COMPLEX FLUIDS FOR ACTIVE DELIVERY IN LAUNDRY APPLICATION
DYE-SURFACTANT INTERACTIONS

BENJAMIN DEVILLIERS

Ph.D. THESIS 2018

Complex fluids for active delivery in laundry application

Dye – Surfactant interactions

Benjamin Devilliers

A thesis submitted in part fulfilment of
the requirements for the degree of
Doctor of Philosophy

Department of Chemistry
Durham University

September 2018

Abstract

Everyone has noticed the yellowing of our white fabrics over time. Consequently, industrial companies have introduced hueing dyes to bring a brightening effect in their soluble unit doses (SUD). However, unwanted staining by the dye can occur when the SUD is badly dissolved and directly in contact with the fabric. Internal P&G works have shown that the risk of staining could be reduced using nonionic surfactants. Thus, this thesis concerns the fundamental understanding of the underlying mechanisms and interactions in complex fluids, focussing on dye-surfactant interactions, to minimise the staining risk and maximise the consumer's benefits.

An increase of the hydrophilicity of the surfactant increased its solubility and cloud point, as expected. Two hueing dyes, E4210 and V200, were tested with two nonionic surfactant series (containing 10 or 13 carbons, with a number of EO groups from 3 to 20). In water, V200 aggregates at a concentration above 2×10^{-5} mol L^{-1}. Using the spectrophotometric method, we observed an interaction between dye and surfactant molecules below their CMC, with an intensity increase of the absorption band. When the CMC is reached, a bathochromic shift occurs due to the dye incorporation into surfactant micelles. E4210 molecules were located at the hydrophilic/hydrophobic interface within surfactant micelles, co-micellising with surfactant. Surfactant interactions decrease the dye deposition onto fabric while the viscosity of the solution increases the risk of fabric staining. For V200, monomers adsorb onto the fabric, depleting monomers from solution. However, the monomer-aggregate equilibrium in solution is quickly re-established with the aggregates dispersing into monomers.

Through observations and data results, it has been found that the dye-surfactant interactions have a role in controlling the dye adsorption kinetics by slowing or limiting the dye-fibre interactions, reducing dye adsorption onto fabric and thus the risk of staining. Surfactants also participate in the dye removal by reducing dye redeposition by keeping dye molecules in suspension within surfactant micelles.

For Eloise and my Family.

Acknowledgements

I wish to express my sincere gratitude and thank my supervisor, Dr Sharon Cooper, for her help, patience, guidance and support in my work as well as in my writing. I also would like to thank my research group and Helen Riggs for their help and guidance in my SAXS and EM works. I also want to thank the PhD students, especially Helen Ramsey and Janet Berry at the beginning of my thesis at Durham as well as the Ritu's students in my office for their help, kindness and to have brought a good atmosphere in the office. Also Ritu Kataky and Richard Thompson from Durham University for their reviewing and help on my first and second year reports.

I also wish to thank the MICSED team, Anna Stanczak, Elise Sabattié, Niamh Ainsworth and Salvatore Croce for their support and collaboration work as well as all the nice moments that we spent together.

I would like to thank Procter and Gamble for all the help and advices they provided me during my secondment at P&G but also during my work at Durham University: my P&G supervisors, Jean-François Bodet, Euan Magennis and Greg Miracle; and other people from P&G: Adam Hayward, Andrew Moon and especially Jef Maes.

To finish, I wish to express my sincere gratitude and thank my family and more especially Eloise Brice who has supported me during these three years and even more with the writing time, for the good and bad moments, to have followed me to Durham and Brussels and to have supervised my writing.

Declaration

The work described in this thesis was carried out in the Department of Chemistry at the University of Durham between October 2014 and September 2017 under the supervision of Dr S. J. Cooper as well as a secondment at Procter & Gamble Brussels Innovation Centre between October 2015 and March 2017 under the supervision of J. F. Bodet. All work is my own, unless otherwise stated in the text, and it has not been submitted previously for a degree at this or any other university.

- Some of the tensiometry data were performed by the analytical department at Procter & Gamble Brussels Innovation Centre.

Statement of copyright

Table of Contents

Glossary

This list has some of the important terms used throughout this thesis. It is not an exhaustive list, any other terms will be defined as and when they occur in the text.

Auxochromes – colour helpers that increase the intensity of the colour

Bathochromic – when an absorption band moves towards longer wavelengths (also called a red-shift).

Chromogen is the coloured molecular structure (often used synonymously with the term chromophore).

Chromophore – the unsaturated building blocks of colour, *e.g.* –N=N–

Colour Index – the descriptive catalogue of synthetic colorants in terms of generic name and constitution (where disclosed) published by the SDC.

Detergency – the removal of unwanted substances from a solid surface through an aqueous bath

Hue – the attribute of colour whereby it is recognised as being predominantly red, blue, yellow, green, *etc*.

Hydrophilic – also called “water loving” is when a molecular entity or of a substituent has an affinity and interacts with polar solvents, in particular with water, or with other polar groups.

Hydrophobic – also called “water hating” is the opposite of hydrophilic and means no affinity for any polar groups or solvents. Hydrophobic molecules tend thus to interact together or with nonpolar molecules or solvents like oils or fats.

Hyperchromic – increase in the intensity of an absorption band.

Hypochromic – decrease in the intensity of an absorption band.

Hypsochromic – when an absorption band moves towards shorter wavelengths (also called a blue-shift).

Solvatochromism – colour change brought about by a change in solvent polarity (solvatochromic).

Surfactants – amphiphilic molecules (having a hydrophilic and a hydrophobic part) acting on the surface tension. Contraction of surface-active agents.

Halochromism – colour change brought about by a change in pH.

List of Symbols and Abbreviations

This list has some of the common symbols and abbreviations used throughout this thesis. It is not an exhaustive list, any other symbols or abbreviations will be defined as and when they occur in the text.

All usual unit described in this list came from their usual use in this thesis. If a different unit is used in a particular case, this will be indicated in the text.

Symbol	Meaning	Usual Unit
a	Area	cm^2
α	Angle	°
A	Absorbance	
a	Activity	
c	Velocity of light	2.9979×10^8 m s^{-1}
C or $[\,]$	Concentration	mol L^{-1}
d	Distance	cm
ε	Molar extinction coefficient	L mol^{-1} cm^{-1}
ε_o	Molar extinction coefficient of the dye in water	L mol^{-1} cm^{-1}
ε_m	Molar extinction coefficient of the dye-surfactant complex	L mol^{-1} cm^{-1}
ε_r	Static dielectric constant	F m^{-1}
E	Energy	J
F	Force	N
f	Fraction	%
G	Free energy	J
γ	Surface/Interfacial tension	mN m^{-1}
h	Planck's constant	6.626×10^{-34} J s

Symbol	Meaning	Usual Unit
H	Enthalpy	J
I	Intensity	
K	Equilibrium constant	
K_b	Binding constant	L mol^{-1}
l	Length	cm
λ	Wavelength	nm
M	Molecular weight	g mol^{-1}
N	Aggregation number	
n_i	Refractive index	
n	Number of mole	mol
n_c	Number of carbon	
n_i	Refractive index	
$P(q)$	Form factor	
$p(r)$	Pair distance distribution	cm
π	Pi	3.14
q	Length of the scattering vector	cm^{-1}
r	Radius	cm
R	Ideal gases constant	8.31451 J K^{-1} mol^{-1}
ρ	density	g L^{-1}
$S(q)$	Structure factor	
T	Temperature	°C
t	Time	s
θ	Contact angle	°
$\vec{\mu}$	Dipole moment	D
V	Volume	L
X	Volume ratio	
Σ	Sum	

Abbreviation	Meaning
AE	Alcohol Ethoxylate
Afnor	Agence francaise de normalisation (French Agency for Standardisation)
AO	Atomic orbital
B-H	Benesi-Hildebrand
BIC	Brussels Innovation Centre
CI	Colour Index
CIE	Commission international de l'éclairage (International commission of lighting)
CMC	Critical micelle concentration
CPP	Critical Packing Parameter
CT	Charge transfer
DRS	Diffuse reflectance spectroscopy
EM	Electron Microscopy
EO	Ethylene Oxide
ESR	Electron Spin Resonance
EtOH	Ethanol
FTIR	Fourier Transformation Infrared
GIFT	Generalised Indirect Fourier Transformation
HLB	Hydrophilic-Lipophilic Balance
HSQCAD	Heteronuclear Single Quantum Coherence spectroscopy
IAS	Image Analysis System
IFT	Indirect Fourier Transformation
INRA	Institut national de la recherche agronomique (National Institute of Agricultural Research)
IR	Infra-Red
LAS	Linear alkyl benzene sulfonate
LC-MS	Liquid chromatography – Mass spectrometry
M	Molar = mol L^{-1}
ME	Microemulsion
MeOH	Methanol
MO	Molecular orbital

Abbreviation	Meaning
MW	Molecular weight
NI	Nonionic
NMR	Nuclear Magnetic Resonance
NOESY	Nuclear Overhauser Effect SpectroscopY
O/W	Oil-in-Water
P&G	Procter & Gamble
PEG	Polyethylene glycol
PDDF	Pair Distance Distribution Function
PdGW	Solvent mixture: 58 % Pdiol, 17 % Glycerin, 25 % Water
Pdiol	1,2-propanediol
SAXS	Small Angle X-ray Scattering
SDBS	Sodium Dodecyl Benzene Sulfate
SDS	Sodium Dodecyl Sulfate
SUD	Soluble Unit Dose
TSP	Trimethylsilylpropanoic acid
UPLC	Ultra-performance liquid chromatography
UV	Ultra-violet
W/O	Water-in-oil
wt%	Weight percentage

COMPLEX FLUIDS FOR ACTIVE

DELIVERY IN LAUNDRY APPLICATION

DYE-SURFACTANT INTERACTIONS

1. Introduction

Since prehistoric time, dyes have been used to colour skins and furs, and are still widely used today to colour fabrics. Fabric dyeing is a big industrial business, and a lot of studies[1,2,3] on the industrial dyeing process and on the interaction of industrial dyes with selected surfactants have been done. Regarding fabrics, the yellowing over time of our white clothes have been largely studied and can come from several origins. Indeed, it has been shown that it can be due to air pollution,[4] citric acid that is used as a crosslinking agent for cotton,[5] bleaches,[6] chemical changes in unsaturated oils,[7] the sunlight on wool,[8] and many more.

In order to counteract this yellowing effect, optical brighteners[9] are widely used in the laundry market. A few years ago, industrial companies like Procter and Gamble (P&G) started to introduce dyes, and particularly hueing dyes or bluing dyes, in their laundry products[10,11] to bring a brightening effect benefit as an additional technology to optical brighteners. Hueing dyes are thus incorporated in the blue part of soluble unit dose (SUD, see Figure 1.1).

Figure 1.1: Soluble unit dose.

Hueing dyes play a key role in the delivery of the brightness demanded by consumers, but there are enormous challenges in producing dyes that have appropriate properties in the formulation, high stability, and the correct deposition characteristics. Overcoming these challenges would lead to a rapid benefit without deleterious effects caused by in particular, over-deposition, giving a bluish tint, or even a blue stain when the fabric conditioning composition comprising a hueing dye is directly in contact with the fabric and poorly dispersed. This staining problem and long term overhue were reported by consumers complaints disclosed by P&G; and research from P&G has shown that the hueing dye staining can be reduced using nonionic surfactants, whereas using anionic surfactants, staining is more apparent.

Interactions occur between dyes and surfactants,[12] affecting adsorption and fixation of the dye onto fabrics. In addition, spectral properties will alter depending upon the solvent surrounding the dye. However, the majority of literature[1,12] in this area reports on the dye-surfactant and the dye fixation onto fabric in an industrial context of fabric dyeing. Hence, the focus is on using large dye concentrated baths to achieve maximum dye deposition, along with better and permanent colouration of the fabrics over time.

Ristić N. et al.[13] have studied the effect of nonionic surfactant treatment on dyeing characteristics of cotton fabrics dyed with direct and reactive dyes. They have thus shown that nonionic surfactants could help the wettability of cotton fabric and help the dyeing by interacting with direct and reactive dyes. Another area of dye-surfactant interactions is hair care. However, they used surfactant cloud point to measure the ability of surfactant to interact with the dye; which can be effective only using nonionic surfactant while anionic and cationic surfactants do not present a cloud point. Moreover, depending on the nonionic surfactant properties, the method to determine the cloud point can differ (discussed later) from one nonionic surfactant to another and thus interfere in the comparison between them.

Another area where dye-surfactant interactions are studied is hair care. Due to the formulation properties to interact with the keratin network polymer of the hair (assimilated to a polyanion), cationic surfactants are mainly used. It seems that cationic surfactants mainly participate to the dyeing by helping the dye diffusion through the hair network but also change the hue behaviour, lightness and chroma by interacting with oxidation dyes.[14]

The innovative aspect of this thesis is to aim the deposition on fabrics with the minimum amount of dye molecules necessary to counteract the fabric yellowing in daily use through a laundry product in the washing machine. This implies the need for a low dye concentration, and importantly, the correct equilibrium between dye adsorption and dye removal onto fabric after all the wash cycles.

Thus, it is important to get a fundamental understanding of the underlying mechanisms and interactions in complex, multi-component mixtures that deliver the dye deposition in the presence of surfactants, in order to minimise risk and maximise benefit to the consumer. For this, a tool -box of analytical techniques and methods was developed for the preparation and the characterisation of complex fluids. In the

first step, simple formulations containing one component, dye or surfactant were investigated and then more complex formulations, containing both surfactant and dye components, were studied to investigate their interactions. In addition, but to a lesser extent the influence of the solvent(s) on the interactions were probed. The main project aims were: 1. the investigation of how spectral properties of key commercial dyes are influenced by solvent and surfactant environments; 2. the examination of the dye-surfactant interactions and properties, 3. the determination of the kinetics of uptake on different model fabrics, and 4. the mechanisms of dye deposition and dye removal in the presence of surfactant.

Chapter 2 presents all the materials used in this thesis, as well as the analytical techniques and methods developed through the thesis to characterise the key dyes and surfactants, their interactions and mechanisms of dye deposition/removal.
Chapters 3 and 4 detail relevant science concerning surfactants and dyes, respectively, their usage and properties and their characterisation.
Chapter 5 characterises the dye-surfactant interactions using the analytical techniques and methods developed in Chapter 2 by considering the influence of the hydrophilic and hydrophobic parts of the surfactants on these interactions. Accordingly, mechanisms of dye-surfactant interactions with the hueing dyes of interest are suggested. Chapter 6 discusses dye adsorption onto fabric and its removal, first without surfactants and then with. By combining the findings with the results of Chapter 5, mechanisms on the role of surfactant on dye deposition are proposed. The Conclusions chapter summarises the observations and hypotheses, and discusses ideas for further work.

References

[1] F. M. Drumond Chequer et al., “Textile Dyes: Dyeing Process and Environmental Impact,” in *Eco-Friendly Textile Dyeing and Finishing*, ed. M. Gunay (InTech, 2013): 151–176.

[2] R. Atav, “Thermodynamics of Wool Dyeing,” in *Thermodynamics - Fundamentals and Its Application in Science*, ed. R. Morales-Rodriguez (InTech, 2012): 247–262.

[3] A. Ali et al., “Study of Interaction between Cationic Surfactants and Cresol Red Dye by Electrical Conductivity and Spectroscopy Methods,” *Journal of Molecular Liquids* 196 (2014): 395–403.

[4] V. S. Salvin, “The Effects of Air Pollutants on Textiles: Whose Problem?,” *Journal of American Association of Textile Chemists and Colorists* 4, no. 10 (1972): 29–32.

[5] Y. Lu and C. Q. Yang, “Fabric Yellowing Caused by Citric Acid as a Crosslinking Agent for Cotton,” *Textile Research Journal* 69, no. 9 (1999): 685–90.

[6] R.B. LeBlanc and A.P. Ingram, “Cause of Bleach-Induced Yellowing of APO-Finished Cotton,” *Textile Research Journal* 32, no. 4 (1962): 284–91.

[7] E. K. C. Park and S. K. Obendorf, “Chemical Changes in Unsaturated Oils upon Aging and Subsequent Effects on Fabric Yellowing and Soil Removal,” *Journal of the American Oil Chemists’ Society* 71, no. 1 (1994): 17–30.

[8] K. R. Millington, “Photoyellowing of Wool. Part 1: Factors Affecting Photoyellowing and Experimental Techniques,” *Coloration Technology* 122, no. 4 (2006): 169–86.

[9] J. E. Tucker, “Reduction of Sunlight Yellowing of Wool Fabric Treated with Fluorescent Brightening Agents,” *Textile Research Journal* 39, no. 9 (1969): 830–35.

[10] E. S. Sadlowski and M. D. Cummings, Laundry detergent compositions with efficient hueing dye, US7208459, issued 2007, The Procter & Gamble Company.

[11] E. S. Sadlowski and M. D. Cummings, Laundry detergent compositions with hueing dye, US7205269, issued 2007, The Procter & Gamble Company.

[12] E. Barni, P. Savarino, and G. Viscardi, “Dye-Surfactant Interactions and Their Applications,” *Accounts of Chemical Research* 24, no. 4 (1991): 98–103.

[13] N. Ristić and et al., “The Effect of Nonionic Surfactant Treatment on Dyeing of Cotton Fabrics,” *Tekstil* 62, (1–2) (2013): 8–13.

[14] H. Yasunaga et al., “Function of Surfactants in Hair Dyeing by Oxidation Dyes 1. Effect on Colour of Hair Dyed by P-Aminophenol and 5-Amino-O-Cresol,” *Sen’i Gakkaishi* 64, no. 6 (n.d.): 145–50.

2. Experimental Methods

All the materials and methods used at Durham University and at P&G Brussels Innovation Centre (BIC) to produce the work that is presented in this thesis are quoted in this chapter, including the characterisation techniques, supplier and the manufacturer of materials and equipment.

2.1. Reagents and Chemicals

2.1.1. Hueing dyes

Two commercial hueing dyes were used in this thesis, supplied by P&G (from Milliken): E4210 and V200, which are respectively purple and blue dyes. Due to their polymeric form and because of the way they are made, they are not in a pure form (in a PEG (Polyethylene glycol) solution and impurities discussed later on Chapter 4) with an effective concentration of 8.00 % and 5.94 % by mass respectively.

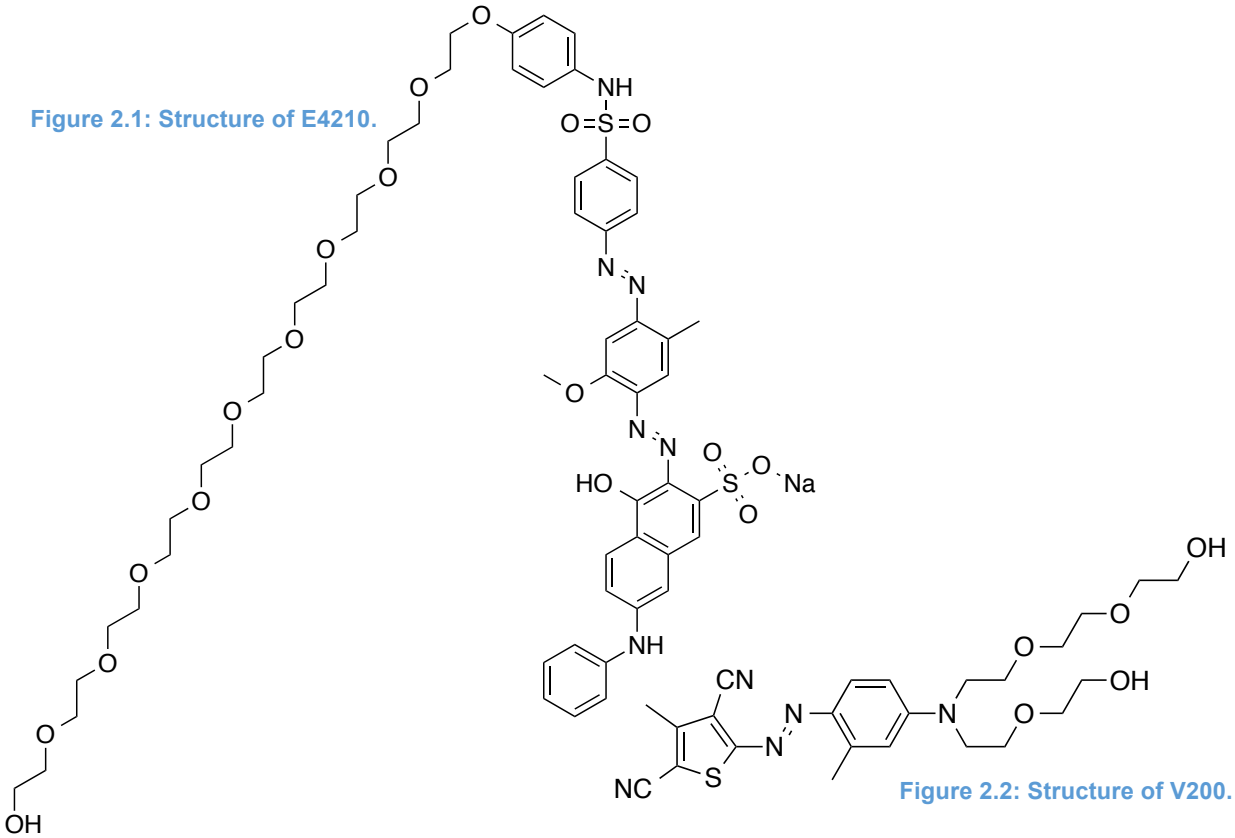

Figure 2.1: Structure of E4210.

Figure 2.2: Structure of V200.

2.1.2. Surfactants

Three surfactants used in this report were supplied by P&G: Lorodac 7-26 (or NI24 AO7; Alcohol, C12-14, ethoxylated; Laureth-4; $C_{12\text{-}14}$-$E_{(>5\text{-}<15)}$), Surfonic L24-9 (or NI24 AO9; Alcohol, C12-14, ethoxylated; $C_{12\text{-}14}$-E_9) and LAS (Linear alkylbenzene sulphonate). Two series of nonionic (NI) surfactants were obtained from BASF: Lutensol® XL types (C_{10}-Guerbet alcohol ethoxylates – Ethylene oxide (EO) from 4 to 14) and Lutensol® TO types (iso-C_{13} Oxo alcohol ethoxylates – EO from 3 to 20) as well as these other surfactants from BASF: Plurafac LF223 (fatty alcohol alkoxylate), sodium dodecylsulfate (SDS) and sodium dodecylbenzene sulfonate (SDBS). However, we have to keep in mind that these commercial surfactants were not in their pure form but were given with an approximate degree of ethoxylation and carbon chain length. Some of them were also diluted in water, this is indicated in the Table 2.1 which summarises the surfactants used in this thesis; HLB (Hydrophilic-Lipophilic Balance) values have been calculated using the Griffin[1] formula for nonionic surfactants and the Davies formula for anionic surfactants (see Chapter 3. Surfactants, 3.3.1.1. CMC and surface tension).

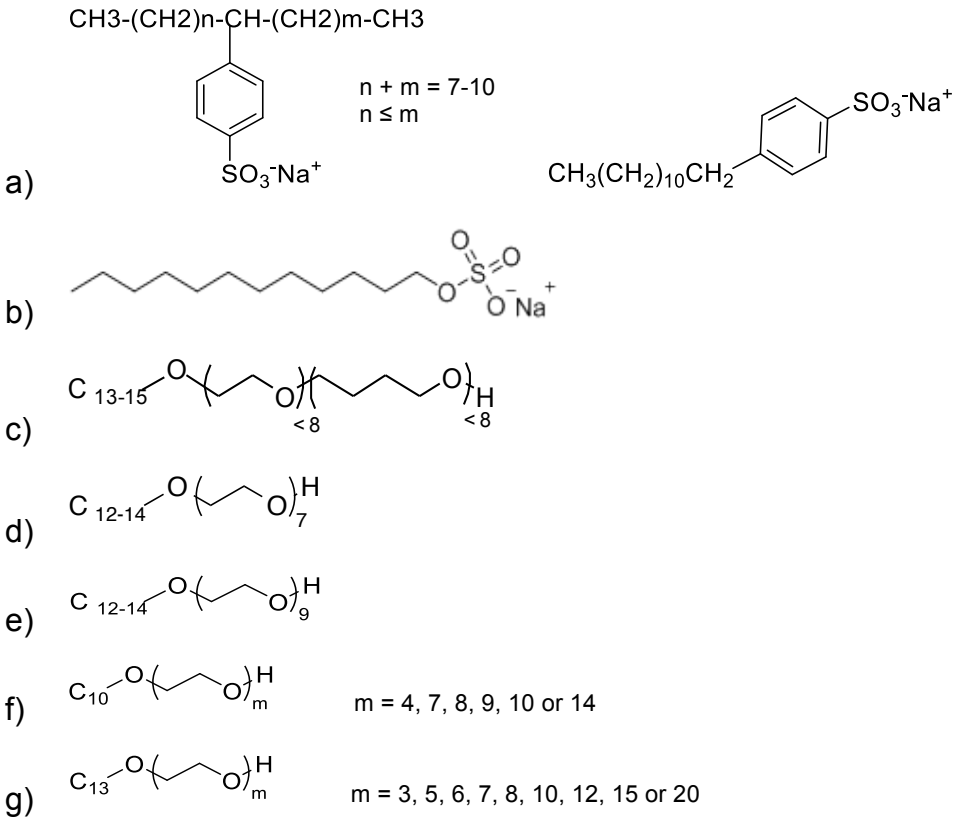

Figure 2.3: Chemical structure of a) LAS and SDBS, b) SDS, c) Plurafac LF223, d) Lorodac 7-26, e) Surfonic L24-9, f) Lutensol XL series and g) Lutensol TO series.

Table 2.1: Surfactants details.

Surfactant	Type	Structure	MW average (g mol^{-1})	HLB	Conc. % by mass
SDS	Anionic	C_{12}-$OSO_3^-Na^+$	288.39	22.10	100 (powder)
LAS	Anionic	C_{13}-C_6H_6-$SO_3^-Na^+$	354.48	12.52	45
SDBS	Anionic	C_{12}-C_6H_6-$SO_3^-Na^+$	342.48	12.04	100 (powder)
Lorodac 7-26	Nonionic	$C_{12\text{-}14}$-$E_{(>5-<15)}$	508.74	12.12	100
Surfonic L24-9	Nonionic	$C_{12\text{-}14}$-E_9	596.84	13.29	100
Plurafac LF223*	Nonionic	$C_{13\text{-}15}E_{<8}$ $P_{<8}$	725.06	14.56	98
Lutensol XL40	Nonionic	$C_{10}E_4$	334.50	10.54	100
Lutensol XL70	Nonionic	$C_{10}E_7$	466.66	13.22	100
Lutensol XL80	Nonionic	$C_{10}E_8$	510.71	13.80	100
Lutensol XL90	Nonionic	$C_{10}E_9$	554.76	14.29	100
Lutensol XP100	Nonionic	$C_{10}E_{10}$	598.82	14.71	100
Lutensol XL140	Nonionic	$C_{10}E_{14}$	775.03	15.92	100
Lutensol TO3	Nonionic	$C_{13}E_3$	332.53	7.95	100
Lutensol TO5	Nonionic	$C_{13}E_5$	420.63	10.47	100
Lutensol TO6	Nonionic	$C_{13}E_6$	464.68	11.38	100
Lutensol TO7	Nonionic	$C_{13}E_7$	508.73	12.12	100
Lutensol TO8	Nonionic	$C_{13}E_8$	552.79	12.75	100
Lutensol TO109	Nonionic	$C_{13}E_{10}$	640.90	13.75	85
Lutensol TO12	Nonionic	$C_{13}E_{12}$	729.00	14.50	100
Lutensol TO15	Nonionic	$C_{13}E_{15}$	861.16	15.35	100
Lutensol TO20	Nonionic	$C_{13}E_{20}$	1081.43	16.29	100

C means the number of carbon

E means the number of ethylene oxide groups

P means the number of propylene oxide groups

* assuming an average of 5 ethylene oxide group and 5 propylene oxide group

2.1.3. Fabrics

In this thesis, five white tracer fabrics with a size of 30 x 30 cm were used, supplied by P&G (from Warwick Equest):

Table 2.2: Fabrics details.

Fabric	Composition	Weight (with tolerance)
Terry	90 % Cotton : 10 % Polyester	300 g m^{-2} (+/- 5 %)
White Knitted Cotton	100 % Knitted Cotton Interlock	255 g m^{-2} (+/- 5 %)
Woven (flat) cotton	100 % Woven Cotton	130 g m^{-2} (+/- 10 g)
Polycotton	65 % Polyester : 35 % Cotton	110 g m^{-2} (+/- 10 g)
Polyester	100 % Polyester	185 g m^{-2} (+/- 5 %)

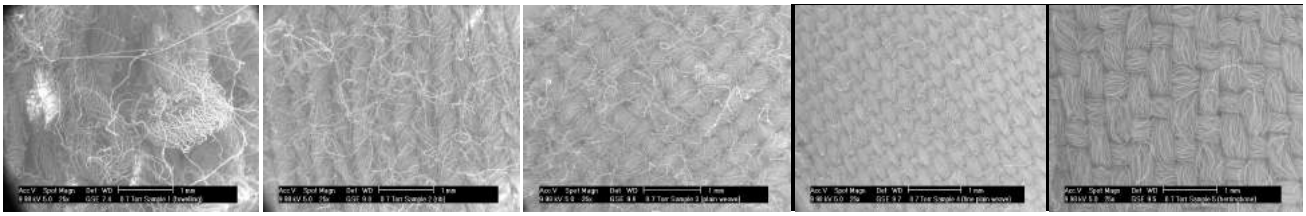

Figure 2.4: Electron microscopy pictures of fabrics: Terry cotton, Knit cotton, Flat cotton, Polycotton and Polyester from left to right.

2.1.4. Other materials

All the solvents and chemicals used were of reagent grade and used without further purification, unless otherwise stated in the text.

- Deionised water (Sartorius Arium 611 ultrapure water system (resistivity less than 18.2 Mohm cm)).
- For the dye purification, decane was obtained from Sigma Aldrich (95 % purity) and chloroform from Fisher Scientific.
- Methanol (MeOH), ethanol (EtOH), glycerol (or glycerine), 1,2-Propandiol (or Pdiol), PEG200, Ethylene Glycol were from Sigma Aldrich.
- Deuterium oxide 99.9 atom % D, contains 0.05 wt. % 3-(trimethylsilyl)propionic-2,2,3,3-d4 acid, sodium salt from Sigma-Aldrich.

NB: In this thesis, PdGW is used as acronym for the following solvent mixture (% by mass): 58 % Pdiol, 17 % Glycerine, 25 % Water.

2.2. Instrumentation

2.2.1. UV-Vis Spectrophotometry

All the spectrophotometry work was performed either at Durham University or at BIC. At Durham University, a Unicam UV4 UV/Vis Spectrophotometer, which has a PMT detector and a variable spectral bandwidth to 0.5 nm, was used. The wavelength range was from 190 nm to 900 nm, with an accuracy of +/- 0.3 nm at 250-500 nm and +/- 0.5 nm at 190-250 and 500-900 nm. The spectra were analysed using VisionPro Version 4.00 software.

Figure 2.5: UV-Vis spectrophotometer used at Durham on the left and at BIC on the right.

At BIC, a Genesys 10S double beam UV-visible spectrophotometer was used, which had a dual silicon photodiodes detector and variable spectral bandwidth to 1.8 nm. The wavelength range was from 190 nm to 1100 nm with a repeatability of +/- 0.5 nm. Spectra were analysed using VISIONlite software. A 6-cell changer was available but the 1-cell holder was used.

In all UV-Vis work, a 1 cm path length cell holder was used and all the sample sizes and volumes are detailed when appropriate.

2.2.2. Tensiometry

Tensiometry work was performed either at Durham University or at BIC.

Tensiometry data from Durham University were obtained at room temperature (22-25 °C) by the pendant drop method using a FTA-200 tensiometer equipped with a High resolution

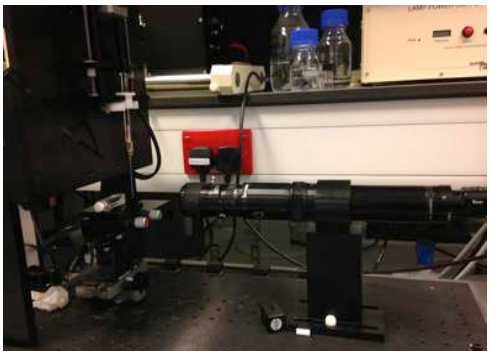

Figure 2.6: Pendant drop tensiometer.

WAT-902B camera from Watec. Drops were formed using a syringe (previously cleaned using a 2-5 % decon surfactant solution for 15 min in an ultrasonic bath then rinsed thoroughly with distilled water) and analysed with the FTA32 2.0 software. All the measurements were done at least in quadruplicate with a fresh drop.

Tensiometry data from BIC were obtained by the analytical department by determining indirectly through the measure of the surface tension of several dilutions of the sample. The serial dilution curves were made using a “Microlab STAR” robotic liquid handling platform from Hamilton Robotics in 96-well plates (Instrument serial number: 2073) and the surface tensions were obtained using a “Delta-8” tensiometer instrument from Kibron, working on the du Noüy-Padday Method (Instrument serial number: 811A250108033). All the measurements were done at 22 °C in at least 4 replicates.

In all tensiometry work, samples were left overnight at room temperature (22-25 °C) as equilibrium time.

2.2.3. Liquid chromatography – Mass spectrometry (LC-MS)

In order to analyse samples from the dye purification, the following LC-MS system was used.

This instrument was setup for flow injection analysis (FIA) or ultra-performance liquid chromatography (UPLC). The solvent flow t from the Acquity UPLC system was introduced into the electrospray ion source which generates positive and negative ions alternately. The operating mass range was 100-2000 u.

The Electrospray Ionisation – Liquid chromatography method with methanol as mobile phase (ESI-LC MeOH) was used to analyse purification samples from a column Acquity UPLC BEH C18 1.7 μm (2.1 mm x 50 mm).

The mobile phase was composed of two solvents: solvent A: water containing formic acid (0.1 %) and solvent B: methanol, with the following gradients:

Table 2.3: Gradient used for the ESI-LC MeOH method.

Time (min)	Flow rate (mL/min)	% by mass A	% by mass B
0	0.6	95	5
0.2	0.6	95	5
4	0.6	5	95
4.5	0.6	5	95
5	0.6	95	5

2.2.4. Optical microscopy

An Olympus BX50 optical microscope was used to look at the different characteristics of surfactant micellar phases (e.g. maltese cross of lamellar phase). This was equipped with a polarising filter, a digital camera and Linksys 32 software to enable image capture and processing. Samples to be viewed were placed between two glasses cover slips and placed on the Linkam heating/cooling block. This block has a central hole (1 mm by 4 mm) to allow light transmission through the sample.

2.2.5. Electron Microscopy (EM)

The structure of the fabric samples was examined at Durham University by electron microscopy using a Philips/FEI XL30 ESEM™ in reduced-vacuum mode, thus enabling the samples to be imaged without applying an electrically-conducting coating. The samples were fixed to microscope stubs using double-sided adhesive carbon pads. The imaging gas was water vapour, and the pump-down cycle used was 0.5–1.0 Torr five times, finishing at 0.5 Torr. The pressure was then adjusted as necessary to obtain an informative micrograph with gaseous secondary electron (GSE) detection.

2.2.6. Image Analysis System (IAS) – Digi Eye box

In order to compare fabric colours and provide more information than visual grading, an IAS was used at BIC to get objective, sensitive and absolute results, which were repeatable and reproducible regarding the staining tests and to compare fabric colours. The Digi Eye box consists of a chamber with a controlled light using a VeriVide T8 D65 lamp (Daylight 6500 K), within CIE Tolerance, a Nikon D90 camera

to take pictures and the Digi Eye v2.81 with chart 3.6 software for the determination of the *L, a* and *b* values (describes in Chapter 4. Dyes 4.1.4. Characterisation of colours) of each stains. Verivide Limited supplies all the system.

2.2.7. Washing machine

A washing machine, Miele W526, was used at BIC to perform all the experiments in real life conditions. Parameters of washing cycle times and temperatures are detailed when appropriate.

2.2.8. Small Angle X-ray Scattering (SAXS)

For SAXS measurements, a Bruker Nanostar SAXS machine was used with X-ray source operating at 40 kV and 35 mA to produce CuKα x-rays with a wavelength of 1.54 Å. The beam was focused passing through cross-coupled Göbel mirrors and a series of pinholes. The liquid sample was placed in a 2 mm thickness capillary and a control temperature system fixed the temperature at 25 °C for all the results.

X-ray diffraction was measured using a Hi-star 2D detector held at 1 m from the sample. The sample and detector were placed under vacuum to minimise the interaction of the beam with air particles. The detector measured the radiation at each angle, and produced the final SAXS diffraction spectrum ($I(q)$ vs q). Results were then analysed by Generalised Indirect Fourier Transformation (GIFT) analysis in order to obtain the pair distance distribution function, $p(r)$, to access the structural parameters.

Figure 2.7: SAXS machine.

2.3. Methods developed and used

2.3.1. Validation method

In order to get a robust and repeatable method, the methods were validated using the method of "accuracy profiles".[2,3,4] This method consists of building a statistical model using an experimental design aimed to test the normality of the dispersion of measurements and estimate the components of the uncertainty of the measurements: the precision, the accuracy and the specificity. Basically, this is a tool to make the decision on the validity of a method graphically.

To be validated, a method must give the guarantee that each result will be sufficiently close to the true value. This means that we have to calculate the probability to get the result at reasonable distance from the true value. For instance, if Z is the result obtained and X is the true value, they are sufficiently close if:

$$-y < Z - X < +y \qquad \text{Eq. 2.1}$$

where -y and +y represent the maximum reasonable distances acceptable for the method (defined by the user). They give the acceptability limits. If these distances are similar for both sides of the true value, the acceptability interval can be written:

$$|Z - X| < y \quad or \quad \frac{|Z - X|}{X} < y\,\% \qquad \text{Eq. 2.2}$$

Then the probability to get the result at reasonable distance from the true value can be given by the following equation, where β represents the tolerance probability.

$$Prob\,(|Z - X| < y) \geq \beta \qquad \text{Eq. 2.3}$$

In order to predict the tolerance limits, several steps must be followed:

- Choose an experimental method and define what we want to measure.
- Define the objectives, which means define the acceptability limits.
- Select the validation samples whose reference values are known.
- Chose an experimental design which will give diverse incertitude sources by, for instance, selecting at least three levels of concentration (covering the calibration domain if this is an indirect method) and doing three replicates of each level for at least three days.
- Collect the data by preparing and independently measuring the 27 samples (3(levels) x 3(replicates) x 3(days)) as well as the same for the reference material. For indirect methods, collect the data from the calibration. The

experiments were repeated on 3 separate days in order to take into account the influence of the temperature or even the manipulation that can differ from day to day.

- Calculate the validation criteria from the results: different statistical steps involving the number of series (days), the number of repetitions (replicates), the number of measures (n° series x n° repetition), the sums of squares of deviations, variances and standard deviations, as well as the t-student coefficient. In probability and statistics, the Student's t-test is usually used to determine the statistical significance of the difference between two sample means where the sample size is small and population standard deviation is unknown
- Calculate the tolerance limits and build the accuracy profile. It consists of a 2D-graphical representation (see example on Figure 2.8) where the concentration levels are represented in the horizontal axis and the tolerance interval limits and the accuracy (acceptability interval) are represented in the vertical axis.
- Interpret the results and decide if the method is validated or not. To validate a method, the recovery yield, corresponding to the results obtained with the method as a percentage of the target value, must be included in the tolerance interval which must be included in the acceptability interval.

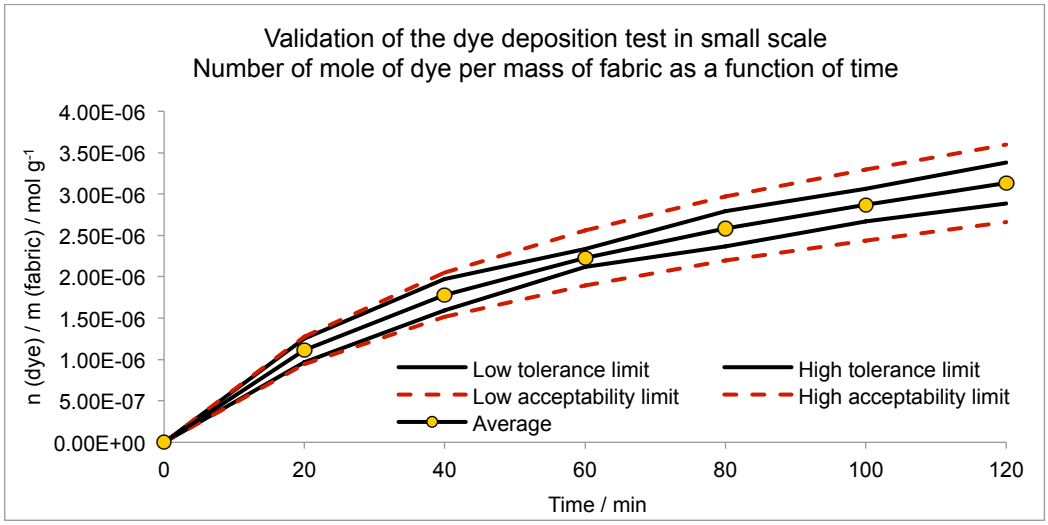

Figure 2.8: Accuracy profile for the validation of the dye deposition test in small scale: accuracy is illustrated as a continuous line with the average number of mole of dye absorbed onto fabric per mass of fabric during time. The limits of the β-expectation tolerance interval are represented by two symmetrical continuous thin lines. The acceptability limits (−15 %, +15 %) are illustrated as dashed lines. Whereas tolerance interval is included into the acceptability limits in the range (0, 120 minutes), the method can be declared as valid over this domain.

This validation method was thus used to validate two procedures used in this thesis (The Benesi-Hildebrand plot for determining surfactant-dye binding constants and the small scale dye adsorption test) by using an Excel file developed by Prof. M. Feinberg, professor at the INRA at Paris (Intitut National de Recherche Agronomique – National Institute of Agronomic Research), for the Afnor (Agence francaise de normalisation – French Agency for Standardisation).

2.3.2. Benesi-Hildebrand plot for the dye-surfactant interaction parameters

Experimentally, the method involved the preparation of several samples of dye-surfactant solution at different surfactant concentrations but with a constant concentration of dye (which has to be kept constant between all the experiments). The stock solutions were left for 60 minutes in an ultrasonic bath for a good dye and surfactant dispersion, and all the samples were then left overnight for stabilisation before analysing them by spectrophotometry. Usually, a dozen samples were prepared that must satisfy two conditions. The first one being that the surfactant concentration ranged from below to above the surfactant CMC for the investigation and visualisation of the dye-surfactant interactions; and the second one being that there are at least 8 samples in the surfactant concentration range ([Surfactant] >> 100 x [Dye]) to allow the determination of K_b. By taking 3 x 3 mL (triplicate), the absorbance of each sample (the dye stock solution, the surfactant stock solution and all dye-surfactant dilutions) was measured by spectrophotometry. By plotting $\frac{1}{[S]_0}$ against $\frac{[D]_0}{\Delta A}$ at the wavelength where ΔA_{max} occurs, it was possible to determine the binding constant of the dye-surfactant complex, K_b, using:

$$\frac{[D]_0}{\Delta A} = \frac{1}{K_b \varepsilon_m l}\frac{1}{[S]_0} + \frac{1}{\varepsilon_m l} \qquad \text{Eq. 2.4}$$

where $[D]_0$ and $[S]_0$ are respectively the dye and surfactant concentration, ΔA is the difference in absorbance between the absorbance of the solution in presence and in absence of surfactant, K_b and ε_m are respectively the binding constant and the molar extinction coefficient of the dye-surfactant complex, and l the path length (equation explained on Chapter 5, 5.1.2. Benesi-Hildebrand equation).

Eq. 2.5 was also used to show the fraction, f, of dye molecules incorporated into surfactant micelles (equation explained on Chapter 5, 5.1.2. Benesi-Hildebrand equation). .

$$f = \frac{\Delta A}{[D]_0 \varepsilon_m} \qquad \text{Eq. 2.5}$$

Also in parallel, we could determine the molar extinction coefficient of the dye-surfactant complex, ε_m, by using the Beer-Lambert Law with the samples having different dye concentration but the same surfactant concentration (far above the surfactant CMC). In this way, it would be possible to compare ε_m from the Beer-Lambert Law and ε_m from the B-H equation and validate the method.

2.3.3. Dye adsorption test in small scale

A method was developed to study the dye deposition on a small scale. The method developed involved the preparation of a dye stock solution at 10^{-4} mol L^{-1} used for the calibration curve and the deposition test. Surfactants were also added in order to study the influence of surfactants on the dye deposition. The stock solution was kept for 60 minutes in an ultrasonic bath for good dye dispersion. Then, at least ten solutions were prepared to get a fresh calibration curve. 10 mL of the stock solution was poured into a vial (volume 28.25 mL; dimension: 2 x 9.5 cm) with a stirrer (12 x 4.5 mm) to mimic the washing bath motion in the washing machine (the stirring was kept constant for all the experiments). A sample of 3 mL of this dye solution was analysed by spectrophotometry giving the absorbance at t = 0 minute. 0.1 g of fabric was then introduced into the vial containing the dye solution (one fabric per vial), which was then analysed spectrophotometrically every 15 minutes during two hours by taking 3 mL of the solution and putting them back into the vial after each measurement to keep the volume of the dye solution constant. The adsorption tests were repeated in triplicate. The absorbance loss (and thus the dye concentration loss in the solution) corresponds to the dye absorbed onto the fabrics, which was determined from the calibration curve.

2.3.4. Staining test in real conditions

In order to work under in realistic conditions, a staining test was done to study the potential staining risk of the developed formulations by comparing them to a reference or to one another. For this, several formulations of the blue top

compartment from the SUD were prepared according to the nonionic formulation from P&G. 1.5 mL of each formulation were then deposited on a pre-wet fabric (with the reference, if needed, for comparison) and left for 45 min. Then a rinsing step was needed, which was performed by dipping the fabric twenty times in water, to remove the excess of dye from the fabric before making a short machine cycle wash at 30 °C (Miele W526 – Program: Cotton; Short: 1h26, Spin speed: 1200 rpm) with 15 g of basic detergent to mimic realistic washing conditions. The fabric was then dried at room temperature. Afterwards, the Digi Eye box was used to determine the L, a and b values (described on Chapter 4, 4.4.1. Characterisation of colours) of each stain. All staining work was done at least in triplicate and the washing machine was rinsed between each test by doing a short cycle wash at 95 °C in order to remove any excess dye that could have been left in the machine.

2.3.5. Dye removal test

Based on the staining test in real conditions, a dye removal test was used to study the ability of a formulation to remove the dye from the fabric. For this, several formulations comprising a surfactant system in solvent without dyes were prepared according to the nonionic formulation from P&G. All fabrics were first dyed in a dye solution of 10^{-4} mol L^{-1} with high agitation during 2 hours to obtain a homogeneous dying, then rinsed by dipping them twenty times in water and dried at room temperature. 6 regions were delimited on each fabric in order to apply formulations and localised where the measurements were to be done. 1.5 mL of each formulation was then deposited on a pre-wet dyed fabric and left for 45 min. Then a rinsing step was needed, which was performed by dipping the fabric twenty times in water, to remove the excess of surfactant before making a short machine cycle wash at 30 °C (Miele W526 – Program: Cotton; Short: 1h26, Spin speed: 1200 rpm) with 15 g of basic detergent to mimic realistic washing conditions. The fabric was then dried at room temperature. Afterwards, the Digi Eye box was used to determine the L, a and b values in the region where the formulations were deposited. We have to note that a first measurement of L, a and b was done after the fabric dyeing step as reference to compare with the L, a and b after the deposition of formulation to quantify the dye removal. Dye removal tests were repeated at least in triplicate.

References

[1] W. C. Griffin, 'Calculation of HLB Values of Non-Ionic Surfactants', *J. Soc. Cosmet. Chem.* 5 (1954): 249–355.

[2] Ph. Hubert et al., "Harmonization of Strategies for the Validation of Quantitative Analytical Procedures: A SFSTP Proposal—part I," *Journal of Pharmaceutical and Biomedical Analysis* 36, no. 3 (2004): 579–86.

[3] Max Feinberg et al., "New Advances in Method Validation and Measurement Uncertainty Aimed at Improving the Quality of Chemical Data," *Analytical and Bioanalytical Chemistry* 380, no. 3 (2004): 502–14.

[4] Max Feinberg, "Validation of Analytical Methods Based on Accuracy Profiles," *Journal of Chromatography A*, Data Analysis in Chromatography, 1158, no. 1–2 (2007): 174–83.

3. Surfactants

3.1. Introduction

A surfactant (contraction of *surface-active agents*) is an amphiphilic molecule that has two parts (see Figure 3.1): one hydrophilic, soluble in polar solvents, called the "hydrophilic head-group", which is an ionic or highly polar group; and another hydrophobic (or lipophilic) part, soluble in non-polar groups, called the "hydrophobic tail", which is generally a linear or branched hydrocarbon chain. In solution, these molecules have the ability to spontaneously adsorb at the surface or interface with their hydrophilic head-groups toward a polar environment and their hydrophobic tails toward a non-polar environment to minimise the interaction with chemical functionalities of opposite affinity (hydrophilic vs. hydrophobic).[1] This situation is energetically more favourable than complete solution in either phase.

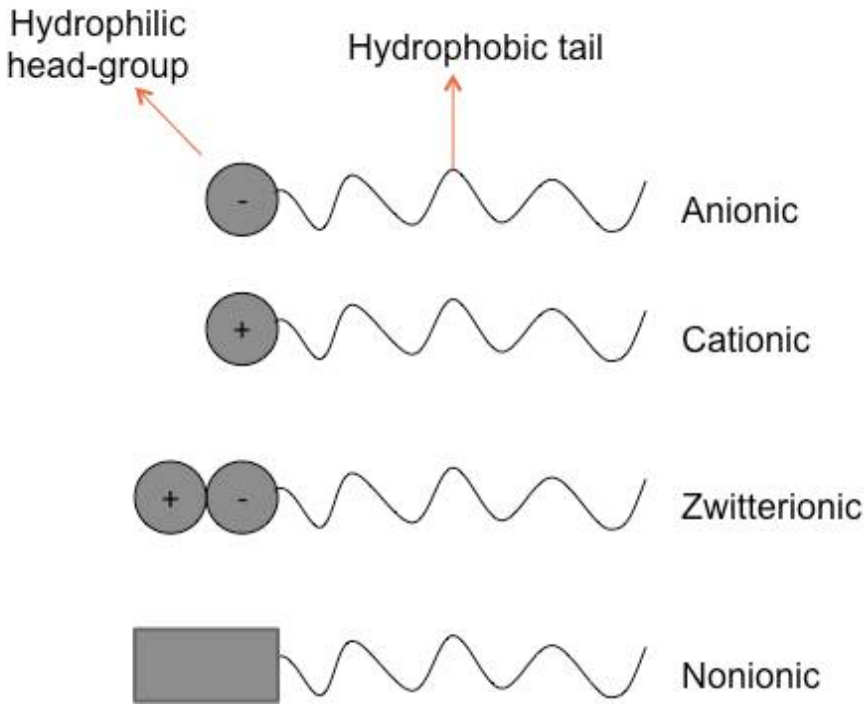

Figure 3.1: The four different main types of surfactants.

Depending on the nature of the hydrophilic group, surfactants are classified as:

- **Anionic:** The head-group is negatively charged, for example:

  $RCO_2^-Na^+$ (soap),

  $RC_6H_4SO_3^-Na^+$ (alkylbenzene sulfonate).

- **Cationic:** The head-group is positively charged, for example:

  $RNH_3^+Cl^-$ (salt of a long-chain amine),

  $RN(CH_3)_3^+Cl^-$ (quaternary ammonium chloride).

- **Zwitterionic:** The head-group is both positively and negatively charged, for example: $RN^+H_2CH_2CO_2^-$ (long-chain amino acid),

  $RN^+(CH_3)_2CH_2CH_2SO_3^-$ (sulfobetaine).

- **Nonionic:** The head-group is non-charged, for example:

  $RCO_2\ CH_2CHOHCH_2OH$ (monoglyceride of long-chain fatty acid),

  $R(OC_2H_4)_nOH$ (polyoxyethylenated alcohol).

Surfactants are widely used for their property of lowering the surface tension, particularly for detergents, wetting agents, emulsifiers, foaming agents, and dispersants.

3.2. Surfactant properties

3.2.1. Surface and interfacial tensions

We make the distinction between the surface, which is the boundary between two phases where one phase is a gas, usually air; and the interface which is a boundary between two immiscible and non-gaseous phases.

The phenomena of surface and interfacial tensions can be explained by the short-range forces of attraction existing between molecules (Van der Waals forces, hydrogen bonding...). Indeed, each molecule within the bulk of a liquid is, on average, subject to equal forces of attraction in every direction. However, those located at the interfacial (or surface) experience unbalanced attractive forces due to a lack of similar molecule with the same forces close to them resulting in a net inward pull (see Figure 3.2) and a potential energy greater than the energy of a

similar molecule in the interior of the bulk. Thus, to minimise this potential energy, mobile molecules will spontaneously leave the surface (or interface) for the interior so as to minimise the surface (or interfacial) area, hence forming droplets of liquid or bubbles of gas, since the spherical shape is the shape with the minimum interactions between the two different phases.

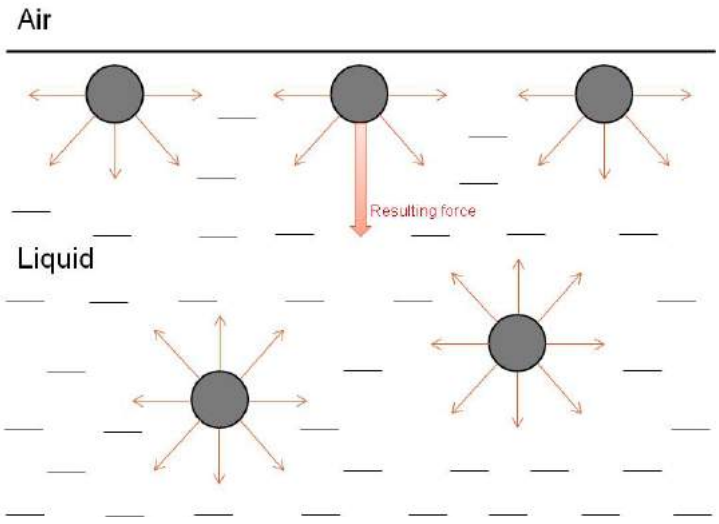

Figure 3.2: Attractive forces between molecules at the surface air-liquid.

The surface tension γ of a liquid can be defined as the force F acting at right angles to any line of unit length l on the liquid surface. This corresponds to the work (free energy) G required to increase the area a of the surface isothermally and reversibly by one unit amount (Eq. 3.1).[2]

$$\gamma = \left(\frac{dG}{da}\right)_{n,p,T} \qquad \text{Eq. 3.1}$$

The surface (or interfacial) tension depends upon the difference in nature of the two phases meeting at the surface (or interface). The more there are dissimilarities in their natures, the higher the surface (or interfacial) tension. Thus, with an accumulation at the surface (or interface), the surfactant molecules will decrease the dissimilarity between both phases and will thus reduce the surface (or interfacial) tension. This phenomenon can be measured by tensiometry as a function of surfactant concentration.

3.2.2. Aggregation of surfactants – Critical Micelle Concentration (CMC)

Surfactants molecules are located at the surface (or interface) as well as, in a small part, in the bulk. When the limit of surfactant concentration at the surface is

reached, the surface (or interfacial) tension cannot be lowered significantly more and remains approximately constant. At this surfactant concentration, further addition of surfactant molecules in the bulk leads, spontaneously, to the surfactant aggregation into micelles with, for a polar liquid environment, their hydrophobic tails pointing inwards and their hydrophilic head groups towards the polar phase (see Figure 3.4). This arises so as to minimise the proximity of the hydrophobic tails with the polar phase (or conversely with their hydrophilic head groups and their hydrophobic tails pointing inwards towards the non-polar phase to minimise the interactions of their polar head groups with a non-polar phase for inverse micelle).[3] This concentration is called the critical micelle concentration (CMC). When micellisation begins, activity does not change with increasing concentration, so interface concentration does not change. Micelles do not form because the interface is full. Figure 3.7 shows that surface is really constant for order of magnitude before CMC.

In aqueous solution, the thermodynamic drive for micellisation is entropy-driven and not enthalpy-driven. This is because when the hydrophobic tails are surrounded by water, the water becomes more structured, forming a cage around the tails, so as to maintain as much hydrogen bonding with other water molecules as possible. This is known as the hydrophobic effect,[4] with the structuring leading to a smaller accessible number of conformations for the water molecules and so a reduction in entropy compared to their

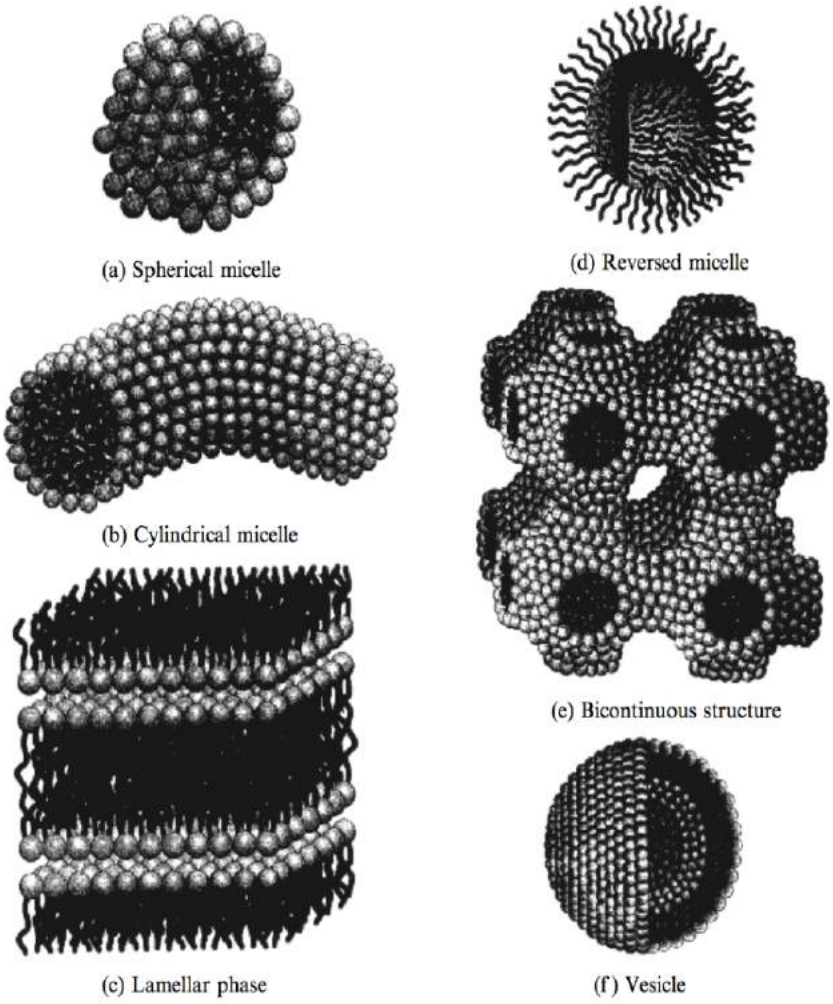

Figure 3.3: Surfactant self-assembly leads to a range of different structures. Reproduced by permission of Wiley-VCH.[3]

entropy in bulk water. Removing the hydrophobic tails from the aqueous environment on micellisation restores the bulk water structure, increasing the water's entropy.

As micelles are dynamic entities, their shapes and structures can change, depending on several parameters like temperature, the type of surfactant and its concentration, other ions within the solution and other water-soluble compounds found, e.g. alcohols. Indeed, surfactants can aggregate to form spherical micelles, cylindrical micelles, and at high enough concentrations, lamellar structures, etc. (see Figure 3.3).

3.2.2.1. Packing parameter and aggregation number

The shape and structure of micelles can be estimated by the critical packing parameter (CPP) firstly described by J.N. Israelachvili *et al.* in 1975.[5] They developed a geometrical model taking into account the thermodynamics of self-assembly. For that, they defined the distortion from spherical shape as a relation between the aggregation number, N, and the area per amphiphile, a. The aggregation number for spherical micelles can be expressed as the ratio between the micellar core volume, V_{core}, and the volume of the hydrocarbon tail, V_{tail} (see Figure 3.4):

$$N = \frac{V_{core}}{V_{tail}} = \frac{4\pi}{3}\frac{r_{mic}^3}{V_{tail}} \qquad \text{Eq. 3.2}$$

where r_{mic} represents the micelle radius.

Alternatively, the aggregation number can be expressed as the ratio between the micellar area, a_{mic}, and the cross-sectional area, a_0, of one surfactant molecule, as follows:

$$N = \frac{a_{mic}}{a_0} = \frac{4\pi r_{mic}^2}{a_0} \qquad \text{Eq. 3.3}$$

Considering Eq. 3.2 and Eq. 3.3 as equal, Eq. 3.4 is obtained, given a critical condition for the formation of spheres:

$$\frac{V_{tail}}{a_0 r_{mic}} = \frac{1}{3} \qquad \text{Eq. 3.4}$$

r_{mic} cannot exceed the extended length of the surfactant alkyl chain, l_c, which is given by:

$$l_c = 1.5 + 1.265 n_c \qquad \text{Eq. 3.5}$$

where n_c is the number of carbon atoms constituting the alkyl chain.

Thus the ratio $V_{tail}/a_0 l_c$, gives a geometric characterisation of a surfactant molecule and is called the CPP. Figure 3.5 shows the expected structure of micelles as a function of the CPP.

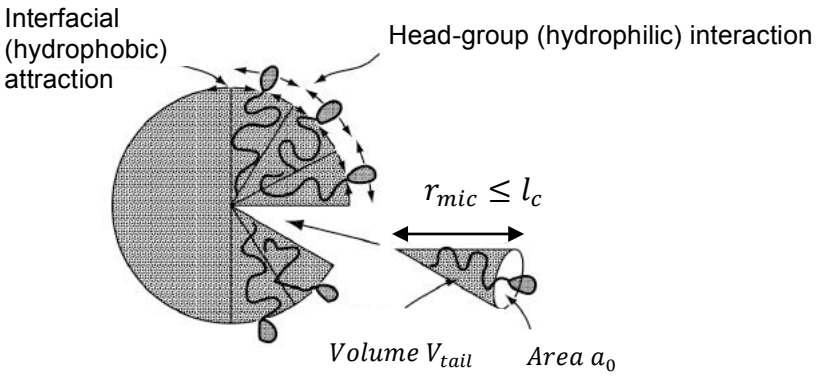

Figure 3.4: The critical packing parameter (CPP) or surfactant number relates to the head group area, the extended length and the volume of the hydrophobic part of a surfactant molecule into a dimensionless number CPP. Reproduced by permission of Wiley-VCH.[3]

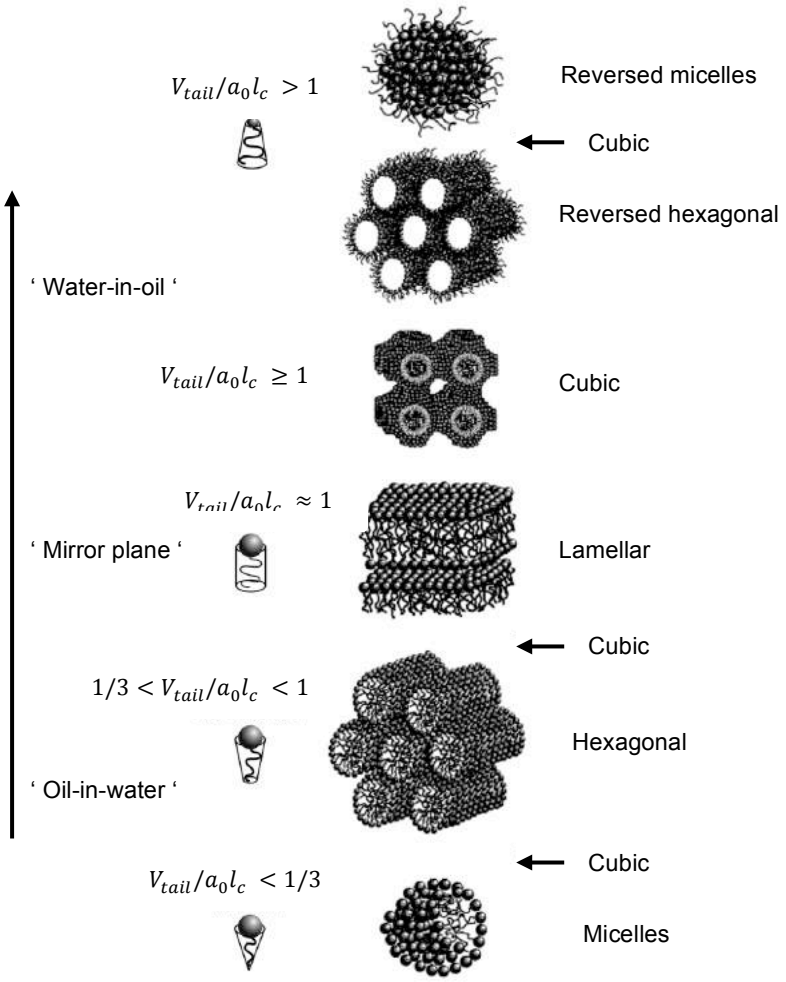

Figure 3.5: Critical packing parameters (CPPs) of surfactant molecules and preferred aggregate structures for geometrical packing reasons. Reproduced by permission of Wiley-VCH.[3]

3.2.2.2. Parameters influencing the CMC

Since the CMC is due to surfactant aggregation in bulk solution, it is obvious that the surfactant structure influences the CMC. The longer the hydrophobic tail, the more hydrophobic the surfactant; and the lower the affinity with water. Thus, in aqueous medium, the CMC decreases as the number of carbon atoms in the hydrophobic tail increases.[1] The type of hydrophilic head-group will also have an effect on the CMC. Since an ionic head-group has stronger interactions with water than a nonionic head group, ionic surfactants are more hydrophilic than nonionic, giving, in aqueous medium, much higher CMCs for ionic surfactants than nonionic surfactants containing an equivalent amount of hydrophobic groups.[1]

Conductivity is a method used to determine the CMC of ionic surfactants. When the surfactant concentration increases, the amount of counterions also increases causing an approximately linear increase of the conductivity as a function of the surfactant concentration. When the CMC is reached, a break of the slope occurs due to the binding of some of the counterions of ionic surfactant to the micelle depending on the degree of ionisation of the micelle. The larger the hydrated radius of the counterion, the weaker the degree of binding; hence the CMC scales for counterions as: $NH_4^+ > K^+ > Na^+ > Li^+$ and $I^- > Br^- > Cl^-$.[1]

The micelle environment can influence the CMC and specifically electrolytes and additives like alcohol, which can interact with the surfactant.[6] By interacting with the hydrophilic head-group, electrolytes decrease its solvation and importantly, also decrease the electrostatic repulsion between head-groups. These effects favour micelle formation and thus decrease the CMC. Regarding alcohols, their presence also tends to decrease the CMC due to the formation of mixed surfactant-alcohol micelles (see below the discussion on solubilisation of alcohols), decreasing the aggregation number.

To finish, the temperature also influences the CMC. Usually, for nonionic surfactants, the CMC decreases with an increasing temperature.[6] This is due to the breaking of hydrogen bounding between water molecules and the polar head-group, which decreases its solvation (see below for the Cloud point). In contrast, ionic surfactants can only form micelles above a certain temperature, known as the Krafft point (see below).

3.2.3. Solubilisation by surfactant

Solubilisation occurs when a substance, whatever its state is (i.e. solid, liquid or gas), is spontaneously dissolved in a solvent. Solubilisation can involve reversible interaction with micelles while forming a thermodynamically stable isotropic solution, which has a lower thermodynamic activity than the non-dissolved substance.[7] J.L. Salager[6] distinguish four types of solubilisation according to the additive's nature (see Figure 3.6):

- When the additive is a non-polar compound, like oil, the solubilisation occurs at the interior of the micelle (Figure 3.6 a)). The micelle is thus swollen and forms a microemulsion with droplets of a few hundred angstroms solubilising a large amount of oil.
- When the additive is amphiphilic, like an alcohol, the solubilisation is called co-micellisation because the micelles contain both amphiphiles (surfactant and alcohol) (Figure 3.6 b)). In this case, the alcohol acts as a co-surfactant; however, it cannot form micelles without surfactants due to its shorter hydrophobic chain. In some cases, co-micellisation with other amphiphilic additives and especially surfactants gives micelles with a large solubilising power due to the synergistic effect between both.
- When the additive is neither soluble in water nor in the hydrophobic interior of the micelle, it may be adsorbed at the micelle surface (Figure 3.6 c)).
- The last type of solubilisation is characteristic of nonionic surfactant micelles where the organic additive is trapped by hydrophilic chains (Figure 3.6 d)).[8]

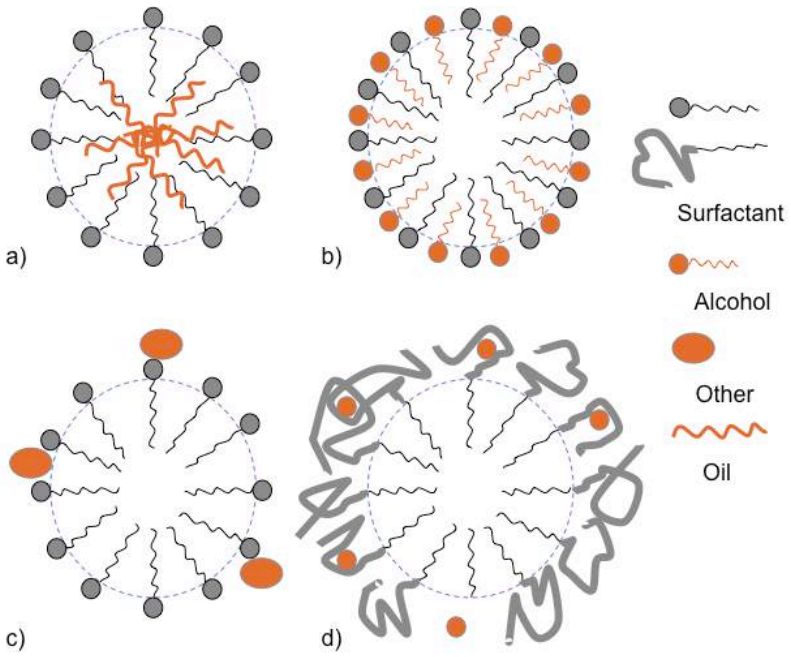

Figure 3.6: Different types of solubilisation by surfactant: a) oil solubilisation in the interior of micelle, b) co-solubilisation of alcohol or amphiphilic additives, c) solubilisation of insoluble additives at the micelle surface, and d) solubilisation by hydrophilic chain of non-ionic surfactants.

3.2.4. Krafft point

The Krafft temperature, or the Kraft point, is the temperature at which an ionic surfactant (typically) starts to experience enhanced solubilisation and can form micelles.[2] Below the Krafft point, the ionic surfactant molecules present in solution are non-associated and their solubility remains too low to reach the CMC.

The Krafft point depends critically on the head-group and counter-ion of the surfactant. The chain length of the hydrophobic tail and the presence of electrolytes also influence the Krafft point of ionic surfactants; for example, the addition of electrolytes increases the Krafft point, and a decrease in the Krafft point can be obtained with branched alkyl chains or bulkier hydrophobic groups (e.g. two alkyl chains).[7]

3.2.5. Cloud point

Conversely to the Krafft point, the cloud point is mainly for nonionic surfactants and represents the temperature at which the solution containing nonionic surfactants separates into two phases, one surfactant rich and the other surfactant poor, and thus becomes cloudy.

The cloud point of nonionic surfactants is due to the fact that their aqueous solubility depends on hydrogen bonding between water and their polyethylene oxide chain. Thus, as hydrogen bonding is not a strong interaction and its strength depends upon the linearity of the bond, an increase in temperature increases thermal motion and weakens this interaction, reducing the surfactant solubility.[7] The cloud point depends on the number of ethylene oxide (EO) groups; an increase in EO content will increase the cloud point.

3.2.6. HLB number

In order to characterise a surfactant, a general rule in emulsion technology is that water-soluble surfactants tend to give oil-in-water (o/w) emulsions and conversely, oil-soluble surfactants give water-in-oil (w/o) emulsions. This concept is known as Bancroft's rule.[9] Bancroft's rule is entirely qualitative. In order to give a relationship between the hydrophilic part and the hydrophobic part, Griffin[10,11] introduced the concept of the hydrophilic/lipophilic balance (HLB) of a surfactant.

The HLB numbers for nonionic surfactants were determined by simple calculations, as follows.

For alcohol ethoxylates and alkylphenol ethxylates:

$$HLB = \frac{wt\%\ ethylene\ oxide}{5} \qquad \text{Eq. 3.6}$$

The commonly used Griffin formula for nonionic surfactants is:

$$HLB = 20 \times \frac{M_H}{M_H + M_L} \qquad \text{Eq. 3.7}$$

where *wt%* is the weight percentage, M_H is the molecular weight of the hydrophilic part of the molecule and M_L is the molecular weight of the lipophilic (hydrophobic) part of the molecule. This formula gives a HLB value between 0 and 20 where 0 corresponds to a totally hydrophobic surfactant and 20 corresponds to a totally hydrophilic surfactant, which allows one to define the application of the surfactant and its dispersibility in water (see Table 3.1).

Table 3.1: Use of Griffin's HLB number concept. Reproduced by permission of Wiley-VCH.[3]

Application		Appearance of aqueous solution	
3 – 6	W/O Emulsifier	1 – 4	No dispersibility
7 – 9	Wetting agent	3 – 6	Poor dispersibility
8 – 14	O/W Emulsifier	6 – 8	Milky dispersion after agitation
9 – 13	Detergent	8 – 10	Stable milky dispersion
10 – 13	Solubilisers	10 – 13	From translucent to clear
12 – 17	Dispersant	13 – 20	Clear solution

However, the last formula does not take into account the polar group of ionic surfactants, thus Griffin's HLB number concept was extended by Davies,[12] who introduced a scheme to assign HLB group numbers to chemical groups which contain an ionic surfactant:

$$HLB = 7 + \Sigma(hydrophilic\ group\ numbers) + \Sigma(hydrophobic\ group\ numbers) \quad \textbf{Eq. 3.8}$$

Some typical group numbers are shown in Table 3.2.

Table 3.2: Determination of HLB numbers according to Davies. Reproduced by permission of Wiley-VCH. [3]

Group	HLB number	Group	HLB number
Hydrophilic		*Lipophilic*	
$-SO_4Na$	20.8	$-CF_3$	- 0.870
$-CO_2K$	21.1	$-CF_2-$	- 0.870
$-CO_2Na$	19.1	$-CH_3$	- 0.475
–N (tertiary amine)	9.4	$-CH_2-$	- 0.475
Ester (sorbitan ring)	6.3	–CH=	- 0.475
Ester (free)	2.4	–CH–	- 0.475
$-CO_2H$	2.1	|	
–OH (free)	1.9		
–O–	1.3		
–OH (sorbitan ring)	0.5		

3.3. Surfactants characterisation

This part characterises the surfactants used in this thesis and discuss the results.

3.3.1. Discussion

3.3.1.1. CMC and surface tension

It is important to know the surfactant CMC since it is at this concentration that many physicochemical properties change. This is the case for the surface tension, where at very low concentration the surface tension is close to the surface tension of water and then decreases when increasing surfactant concentration, to stabilise at an almost constant value after the CMC.

Thus the CMC of each surfactant was determined by tensiometry either at Durham University or at BIC in water at a concentration range comprising the expected CMC range. Note that only a few surfactants were characterised at Durham but the results were consistent with those obtained at P&G. Thus, as the temperature could be kept constant for all the tensiometry work at P&G, compared to Durham, and since all the surfactants were characterised, only surfactant's CMC from P&G are shown in the Figure 3.7 and are summarised in Table 3.3.

Table 3.3: Results of CMC and surface tension of surfactants.

Surfactant		CMC (mg L^{-1})	CMC (mol L^{-1})	Surface tension at the CMC (mN m^{-1})	HLB
Lutensol TO3	$C_{13}E_3$	71.28	2.14×10^{-4}	31.00	7.95
Lutensol TO5	$C_{13}E_5$	34.65	8.24×10^{-5}	30.95	10.47
Lutensol TO6	$C_{13}E_6$	43.69	9.40×10^{-5}	31.59	11.38
Lutensol TO7	$C_{13}E_7$	64.34	1.26×10^{-4}	30.52	12.12
Lutensol TO8	$C_{13}E_8$	94.34	1.71×10^{-4}	31.62	12.75
Lutensol TO109	$C_{13}E_{10}$	132.01	2.06×10^{-4}	32.30	13.75
Lutensol TO12	$C_{13}E_{12}$	169.85	2.33×10^{-4}	34.97	14.50
Lutensol TO15	$C_{13}E_{15}$	152.30	1.77×10^{-4}	36.30	15.35
Lutensol TO20	$C_{13}E_{20}$	231.00	2.14×10^{-4}	38.15	16.29

Surfactant		CMC (mg L^{-1})	CMC (mol L^{-1})	Surface tension at the CMC (mN m^{-1})	HLB
Lutensol XL70	$C_{10}E_7$	481.49	1.03×10^{-3}	29.82	13.22
Lutensol XL80	$C_{10}E_8$	659.64	1.29×10^{-3}	30.17	13.80
Lutensol XL90	$C_{10}E_9$	874.38	1.58×10^{-3}	30.89	14.29
Lutensol XL100	$C_{10}E_{10}$	986.42	1.65×10^{-3}	31.01	14.71
Lutensol XL140	$C_{10}E_{14}$	1418.53	1.83×10^{-3}	33.49	15.92
SDBS	C_{12}-C_6H_6-$SO_3^-Na^+$	38.52	1.11×10^{-4}	32.52	12.04
LAS	C_{13}-C_6H_6-$SO_3^-Na^+$	525.00	1.57×10^{-3}	37.50	12.52
SDS	C_{12}-$OSO_3^-Na^+$	1090.00	3.78×10^{-3}	34.40	22.10

It can be seen from these results and more specifically on Figure 3.7. 4) that an anionic surfactant has a CMC higher than a nonionic surfactant with the same hydrophobic part (e.g. by comparing $C_{13}E_{10}$ with LAS with C_{13} in this case). This means that more anionic surfactant molecules are needed before a micelle is formed compared to nonionic surfactant molecules, due to the electrostatic repulsion which occurs between ionic head groups in anionic surfactant molecules. Regarding the anionic surfactants, the LAS has 13 carbons while the SDBS has 12 carbons for the "same" structure; in this case, the LAS should have a lower CMC than the SDBS. However, the branching of the benzene sulfonate group within the alkyl chain increases the solubility[6] of the LAS and thus its CMC compared to the linear form (see Figure 2.3 in Chapter 2). Moreover, the benzene group gives more hydrophobicity to the SDBS and the sulfate group gives more hydrophilicity to the SDS compared to the sulfonate group of the SDBS; this explains the huge difference in the CMC between them. Figure 3.7. 1) and 2) show the influence of the number of EO units on the CMC while Figure 3.7. 3) shows the influence of the carbon chain length on the CMC. A surfactant which is more hydrophilic (either with more EO groups or with a shorter carbon chain length) will have more affinity with water molecules than a more hydrophobic surfactant. Thus, water molecules will be able to solvate more hydrophilic surfactant molecules before leading to a higher CMC.

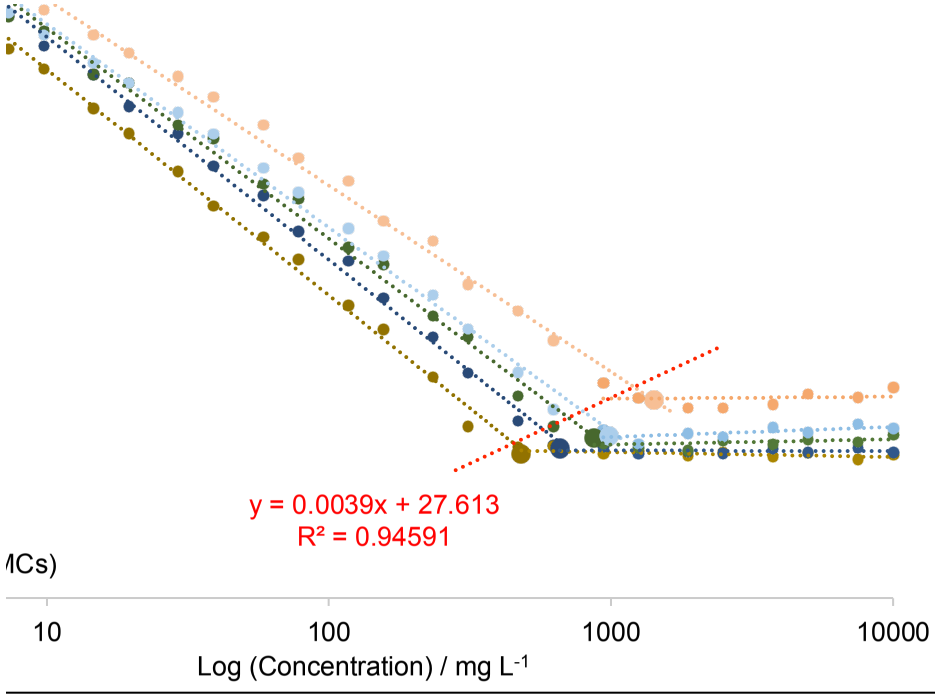
y = 0.0039x + 27.613
R² = 0.94591
ICs)
10
100
1000
10000
Log (Concentration) / mg L-1

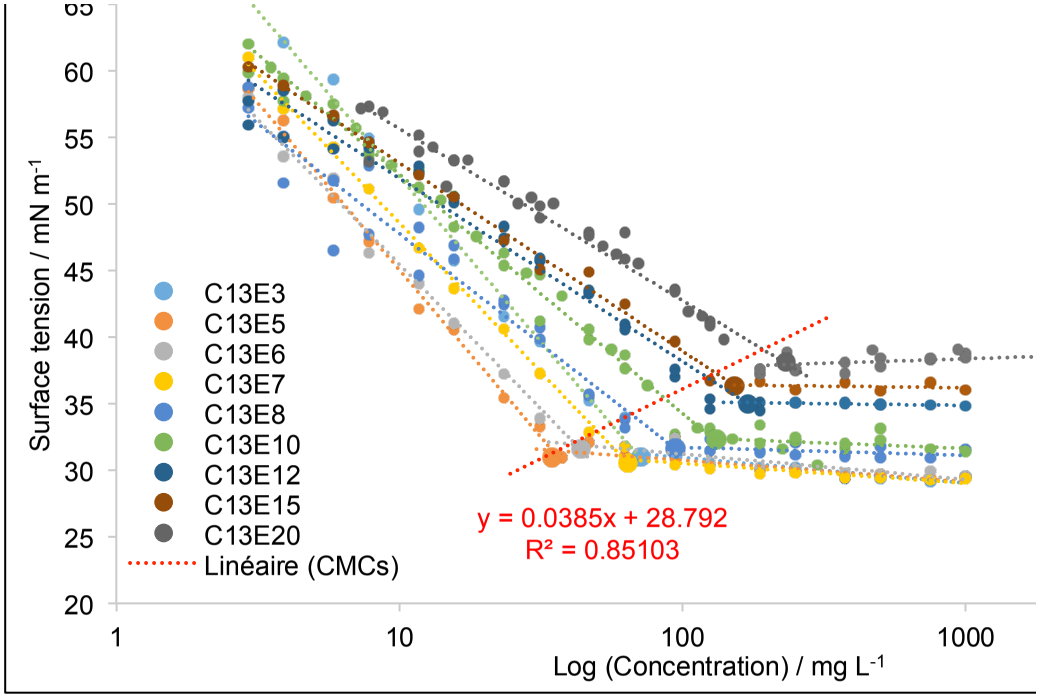
Surface tension / mN m-1
65
60
55
50
45
40
35
30
25
20
C13E3
C13E5
C13E6
C13E7
C13E8
C13E10
C13E12
C13E15
C13E20
Linéaire (CMCs)
y = 0.0385x + 28.792
R² = 0.85103
1
10
100
1000
Log (Concentration) / mg L-1

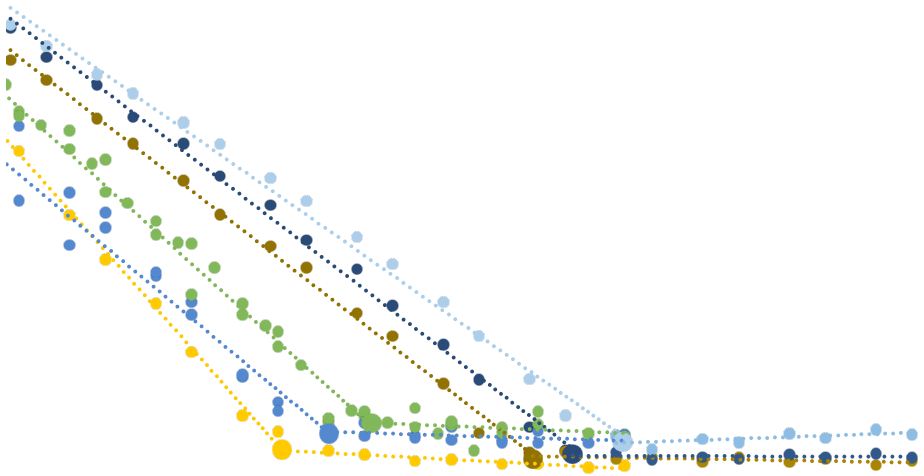
parison between series with the same number of EO

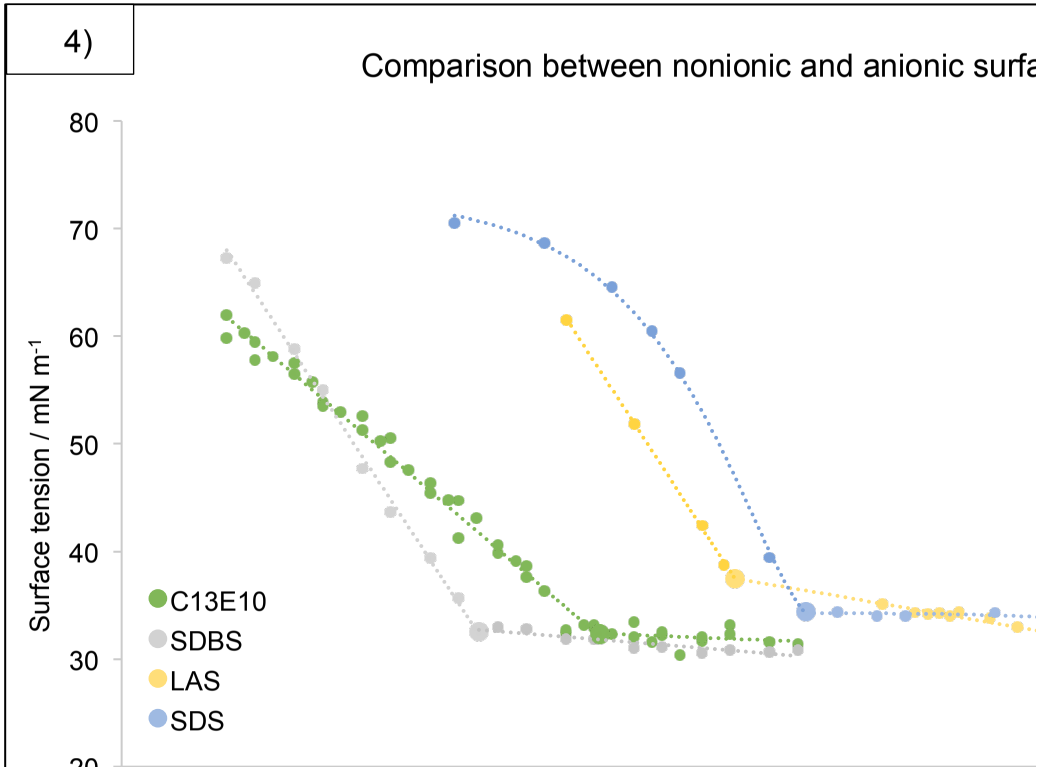
4)
Comparison between nonionic and anionic surfa
Surface tension / mN m-1
80
70
60
50
40
30
C13E10
SDBS
LAS
SDS

This is apparent from Figure 3.7. 1) and 2), where the CMC increases when the number of EO group and the HLB increase as follows: $CMC_{(C10E7)} < CMC_{(C10E8)} < CMC_{(C10E9)} < CMC_{(C10E10)} < CMC_{(C10E14)}$; and with Figure 3.7. 3), where the CMC increases when the carbon chain length decreases as follows: $CMC_{(C10E7)} > CMC_{(C13E7)}$; $CMC_{(C10E8)} > CMC_{(C13E8)}$ and $CMC_{(C10E10)} > CMC_{(C13E10)}$

3.3.1.2. Phase diagrams

Binary systems of surfactants in water were investigated to study their aggregation behaviour in water as a function of the surfactant concentration. Samples were prepared from a concentration range from 95/05 to 10/90 water/surfactant w/w % and kept at room temperature. For both the surfactants studied, namely LAS and Lordodac, 95/05 water/surfactant w/w % corresponds to a concentration above the CMC. However, for all the LAS samples, the effective concentration (45 w/w %) was not taken into account. This means that when a sample at 50/50 w/w % was prepared, there was 50 w/w % of water and 50 w/w % of LAS at 45 w/w % (see Figure 3.8 for the true surfactant concentrations). Moreover, from the LAS at 45 w/w %, one can observe a phase separation at room temperature into a water-rich phase and surfactant crystalline phase. Thus, a micellar system from 95/05 to 55/45 water/LAS w/w % was obtained but poor results above this concentration (i.e., gel plus undissolved surfactant) occur, which can be defined as the solubility limit of LAS (almost 370 g L^{-1} of LAS).

95/05 90/10 85/15 80/20 75/25 70/30 65/35 60/40 55/45 50/50 45/55 40/60 35/65 30/70 25/75 20/18 15/85 10/90

98/02 95/05 93/07 91/09 89/11 86/14 84/16 82/18 80/20 77/23 75/25 73/27 71/29 68/32 66/34 64/36 62/38 59/41

Figure 3.8: Water/Surfactant solution (in w/w %) used for binary systems. Surfactant: Lorodac on the top and LAS on the bottom.

Using an optical microscope equipped with a polarisation system (see Chapter 2), results shown in Figure 3.9 were obtained, which summarises binary systems at room temperature. The liquid crystalline phases can be differentiated by their birefringence since hexagonal and lamellar phases are birefringent; in addition, Maltese crosses are specific to lamellar phase (see Figure 3.10).

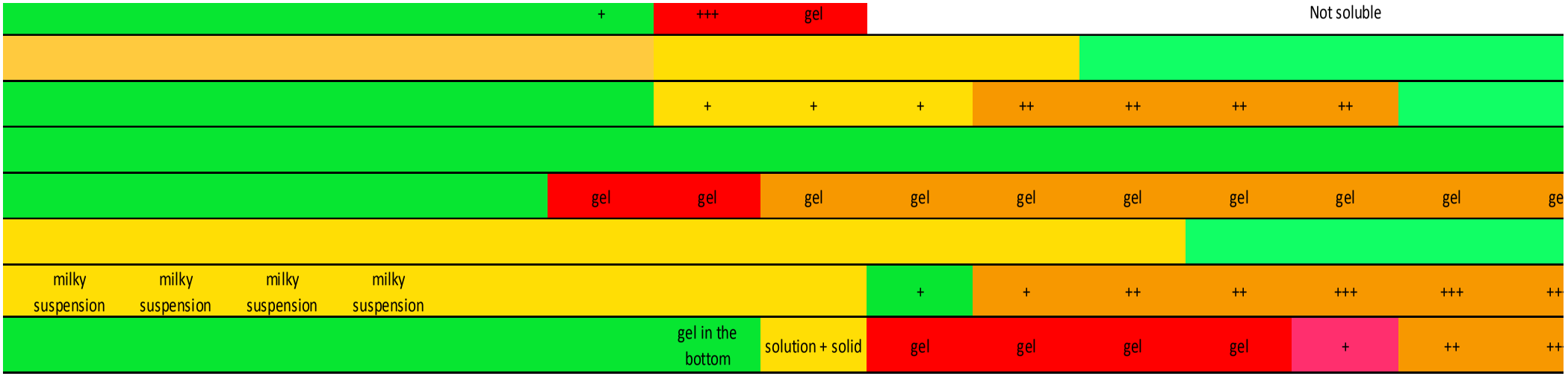

elles

rse Micelles

ses

ases

.

al

f viscosity

urfactant in water at room temperature.

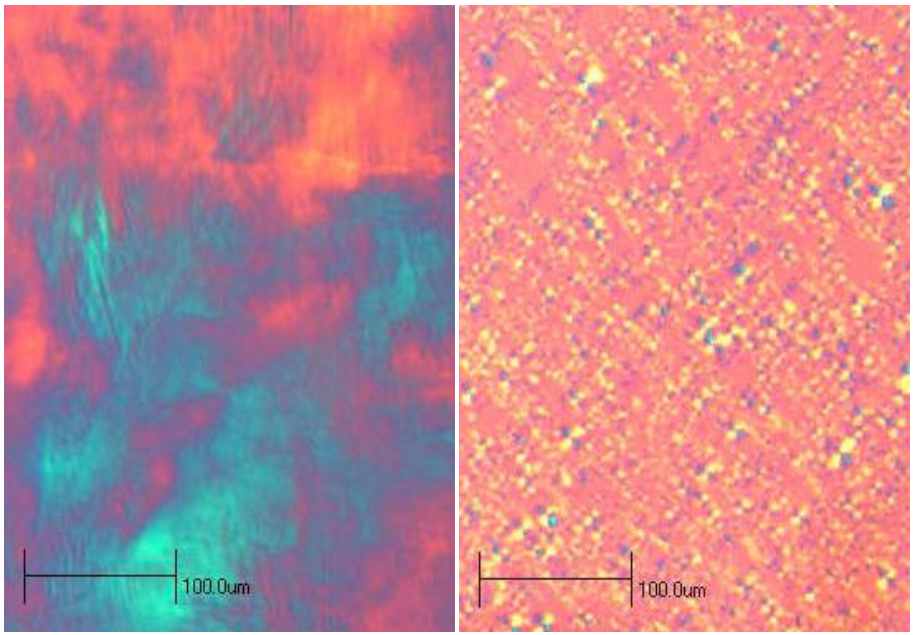

3.3.1.3. Cloud points

It has been shown that the cloud point can be used to evaluate the ability of surfactant to interact with dye, i.e. the higher the cloud point the more intense interaction.[13] Indeed, in the same way as electrolytes interact more or less with surfactant and influence the surfactant's cloud point, the same analogy can be done studying dyes. For this reason, the cloud point of the Lutensol TO and Lutensol XL series was determined experimentally in order to investigate the relationship between cloud point and binding constant. Several methods exist to determine the cloud point of a non-ionic surfactant, depending on its degree of ethoxylation and thus its hydrophilicity. The procedure does not change between each method, only the method of surfactant dissolution. For a surfactant with a low degree of ethoxylation (more hydrophobic), a diethylene glycol monobutyl ether solution in water (C = 250 g L^{-1}) is used for a better surfactant dissolution. For a medium surfactant giving a clear solution in water, 1 g of surfactant is usually diluted in 100 mL of water. However, for surfactant with a high degree of ethoxylation (more hydrophilic), a NaCl solution in water (C = 50 g L^{-1} or 100 g L^{-1}) is used in order to attain a temperature above 100 ºC, which is the normal boiling point of water.

In our case, as a range of ethoxylation from low to high occurs and because the cloud point of the most hydrophilic surfactant is lower than 100 °C, the following method to determine the cloud point for ease of comparison was used. 5 g of surfactant were mixed with 25 g of diethylene glycol monobutyl ether (solution at 250 g L^{-1} in water) to give a transparent solution at room temperature. The solution was heated until it became cloudy and then it was removed from the heating. Under agitation, the temperature was taken when the solution became transparent again, giving the cloud point. The experiment was repeated five times and the results are shown in Figure 3.11, in parallel with the HLB calculated from the Davies' equation.

There is no exact relation between the cloud point and HLB values but we can see that for both, the cloud point and the HLB variation have a similar shaped curve, increasing asymptotically with the degree of ethoxylation. At low degree of ethoxylation, adding one more ethoxylate group widely affects the cloud point and the HLB. But at a certain number of ethoxylate group – around 7 EO – the cloud point and the HLB, do not increase that much. This is explained by the fact that only

the few first EO are effective in the HLB by interacting with six water molecules on average. Then, the EO chain forms a zigzag and the maximum hydratation ability of each EO is decreased.[14]

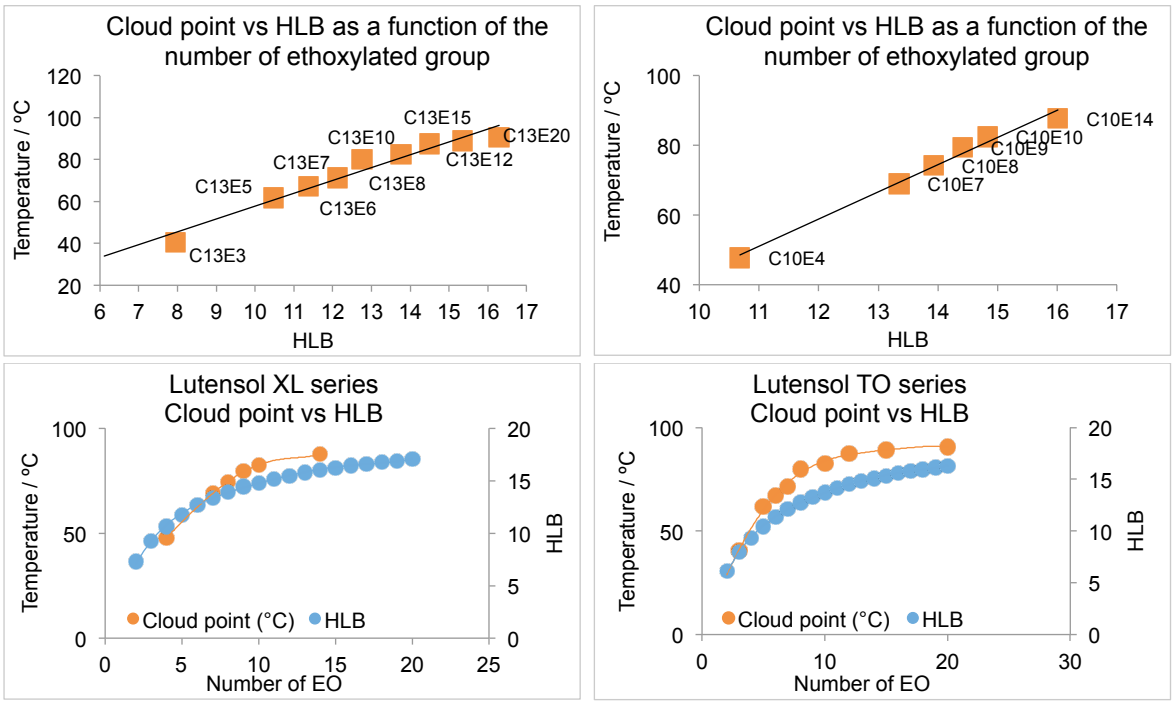

Figure 3.11: Graphs representing the Cloud Point and the HLB as a function of the degree of ethoxylation (number of EO) for the Lutensol XL series (C10) on the left and the Lutensol TO (C13) series on the right.

3.3.2. Conclusion

As shown from the results and the literature review, the structure of a surfactant plays a major role in its properties. Indeed, a surfactant which is highly hydrophilic will have a higher HLB and more interactions with water molecules, allowing better solubilisation and thus increased CMC and cloud point. Conversely, a surfactant that is rather hydrophobic will have a lower HLB and less interactions with water molecules and will have a tendency to aggregate at a lower concentration, thus decreasing its CMC and its cloud point.

There are several ways to affect the hydrophilicity/hydrophobicity of a surfactant. Regarding the hydrophobic part, which is usually an alkyl chain, the shorter the chain, and the more hydrophilic the surfactant. However, for the same number of carbon atoms, branching will bring less hydrophobicity than a linear chain. Regarding the hydrophilic part, for a nonionic surfactant, the longer the ethoxylated chain, the more hydrophilic the surfactant, whilst an anionic surfactant will be more hydrophilic than a nonionic surfactant provided it is above its Krafft temperature.

References

[1] M. J. Rosen, *Surfactants and Interfacial Phenomena*, 3rd ed (Wiley-Interscience, 2004).

[2] J. S. Duncan, Shaw, *Introduction to Colloid and Surface Chemistry*, 4th ed

[2] J. S. Duncan, Shaw, *Introduction to Colloid and Surface Chemistry*, 4th ed (Butterworth-Heinemann, 1992).

[3] Krister Holmberg, ed., *Surfactants and Polymers in Aqueous Solution*, 2nd ed (Wiley-Interscience, 2003).

[4] Noel T. Southall, Ken A. Dill, and A. D. J. Haymet, "A View of the Hydrophobic Effect," *The Journal of Physical Chemistry B* 106, no. 3 (2002): 521–33.

[5] Jacob N. Israelachvili, D. John Mitchell, and Barry W. Ninham, 'Theory of Self-Assembly of Hydrocarbon Amphiphiles into Micelles and Bilayers', *Journal of the Chemical Society, Faraday Transactions 2: Molecular and Chemical Physics* 72 (1976): 1525–1568.

[6] J.L. Salager, 'Surfactifs En Solution Aqueuse', Cahier FIRP F201A (1993).

[7] M. R. Porter, *Handbook of Surfactants* (Springer, 2013).

[8] Kazuhiko Kandori, Robert J McGreevy, and Robert S Schechter, 'Solubilization of Phenol in Polyethoxylated Nonionic Micelles', *Journal of Colloid and Interface Science* 132, no. 2 (1989): 395–402.

[9] Eli Ruckenstein, "Microemulsions, Macroemulsions, and the Bancroft Rule," *Langmuir* 12, no. 26 (1996): 6351–53.

[10] W. C. Griffin, 'Classification of Surface-Active Agents by HLB', *J. Soc. Cosmet. Chem.* 1 (1949): 311–26.

[11] W. C. Griffin, 'Calculation of HLB Values of Non-Ionic Surfactants', *J. Soc. Cosmet. Chem.* 5 (1954): 249–355.

[12] J. T. Davies, *Interfacial Phenomena* (Academic press, 2012).

[13] Nebojša Ristić, Miodrag Šmelcerović, and Ivanka Ristic, 'The Effect of Nonionic Surfactant Treatment on Dyeing of Cotton Fabrics', *Tekstil: Journal of Textile & Clothing Technology* 62 (2013).

[14] Xiaowen Guo, Zongming Rong, and Xugen Ying, 'Calculation of Hydrophile–lipophile Balance for Polyethoxylated Surfactants by Group Contribution Method', *Journal of Colloid and Interface Science* 298, no. 1 (2006): 441–50.

4. Dyes

4.1. Introduction

Colours are everywhere around us and play an important part in our everyday lives; they can induce mood changes and they can make us feel things differently.[1]

Today, there are all kinds of dyes, either natural or synthetic. One of the main fields of application of dyes is textile dyeing and this thesis will focus on this topic.

For instance, liquid detergents have inherent dyes in terms of textile dyeing; they are principally used to give a colour to the liquid detergent product to be more appealing. However, recently brighteners and hueing dyes have been developed in liquid detergent formulations to give a brightening effect to the product by interacting with textile fibres, particularly to white fabrics. This study will focus on those hueing dyes incorporated in liquid detergents and particularly, Chapter 5, on their interactions with surfactants, since these interactions can affect the dye deposition onto fabric.

4.1.1. Origin of colour and interaction with light

Colour is born from the interaction between a light source and an object which is perceived by the human eyes. Human eyes are sensitive to a certain region of the electromagnetic spectrum called the visible light region, corresponding to radiation within the very narrow wavelength range 360-780 nm.[2] Normal white light is composed of this entire wavelength range. An object can selectively absorb certain wavelengths of visible light and the remaining wavelengths of light (also called the complementary colour) are transmitted or reflected; these define the colour observed (see Figure 4.1). If the object absorbs all the wavelengths of light, it will appear black; and conversely, if all the wavelengths of light are reflected, the object will appear white. This explains why, when it is sunny, wearing black clothes makes you

warmer than white clothes. The black one will absorb the light with an energy converted into heat while the white one will reflect the light.

The absorption of visible light energy by a molecule leads to an electronic transition due to the excitation of an electron in the molecule from a low energy state, or ground state, to a higher energy state, or excited state. The difference of energy between these two states is given by Planck's equation:

$$\Delta E = hc/\lambda \qquad \text{Eq. 4.1}$$

where h is Planck's constant, c is the velocity of light and λ is the wavelength of light absorbed.

Table 4.1 shows the relationships between colours absorbed (wavelengths adsorbed) and the colours observed (wavelengths reflected). For example, a dye that absorbs the yellow colour (i.e. in the range 560-595 nm) will appear violet or blue. This is the mechanism used for hueing dyes that absorb the yellowish colour from white fabrics to give a bluish colour that makes it whiter. Another way to directly see the complementary colour is to use the colour wheel (see Figure 4.1).

Table 4.1: Colour absorbed versus colour observed (complementary colours). Reproduced by permission of Wiley-VCH).[3]

Wavelength absorbed (nm)	Colour absorbed	Colour observed
400 - 435	Violet	Greenish-yellow
435 - 480	Blue	Yellow
480 - 490	Greenish-blue	Orange
490 - 500	Bluish-green	Red
500 - 560	Green	Purple
560 - 580	Yellowish-green	Violet
580 - 595	Yellow	Blue
595 - 605	Orange	Greenish-blue
605 - 750	Red	Bluish-green

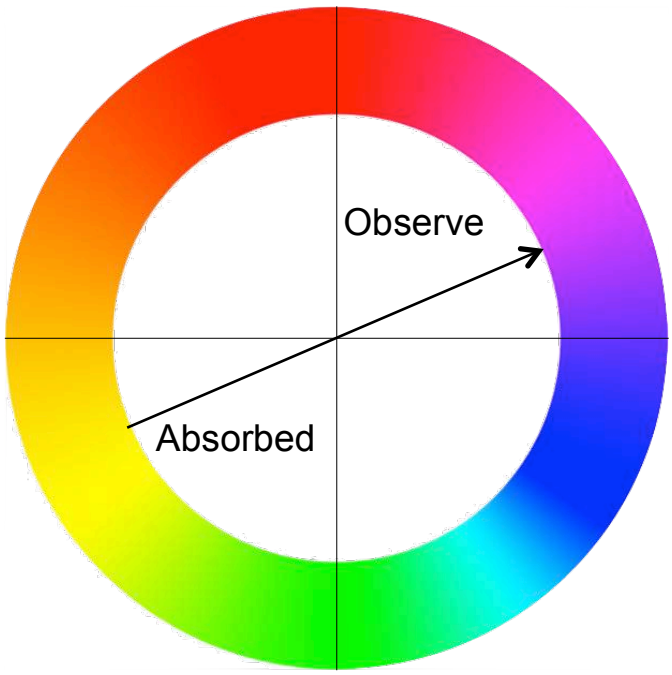

Figure 4.1: Colour wheel.

The most useful technique for characterising the colour of dyes is UV/visible spectroscopy, from which the colour can be defined in terms of three attributes: hue (or shape), strength (or intensity) and brightness. The hue of a dye is determined by the absorbed wavelengths of light, i.e. by the λ_{max} value obtained from the UV/visible spectrum if there is a single visible absorption band. An incident light, I_0, from a light source will pass through a sample and a transmitted light, I_t, will result as shown on Figure 4.2. The absorbance is thus defined as following:

$$A = -log\frac{I_0}{I_t} \qquad \text{Eq. 4.2}$$

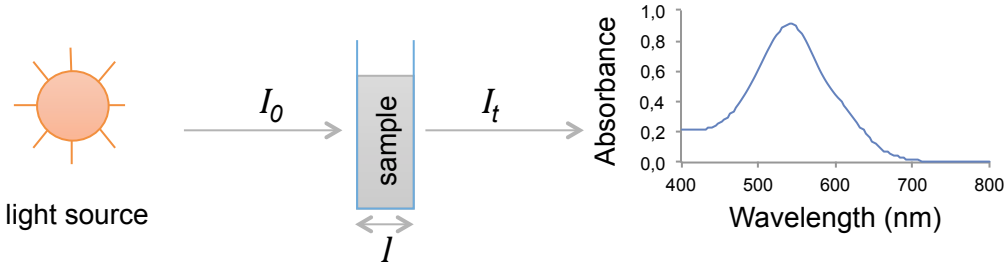

Figure 4.2: Absorbance

The strength or intensity of the colour of a dye is given by the molar extinction coefficient (ε) at its λ_{max} value, which can be determined by using the Beer-Lambert law from the UV/visible spectrum:

$$A = \varepsilon Cl \qquad \text{Eq. 4.3}$$

where A is the absorbance of the dye at a particular wavelength (typically at λ_{max}), ε is the molar extinction coefficient at this wavelength, C is the concentration of the dye and l is the path length of the cell (commonly 1 cm). In order to use the Beer-Lambert law, the absorbance against the dye concentration must be linear; usually at low dye concentration. Moreover, deviation from the law may occur when dyes show molecular aggregation in solution.

Brightness can be described by the shape of the absorption band. A narrow absorption band is characteristic of bright colours, while dull colours are characterised by a broad adsorption band.[2]

4.1.2. Colour and chemical functions

To have a colour, a dye has to absorb light in the visible spectrum (360–780 nm). To efficiently achieve this, the dye must have at least one chromophore (responsible for the colour). A chromophore is commonly an electron-withdrawing group composed of atoms having one or more double bonds which must be part of a conjugated system, i.e. a structure with alternating double and single bonds exhibiting resonance, which is a stabilising force in organic compounds.[2] When this conjugated system is sufficiently long, or associated with one or more auxochromes (see below), there is a creation of a delocalised electronic cloud that can resonate with the incident radiation and thus absorb it.

In 1876, Otto Witt[3] suggested a theory that defines chromophores as responsible for the colourful appearance of organic dyes, since they absorb certain wavelengths while others are reflected giving the colour to the dye. He also defines auxochromes as ‘‘salt-forming” colour helpers that increase the intensity of the colour. These auxochromes are electro-releasing groups which, by releasing an electron by ionisation, are capable of changing the frequency of absorption of a chromophore by increasing the electronic delocalisation and thereby changing the absorption energies. Due to this action, which is similar to extending the length of the conjugated system, they are responsible for the bathochromic (or red shift to longer wavelength) and hypochromic (or blue shift to shorter wavelength) effects (see Figure 4.3). They also have an influence on the dye solubility and on the bonding to the target.[2]

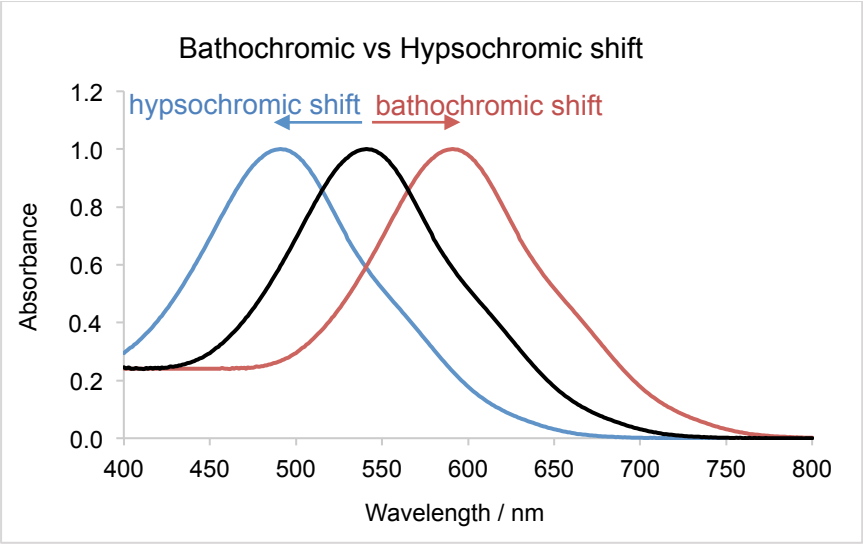

Figure 4.3: Bathochromic and hypsochromic shifts.

The most important chromophores are the azo (–N=N–), carbonyl (–C=O), methine (–CH=) e.g. in benzene, nitroso (–N=O) and nitro ($–NO_2$) groups. For auxochromes, we can encounter several types; the acidics: –OH, –COOH and $–SO_3H$; the basics: $–NH_2$, –NHR and $–NR_2$; and the halogens: –I, –Br and –Cl.

Another factor that can affect the colour of the dye is the pH. This phenomenon is called halochromism and can be used as a pH indicator. For example, this is the case for phenolphthalein, which is a pH indicator due to its structure that changes with pH as follows:

Acidic condition

pH: 0 - 8.2

Colourless

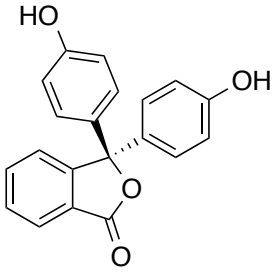

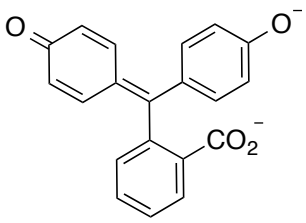

Basic condition

pH: 8.2 - 12

Pink to fuchsia

Figure 4.4: Dye used as pH indicator.

The chromophore, conjugated system and auxochrome form a complex also called the donor-acceptor chromogen. Modern theories of chemical bonding can explain the causes of colour in detail.

4.1.3. The cause of colour

The colour of an object or a molecule can be caused from a variety of physical and chemical mechanisms, as described by Nassau.[3] The molecular orbital approach will be discussed in this section. [2] Quantum theory describes electrons in matter as being contained in regions of high probability, called orbitals. Molecular orbitals (MO) are generated by overlap of atomic orbitals (AO) and have a characteristic shape, size and energy. Direct or 'end-on' overlap gives σ and σ* orbitals, corresponding to the lower energy bonding orbital occupied by two electrons and the higher energy anti-bonding orbital often remaining unoccupied, respectively. Indirect or 'sideways' overlap gives π and π* orbitals, corresponding to a singly occupied orbital and (often) unoccupied orbital respectively from a conjugated system. In addition, n-orbitals (non-bonding orbitals) correspond to an atomic orbital containing inner shell or 'lone-pair' electrons that are incapable of combination because they do not overlap in space and energy with other AO's (see Figure 4.5).

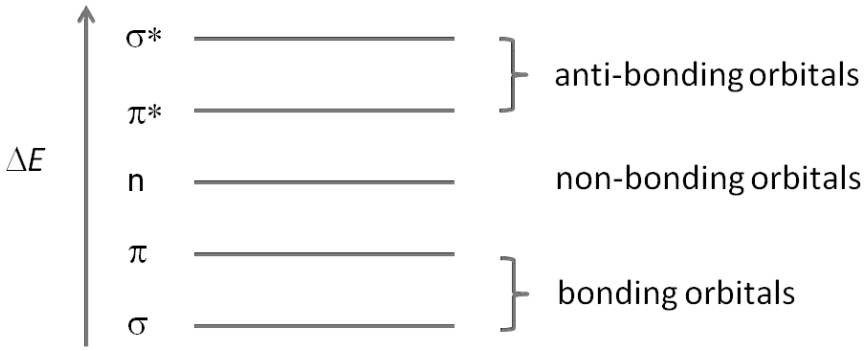

Figure 4.5: Electronic energy level of a simple molecule.

Thus, by absorbing light, an increase of electronic energy occurs promoting an electron from the ground state (lowest electronic state fully occupied – σ or π bonding electron associated with a covalent bond or a non-bonding n electron) to the excited state (higher empty electronic state – anti-bonding level). The difference of energy (ΔE) between the two states defines the wavelength of light absorbed and thus the colour observed (complementary colour) which is specific to each molecule. The absorption of light by organic dyes is due specifically to π-π* transitions rather than σ–σ* transitions, which are of much higher energy, usually in the far UV region.

4.1.4. Characterisation of colours

Similar to the use of the spectrophotometer to obtain the spectrum of a dye, the colorimeter is widely used to characterise and compare colour.[4] It expresses the colour in a colour system, called CIEL*a*b* for Commission internationale de l'éclairage (International commission of lighting in English), which characterises a colour by three parameters (see Figure 4.6). The L value corresponds to the lightness and is comprised of a number between 0 and 100 (black: L = 0; white L = 100); and the parameters a and b correspond to the red-green and the yellow-blue parameters respectively (a and b values comprised between -120 and 120). Usually, to compare our blue hueing dye, the b value is mainly used, as well as the ΔE which measures the overall colour difference between two samples from Eq. 4.4.

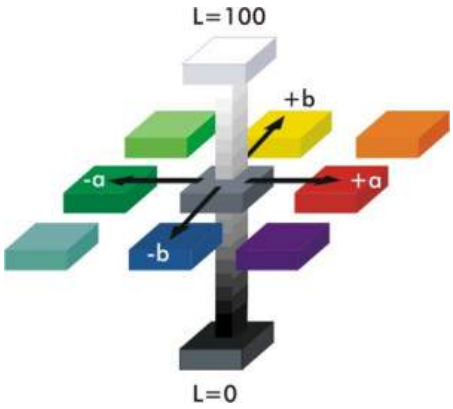

Figure 4.6: Colour system.

$$\Delta E = \sqrt{\Delta L^{*2} + \Delta a^{*2} + \Delta b^{*2}} \qquad \text{Eq. 4.4}$$

4.1.5. Classification

In terms of colorants, we can define two classes: dyes and pigments. In general, dyes have low to moderate molecular weights and good solubility, whereas pigments are bigger and difficult to disperse, and generally require the use of appropriate dispersing agents.[4]

As there are several kinds of fabrics, which differ in their chemical composition, there are several classes of dyes capable of interacting with specific fabrics. There are several ways to classify dyes, either according to their chemical structure or according to their use and method of application. The *Colour Index*[5] (CI), is the most important reference work for dyes and pigments used in the colouration of textiles. This divides dyes into groups based on the type of dying process used. This classification is shown in Table 4.2. Table 4.3 shows the classification in terms of chemical functionality and is particularly based on the chromogen structure.

Table 4.2: Usage classification of dyes. Reproduced by permission of Wiley-VCH.[6]

Class	Principal substrates	Method of application	Chemical types
Acid	nylon, wool, silk, paper, ink and leather	usually from neutral to acidic dyebaths	azo(including premetallized), anthraquinone, triphenylmethane, azine, xanthene, nitro and nitroso
Azoic components and compositions	cotton, rayon, cellulose acetate and polyester	fibre impregnated with coupling component and treated with a solution of stabilised diazonium salt	azo
Basic	paper, polyacrylonitrile, modified nylon, polyester and inks	applied from acidic dyebaths	cyanine, hemicyanine, diazahemicyanine, diphenylmethane, triarylmethane, azo, azine, xanthene, acridine, oxazine, and anthraquinone
Direct	cotton, rayon, paper, leather and nylon	applied from neutral or slightly alkaline baths containing additional electrolyte	azo, phthalocyanine, stilbene, and oxazine
Disperse	polyester, polyamide, acetate, acrylic and plastics	fine aqueous dispersion is often applied by high temperature/ pressure or lower temperature carrier methods; dye may be padded on cloth and baked on or thermofixed	azo, anthraquinone, styryl, nitro, and benzodifuranone
Fluorescent brighteners	soaps and detergents, all fibres, oils, paints and plastics	from solution, dispersion or suspension in a mass	stilbene, pyrazoles, coumarin, and naphthalim ides
Food, drug and cosmetic	foods, drugs and cosmetics		azo, anthraquinone, carotenoid and triarylmethane
Mordant	wool, leather and anodized aluminium	applied in conjunction with Cr salts	azo and anthraquinone
Oxidation bases	hair, fur and cotton	aromatic amines and phenols oxidised on the substrate	aniline black and indeterminate structures
Reactive	cotton, wool, silk and nylon	reactive site on dye reacts with functional group on fibre to bind dye covalently under influence of heat and pH (alkaline)	azo, anthraquinone, phthalocyanine, formazan, oxazine, and basic
Solvent	plastics, gasoline, varnishes, lacquers, stains, inks, fats, oils and waxes	dissolution in the substrate	azo, triphenylmethane, anthraquinone, and phthalocyanine
Sulfur	cotton and rayon	aromatic substrate vatted with sodium sulfide and reoxidised to insoluble sulfur-containing products on fibre	indeterminate structures

Class	Principal substrates	Method of application	Chemical types
Vat	cotton, rayon and wool	water-insoluble dyes solubilised by reducing with sodium hydrogensulfite, then exhausted on fibre and reoxidised	anthraquinone (including polycyclic quinones) and indigoids

Table 4.3: Chromogens structure classification.[4] Examples are shown below this table in Figure 4.7.

Class	Characteristic structure	Hues	Example
Azo dyes	Azo group (-N=N-). Linking two sp^2 hybridised carbon atoms, and most often joins two aromatic rings such as a benzene or naphthalene ring but also to a heterocyclic aromatic ring or to a group having an enolisable carbon.	A wide range of hues covering the entire visible spectrum. Moderate to high colour strength.	(1)
Anthraquinone dyes	carbonyl group (C=O) Anthraquinone structure consists of two benzene rings joined by two carbonyl groups at adjacent position of the ring.	A broad range of hues depending on the substitution. Do not have colour strength as high as azo but they are known for their lightfastness, particularly in the blue range.	(2)
Polymethine dyes	Diverse in structure. In general, electron-donating group and an electron-accepting group connected by a series of methines (=CH-).	Moderate to high tinctorial strength and varying degrees of lightfastness.	(3), (4)
Triphenylmethane dyes	Three aromatic rings attached to a central sp^2 carbon bearing a positive charge.	Some of the highest colour strength of any colorant known. Poor lightfastness and colour stability at hight pH. Colour range limits to the range of violet to green.	(5)
Heterocyclic analogs of triphenylmethane dyes	Two main subclasses: - a heteroatom bridge between two of the aromatic rings - a heteroatom replacing the sp^2 central carbon in addition to the bridge	High colour strength but fairly poor lightfastness.	(6)

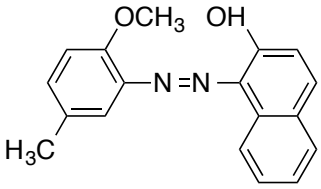

(1) Solvent Red 17

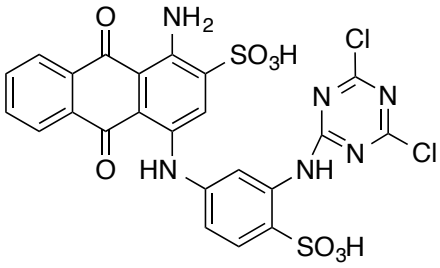

(2) Reactive Blue 4

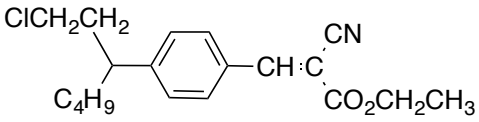

(3) Disperse Yellow 31

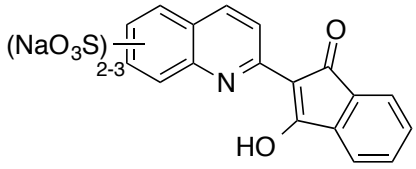

(4) CI Yellow 3

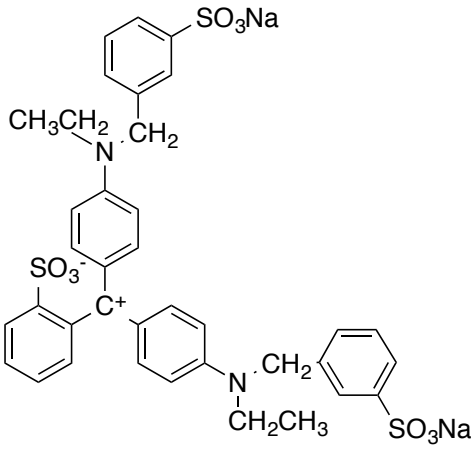

(5) CI Food Blue 2

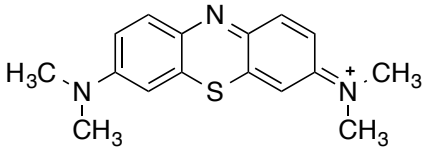

(6) Basic Blue 9

Figure 4.7: Example of dyes corresponding to the examples in the Table 4.3.

4.1.6. Dye aggregation

Due to the accumulated intermolecular van der Waals attractive forces between dye molecules, self-association can occur in solution when dyes are in large numbers. This dye aggregate, compared to the monomeric dye, presents distinct changes in the absorption band and can be seen by UV-Vis spectrophotometry by a spectral shift. Aggregation exists in two self-associations: J-aggregates and H-aggregates.

J-aggregate (J for Jelly who discovered them[7,8]) presents a typical bathochromic shift, i.e., shifts to a longer wavelength (red range), whereas an H-aggregate presents a hypsochromic shift, i.e., shifts to a shorter wavelength (blue range) – described in Figure 4.3. The differences between both have been explained in terms of molecular exciton coupling theory, i.e., coupling of transition moments of the constituent dye molecules due to their stacking to form dye crystals: plane-to-plane and end-to-end for H- and J-aggregates, respectively. By considering the dye molecules as dipoles, it can be seen that the excited state of the dye aggregate splits into two levels through the interaction of transition dipoles.[9] Thus, the transition to the upper state differs by the angle α, called the angle of slippage, between the line of centres of a column of dye molecules, which is specific for each aggregate and leads to a red shift if $\alpha < 32\,^{\circ}$ and to a blue shift if $\alpha > 32\,^{\circ}$ (see Figure 4.8).[10]

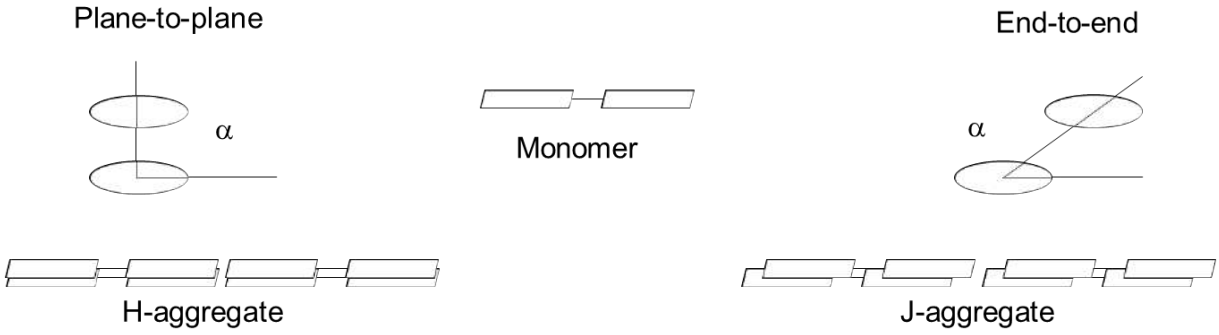

Figure 4.8: Schematic representation of the H- and J-aggregates regarding the angle of slippage α.

Dye aggregation is favoured when a strong dispersion force is associated with the high polarisability of the chromophoric chain of the dyes in aqueous solution. The high dielectric constant of water facilitates the aggregation process by reducing the electrostatic repulsion between similarly charged dye molecules. However, dye aggregation occurs also in mixed solvents and in heterogeneous media, e.g. micelles.

4.1.7. Interactions with solvents

It is well known that solvents have an influence on the rates and equilibrium positions of chemical reactions, as well as the position and intensity of absorption bands in UV(Ultra-Violet)/vis/near-IR, IR (Infra-Red), NMR (Nuclear Magnetic Resonance) and ESR (Electron Spin Resonance) spectroscopy.[11] Solvents are classified in two groups according to their ability to form hydrogen-bonds (protic solvents) or not (aprotic solvent). Solutes (i.e. chromophores for dyes) or solvents can possess active sites for hydrogen bonding or have the ability to form charge transfer (CT) type complexes. These molecular interactions occur in a short-range and are mainly governed by mass-action-law. The charge transfer complex formation will change the electronic state of the molecule, and thus its absorption spectra, compared to the free molecule in the gas phase.[12] This phenomenon is called solvatochromism. Other molecular interactions between solutes and solvents take place like the dispersion force (electrostatic in nature), dipole-dipole interaction, etc.

In order to characterise a solvent, the solvent polarity is used, which takes into consideration physical constants such as the static dielectric constant (ε_r), the permanent dipole moment ($\vec{\mu}$) and the refractive index (n_i). There are two kinds of solvatochromism. The first one is the “negative solvatochromism” which is defined by a hypsochromic shift of the UV/vis/near-IR absorption band, with increasing solvent polarity. And the “positive solvatochromism” which is defined by a hypsochromic shift, increasing with solvent polarity.[10] As explained in 4.1.3. The cause of colour, the electronic spectra comes from the electron transition between two electronic states. These two electronic states are defined as the ground-state and the excited state, which differ from each other in electron distribution, dipole moment and special molecular configuration. The spectral shift is caused by the differential solvation of the ground and first excited state of the chromophore. Thus, a negative solvatochromism is the result of a better stabilisation of the ground-state molecule by solvation rather than the molecule in the excited state by increasing the solvent polarity (i.e. the ground state is more polar than the excited state). Conversely, a better stabilisation of the molecule in the first excited state by increasing the solvent polarity (i.e. a more polar excited state), will lead to a positive solvatochromism.

In general, a strong solvatochromism occurs when dye molecules exhibit a large change in their permanent dipole moment upon excitation. When the dipole moment

increases during the electronic transition ($\vec{\mu}_{ground\ state} < \vec{\mu}_{exited\ \ state}$), a positive solvatochromism normally results. Conversely, a decrease of the solute dipole moment upon excitation ($\vec{\mu}_{ground\ state} > \vec{\mu}_{exited\ state}$) leads to a negative solvatochromism. In 1878, Kundt[13] proposed a rule where it is stated that the maximum of absorption of a solute shifts to a longer wavelength with increasing solvent dispersion forces. Note that Kundt's rule is often applied with the refractive index replacing the dispersion force.[14] The connection between an increased refractive index and increased polarity arises because the refractive index, n_i, is given by: $n_i = \sqrt{\varepsilon_r \mu_r}$, where ε_r is the relative permittivity (also known as the dielectric constant) and μ_r is the relative permeability, with non-magnetic materials having $\mu_r \approx 1$ at optical frequencies so that $n_i \approx \sqrt{\varepsilon_r}$. The relative permittivity of a material measures the decrease in Coulombic force between charges when immersed in the material and so tends to be greater for polar materials than non-polar ones, thereby explaining the connection between increased refractive index and polarity. However, relative permittivity is also high for atoms that are easily polarisable, such as iodine, so the connection should be used with care.

Comparable to the solvent effect on the electronic adsorption spectra of dye solution, surfactants can exhibit a similar effect at low concentration but also above the CMC if the dye fully bonds to the micelle, thus changing the local environment surrounding the dye.

4.2. Dye characterisation

In this part, the two dyes, E4210 and V200, used in this thesis will be characterised and the results will be discussed.

4.2.1. Discussion

4.2.1.1. Dye purification

As E4210 was a non-pure commercial product in a solvent (Polyethylene glycol) and impurities were present (8 % purity, as quoted by the supplier), purification was needed in order to study only the dye-surfactant interactions and minimise other compounds present in the commercial dye, which could affect the dye-surfactant interactions or the dye deposition onto fabrics. Impurities could be, for example, the presence of E4210 without its ethoxylated chain. For this, a solvent extraction using 10 mL of chloroform per gram of dye and 13 mL of decane per gram of dye was performed twice by dissolving the dye in chloroform and then adding decane. The solution was then removed to leave only the dye on the funnels walls. E4210 is soluble in chloroform but not soluble in decane, whereas decane and chloroform are miscible and colourless. During the solvent extraction, it was observed that the solvent mixture took a red colour whereas the separating funnel walls were purple, being completely covered by the dye. After removing the solvent mixture, the dye present on the separating funnel walls was diluted in water and collected. After analysis of the solvent mixture and the dye present on the separating funnel walls by LC-MS, it could be shown that the solvent mixture contained all the solvent and impurities from the commercial dye (plus a little amount of dye) whilst the dye present on the separating funnel walls was almost pure. To complete the dye purification process, residual organic solvent and the water were removed using a rotary evaporator to obtain the purified E4210. However, as no standard for E4201 was available, the purity could not be accessible by LC-MS. The dye identification was done using mass spectrometry, revealing peaks due to the dye hydrophilic and hydrophobic components (see Figure 4.9 - Figure 4.12). Note that only E4210 have been purified. Indeed, due to the aggregation of V200 molecules in water (described later on), the latter was not used for the determination of the dye-surfactant complex binding constant (this will be discussed later in this chapter and in chapter 5).

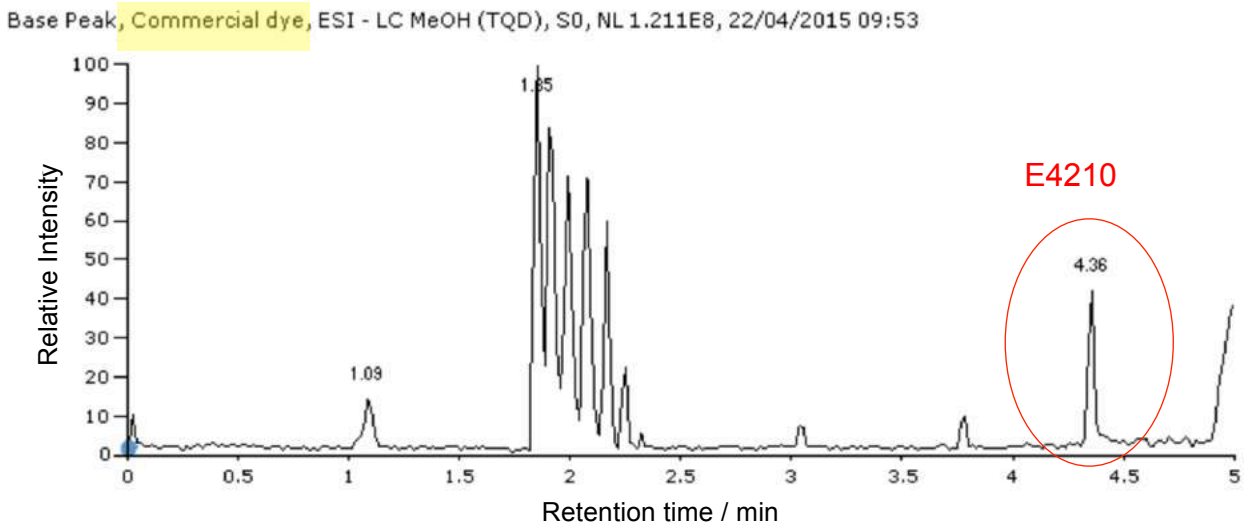

Figure 4.9: LC spectrum of commercial E4210.

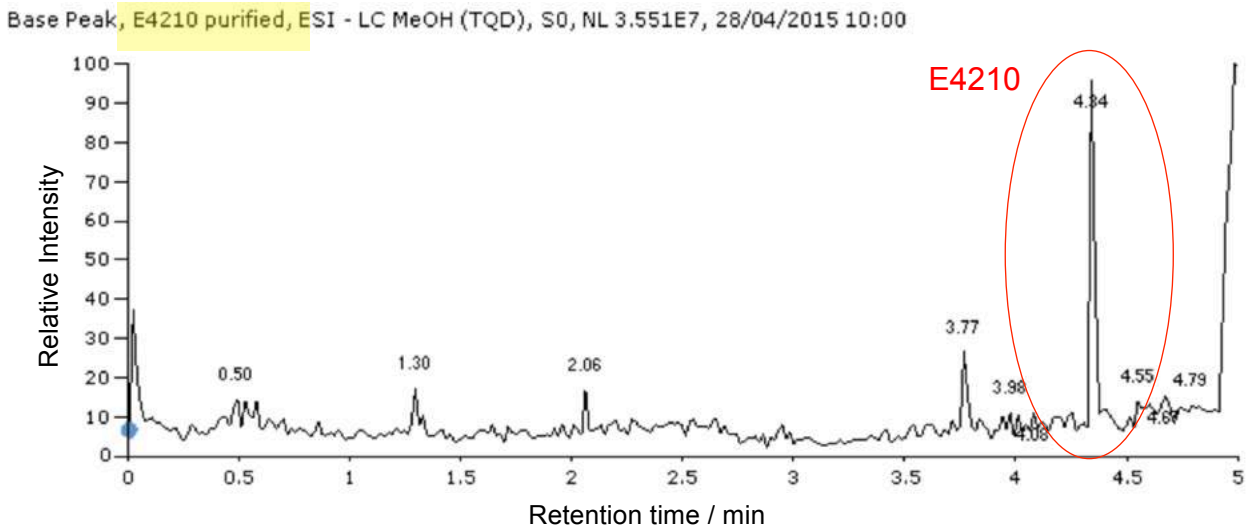

Figure 4.10: LC spectrum of purified E4210 present on the separating funnel walls.

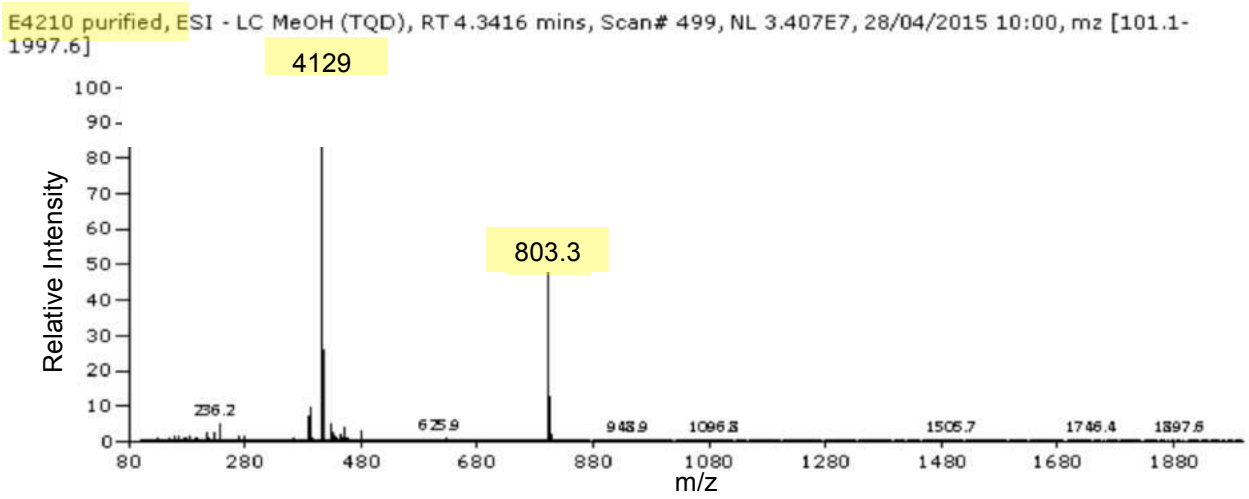

Figure 4.11: Mass spectrum of E4210 (peak at RT = 4.3416 mins).

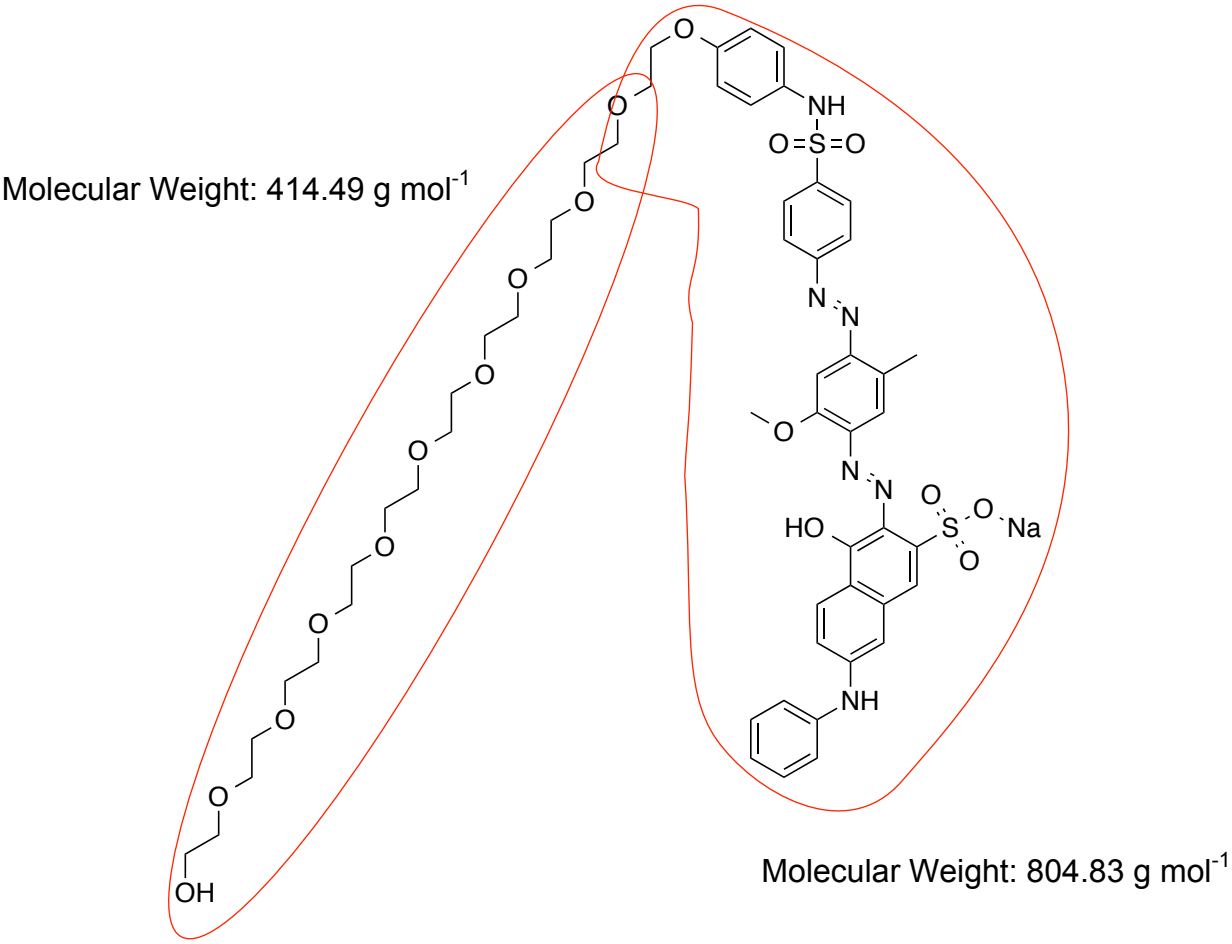

Figure 4.12: Structure of E4210 with molecular weight corresponding to the mass spectrum.

4.2.1.2. UV-Vis spectra

UV-Vis spectra were obtained in order to find the wavelength at the maximum absorption and to calculate the molar extinction coefficient of each dye, which was required to determine the binding constant of the dye-surfactant complex later. Moreover, it was suitable for the determination of the dye concentration to be used for the other experiments (e.g. the dye sorption onto fabrics), since it was required to have a dye concentration to be not too high but sufficient so that it would still present an absorbance that allowed visualisation of the dye after sorption onto fabrics. When the noise was too significant, the Savitzky-Golay method[15] was used to get smooth curves. Note that λ_{max} were determined manually for all the spectra.

All UV-Vis measurements were performed on dye samples in water at room temperature for a concentration range of 1.27×10^{-5} to 1.27×10^{-4} mol L^{-1} for commercial V200; 4.42×10^{-6} to 1.51×10^{-4} mol L^{-1} for commercial E4210 and 8.52×10^{-7} to 1.70×10^{-4} mol L^{-1} for purified E4210 (respectively Figure 4.13, Figure 4.14 and Figure 4.15).

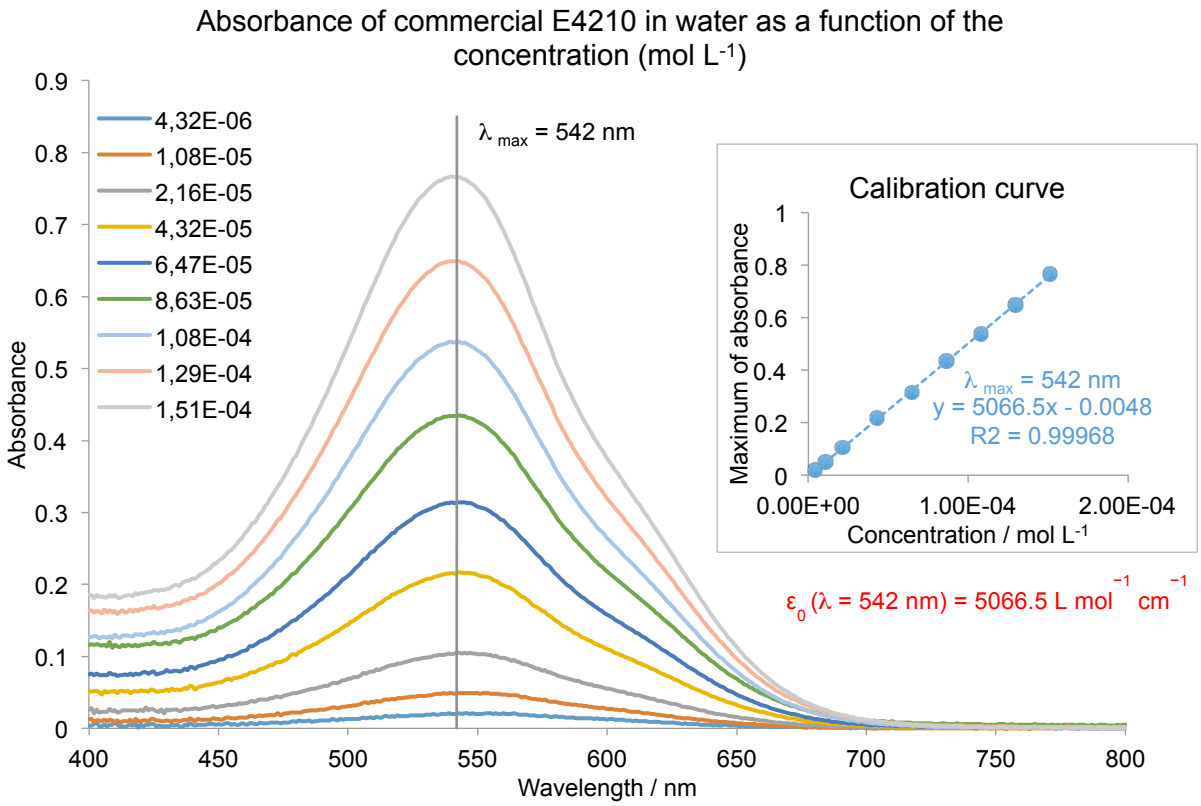

Figure 4.13: Absorbance of commercial E4210 in water as a function of the concentration.

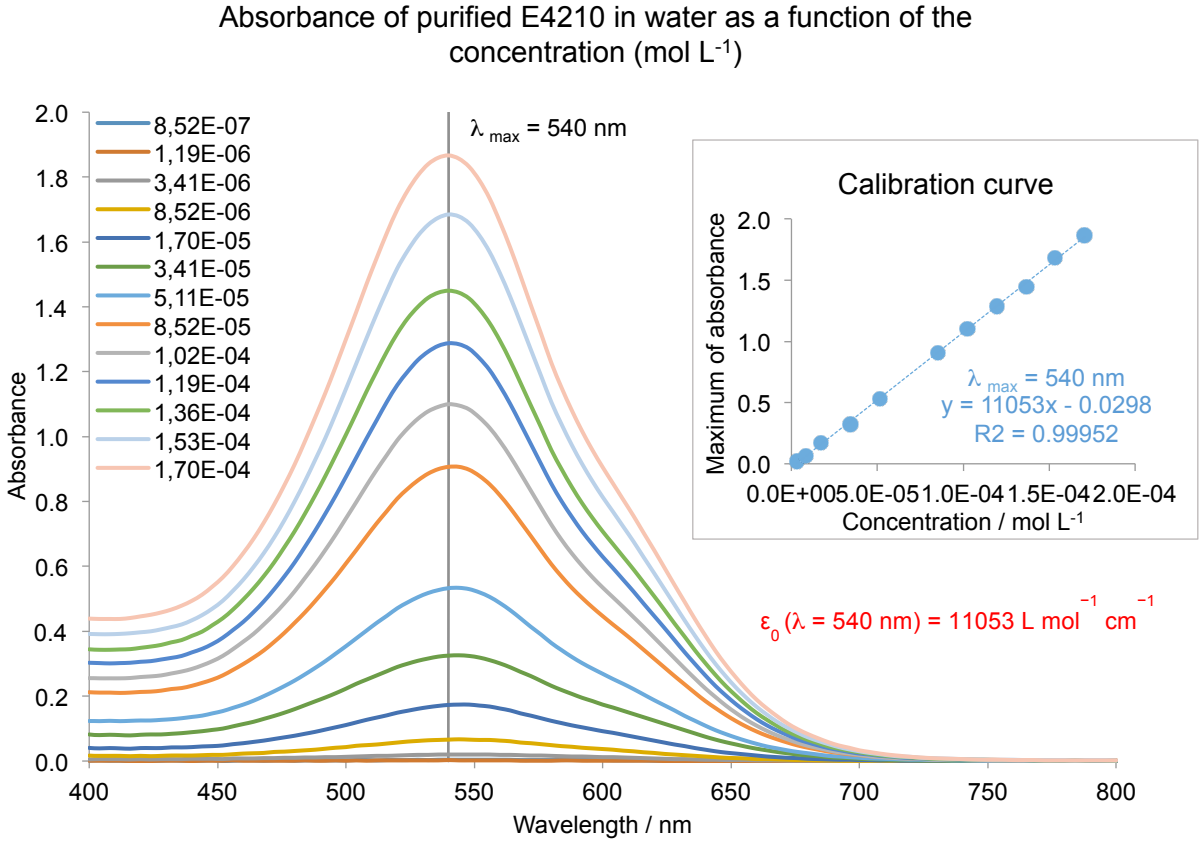

Figure 4.14: Absorbance of purified E4210 in water as a function of the concentration.

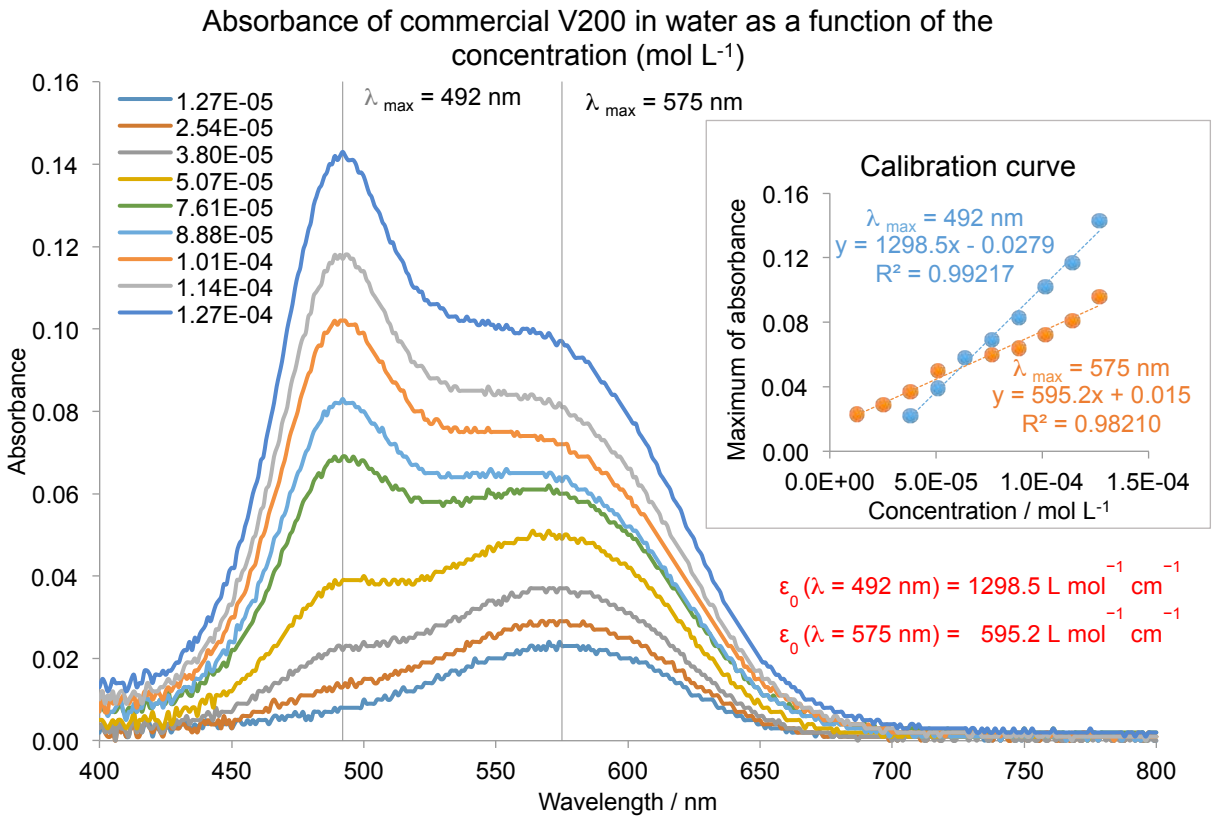

Figure 4.15: Absorbance of commercial V200 in water as a function of the concentration.

The linear relation between absorbance and dye concentration (R^2 values are listed in Table 4.4) indicates the validity of the Beer-Lambert Law at these concentration ranges. Thus, the molar extinction coefficient of each dye was determined using the Beer-Lambert Law. All the results are shown in Table 4.4.

Table 4.4: Results for dye UV-Vis spectrophotometry in water.

	Commercial V200		Commercial E4210	Purified E4210
Concentration range (mol L^{-1})	1.27×10^{-5} to 1.27×10^{-4}		4.42×10^{-6} to 1.51×10^{-4}	8.52×10^{-7} to 1.70×10^{-4}
λ_{max} (nm)	492	575	542	540
A_{max} for $C = 10^{-4}$ mol L^{-1} from the calibration curve	0.1020	0.0445	0.5019	1.0755
ε at λ_{max} (L mol^{-1} cm^{-1})	1298.5	595.24	5066.5	11053
R^2 from the calibration curve	0.99217	0.98210	0.99968	0.99952

In Figure 4.15, for commercial V200 at low concentration, the band absorption at 575 nm predominates, whereas in more concentred solutions, the peak at 492 nm dominates, showing a hypsochromic shift, i.e. a shift to a shorter wavelength. As described in the literature part (see 4.1.6 Dye aggregation), this shift shows a dye aggregation suggestive of an H-aggregate with a plane-to-plane stacking. At low concentrations, V200 is primarily in the form of monomers due to a good solvation of each monomer, while when the dye concentration increases (above 2 x 10^{-5} mol L^{-1}), the solvent cannot solvate each monomer dye and dye aggregates are formed. Thus, the first adsorption maxima at 492 nm can be assigned to the dye aggregate and the second adsorption maxima at 575 nm to the dye monomer. Also, as shown in Figure 4.16 and Figure 4.17, the difference of the absorption maxima can be clearly observed, as well as the difference in the colour of the solution and sedimented aggregate when appreciable aggregation has occurred after a long time.

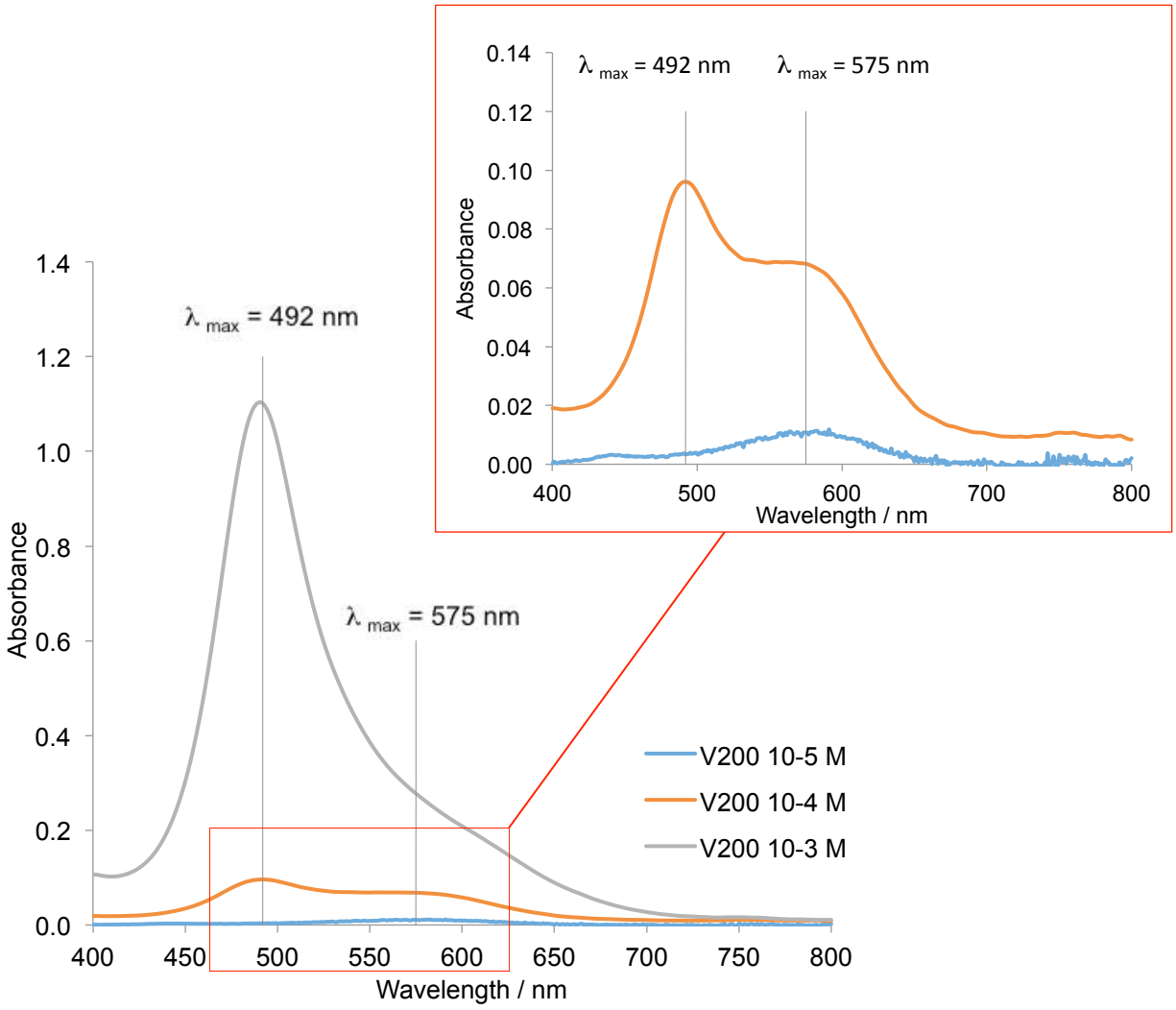

Figure 4.16: Adsorption maxima of the V200 monomer and aggregate.

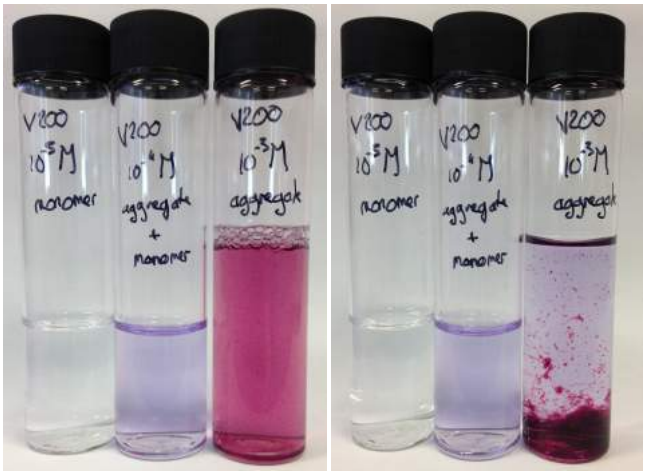

Figure 4.17: Influence of V200 concentration: 10^{-5}, 10^{-4} and 10^{-3} mol L^{-1} respectively from the left to the right (after some time for the picture on the right).

Regarding E4210, neither a new absorption band nor a considerable shift of absorption maximum was observed with increasing concentration for both commercial E4210 and its purified form (Figure 4.13 and Figure 4.14, respectively). Moreover it can be observed that there are no significant changes in the absorption maximum (+/- 2 nm) between the commercial and purified samples, which can lead to say that compounds added to the dye in the commercial form have no direct interaction with the dye absorbance mechanism. Note that the molar extinction coefficient for the commercial form is only approximatively half that of the purified form, whereas its concentration is 1/12 that of the purified form approximately. This is likely because of the impurities absorbing at this wavelength. For example, the presence of E4210 without its ethoxylated chain in the commercial form could be an impurity. In this way, it would adsorb at the same wavelength as E4210 but without its ethoxylate chain it is not dissolved in chloroform and thus flushed away.

It can also be observed that for the same dye concentration of 10^{-4} mol L^{-1}, the maximum of absorbance is lower for V200 than for E4210. This might also be due to the difference in chemical structure and the quantity of dye in the commercial form (effective concentration of 8.00 % for E4210 and 5.9 % for V200).

E4210 does not present aggregation at high concentration probably due to its long ethoxylated chain which can cause its good solvation by polar solvents and avoid its aggregation. Moreover, E4210 is a more efficient technology than V200 in terms of deposition onto several kinds of fabrics (due to its long ethoxylated chain – in the same way, it will increase interactions with polar functions encountered in fabrics like

cotton); however, the improved performance comes with a higher risk of staining, which has to be solved in order to avoid this. For all the next experiments using E4210 and V200, a concentration of 10^{-4} mol L^{-1} of the commercial form (i.e. at an effective dye concentration of 10^{-4} mol L^{-1} x 8.00 % and 10^{-4} mol L^{-1} x 5.9 % respectively) was used since this concentration was suitable to visualise the dye loss due to the dye sorption onto fabrics for both dyes. Moreover, because E4210 is a more efficient technology than V200, all the experiments were done using E4210 while V200 was used mainly in the dye deposition onto fabrics' chapters.

4.2.1.3. CMC and surface tension

As E4210 has a long ethoxylated chain, we can suggest that it may possess a surfactant-like behaviour, i.e., potentially a micellar aggregation at higher concentrations in an aqueous system. Thus the possible CMC of E4210 was investigated by tensiometry (see chapter 2 on Experimental methods) at room temperature in water at a concentration range of 192 mg L^{-1} to 12000 mg L^{-1} (see Figure 4.18). In order to be sure that the surface tension measured is ascribed to the dye and not impurities, the purified form of E4210 were used.

It can be observed that at a certain concentration: 337 mg L^{-1}, the surface tension decreases more slowly after this concentration than before. This is typical of surfactant behaviour and the micellisation phenomenon; it can thus be suggested that the ethoxylated chain corresponds to the hydrophilic part and the rest to the "hydrophobic" part. However the surface tension of 59.3 mN m^{-1} at the CMC (270 mg L^{-1}) is not really far from the water surface tension (72.8 mN m^{-1}) due to the polar function within the "hydrophobic" part.

Thus E4210 can be seen as a dye possessing a surfactant-like behaviour, but being more polar than a surfactant. Nevertheless, even if more points could be taken at higher and lower concentrations closer to the potential dye CMC to better show the influence of the concentration of E4210 on the surface tension, it is ascertain that E4210 does not form micelles on its own in laundry applications. Indeed, E4210 is used at very low concentration in laundry formulation, which is significantly under its potential CMC. However, it may co-micellise with detergent surfactants. Note that as the surfactant's CMC in presence of dye was not measured, it was not possible to

compare it with the surfactant's CMC itself and put in evidence any synergy between dye and surfactant on the surface tension reduction.

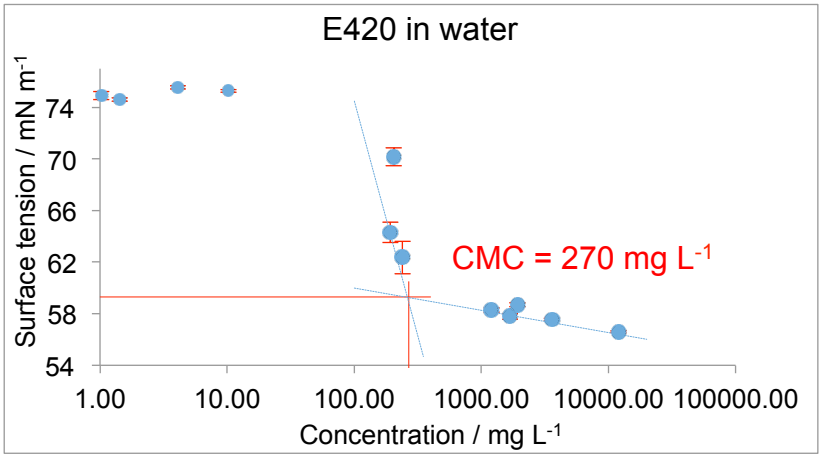

Figure 4.18: Surface tension of E4210 in water as a function of the concentration.

4.2.1.4. Dye-Solvent interactions

In order to study the influence of different solvents whilst keeping the dye concentration constant, a stock solution of E4210 and V200 was prepared in water at 10^{-3} mol L^{-1} and then mixed 1 mL of the stock solution with 9 mL of solvent in order to get a dye concentration of 10^{-4} mol L^{-1}. All the samples (see Figure 4.19) were then analysed by spectrophotometry in triplicate and the results are presented below. Also, to better compare the influence of the solvent, each curve have been normalised using the following equation (also used for all future normalisations):

$$x_n = \frac{(x - the\ last\ data\ of\ the\ serie)}{the\ maximum\ value\ in\ the\ serie} \qquad \text{Eq. 4.5}$$

where x and x_n represent the original value and the normalised value respectively.

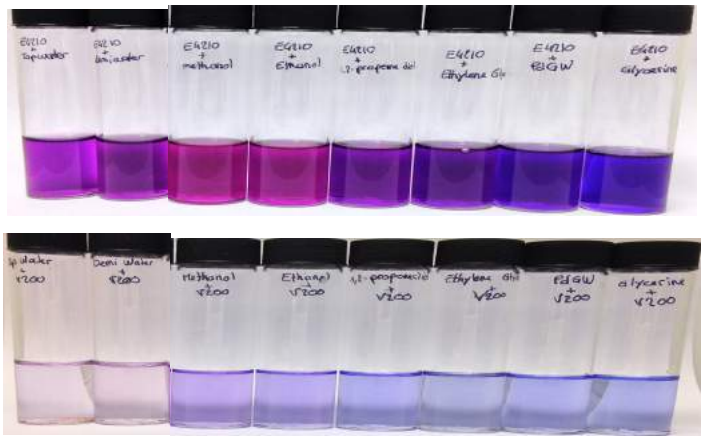

Figure 4.19: Influence of the solvent on E4210 (on the top) and on V200 (on the bottom). Solvent used from left to right: Tap-water, Demi-water, Methanol, Ethanol, 1,2-propane diol (Pdiol), Ethylene Glycol, PdGW (58 % Pdiol, 17 % Glycerine, 25 % Water) and Glycerine.

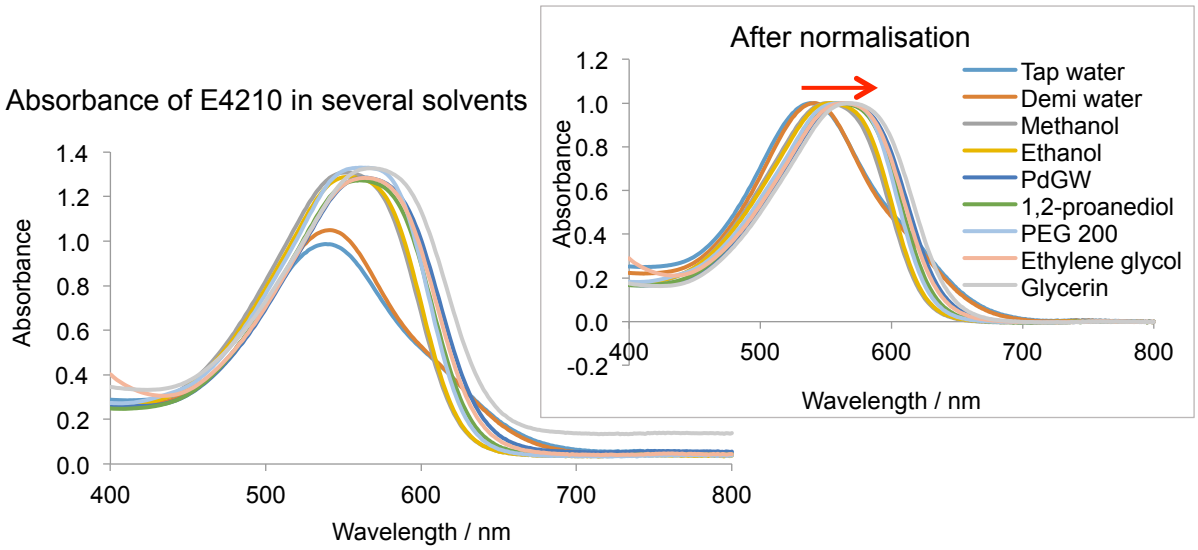

Figure 4.20: Influence of the solvent on the E4210 absorption band.

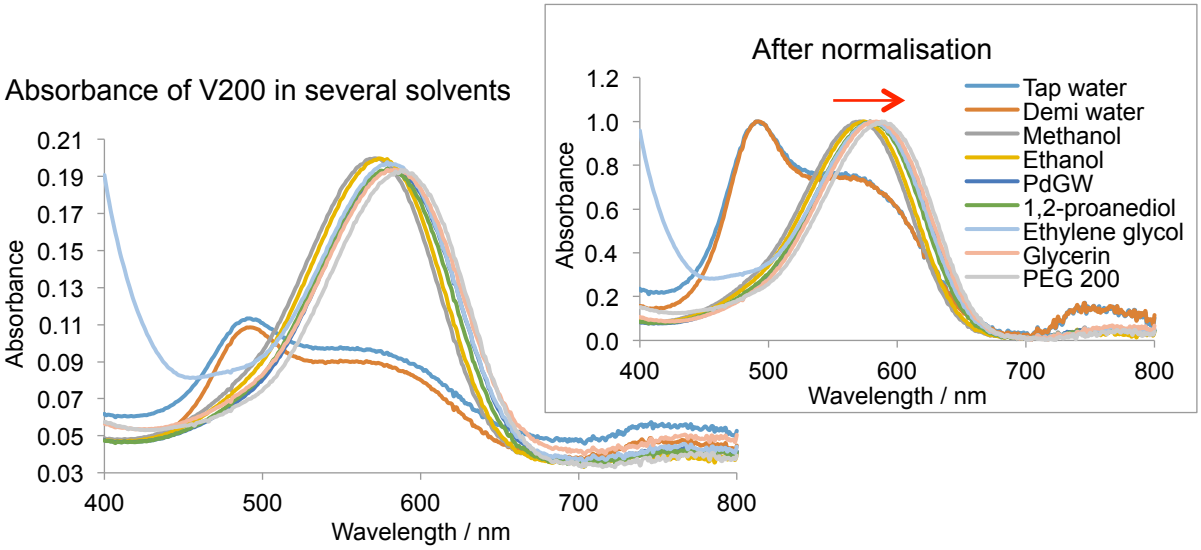

Figure 4.21: Influence of the solvent on the V200 absorption

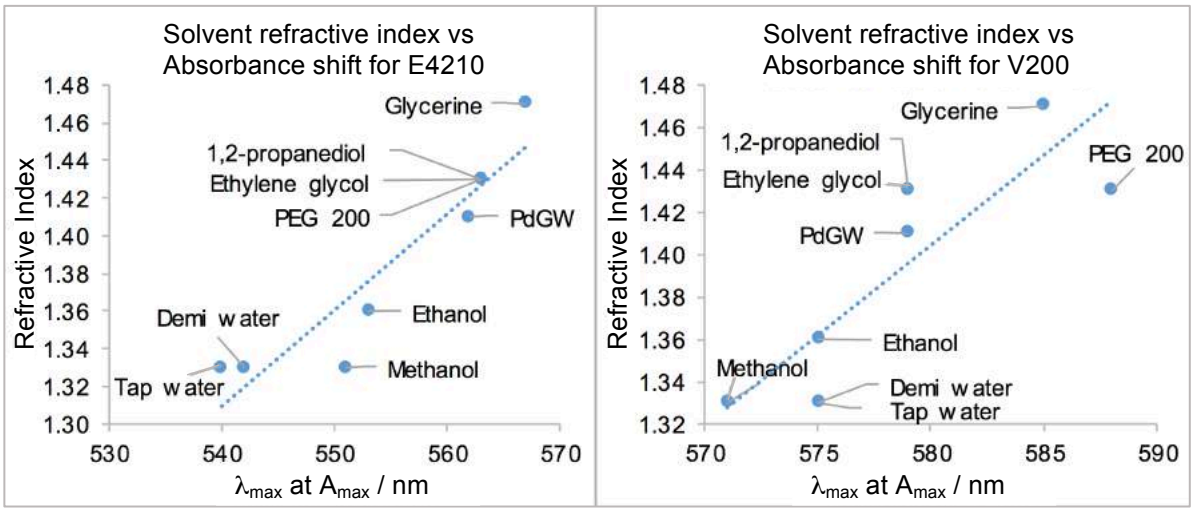

Figure 4.22: Relation between the solvent refractive index and the absorbance shift due to the solvent for E4210 and V200.

In Figure 4.20 and Figure 4.21, changes in the shape and position of the E4210's and V200's absorption bands can be observed respectively, as a function of the solvent. Regarding the solvent effect on V200, two peaks can be observed in water (the first one corresponding to the aggregate and the second peak, at longer wavelength, corresponding to the monomer) while there is only one peak for the other solvents. Thus, it can be assumed that only the monomer form of the dye is present in these solutions, given that the solvents are better able to solubilise the dye so dye aggregation is unlikely.

The effect of the solvent, i.e. the solvatochromism is caused by differential solvation of the ground and first excited state of the chromophore. As the polarity was not always accessible for each solvent in the literature, the refractive index of the solvent was used as a characteristic value as suggested by Kundt (see 4.1.7. Interactions with solvents). From Figure 4.22, as expected, a bathochromic shift of the dye absorption band shift to a longer wavelength with the increasing refractive index of solvent was observed. Indeed, by normalisation of the curves in Figure 4.20 and Figure 4.21, the shift in position can be observed to longer wavelength with the increase of the refractive index of the solvent.

The influence of the solvent on the dye deposition by putting approximately 0.1 g of polycotton in each sample for two hours has been also tested. Note that no agitation was added. The fabrics are shown in Figure 4.23.

Figure 4.23: Influence of the solvent on the dye deposition onto polycotton with E4210 on the top and V200 on the bottom. Solvent used from the left to the right: Tap-water, Demi-water, Methanol, Ethanol, 1,2-propane diol (Pdiol), Ethylene Glycol, PdGW (58 % Pdiol, 17 % Glycerine, 25 % Water) and Glycerine.

An influence of the solvent on the deposition for both dyes can be seen. In particular with water where the dye deposition is high, it is reduced a lot with the other solvent. Even if the colour intensity on each piece of fabric was not measured, it seems that the deposition follows this order from the highest to the lowest: water/tap water, glycerine, methanol/ethanol, PdGW, ethylene glycol. Note that the fabric colouration does not depend upon the solution colour (which changes with solvent), only with the dye colour. Once the dye is out of the solution, the fabric gets the original dye colouration. The increase in dye deposition could be explained either by a reduced affinity of the dye by the solvent, and/or by the wettability of the fabric by the solvent since the dye deposition is mainly driven by the transport of dye molecules to the fibre, which is poor if the fabric is not wetted effectively by the solvent. As this experiment was merely to observe the effect of the solvent on the dye deposition, this would need more investigation on the reason why this difference occurs.

4.2.2. Conclusion

E4210 and V200 are two azo polymeric dyes. They both absorb light in the yellowish region of the visible light, at 540 nm for E4210 and 575 nm for V200, and the purple/blue region of the visible light are reflected giving their colour. Due to this and their ethoxylated chains which brings more interactions with fabric fibers, they are good hueing dyes.

V200 aggregation occurs at a dye concentration above 2×10^{-5} mol L^{-1} in water. As E4210 is a more efficient technology than V200 and does not present any aggregation that could perturb the study of dye-surfactant interactions, E4210 was mainly used for the next experiments. Moreover, as no real changes in the absorbance between the commercial and the purified form have been shown, the commercial form was used for all the remaining experiments. Furthermore, as the E4210 commercial effective concentration is at 8.00 %, it is quite time consuming and expensive to purify enough dye for all our experiments.

The solvatochromic effect of the solvents has been shown on both hueing dyes, which shifts the absorption band to a longer wavelength with increasing refractive index of the solvent. This could be used to give an idea of the polarity of any solvent. However, in this thesis, this will also be useful to visualise the dye-surfactant interactions since when the surfactant concentration reaches the CMC, the dye molecules will be interacting with the surfactant micelles, thus changing the electronic environment surrounding the dye molecules.

References

[1] Zena O'Connor, "Colour Psychology and Colour Therapy: Caveat Emptor," *Color Research & Application* 36, no. 3 (2011): 229–34.

[2] R. Christie, *Colour Chemistry*, 2001.

[3] R. L. Allen, *Colour Chemistry* (Springer Science & Business Media, 2013).

[4] G. Broze, *Handbook of Detergents: Properties* (CRC Press, 1999).

[5] Society of Dyers and Colourists and American Association of Textile Chemists and Colorists, *Colour Index* (Bradford, 1971).

[6] W. Herbst, K. Hunger, and G. Wilker, *Industrial Organic Pigments: Production, Properties, Applications*, 3. ed (Wiley-VCH, 2004).

[7] E. E. Jelly, *Nature*, no. 138 (1936): 1009.

[8] E. E. Jelly, *Nature*, no. 139 (1937): 631.

[9] M. Kasha et al., "The Exciton Model in Molecular Spectroscopy," *Pure. Appl. Chem.*, no. 11 (1965): 371–492.

[10] G. B. Behera, P. K. Behera, and B. K. Mishra, 'Cyanine Dyes: Self Aggregation and Behaviour in Surfactants. A Review', *J. Surface Sci. Technol.* 23, no. 1–2 (2007): 1–31.

[11] C. Reichardt, 'Solvatochromic Dyes as Solvent Polarity Indicators', *Chemical Reviews* 94, no. 8 (1994): 2319–2358.

[12] N. Mataga and T. Kubota, 'Solvent Effect on the Electronic Spectra.pdf', in *Molecular Interactions and Ionic Spectra* (New York: Marcel Dekker, INC., 1970), 371–410.

[13] A. Kundt, *Ann. Phys. U. Chem. (Jubelband)*, 1874, 615–24.

[14] A. L. LeRosen and Charles E. Reid, 'An Investigation of Certain Solvent Effect in Absorption Spectra', *The Journal of Chemical Physics* 20, no. 2 (1952): 233–36.

[15] P. A. Gorry, 'General Least-Squares Smoothing and Differentiation by the Convolution (Savitzky-Golay) Method', *Analytical Chemistry* 62, no. 6 (1990): 570–573.

5. Dye Surfactant Interactions

Dye-surfactant associations are important in the dyeing processes and have been studied a lot in aqueous solutions. Surfactants are introduced in the dyebath to assist with the dyeing by playing the role of solubilisers for water insoluble dyes, breaking down dye aggregates in order to accelerate adsorption processes onto fibres, or by performing the role of auxiliaries to improve the dye adsorption, or to strengthen the dye binding, or very often, by performing the role of a levelling agent (controlling the rate of exhaustion of dye so that it is taken evenly and slowly; and helping the migration of the dye after initial uneven sorption onto fibre).[1]

5.1. Introduction

5.1.1. UV-Vis spectroscopy as a visual tool

The most common technique used to study the dye-surfactant interactions is UV-Vis spectrophotometry, which can reveal dye aggregates, premicellar dye-surfactant complexes and dyes incorporated into a micelle.[2,3,4] Basically, two types of interactions between dye and surfactant may be observed depending on the chemical structure of both dye and surfactant: at a low concentration below the CMC, a decrease in the absorbance with appearance of a new band indicates the formation of a dye-surfactant complex; whilst at high micelle concentrations, an increase of the extinction coefficient with a red shift indicates the incorporation of the dye into micelles. Several authors, including S. Go Göktürk[5,6] and R. Tehrani-Bagha,[7,8] who studied dye-surfactant interactions, found that non-Coulombic interactions (mainly hydrophobic) play a major role in binding compared to

electrostatic interactions; however, these interactions depend mostly on the chemical structures of both dye and surfactant.

5.1.2. Benesi-Hildebrand equation

In 1949, Benesi-Hildebrand,[9] B-H, developed equations which are still the most popular methods to determine the binding constant between dye and surfactant, K_b, and the fraction of dye bounded to micelles, f, spectrophotometrically.

At equilibrium, dye-surfactant interactions can be written as:

$$D + S \overset{K_b}{\leftrightarrow} DS \qquad \text{Eq. 5.1}$$

where D is the dye, S is the surfactant, and DS is the dye-surfactant complex.

Thus, the binding constant of the dye-surfactant complex, K_b, is defined by:

$$K_b = \frac{[DS]}{[D][S]} \qquad \text{Eq. 5.2}$$

where $[DS]$, $[D]$ and $[S]$ are the dye-surfactant complex, the dye and the surfactant concentrations, respectively.

with

$$[D]_0 = total\ D\ (uncomplexed\ and\ complexed) = [D] + [DS] \qquad \text{Eq. 5.3}$$

$$[S]_0 = total\ S\ (uncomplexed\ and\ complexed) = [S] + [DS] \qquad \text{Eq. 5.4}$$

giving

$$K_b = \frac{[DS]}{([D]_0 - [DS])([S]_0 - [DS])} \qquad \text{Eq. 5.5}$$

Note that concentrations are used instead of activities for the equilibrium constant, which is strictly only valid if the solutions are ideal while micelle-forming surfactants are definitely not ideal solutes.

In order to determine K_b and use the Benesi-Hildebrand equation,[9] the surfactant concentration must be hundreds of times higher than the dye concentration.

Thus, if $[S]_0 >> [D]_0$, then $([S]_0 - [DS]) \approx [S]_0$ so:

$$K_b = \frac{[DS]}{([D]_0 - [DS])[S]_0} \qquad \text{Eq. 5.6}$$

rearranging gives,

$$[DS] = \frac{K_b[S]_0[D]_0}{1 + K_b[S]_0} \qquad \text{Eq. 5.7}$$

Beer's law gives for the charge transfer (CT) absorption, A_m, of the DS complex:

$$A_m = \varepsilon_m l[DS] = \varepsilon_m l\left(\frac{K_b[S]_0[D]_o}{1+K_b[S]_0}\right) \quad \text{Eq. 5.8}$$

where ε_m is the molar extinction coefficient of the dye fully bounded to the micelles; and A_m is obtained from the additive law of absorbance:

$$A = A_0 + A_m \quad \text{Eq. 5.9}$$

$$A_m = A - A_0 = \Delta A \quad \text{Eq. 5.10}$$

with A, A_0 and A_m, respectively being the absorbance measured, the absorbance of the dye without surfactant and the absorbance of the dye fully bounded to the micelles.

Also, typically, l = 1 cm. Rearranging Eq. 5.8, the B-H equation is:

$$\frac{[D]_0}{\Delta A} = \frac{1}{K_b \varepsilon_m l}\frac{1}{[S]_0} + \frac{1}{\varepsilon_m l} \quad \text{Eq. 5.11}$$

There are several variants of the B-H equation, however, the following one will be used in our experiments,[10] in order to determine ε_m and K_b separately.

The fraction, f, can be calculated as:

$$f = \frac{[DS]}{[D]_0} \quad \text{Eq. 5.12}$$

or experimentally:[11]

$$f = \frac{\Delta A}{[D]_0 \varepsilon_m} \quad \text{Eq. 5.13}$$

The standard free energy of dye-surfactant complex formation,[12] $\Delta G°$, can be estimated from values of K_b and written as:

$$\Delta G° = -RTlnK_b \quad \text{Eq. 5.14}$$

where, R is the gas constant and T is the temperature.

5.1.3. Dye-surfactant interactions

Using the Benesi-Hildebrand method, it has been found that the binding of dye to micelle depends on the type of surfactant used and on the dye structure. It has also been found that the presence of cosolvents decreases the binding to sodium dodecyl sulfate (SDS) micelles at low concentration and totally inhibits it at a certain concentration due to the cosolvents' ability to counteract the hydrophobic association.[6]

S. Yefimova[13] has shown that for interactions between a cationic dialkylacarbocyanine perchlorate ($DiOC_n$) dye with different alkyl chain lengths and the anionic surfactant SDS, the binding constant of oppositely charged dyes and surfactant micelles is controlled by both electrostatic and hydrophobic forces. However, even a small increase of the dye alkyl chain length causes an abrupt nonlinear increase in the fraction of micellised dye molecules, highlighting that the hydrophobic interactions play a major role in the dye incorporation into micelle. Similarly, M. Sarkar and S. Poddar[4] have found that the length of the alkyl hydrocarbon chain of the nonionic surfactants can influence the stability of the dye-surfactant complex, i.e., the greater the chain length, the more stable the complex.

It has also been shown that the degree of association decreases with an increase of temperature,[14] which is more pronounced in nonelectrolyte solutions.

A. R. Teharani-Balgha and K. Holmberg[8] have shown that the majority of dyes have polar substituents, such as hydroxyl and amino groups, which can interact with surfactant polar head groups by a combination of intermolecular interactions and improve the solubilisation. They also found that in some cases, particularly with cationic surfactants, the ionic head group can induce ionisation of the dye and the ionic dye can then interact favourably with the oppositely charged surfactant.

5.1.4. Location of the dye in micelles

5.1.4.1. UV-Vis spectrophotometry method

The location of the dye in the surfactant micelles can be assessed by UV-Vis spectrophotometry by comparing absorption spectra of dyes in micelles and in solvents with different polarities. Indeed, as it has been described in Chapter 4, 4.1.7. Interaction with solvents, the environment surrounding the dye influences its absorption spectra. Moreover, there exists a polarity gradient from the very hydrophobic core of the micelle towards the hydrophilic head group region (see Figure 5.1). Thus, if the UV-Vis spectrum of the dye in the surfactant micelle has a similar shape to the dye spectra when it is dissolved in nonpolar solvents (solvents with a low polarity index), it can be assumed that the dye is located in the hydrophobic inner core of the micelles. Conversely, if the spectrum of the dye in the surfactant micelle has a similar shape to the one of the dye when it is dissolved in

more polar solvents (solvents with a higher polarity index), it can be assumed that the dye is located in the semi-polar outer part of the micelle.[8]

With this method, it has been demonstrated[8] that different surfactants work best for different dyes. In general, nonionic surfactants have a higher solubilisation power than anionic and cationic surfactants due to the dye's accommodation, not only in the inner hydrocarbon part of the micelle but also in the head group shell.

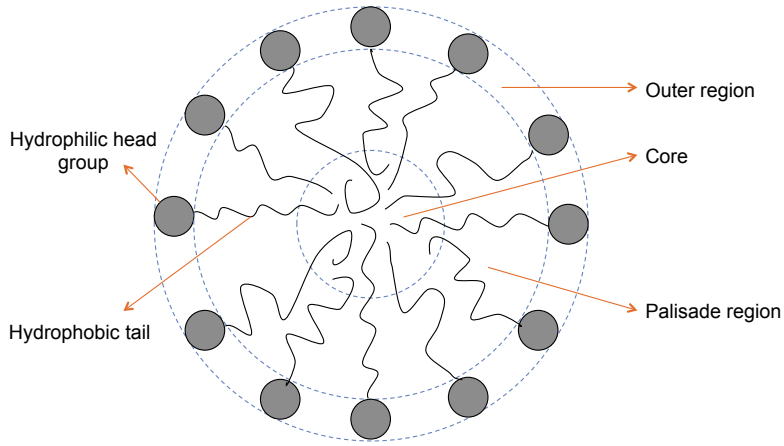

Figure 5.1: A surfactant micelle in water. Three different regions can be identified: the outer region, the palisade region and the core.

5.1.4.2. SAXS method

Small angle X-rays scattering (SAXS) is a widely used technique to determine the structure of particle systems, including crystal structures, for particle sizes or shapes in the size range from 1 to 100 nm.[15] SAXS is also an accurate and non-destructive analytical method; it can be useful to study internal structure of colloidal particles such as micelles.

5.1.4.2.1. Interaction of X-rays with structure

X-rays are electro-magnetic waves with typical wavelengths of 0.1 to 10 nm and can be described by particles called photons. When X-rays hit a material, we can observe three phenomenon: one fraction will pass through the sample, another one will be absorbed and transformed into other forms of energy (heat, fluorescence radiation, etc.) and one will be scattered into other directions of propagation. When an atom is irradiated with an x-ray photon and absorbs it, an electron can be expelled using up the X-ray energy. The atom will be thus in an unstable situation and will want to restore the original configuration by rearranging the remaining electrons. This results in the emission of fluorescence radiation, i.e., X-rays with

other wavelengths than the incident radiation. When the X-rays are scattered, this can be with or without a loss of energy and thus they can have a different wavelength than the incident radiation or keep the same wavelength. The scattered radiations are observed by the detector with an angle 2θ, thus, a plot can be created showing the intensity of the scattered radiation against the angle of scattering.[16]

5.1.4.2.2. Particles in solution

When using X-rays scattering techniques on solutions containing particles such as micelles, two types of scattering must be considered.

5.1.4.2.2.1. Form factor P(q)

In the case of diluted solutions, scattering occurs primarily within each particle, i.e. it is an intraparticle scattering. The scattered waves from a single particle then interfere with each other to give the scattering pattern observed on the detector (see Figure 5.2).

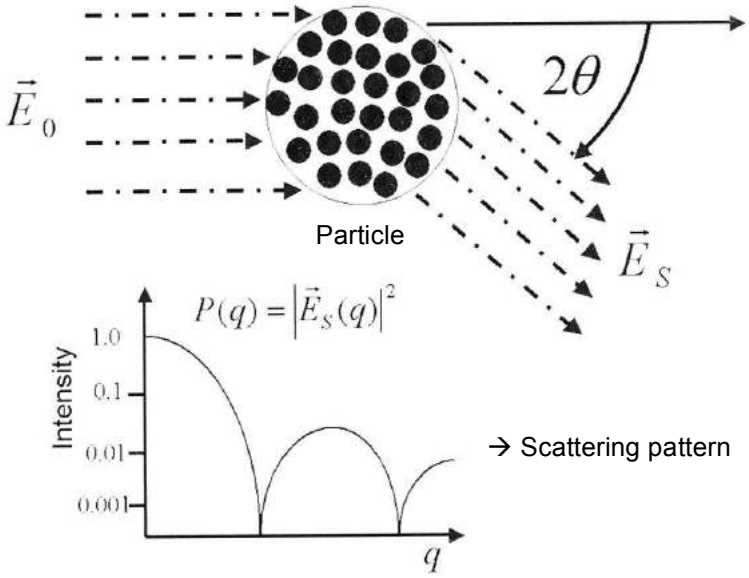

Figure 5.2: The form factor, P(q), of a particle is an interference pattern, the oscillations of which are typical of the particle's shape.

This pattern oscillates as a function of the shape (or the form) of the particle; it is therefore called "the form factor" P(q), where q represents the length of the scattering vector which is defined by the following equation:

$$q = \frac{4\pi}{\lambda} \cdot \sin(\theta) \qquad \text{Eq. 5.15}$$

If the sample is diluted (a dilute system of particles is defined for SAXS, when the distances between the particles are large in comparison to the wavelength λ), the observed scattering pattern corresponds to the form factor of one particle only, provided that the particles are all identical in shapes and sizes (i.e., monodisperse samples). If the particles have different sizes (i.e., polydisperse samples), we will obtain the average scattering pattern of the whole sample.

5.1.4.2.2.2. Structure factor S(q)

At high concentrations, the distances between the particles are of the same order of magnitude as the distances within the particles. Thus, in addition to intraparticle scattering, interparticle scattering must be taken into consideration. This interaction between particles is called “the structure factor” S(q) and it is necessary for the description of interacting systems and depends on the relative locations of the individual particles. S(q) depends on four factors: the radius of particles, the polydispersity of the solution, the charge of the particles, and the volume fraction (fraction of the solution volume that is taken up by the particles).[17] In crystallography, the structure factor is also called “the lattice factor”, because it contains the information about the positions of the particles with respect to each other. Concentration effects become particularly visible at small angles and can result in the formation of an additional peak or shoulder in the I(q) vs. q plot (see Figure 5.3). If the particles concentration is relatively low, the interactions between particles are decreased and repulsive interactions are more important; this generates a decrease in intensity at small q-values. In contrast, an intensity increase indicates attractive interactions at high concentration due to reducing space between particles, which may ultimately produce aggregation.

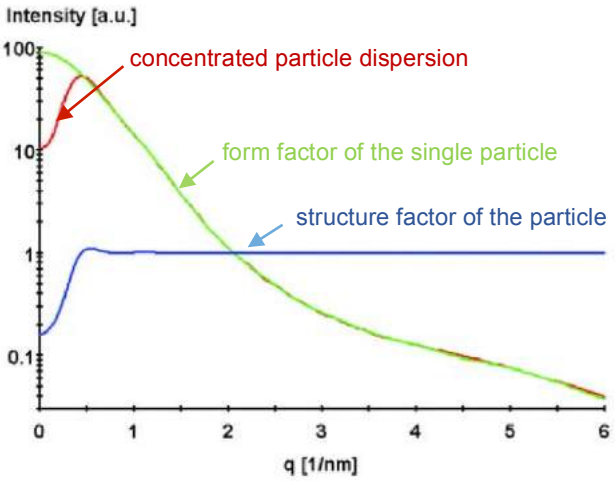

Figure 5.3: The SAXS profile of (red) a concentrated particle dispersion is the product of (green) the form factor of the single particle with (blue) the structure factor of the particle positions.

If the arrangement of particles is more ordered and periodic (i.e., crystalline-like lamellar phases), the broad peak can develop into a more-pronounced and narrow peak, which is called a Bragg peak. This indicates that the mean distance (d_{Bragg} in nm) between the aligned particles can be related to the position of its maximum (q_{Peak}) by using Bragg's law:

$$d_{Bragg} = \frac{2\pi}{q_{Peak}} \qquad \text{Eq. 5.16}$$

5.1.4.2.3. SAXS measurements and analysis

In SAXS, a long exposure time is the recipe for data of good quality. Before starting a SAXS measurement, it is important to know that one SAXS measurement consists of two experiments. The first is to determine the scattering from the matrix material (e.g., the solvent) and the second to determine the scattering from the particle system. Then we can obtain the scattering, $\Delta I(q)$, from the particles alone by subtracting the scattering of the matrix material $\Delta I_{M,exp}(q)$ to the scattering of the sample $\Delta I_{S,exp}(q)$ using the following equation:

$$\Delta I(q) = I_{S,exp}(q) - I_{M,exp}(q) \qquad \text{Eq. 5.17}$$

When a particle with the electron density of ρ_1 is embedded into a matrix of electron density ρ_2, the scattered intensity of the particle becomes:

$$\Delta I_1(q) = I_0 \cdot (\Delta\rho)^2 \cdot V_1^2 \cdot P(q) \qquad \text{Eq. 5.18}$$

where $\Delta\rho = \rho_1 - \rho_2$ and V is the sample volume.

An ensemble of N identical particles consequently causes an intensity of,

$$\Delta I(q) = N \cdot \Delta I_1(q) \cdot S(q) \qquad \text{Eq. 5.19}$$

Once the intensity of particles alone is recorded, we can summarise Eq. 5.18 and Eq. 5.19:

$$\Delta I(q) \propto P(q) \cdot S(q) \qquad \text{Eq. 5.20}$$

The Indirect Fourier Transformation (IFT) is usually used for the model-free evaluation of small-angle scattering data on dilute samples. However, for higher particle concentrations, the particle interactions cannot be neglected. To solve this problem, the Generalised Indirect Fourier Transformation (GIFT) method was developed. It takes into account the simultaneous determination of the form factor (intraparticle contributions) and the structure factor (interparticle contributions) for the model independent evaluation of scattering data with a minimum of *a priori* information.[18]

GIFT analysis is used to convert the scattering curve, $I(q)$ vs q, into the pair distance distribution function (PDDF), $p(r)$, which gives a histogram of distances found inside the particle. Thus the plot of $p(r)$ against r can give us a quick classification of the shape by identifying the key features as shown in Figure 5.4.

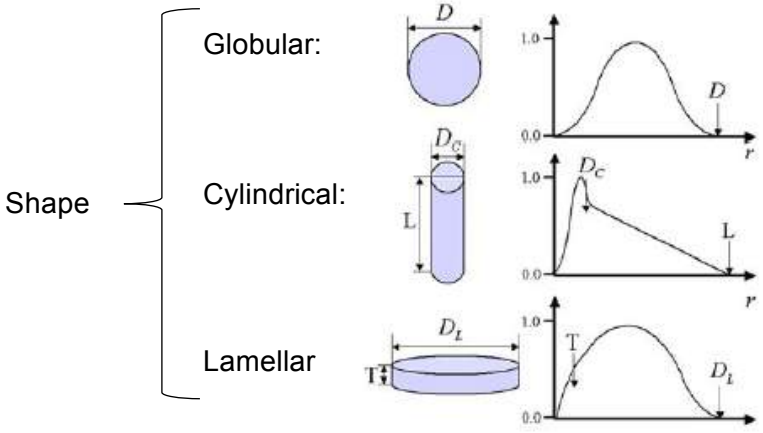

Figure 5.4: The key features of the PDDF, which are indicative for the particle shape.

Inhomogeneous particles, like core-shell, can also be quickly identified since the core-shell particle has a different electron density between the core and the shell. Thus, we can observe a dip in the PDDF, which can even go to negative values (see Figure 5.5) when the contrast of one region is smaller than the one of the matrix material. Note if the core radius is significantly larger than the shell thickness, the second peak can be smaller than the first, in contrast to the case depicted in Figure 5.5.

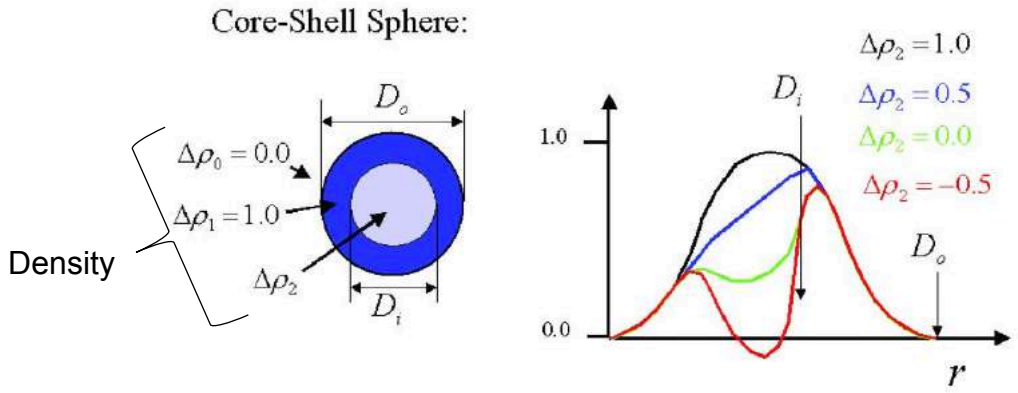

Figure 5.5: The PDDFs of core-shell particles.

Similar to core-shell particles, it is easy to recognise the PDDFs of aggregates. Indeed, they show a second peak too, but this time always smaller than the first peak (see Figure 5.6) and always positive since the electron density is the same.

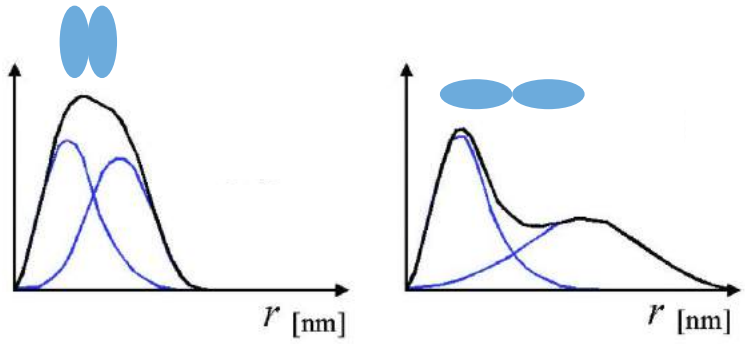

Figure 5.6: The aggregate of two subunits make a PDDF which can be recognised by a second peak.

GIFT analysis thus allows us to obtain the form structure and size for sphere and core-shell particles. However, it is not so useful for the analysis of bicontinuous microemulsions since these structures contain interconnected channels rather than isolated particles.

5.1.4.3. ^{1}H NMR method

Another method to study the dye location in micelles is to use ^{1}H NMR by looking at the variation in the chemical shifts of the surfactant with dye concentration.[19] As the origin of these chemical shift variations is the magnetic susceptibility anisotropy of the aromatic dye molecules, the protons from the surfactant close to the dye molecules undergo a large shift. Thus, the chemical shift provides information on the dye location within the surfactant micelles and the manner in which dye solubilisation shifts the ^{1}H NMR lines of the surfactant molecules strongly depends on the surfactant type and, to a lesser extent, on the dye molecule.

5.2. Discussion

In this part will be presented and discussed all the results obtained using the method developed to get the binding constant of a dye-surfactant complex. The validation method was used as described in Chapter 2, 2.3.1. Validation method. However, this validation method is typically used to validate analytical methods by comparing results obtained by a new method with an older method (which they would like to change/improve for some reasons) or with a reference material. However, there was neither reference material nor standard method to get the binding constant of a dye-surfactant complex, using both dyes, with none being reported in the literature. Thus, the Excel file was modified in order to compare all the results with the average of all the measurements as a reference. Moreover, different levels of concentrations are usually used in the validation method. As the dye concentration has been fixed for all the experiments, different wavelengths were studied in order to know at which wavelength to be to determine the binding-constant (either at the maximum of absorption of the dye, or at the maximum of absorption of the dye-surfactant complex or at others). The validation of the method developed to obtain the binding constant of a dye-surfactant complex has given a good repeatability; in particular tolerance probability and acceptability limit values (90 % and 15 %, respectively) were quite reasonable, which validated the method for a wavelength corresponding to the maximum of absorbance of the dye-surfactant complex.

5.2.1. Visualisation of the dye-surfactant interactions and K_b

Using the method developed (see Chapter 2, 2.3.2. Benesi-Hildebrand plot for the dye-surfactant interaction parameters), the interactions between E4210 and V200 with several nonionic surfactants and a few anionic surfactants were studied. Two examples, one with $C_{13}E_{10}$ and purified E4210 and another one with $C_{10}E_{10}$ and commercial V200, are presented (Figure 5.7 and Figure 5.9 respectively) and discussed below. The results were obtained at room temperature (≈ 25 °C) with a constant dye concentration and as a function of the surfactant concentration, before and after normalisation (the same process as explained in Chapter 4, 4.2.1.4. Dye-Solvent interactions). The difference in absorbance of the dye in the absence and in the presence of surfactant, as well as the fraction of dye molecules incorporated in the surfactant micelles were investigated.

The extent of interactions between E4210 and $C_{13}E_{10}$ are apparent from Figure 5.7 and Figure 5.8. In the first place, it has to be remembered that the maximum of absorption of purified E4210 in water is at 542 nm and the CMC of $C_{13}E_{10}$ is 2.06 x 10^{-4} mol L^{-1}. Moreover, the absorbance of the surfactant in the range of wavelengths studied (between 400 nm and 800 nm) was performed and no absorption band from the surfactant itself occurred – the same for all the surfactants studied. Figure 5.7, representing the absorbance of purified E4210 at constant concentration as a function of the concentration of $C_{13}E_{10}$ from below its CMC to above the CMC, allows to probe the dye-surfactant interactions. Indeed, the first aspect apparent from the UV-vis spectra is that the addition of surfactant to a constant concentration of E4210 causes a little increase in the absorbance of E4210, suggesting a dye-surfactant interaction that makes light absorption at this wavelength more likely. The increase in absorbance with surfactant concentration is significantly reduced at higher surfactant concentrations with a bathochromic shift to a longer wavelength, which appears when the CMC is reached and then remains constant with the surfactant concentration – in the legend entry, the surfactant concentrations above the CMC are shown in red.

This solvatochromism effect is due to the change in the local environment surrounding the dye, which influences its electronic structure and thus its photophysics by the differential solvation of the ground and first excited state of the chromophore.[20] Thus the bathochromic shift is probably due to the reduction of the surrounding medium's polarity when the dye resides in the surfactant micelles, which better stabilise the excited state of the dye than the dye in the ground state. This hypothesis is backed up by the fact that on the graphs, the bathochromic shift is most apparent at surfactant concentrations above its CMC (concentration in red). Thus, it can be suggested that before the surfactant CMC, an interaction between E4210 and surfactant exists, causing an increase in the absorbance intensity. The surfactant is thus complexed to a degree with the dye and its concentration needs to be increased relative to a system without dye, for micelles to form. The CMC of the surfactants in the presence of E4210 was not directly measured. However, it can be observed on Figure 5.8 C), which shows the absorbance of E4210 as a function of the concentration of $C_{13}E_{10}$, a change in slope at 3.40 x 10^{-4} mol L^{-1} which could correspond to the CMC of $C_{13}E_{10}$ in presence of purified E4210 while it was measured at 2.06 x 10^{-4} mol L^{-1} in absence of E4210.

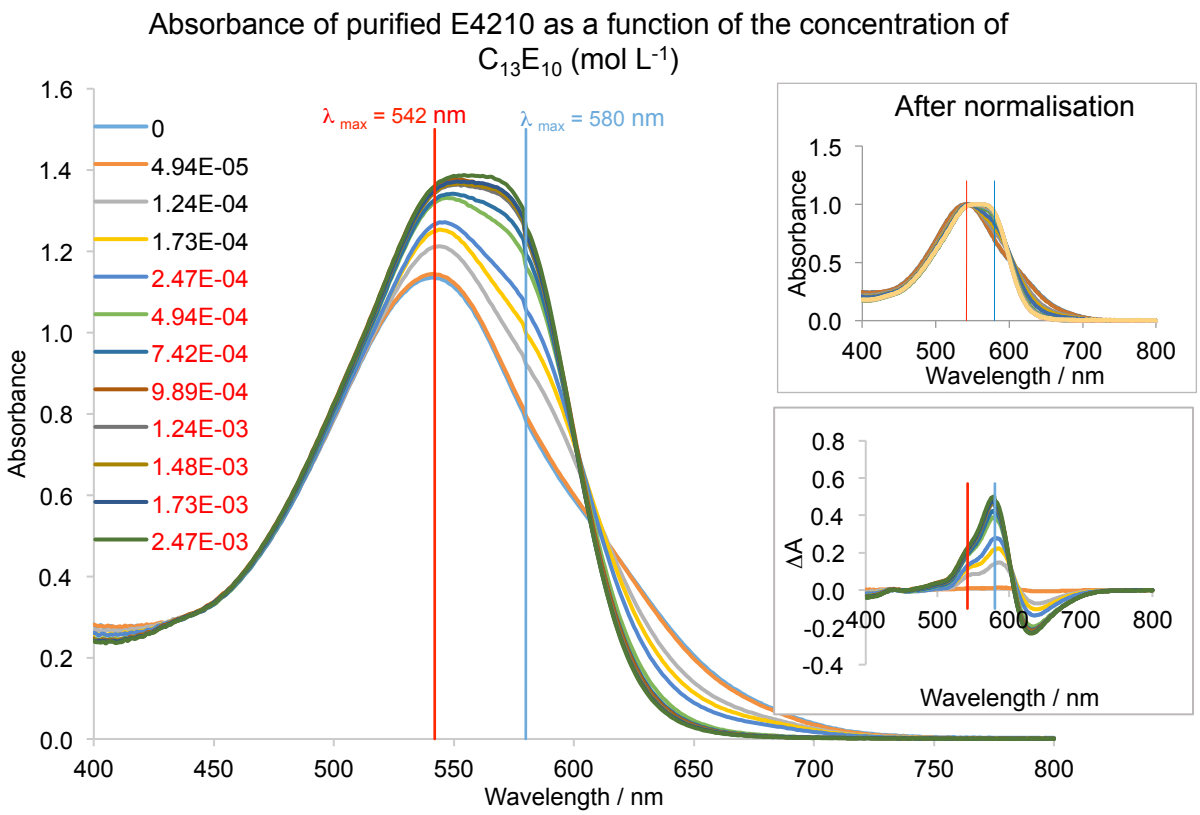

Figure 5.7: Interactions of purified E4210 with $C_{13}E_{10}$. Major graph: absorbance of commercial E4210 as a function of the concentration of $C_{13}E_{10}$. Graph on the top right: curves after normalisation. Graph on the bottom right: differences of dye absorption in presence and in absence of surfactant.

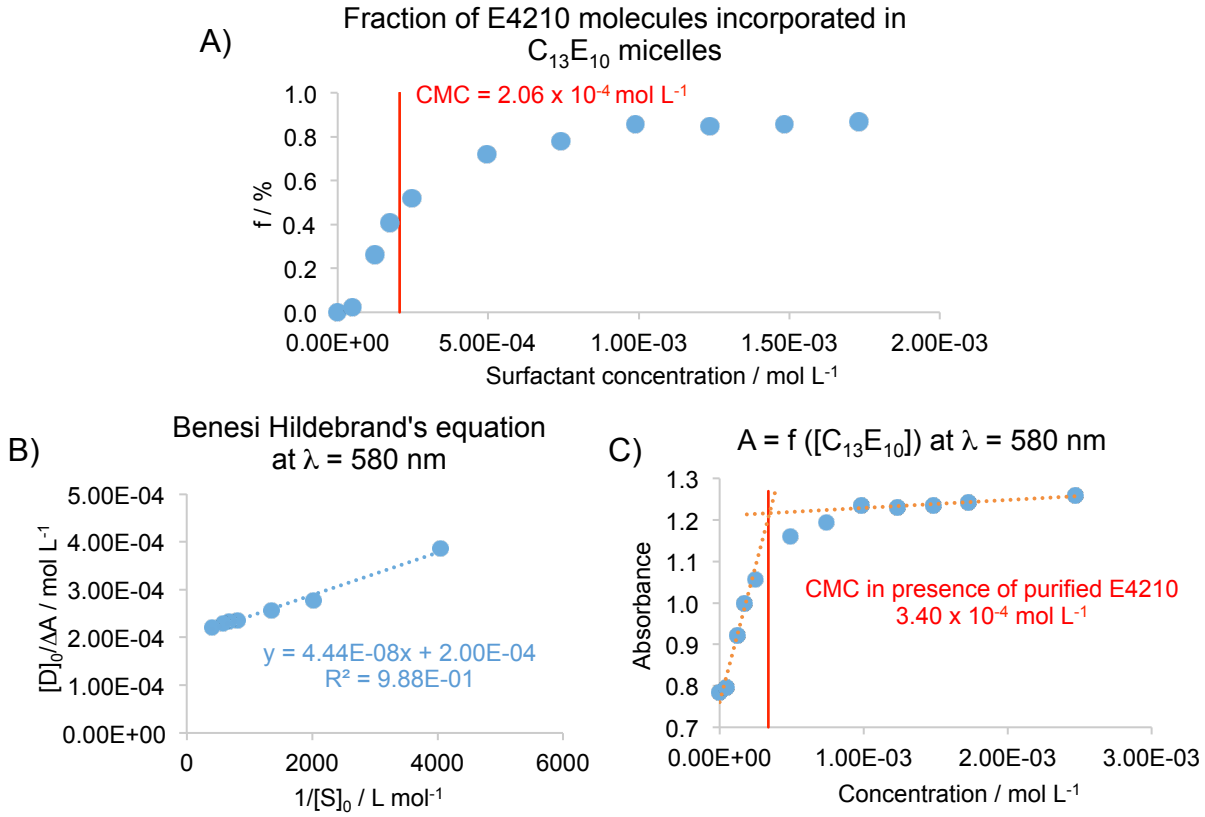

Figure 5.8: A) Fraction of E4210 molecules incorporated in $C_{13}E_{10}$ micelles, B) Benesi Hildebrand's equation used for the E4210-$C_{13}E_{10}$ complex at λ = 580 nm, and C) the absorbance of the E4210-$C_{13}E_{10}$ complex as a function of the concentration of $C_{13}E_{10}$ at λ = 580 nm on the bottom right.

When the bathochromic shift appears, it can be suggested that a significant proportion of dye molecules now reside within surfactant micelles, thus causing a change in the local environment surrounding the dye and hence this bathochromic shift. Figure 5.8 A) also confirms this where almost 100 % of dye molecules are incorporated in micelles after the surfactant CMC.

The graph representing ΔA = f (λ) on Figure 5.7 was obtained by subtracting the absorbance of the dye only from the absorbance of the dye in presence of surfactant, in order to allow the selection of the wavelength where only the dye-surfactant complex occurs, which will be used to calculate the binding constant of the dye-surfactant complex. From this graph, the appropriate wavelength to represent only the dye-surfactant complex was 580 nm. Thus, using the BH equation (Eq. 5.11) at $A = \Delta A_{max}$ (λ = 580 nm in this case), a concentration of dye of 10^{-4} mol L^{-1} and using only surfactant concentrations superior to 1.00×10^{-2} mol L^{-1} (i.e. 100 x [D]), we obtained $K_b = 4.50 \times 10^3$ L mol^{-1} and $\varepsilon_m = 5.01 \times 10^3$ L mol^{-1} cm^{-1} from Figure 5.8 B).

Since the dye concentration has an influence on K_b, it is important to keep the dye concentration constant in all experiments in order to be able to compare all the results together.

Regarding the interactions between commercial V200 and $C_{10}E_{10}$ apparent from Figure 5.9 and Figure 5.10, the same trend can be observed. As a reminder, the maximum of absorptions of V200 are 491 nm and 575 nm for the dye aggregate and the dye monomer, respectively with ε_0 = 1298.5 L mol^{-1} cm^{-1} and ε_0 = 595.2 L mol^{-1} cm^{-1} for the dye aggregate and the dye monomer. From Figure 5.9, we can see that at low surfactant concentration, the absorbance of the monomer increases compared to the case with no surfactant, while the absorbance from the aggregate decreases until it disappears due to its dispersion into monomer favoured by the greater surfactant-dye interaction. The dispersion of aggregates into monomers is visible to the naked eye due to the difference in the wavelength for the absorption maximum between the dye aggregate (at 491 nm) and monomer (at 575 nm). This explains the difference in colouration after the CMC (sample nº 5), on Figure 5.10. Then, when the surfactant's CMC is reached (CMC = 4.68 x 10^3 mol L^{-1}), there is a bathochromic shift in the absorption band from 575 nm to 592 nm showing a new environment surrounding the dye molecules.

The normalisation graph also shows the shift in the absorption band to longer wavelength. It can thus be suggested that before the CMC, an interaction between V200 and surfactant exists causing an increase in the absorbance intensity and the dispersion of dye aggregates into monomers. The surfactant is thus complexed to a degree with the dye and its concentration needs to be increased to form micelles as shown with the example of $C_{13}E_{10}$ with purified E4210. When the bathochromic shift appears, we can suggest that a significant proportion of dye molecules now reside within the surfactant micelles; thus causing a change in the local environment surrounding the dye and thus this bathochromic shift.

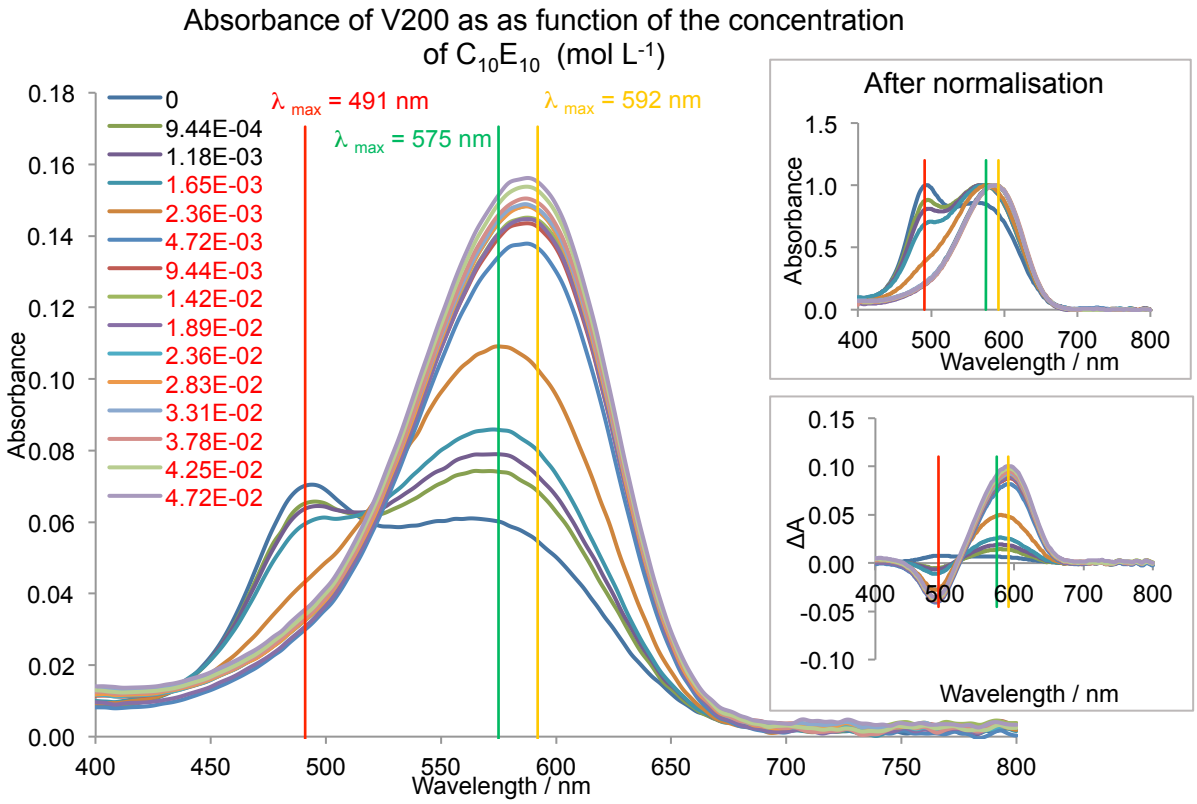

Figure 5.9: Interactions of V200 with $C_{10}E_{10}$. Major graph: absorbance of E4210 as a function of the concentration of $C_{10}E_{10}$. Graph on the top right: curves after normalisation. Graph on the bottom right: differences of dye absorption in presence and in absence of surfactant.

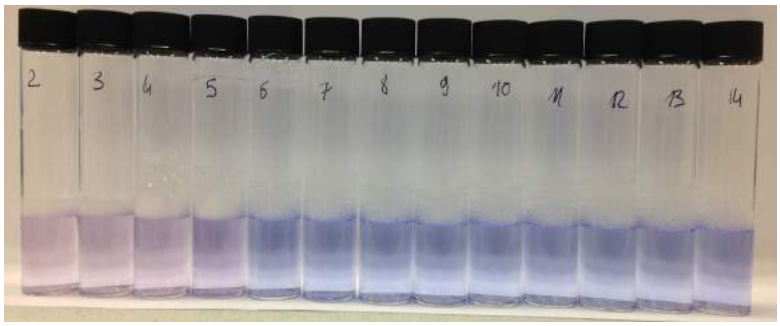

Figure 5.10: Interactions of V200 with $C_{10}E_{10}$: samples used for the study with constant V200 concentration and several concentration of $C_{10}E_{10}$.

Because of the hypsochromic shift from 575 nm to 492 nm due to the dye aggregation of V200, it was not possible to determine the binding constant of V200 with surfactants nor the fraction of dye molecules incorporated in surfactant micelles. This is one limit of the method using dye. Another limit of the method is apparent when using more hydrophobic surfactants, as this leads to cloudy solutions which are not convenient for the spectrophotometric analysis as scattering occurs. This is the case for example for $C_{10}E_7$, which is not sufficiently soluble in water to form transparent and homogeneous solutions in the surfactant concentration range studied. In this case, a high base line is obtained due to the scattering of the light by surfactant molecules distorting the results (see Figure 5.11). In order to avoid this and get transparent and homogeneous solutions, one method is to replace the water with an ethanol solution at 40 % by volume. However, due to the solvatochromism effect seen previously, the absorption band of the dyes is shifted in the EtOH 40 % in the same wavelength range as the dye-surfactant complex, disrupting the direct visualisation of the dye-surfactant interactions and thus the determination of the binding constant using the method developed (see the example of E4210 with $C_{13}E_{10}$ in EtOH 40 % in Figure 5.12). Moreover, the ethanol is a cosolvent and, as discussed in 5.1.3. Dye-surfactant interactions, a cosolvent can decrease the binding of the dye to the surfactant micelles at low concentration and totally inhibits it at higher concentrations.

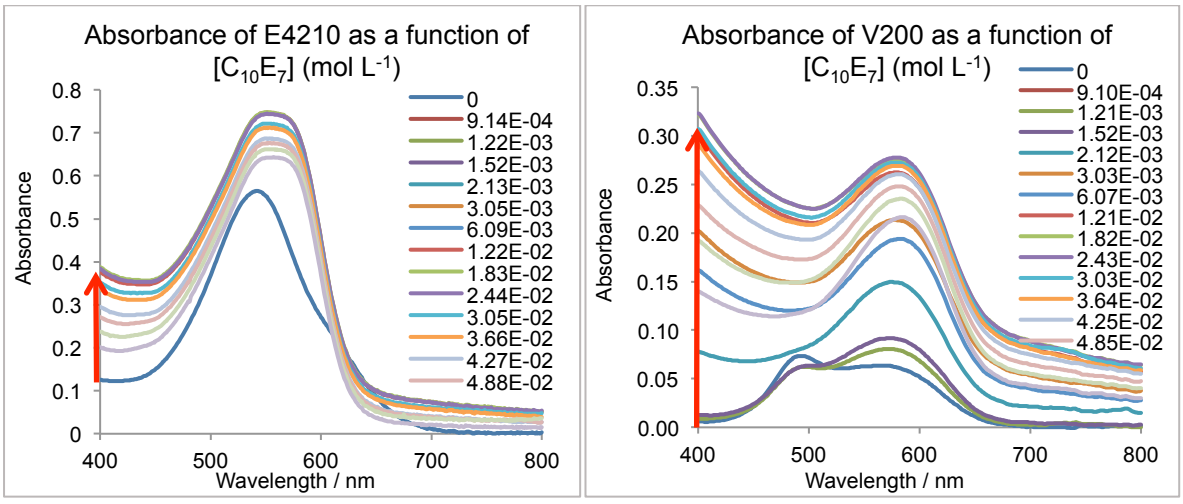

Figure 5.11: Interactions of $C_{10}E_7$ with E4210 on the left and V200 and the right.

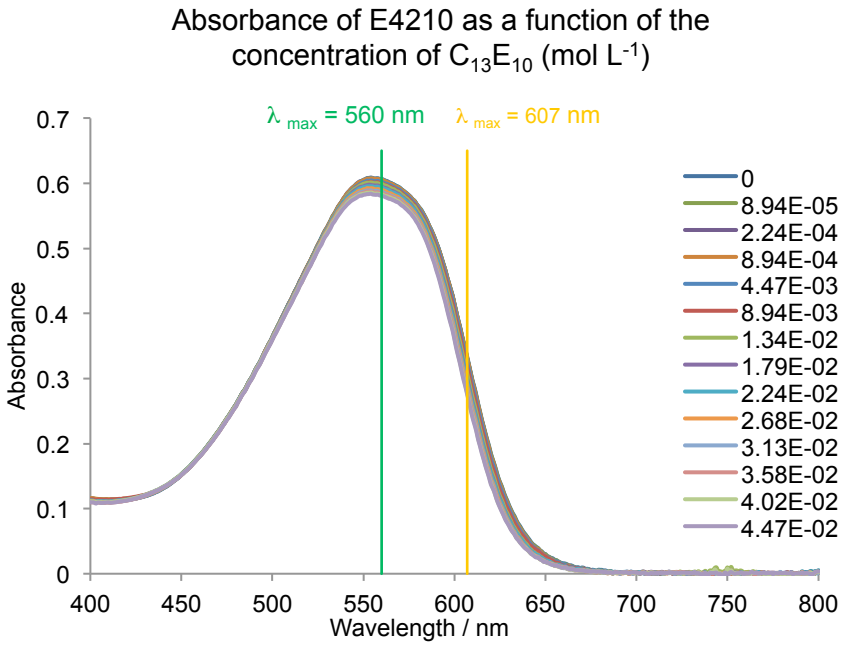

Figure 5.12: Interactions of E4210 with $C_{13}E_{10}$ in an EtOH 40 % solution.

Due to these two limits of the method, we have only studied the binding constant of the dye-surfactant complex with E4210 and sufficiently soluble surfactants that produce homogeneous and transparent solutions. All the measurements were done in triplicates, the results using the commercial form of E4210 are summarised on Table 5.1.

Table 5.1: Binding constant, K_b, and ε_m of E4210-surfactants complexes using the commercial form of E4210.

Surfactant	$K_b \times 10^3$ (L mol^{-1})	Error %	$\varepsilon_m \times 10^3$ (L mol^{-1} cm^{-1})	Error %	Absorbance at the plateau
C13E8	- 3.19	25.28 %	4.50	0.41 %	0.487
C13E10	- 0.90	5.33 %	4.18	0.27 %	0.459
C13E12	- 1.01	5.94 %	4.47	0.88 %	0.477
C13E15	- 0.72	5.32 %	4.34	0.38 %	0.466
C13E20	- 0.61	7.39 %	4.22	0.77 %	0.453
C10E7	- 0.83	11.57 %	4.61	0.75 %	0.489
C10E8	- 2.66	22.15 %	4.61	0.16 %	0.496
C10E9	- 4.71	26.99 %	4.62	0.29 %	0.498
C10E10	- 2.27	12.61 %	4.61	0.48 %	0.494
C10E14	- 0.95	6.57 %	4.44	0.74 %	0.478
LAS	- 1.01	5.94 %	4.46	0.88	0.478
SDBS	- 34.38	7.87 %	4.70	0.21 %	0.515

Looking at the results obtained, it can be observed that the binding constant values obtained for the dye-surfactant complexes using the commercial form of E4210 are negative, which does not make sense since by definition a binding constant is a concentration ratio. These negative values are explained by the fact that the purified form of E4210 was used for the validation method, while the commercial form of E4210 was used in the experiments for the reasons explained earlier. Thus, the same concentration of E4210 raw material was used, i.e. 10^{-4} mol L^{-1} for both experiments using the purified and the commercial form, while the effective concentration of dye molecule should have been used. Indeed, the effective concentration of dye molecules in the commercial form is only of 8.00 % by mass of dye molecules diluted in polyethylene glycol, while in the purified form the concentration of dye molecules should be much higher. Even though the exact purity degree of the purified E4210 could not be assessed, an idea of it can be made by looking at the LC spectrum of the commercial and purified forms of E4210 (see Chapter 4, 4.2.1.1. Dye purification) and also by the fact that the molar extinction coefficient of the purified E4210 is double that of the commercial E4210 (11053 L mol^{-1} cm^{-1} and 5066.5 L mol^{-1} cm^{-1} respectively). The difference in absorbance intensity is also visible by comparing Figure 5.7 and Figure 5.13, which shows the absorbance of the purified E4210-$C_{10}E_{10}$ complex and commercial E4210-$C_{13}E_{10}$, respectively, as a function of the surfactant concentration. Because of this, the effective concentration of dye molecules is much lower in the experiments using the commercial form of E4210 compared to the purified form and we can clearly see the impact by comparing the experiment using the purified and the commercial forms (see Figure 5.7 and Figure 5.13 respectively).

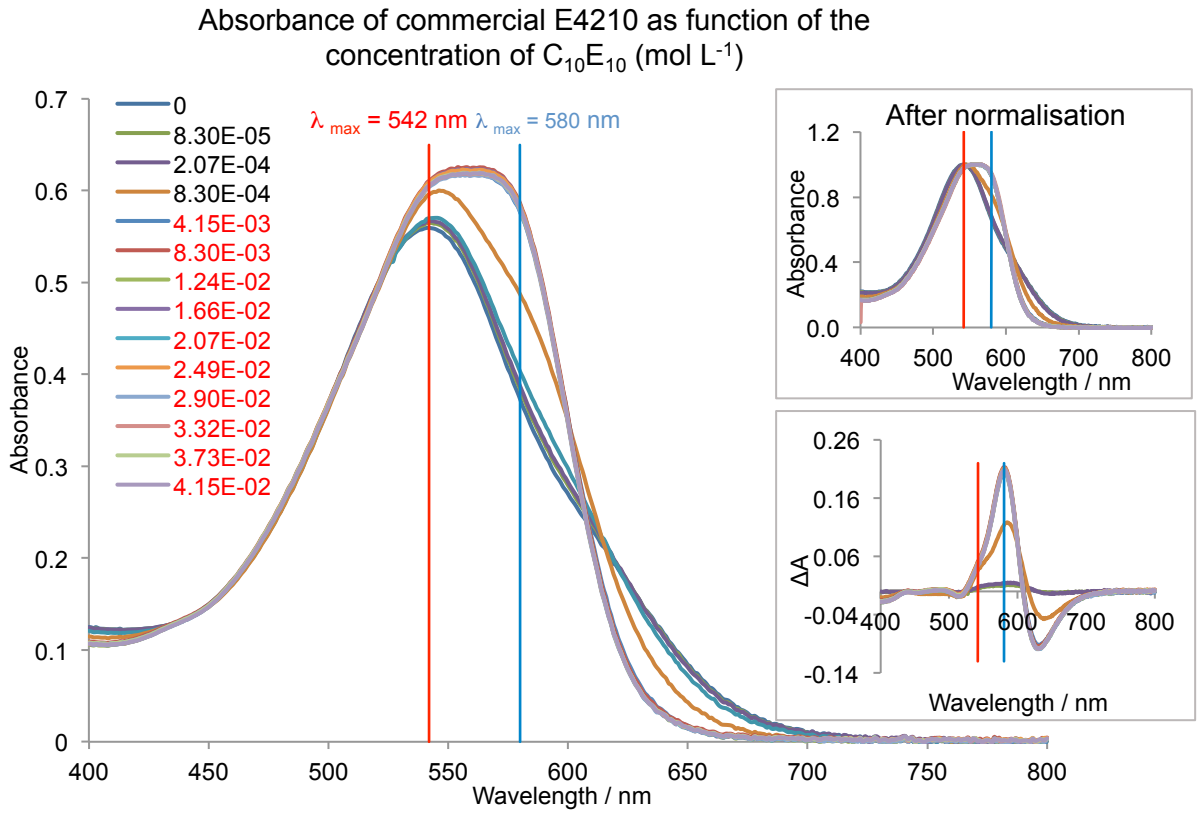

Figure 5.13: Interactions of commercial E4210 with $C_{10}E_{10}$. Major graph: absorbance of commercial E4210 as a function of the concentration of $C_{10}E_{10}$. Graph on the top right: curves after normalisation. Graph on the bottom right: differences of dye absorption in presence and in absence of surfactant.

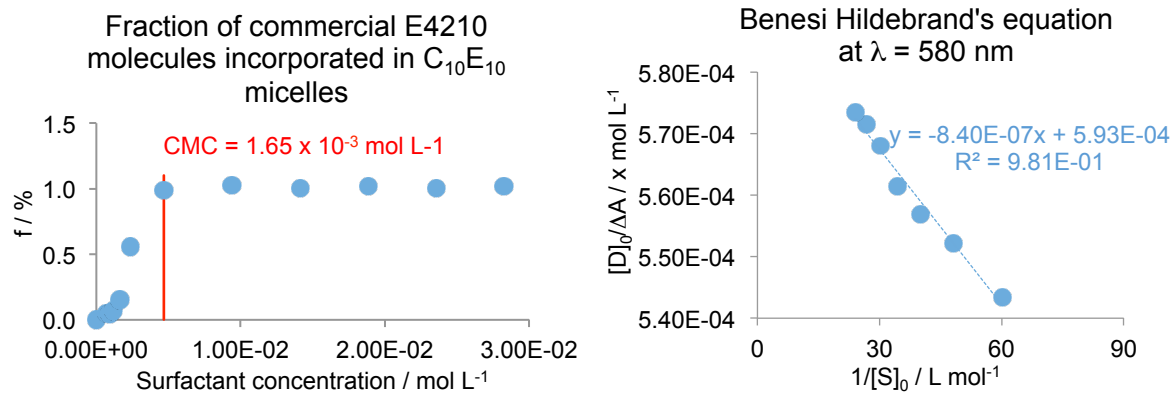

Figure 5.14: Fraction of E4210 molecules incorporated in $C_{10}E_{10}$ micelles on the left, Benesi Hildebrand's equation used for the E4210-$C_{10}E_{10}$ complex at λ = 580 nm on the right.

The method used to determine the binding constant of the dye-surfactant complex was built with the purified E4210-$C_{10}E_{10}$ complex using a surfactant concentration range from below to above its CMC whilst also satisfying $[S]_0 > 100 \times [D]$ in order to be able to measure the binding constant of the complex. Thus a good dye concentration satisfying the B-H equation, but also allowing us a good visualisation in terms of absorbance intensity using the purified E4210 was fixed at 10^{-4} mol L^{-1}. It can be observed in Figure 5.7 a progressive increase of the absorbance at the maximum of absorbance at 542 nm (due to dye-isolated surfactant molecule

interactions) and 580 nm (due to dye molecules incorporated into the micelles) until a plateau is obtained. When the plateau is reached, this means that almost all of the dye molecules are incorporated in surfactant micelles. Before the plateau, the absorbance is increasing with the surfactant concentration and so we obtain a positive gradient in the plot of the B-H equation and thus a positive binding constant of the dye-surfactant complex (see Figure 5.8). Moreover, looking at the fraction of dye molecules incorporated in surfactant micelles (see Figure 5.8), it can be observed a nice curve where almost 50 % of dye molecules are incorporated in surfactant micelles at the surfactant's CMC and where the plateau is almost reached at the last surfactant concentration used. Thus, the mistake was to reuse this method with the commercial E4210 at the same concentration of raw material as the purified E4210, thereby failing to take into account the reduced effective concentration of E4210 in the commercial form. There is only 8.0 % by mass of dye molecules in the commercial E4210 form, so the concentration of dye molecules is much lower compared to the surfactant concentration. Indeed, it can be clearly observed on Figure 5.13 and Figure 5.14 that all the dye molecules are incorporated in surfactant micelles at the surfactant's CMC, thereby, the plateau is already reached, being outside the study range. Because of this, the absorbance is slightly decreasing when the surfactant concentration increases likely due to another mechanism which comes into place, giving a negative gradient to the B-H equation plot and thus a negative K_b.

A possible way to obtain a binding constant using the data might have been to take the effective concentration of dye molecule in the commercial E4210 as well as the surfactant concentration just before the plateau as the maximum of surfactant concentration and estimate the absorbance value below this surfactant concentration by assuming a linear increase of the absorbance with surfactant concentration. However, this is not possible as it can be observed in Figure 5.8, the absorbance is not increasing linearly with surfactant concentration. Thus it is not possible to use and analyse the data. However, as it has been seen that the absorbance at a constant concentration of dye is increasing with the increase of surfactant concentration until reaching a plateau, the absorbance at this plateau has been recorded (see Table 5.1 and Figure 5.15) assuming that the higher the absorbance at the plateau, the greater the dye-surfactant interaction. Note that the error in the absorbance values in Table 5.1 was less than 0.5 %.

Thus, a tentative hypothesis will be made to interpret these results of absorbance at the plateau. Further experiments with lower dye or surfactant concentrations so that the plateau is not reached would need to be undertaken to obtain accurate binding constants.

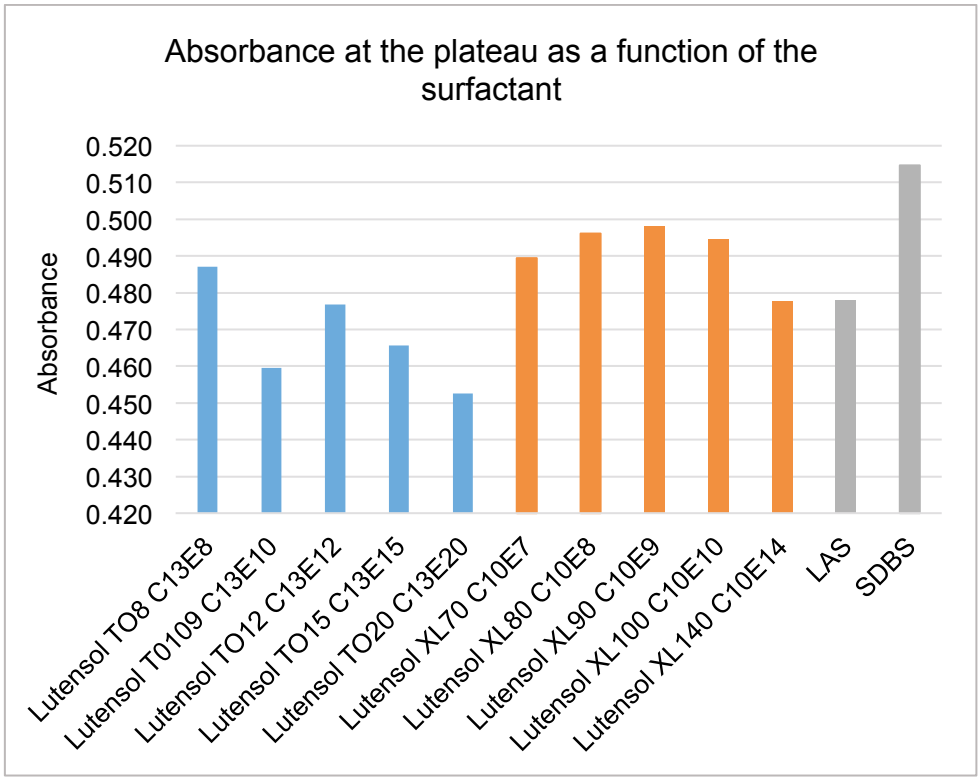

Figure 5.15: Absorbance at the plateau as a function of the surfactant.

From Figure 5.15, looking at the two nonionic surfactants series, it can observed that the absorbance at the plateau, and thus potentially the dye-surfactant interactions, increases until a maximum – corresponding to 12 ethylene oxide groups for the $C_{13}E_j$ series (if we don't take into account the value for $C_{13}E_8$) and to 9 ethylene oxide groups for the $C_{10}E_j$ – and then decreases. Furthermore, it has to be remembered that E4210 has an ethoxylated chain with an approximate number of 10 ethylene oxide groups. As both ethoxylated chains of the dye and the nonionic surfactant are interacting together (see 5.2.2. Dye location in surfactant micelles), this could explain a maximum of interaction between the dye and the surfactant when the ethoxylated chain is almost identical in length. Moreover, note that $C_{13}E_{12}$ and $C_{10}E_9$ have a similar HLB value of 14.50 and 14.29 respectively, which may reflect the hydrophobic/hydrophilic character of E420. However, this is only a hypothesis since data are limited for comparison.

If the two surfactant series are now compared, it can be observed that the absorbance at the plateau, and thus potentially the dye-surfactant interactions for the $C_{13}E_j$ series are lower than for the $C_{10}E_j$ series. NMR has shown (see 5.2.2. Dye location in surfactant micelles) that E4210 is interacting with the hydrophobic part of the surfactant, even if this is to a lesser extent compared to the hydrophilic part. Hence the hydrophobic chain length might be expected to affect dye-surfactant binding and the resulting absorbance. However, further studies are required to understand the effect of the alkyl chain length on dye-surfactant interactions. But it has to be noticed that it is not possible to do this for all the C_nE_j surfactant series, though, because surfactants with a number of carbons inferior to 10 and superior to 13 with a range of number of ethylene oxide groups are either not available or too expensive. Moreover, by increasing or decreasing the number of carbons of a nonionic surfactant, the latter may be less soluble in water or lose its surfactant properties, respectively. Furthermore, M. Sarkar and S. Poddar[4] have found that the greater the chain length, the more stable the complex; thus either the data obtained are not enough to observe the same conclusion as explained or it depends on the structure of the dye since they were working on the methyl violet cationic dye while an azo polymeric dye having a long ethoxylated chain, which increases the interactions with the hydrophilic part of the surfactant micelles, was used in this thesis.

Now Looking at the two anionic surfactants, it can be noted that even if LAS and SDBS only differ by the position of the benzene sulfonate group, either in the middle (LAS) or at the end (SDBS) of the carbon chain respectively, there is a big difference between them in the absorbance at the plateau, and thus potentially the dye-surfactant interactions. Indeed, the absorbance at the plateau of the E4210-SDBS complex is greater than the E4210-LAS complex and the E4210-nonionic surfactant complexes. However, this thesis was more intentionally focused on dye interactions with nonionic surfactants and so further study is required to elucidate the role of chain architecture on the interactions of anionic surfactants with E4210.

In order to know the influence of another surfactant on the binding constant of the dye-surfactant complex, the absorbance of the dye-surfactants complex as a function of the ratio of two surfactants in a binary system was studied. For a higher clarity, the term of “dye-surfactant complex” refers to the interactions of one dye with

one surfactant, and the term of “dye-surfactants complex” (with an s in surfactant) refers to the interactions of one dye with two surfactants in this case. As the same method was used to obtain the binding constants, negative values of K_b were also obtained for the same reasons. Thus, as previously and still in the hypothesis where the intensity of the absorbance at the plateau would be correlated to the intensity of the dye surfactant interactions, these absorbance were reported to produce the four binary systems presented in Figure 5.16.

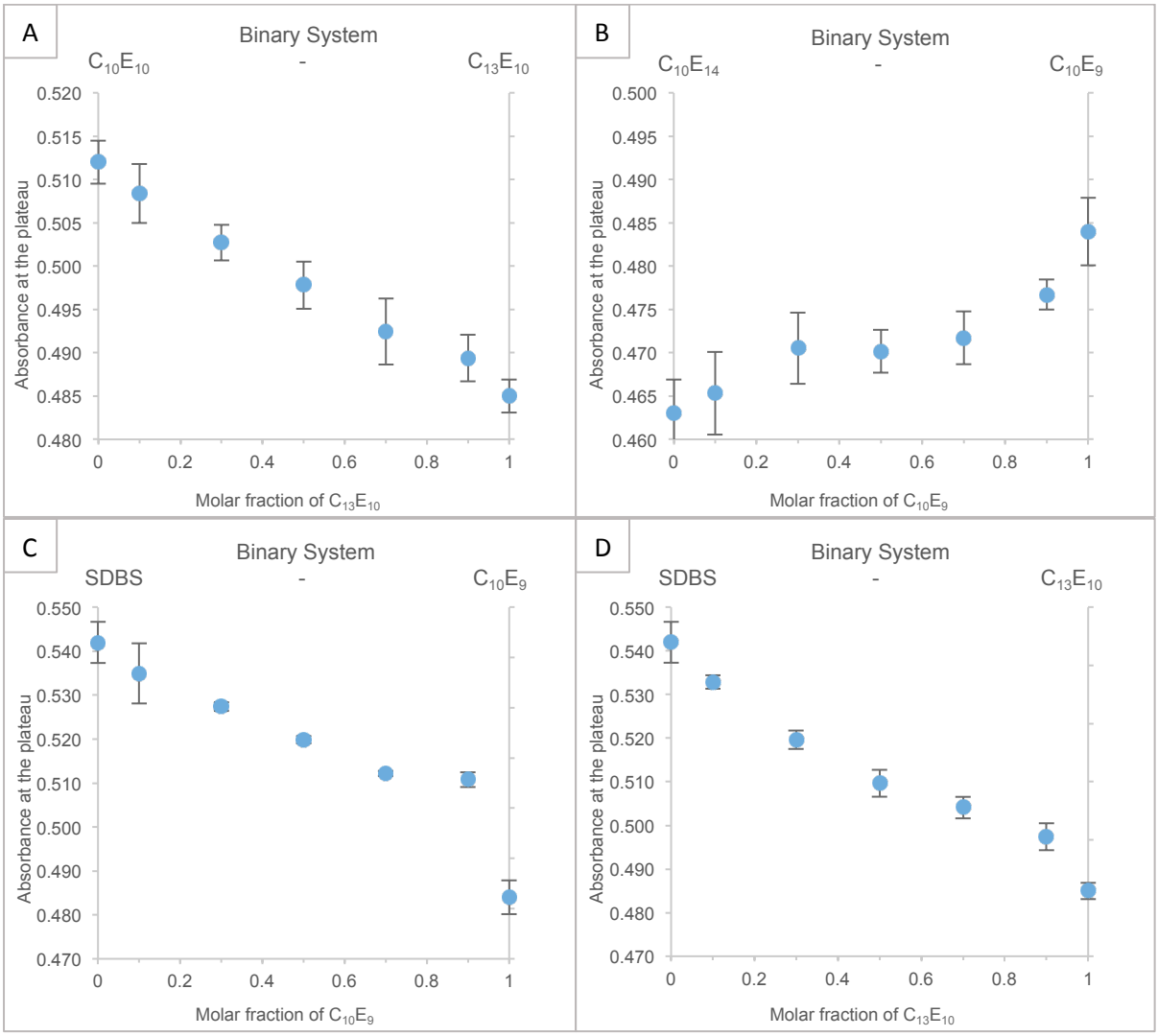

Figure 5.16: Evolution of the absorbance at the plateau of the dye-surfactants complex in several surfactant binary systems of A) $C_{10}E_{10}$ - $C_{13}E_{10}$, B) $C_{10}E_{14}$ - $C_{10}E_9$, C) SDBS - $C_{10}E_9$ and D) SDBS - $C_{13}E_{10}$.

First of all, it has to be noticed that the absorbance at the plateau of dye-surfactant complexes – with one surfactant – are a bit different with those reported in Table 5.1. This is likely due to the fact that the E4210’s stock solution used for the study of the interaction of one surfactant was different with the one used for the study using two surfactants, which could lead to a small variation in dye

concentration influencing the absorbance. From Figure 5.16, it can be observed that the absorbance at the plateau, and thus potentially the dye-surfactant interactions, seems to evolve linearly suggesting that the total interaction depends on the ratio of each surfactant. However, as synergic effects can occur regarding the CMC of a surfactant mixture leading to a nonlinear behaviour,[21] in the same way, the binding constant of a dye with a surfactant mixture should not be linear. Again, this would require further studies to rule on this.

5.2.2. Dye location in surfactant micelles

In order to know the location of the dye molecules within the surfactant micelles, three complementary methods were used.

5.2.2.1. UV-Vis spectrophotometric method

In the first instance, in order to know the location of the dye molecules within the surfactant micelles, the spectrophotometric method described in 5.1.4. Location of the dye in micelles was used. For this, as both dyes are not soluble in alkane solution which could mimic the hydrophobic part of nonionic surfactants (like decane – C10), the adsorption band of the dyes was compared in a surfactant solution at high concentration – in order to have a large amount of dye molecules incorporated in surfactant micelles – with the adsorption band of the dyes in PEG 200 to mimic the ethoxylate environment of the hydrophilic part of the nonionic surfactants. The results are also compared to the dye absorption in water without any surfactant, see Figure 5.17. For both dyes, the adsorption band of the dye in surfactant solution and the dye in PEG200 solution are very similar and different to that of the aqueous dyes without surfactant, suggesting the location of dye molecules is in the hydrophilic part of micelles for E4210 and V200, so that the dyes are interacting predominantly with the ethoxylate chain of the nonionic surfactants. However, this method just gives an idea on the environment surrounding the dye molecules without any certainty; it is not possible to affirm if the dye molecules are located at the surface of the micelles, or if they are trapped in the ethoxylate chains or if they are at the interface between the hydrophilic and the hydrophobic part as shown in Figure 5.18. A SAXS study could bring information about the location of the dye within the micelle and an NMR study will bring greater insight into the nature of the dye-surfactant interactions.

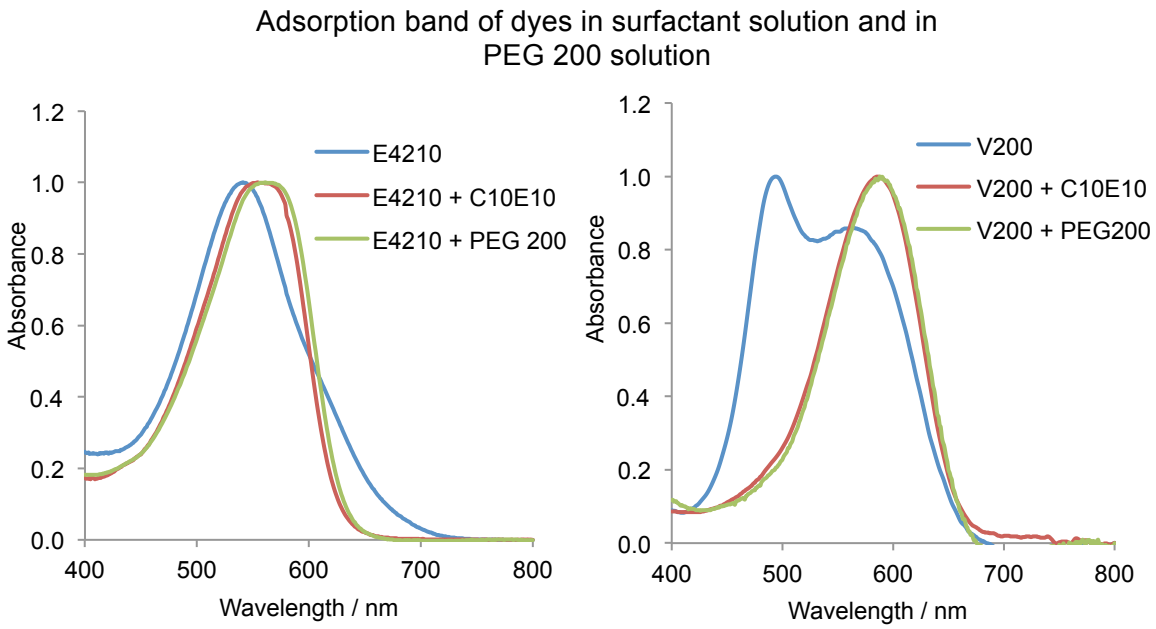

Figure 5.17: Comparison of the adsorption band of E4210 and V200 in surfactant solution and in PEG 200.

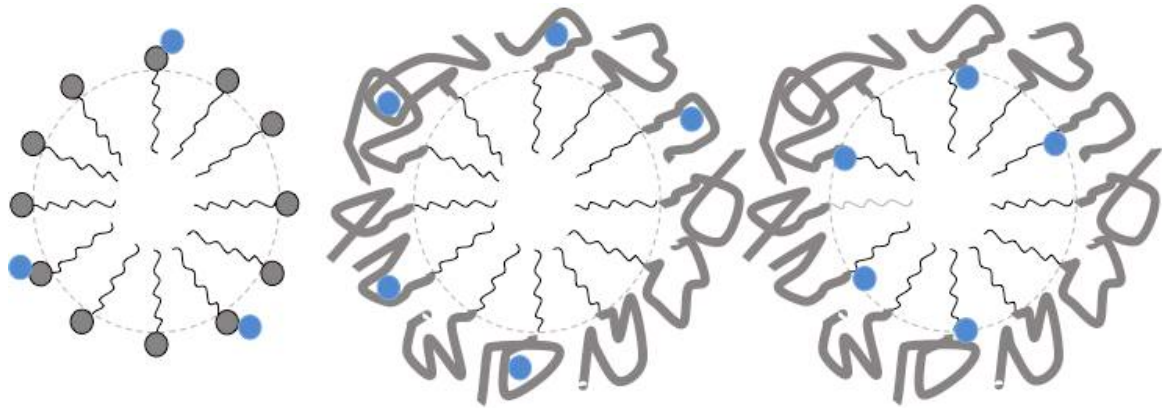

Figure 5.18: Dye molecules location in NI surfactant micelles.

5.2.2.2. SAXS method

As SAXS is widely used to access the micelle size of surfactant system above its CMC, this method was used to find the dye molecules' location within the surfactant micelles to greater precision than the spectrophotometric method. Indeed, the SAXS allows the determination of the micelle diameter, D_0. If the difference in electron density between the hydrophilic and the hydrophobic parts in comparison to the matrix material is important, it can be possible to determine the inner core diameter of the micelle, D_1, corresponding to the hydrophobic part; and thus by the difference, the outer core of the micelle, corresponding to the hydrophilic part. Thus, by comparing the results of the surfactant micelle itself and the surfactant micelle in the presence of dye molecules, it should be possible to locate the dye molecules within the surfactant micelles (see Figure 5.19).

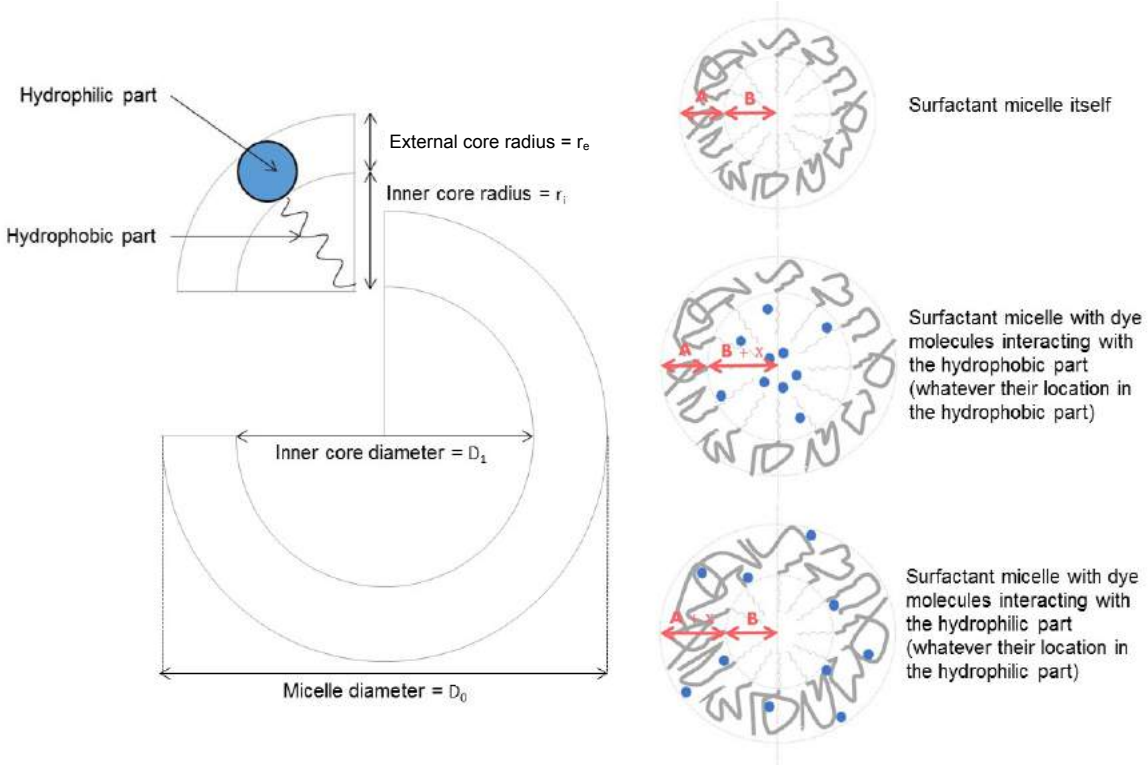

Figure 5.19: Surfactant micelle dimensions and possible results from the SAXS.

Thus, using SAXS, two anionic surfactants have been studied, SDS and SDBS as well as two nonionic surfactant with 10 carbons, $C_{10}E_{10}$ and $C_{10}E_{14}$, and two nonionic surfactants with 13 carbons, $C_{13}E_{10}$ and $C_{13}E_{20}$. For this, the preparation of two samples of each surfactant in deionised water at a concentration of 20 mM was performed – a surfactant concentration above the CMC but not too high, giving a mass percentage from 0.59 to 2.16 % depending on the surfactant, in order to minimise the impact of the structure factor S(*q*). For each surfactant, one sample contained only the surfactant in deionised water and the other one contained the dye E4210 at a concentration of 200 mM (in order to give an approximate dye concentration of 20 mM since the E4210 effective concentration is of 8.00 %). SAXS was performed on each sample for 7 hours and then the resulting *I*(*q*) vs. *q* plot was analysed by GIFT method in order to obtain the PDDF, p(r), to access the micellar shape and structure. An example of the results obtained for $C_{10}E_{10,}$ $C_{13}E_{10}$ and SDBS in absence and in presence of E4210 is presented in Figure 5.20 and all the results are summarised in Figure 5.23. The analysis was first done using only the form factor and then was validated using the structure factor. Essentially no change was seen between both results, confirming that at these surfactant concentrations, the interparticle scattering giving rise to the structure factor was negligible.

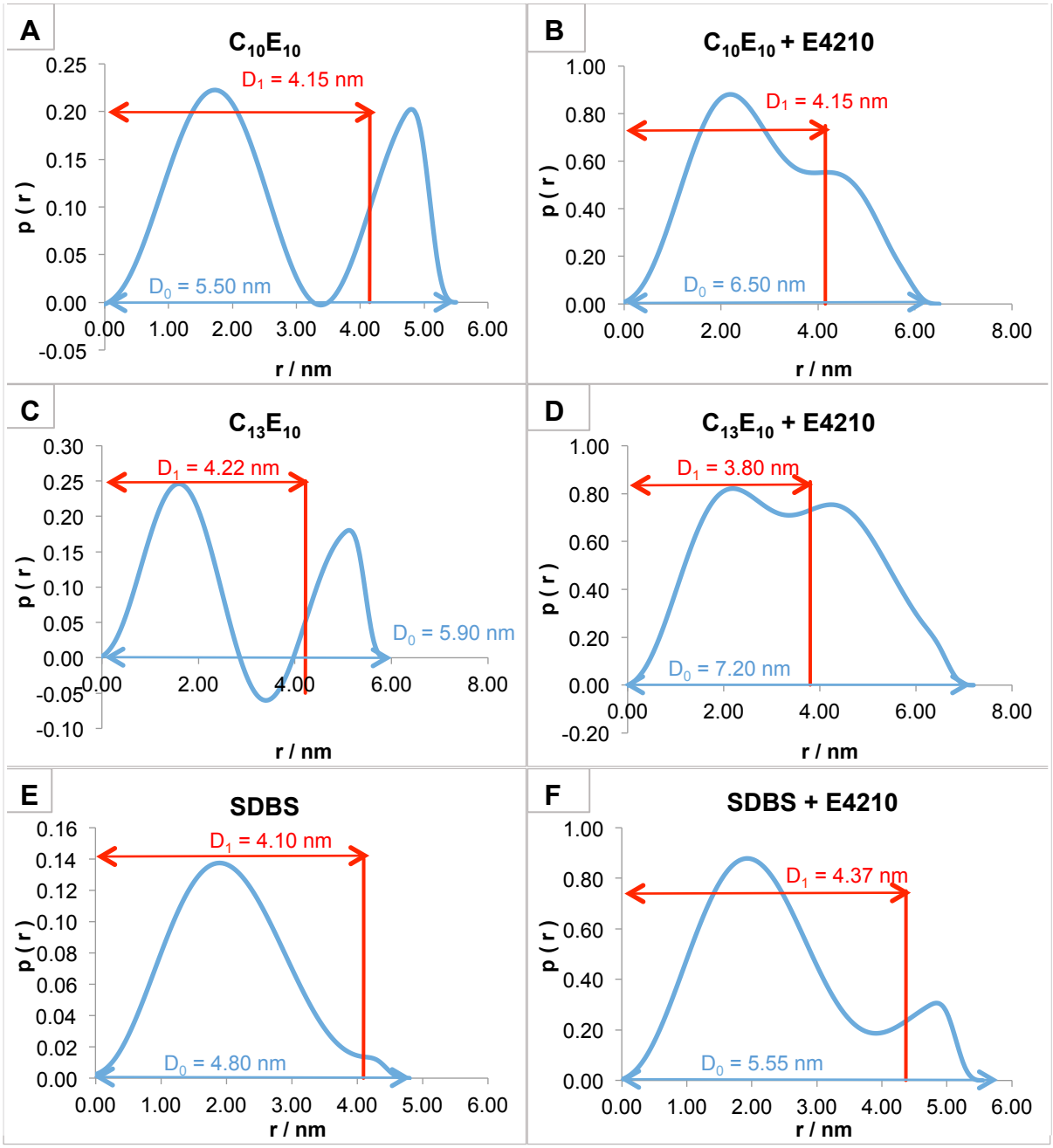

Figure 5.20: Pair distance distribution function, PDDF, for A) $C_{10}E_{10}$, B) $C_{10}E_{10}$ in presence of E4210, C) $C_{13}E_{10}$, D) $C_{13}E_{10}$ in presence of E4210, E) SDBS and F) SDBS in presence of E4210.

In order to compare the experimental results with the theory, the theoretical length of one surfactant molecule was calculated to have an idea on the micelle radius length (see Figure 5.22). For this, a length of 0.154 nm was used for the C-C bond, and an angle of 109.5 ° for the hydrocarbon chain, so that three consecutive carbons in a trans conformation have a length of 0.252 nm. A length of 0.134 nm was used for the C=C bond, 0.109 nm for the C-H bond, 0.150 nm for the C-O bond, 0.105 nm for the O-H bond, 0.183 nm for the C-S length, 0.1481 nm for the S-O bond, and 0.142 nm for the S=O length,[22] alongside angles of 117.4 ° for the angle C=C-C,

109.5 ° for the angles of C-O-C, O-S-O, O-S=O and C-S-O; and 105° for the angles of C-O-C and C-O-H determined from the VSEPR (Valence Shell Electron Pairs Repulsion) theory[23] (see Figure 5.21), which is based on the fact that the spatial structure of a molecule depends on the arrangement of the electrons around the central atom. As surfactant molecules do not adopt all-trans conformations at ambient temperatures, thus a correction coefficient of 0.8 was have been used to mimic some gauche conformations being present. That is why a size of 5.89 nm for 20 ethoxylated groups can be observed while the size obtained for 10 ethoxylated groups is 2.98 nm (see Figure 5.23).

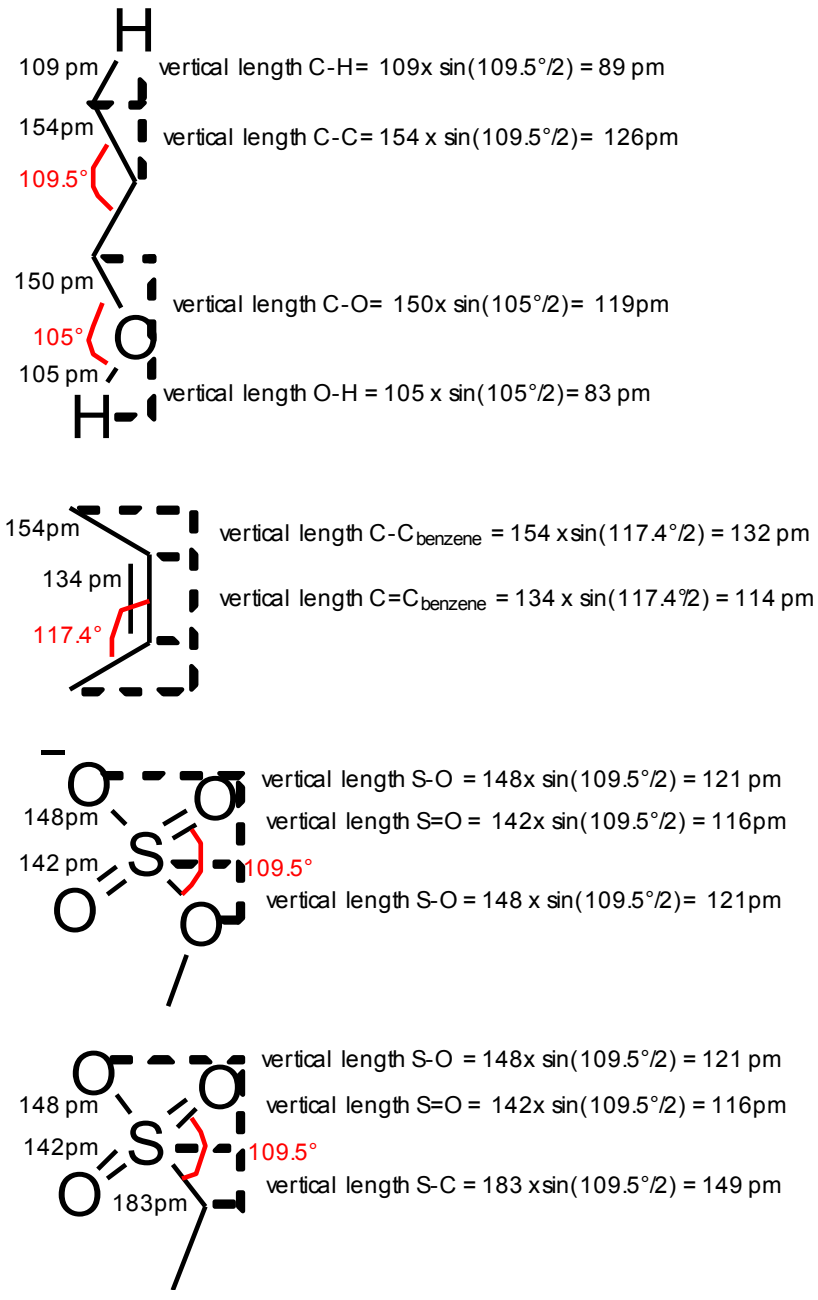

Figure 5.21: Chemical structures, lengths and angles of bonds.

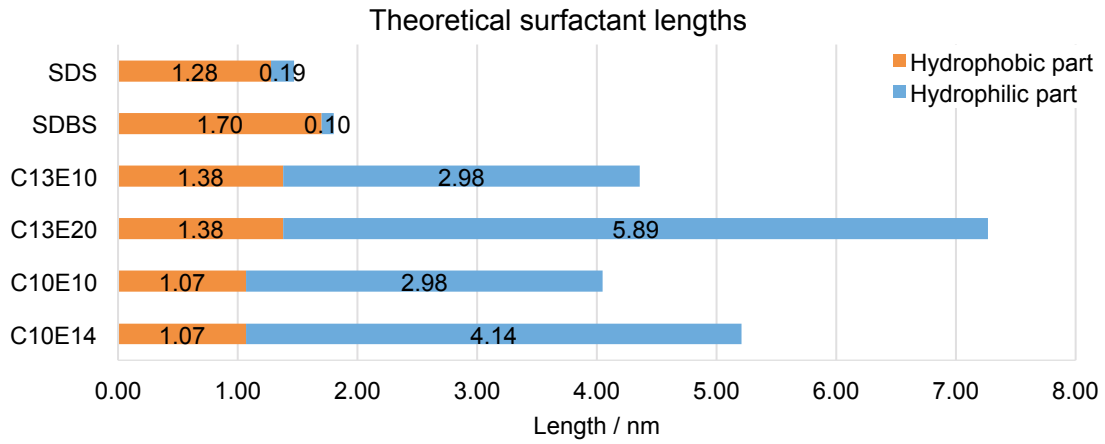

Figure 5.22: Theoretical structural lengths of the different surfactant micelles.

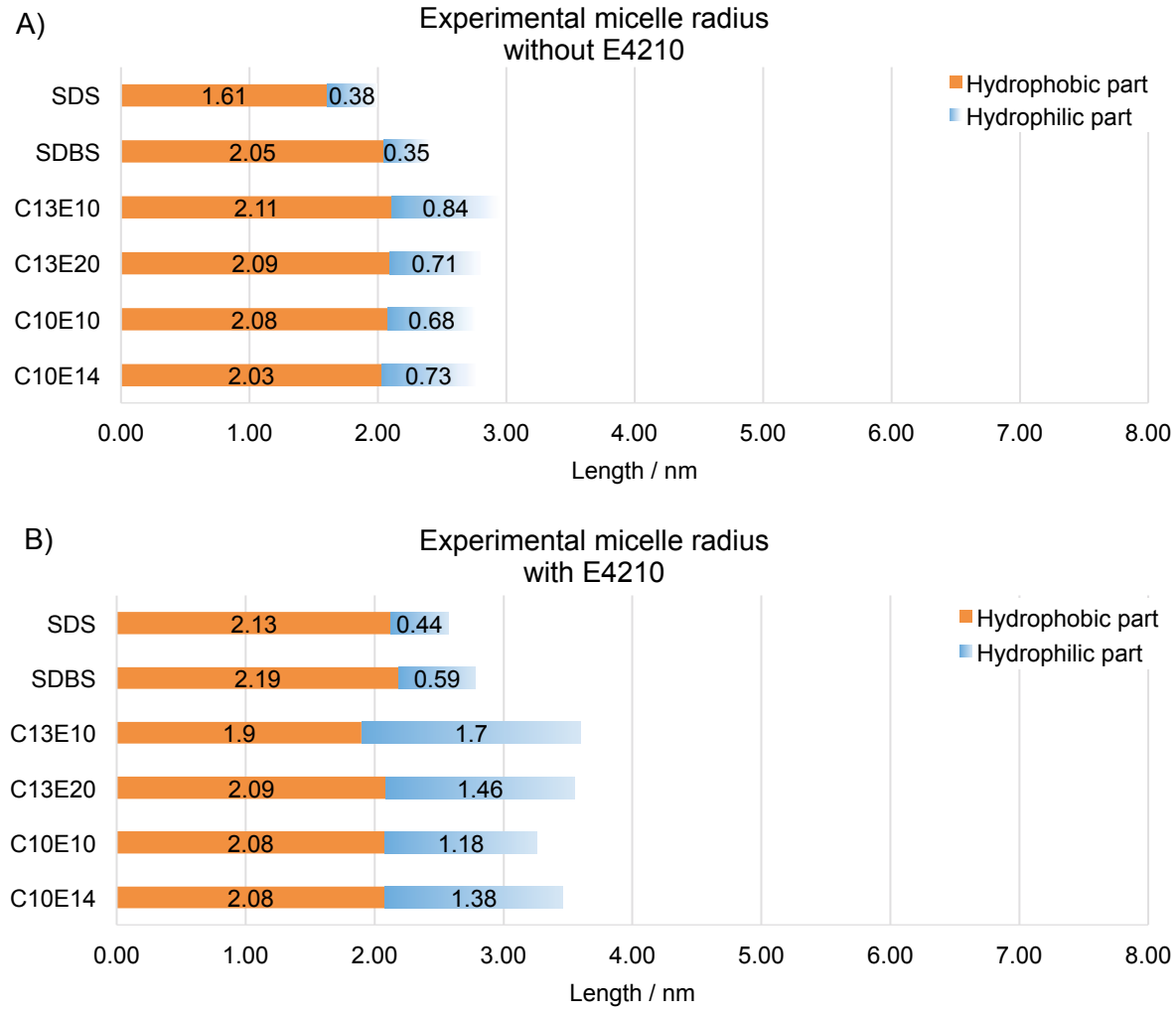

Figure 5.23: Experimental structural lengths of the different surfactant micelles A) in absence and B) in presence of dye molecules (E4210).

First of all, looking at the PDDF of $C_{10}E_{10}$ in absence and in presence of E4210 on Figure 5.20 A) and B) respectively, it can be easily distinguished two peaks in the absence of dye molecules, while in the presence of dye molecule they are quite

close, with the first one higher than the second one. Aggregate systems have this arrangement, but so do core-shell particles with significantly larger core radii than shell thicknesses, and in our systems, the micelles are core-shell structures.

Now looking at and comparing Figure 5.22 and Figure 5.23 A) and B) showing the structural lengths obtained theoretically and experimentally in the absence and presence of E4210, respectively, a difference is immediately observed in the hydrophilic part length between the theoretical and experimental values for the nonionic surfactants. Indeed, the values obtained by SAXS are really short compared to the theoretical values for these nonionic surfactants. This is because when using the SAXS, the difference in electron density between the core and the shell regarding the matrix material is used to produce the PDDF. However, in this case, water molecules are present in the outer region of the nonionic surfactant micelles, which give an outer region of the shell with an electron density close to the matrix material (water molecules). This is why on the PDDF, it is only observed a short part of the hydrophilic part which corresponds to the part closest to the hydrophobic part where less water molecules are present. The fact that only slightly longer lengths in the presence of dye molecules are obtained suggests that dye molecules are localised close to the hydrophobic-hydrophilic border. Otherwise, if they were localised in the middle of the hydrophilic part or even at the surface of the micelles, this should affect a lot the difference in electron density compared to the matrix material and the hydrophilic length should be more observed on the PDDF.

Knowing this, only the hydrophobic part length obtained experimentally (without E4210) can be compared with the theoretical lengths. Thus, it can be observed that the experimental results have closer agreement with the theoretical values, compared to the hydrophilic case, but in this case, the experimental values are longer than theory predicts, particularly for the nonionic surfactants. However, the nonionic surfactants are not pure, and have a range of hydrocarbon lengths and this is the most likely reason for the increased experimental values.

Now comparing the results obtained in the absence and presence of E4210, it can be observed for the nonionic surfactants that the hydrophobic part remains almost constant while an increase of approximately 0.7 nm of the hydrophilic part in the presence of E4210 is observed. Regarding the anionic surfactants, as the hydrophilic part is really short, an increase of approximately 0.8 nm divided between the

hydrophobic and the hydrophilic part can be observed. Thus, all these results show a localisation of E4210 molecules in the hydrophilic part close to the hydrophobic part. To conclude, the SAXS is a good method to localise dye molecules in surfactant micelles. However, the NMR method is the best one to use to get more information about the interactions between dye and surfactant molecules.

5.2.2.3. ^{1}H NMR method

In order to get more information on the interactions between dye and surfactant molecules and hence their relative locations, NMR studies were performed with E4210 and 6 surfactants (the same used for the SAXS study: $C_{10}E_{10}$, $C_{10}E_{14}$, $C_{13}E_{10}$, $C_{13}E_{20}$, SDS and SDBS) comprising ^{1}H, NOESY and HSQCAD studies. The NOESY (Nuclear Overhauser Effect SpectroscopY) method's aim is to identify spins undergoing cross-relaxation and to measure the cross-relaxation rates; moreover, it only depends on the spatial proximity between protons. In other words, the cross peaks of a NOESY spectrum indicate which ^{1}H's are close to some other ^{1}H's in space. The HSQCAD method (Heteronuclear Single Quantum Coherence spectroscopy) was used as a complement for the interpretation of ^{1}H spectra since it correlates ^{1}H and ^{13}C spectrum in order to attach one proton to its bonded carbon.

All samples were prepared in deuterium oxide containing 0.05 *wt.* % of Trimethylsilylpropanoic acid (TSP), which is used as an internal reference at 0 ppm. Thus, one sample of each surfactant at 20 mM and a sample of E4210 at 200 mM (in order to give an approximate dye concentration of 20 mM since the E4210 has an effective concentration of 8.00 %) were prepared in order to identify each part of the molecules in the spectra. Then a sample of E4210 with each surfactant at the same concentration for comparison was prepared. Some spectra are presented below for the discussion with all the spectra and ^{1}H NMR interpretations presented in appendix.

First of all, as E4210 is a big and complex molecule with six aromatic rings, even if some peaks (see appendix) to the right protons could be attributed, it was quite difficult to attribute each peak to the respective protons. Moreover, the high concentration of polyethylene glycol and impurities in E4210 raw material increases the complexity. Note that, only the commercial form was used for the NMR study. Regarding surfactants, each peak could be attributed to the right proton (see appendix). However, the HSQCADs of nonionic surfactants correlates the $-CH_3$

proton to several carbons while there is only one $-CH_3$ on each nonionic surfactant molecules localised at the end of the hydrophobic chain. This shows the non-purity of the nonionic surfactant raw materials discussed previously, since a particular proton would also correlate to a shorter/longer carbon chain.

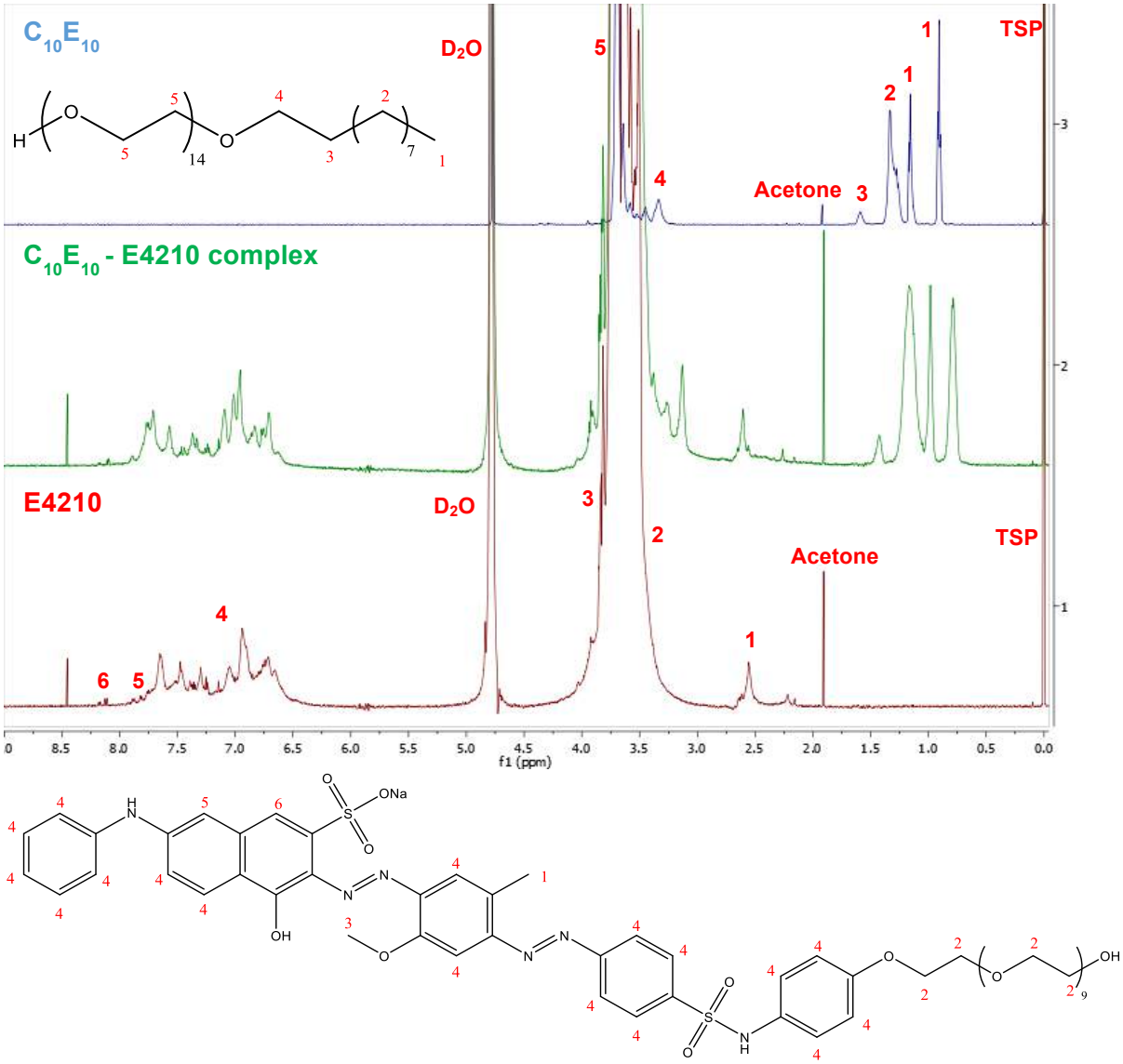

Figure 5.24: ^{1}H NMR of $C_{10}E_{10}$ in blue (on the top), of the E4210-$C_{10}E_{10}$ complex in green (in the middle) and of E4210 in red (at the bottom).

For the discussion, the results for the E4210-$C_{10}E_{10}$ complex will be used as example, which was compared to $C_{10}E_{10}$ only and E4210 only. Note that the other nonionic surfactants differ only by the number of carbons and/or the number of ethylene oxide groups, so they gave essentially the same results; only the intensity of the shift changes. Regarding the two anionic surfactants studied (SDS and SDBS), they were interpreted with the same method. Moreover, as they do not possess an ethoxylated chain like the nonionic surfactants, the shift of the dye

ethoxylated chain in the dye-surfactant complex has been used compared to the dye ethoxylated chain without surfactant as a reference in order to compare the intensity of the dye-surfactant interaction between each surfactant.

Looking at the Figure 5.24, the difference between the ^{1}H spectrum of the dye-surfactant complex with the surfactant and the dye can be observed. The shift of the peaks can also be visualised in Figure 5.25 where the three spectra are superimposed.

By taking the peak value of a) the ethoxylated chain of the dye, b) the surfactant and c) the dye-surfactant complex (see Figure 5.25), a chemical shift at 2217.57 Hz, 2251.53 Hz and 2219.25 Hz is obtained, respectively; giving a delta shift of 32.28 Hz between the dye-surfactant complex and the surfactant, and of 1.68 Hz between the dye-surfactant complex and the dye. Note that we can observe bigger delta shifts looking at other peaks (e.g. around 100 Hz for the surfactant carbon chain – see appendix), so these values are relatively small. The delta shifts of the ethoxylated chain between E4210 and each surfactant and dye surfactant complex are reported in Table 5.2. Note that spectra were recorded in a 600 MHz instrument so that the frequency in Hz is obtained from the chemical shift in ppm by the following relation:

$$\text{Chemical shift (ppm)} \times 600 = \text{Frequency (Hz)} \qquad \textbf{Eq. 5.21}$$

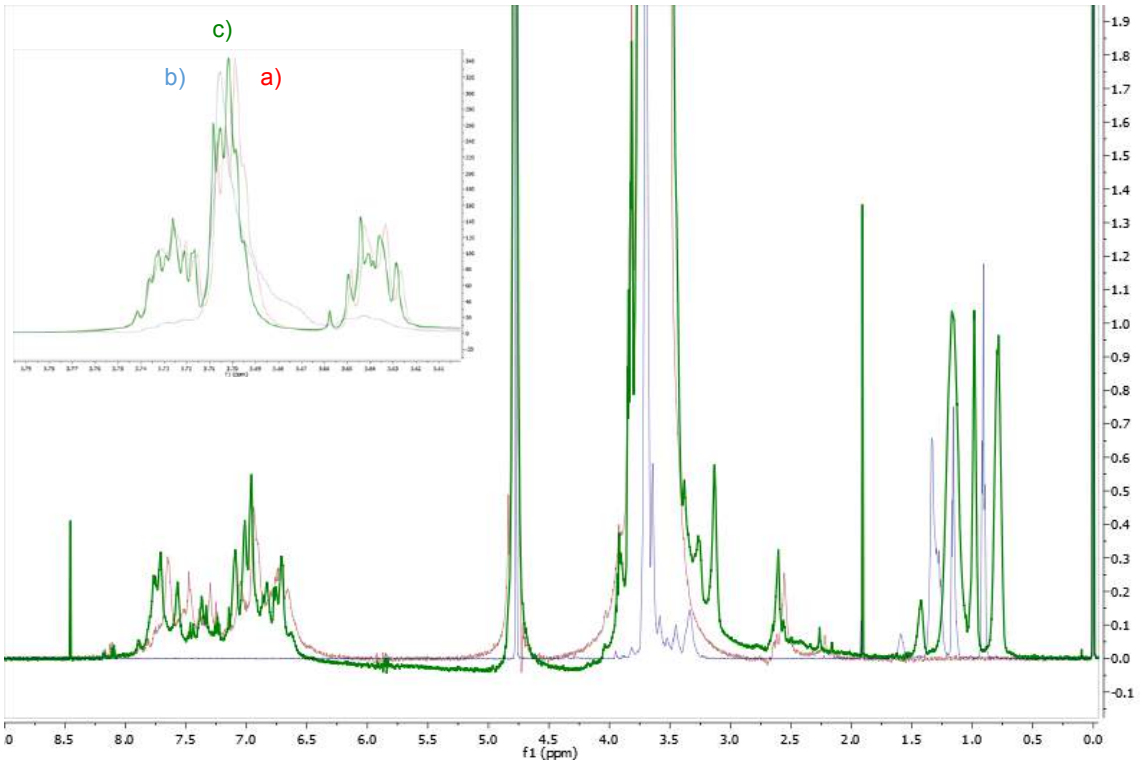

Figure 5.25: ^{1}H NMR superimposed of $C_{10}E_{10}$ in blue, E4210-$C_{10}E_{10}$ complex in green and of E4210 in red.

Table 5.2: Chemical shift of the ethoxylated chain of the dye and dye-surfactant complex; with the delta shift between each other.

Surfactant	E4210 shift / Hz	E4210-surfactant shift / Hz	Delta shift (/Hz) between dye-surfactant complex and surfactant / dye
C10E10	2217.57	2219.25	1.68
C10E14	2217.57	2219.37	1.80
C13E10	2217.57	2219.07	1.50
C13E20	2217.57	2219.76	2.19
SDS	2217.57	2216.56	1.01
SDBS	2217.57	2216.39	1.18

In Table 5.2, it can be clearly observed that the delta shift for the two anionic surfactants between the ethoxylated chain of the dye in absence and in presence of surfactant is lower than for the four nonionic surfactants. This supports the fact that the dye-surfactant interactions are more important for nonionic surfactants than anionic surfactants with almost the same carbon chain lengths. Moreover, by comparing the delta shift between the ethoxylated chain of the dye in absence and in presence of surfactant of $C_{10}E_{10}$ with $C_{10}E_{14}$, and $C_{13}E_{10}$ with $C_{13}E_{20}$, it can be observed that the delta shift, and thus the dye-surfactant interactions, are greater for increasing numbers of ethoxylated groups. In comparison, for increasing number of carbons ($C_{10}E_{10}$ to $C_{13}E_{10}$), the delta shift decreases slightly. But this would need more results to validate this trend.

Now looking at the difference between the NOESY of the complex (E4210-$C_{10}E_{10}$) with the surfactant ($C_{10}E_{10}$) and the dye (E4210) in Figure 5.26 and Figure 5.27 respectively, new spots can be observed – and also for all the dye-surfactant complexes studied (see appendix) – that are not present in the NOESY of the surfactant and the dye.

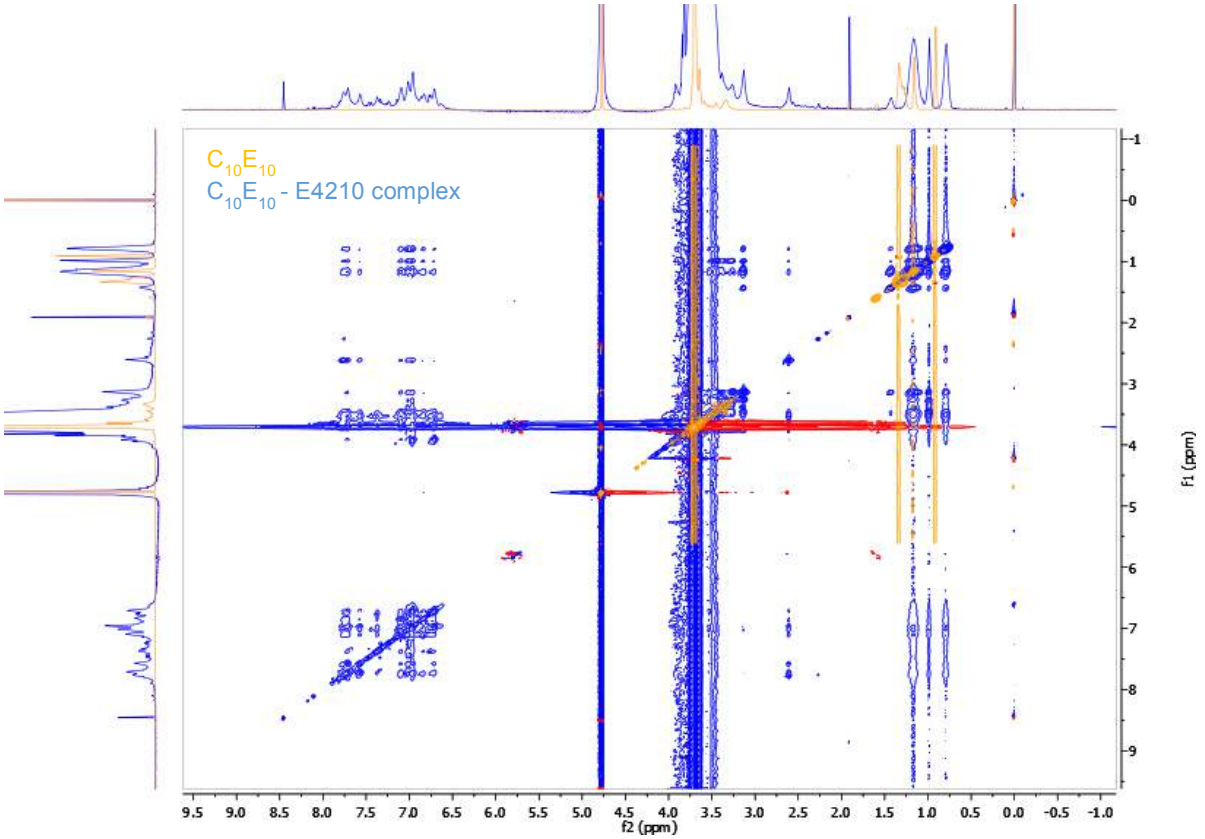

Figure 5.26: Superimposed NOESY of the surfactant $C_{10}E_{10}$ in yellow and the dye-surfactant complex E4210-$C_{10}E_{10}$ in blue.

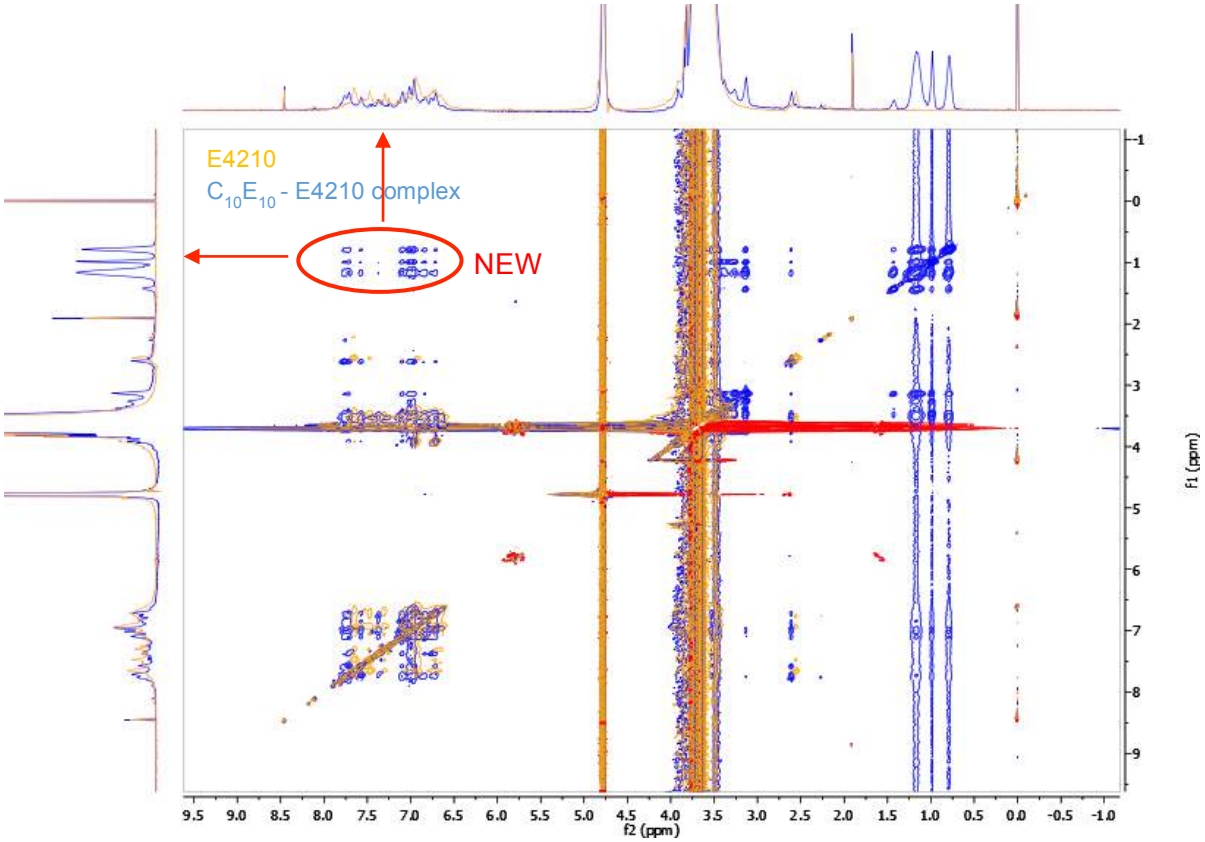

Figure 5.27: Superimposed NOESY of the dye E4210 in yellow and the dye-surfactant complex E4210-$C_{10}E_{10}$ in blue.

By looking at the ^{1}H NMRs above and on the left of the NOESY, it can be observed that the new spots are coming from the aromatic part of the dye and the carbon chain of the surfactant. This means that they are close to each other in space and thus that they are probably interacting together.

To conclude, when it is possible to use this technique, the NMR is the best method to use in order to know the exact location of the interactions between two compounds – dye and surfactant in this case. Now, from all the experiments it can be affirmed that the dye is located within the hydrophilic part of the micelles with both ethoxylated chains from the dye and the surfactant interacting together, but also close to the hydrophobic part of the micelles, so that it is also interacting with the aromatic part of the dye. Finally, it can be concluded that the dye is located at the hydrophilic/hydrophobic interface and in this aspect, it is similar to a co-surfactant.

5.3. Conclusion

The spectrophotometric method enables a good visualisation of the dye-surfactant interaction and the Benesi-Hildebrand equation is a simple method to access the binding constant of the dye-surfactant complex. However, there are some parameters to be careful of, like the concentration of the dye regarding the surfactant concentration, or again the dye concentration and the temperature which has to be constant throughout the experiments since it can impact a lot on the final result. Moreover, using UV-vis spectroscopy, the choice of the solvent is important due to the solvatochromic effect, as well as the choice of the surfactant, which has to be completely soluble to give a transparent and homogeneous solution.

The UV-vis spectroscopy allowed us to visualise the incorporation of dye molecules in surfactant micelles with the shift of the absorption band caused by a change in the local environment surrounding the dye influencing the electronic structure of the chromophore. Regarding V200, the dissolution of the aggregates helped by the surfactant is first observed. Due to this phenomenon, only E4210 was studied using the B-H equation. However, using the B-H equation in a UV-Vis spectrophotometric method, it is important to be careful on raw materials and concentration ranges of study. The dye must not be in an aggregate form and the surfactant must be totally soluble in the concentration range of study. The dye must be in a concentration leading to acceptable absorbance intensity – being careful to use the effective concentration of dye molecules if it is diluted in a solvent – and has

to be kept constant in a study to avoid fluctuations in results – it is preferred to use the same dye stock solution for one study. Regarding the surfactant concentration, it must satisfy $[S]_0 > 100 \times [D]_0$ to validate the B-H equation but it should not be so high that an absorbance plateau is reached. In this thesis, by mistake, the effective concentration of E4210 molecules was not taken into account in the experiments. Consequently a huge difference in concentration between dye and surfactant concentration was obtained with effectively all the dye being incorporated into the surfactant micelles for all the surfactant concentrations studied. This led to a plateau of the maximum of absorbance that makes the B-H equation unusable, giving negative values of the binding constant for the dye-surfactant complex. For this reason, the hypothesis where the absorbance at the plateau would be correlated with the intensity of the dye-surfactant interaction was made, i.e. the greater the absorbance at the plateau, the greater the interactions between the dye and surfactant molecules. Making this hypothesis, it could be thus observed that as a function of the number of EO in a nonionic surfactant series, the absorbance at the plateau, and thus potentially the dye-surfactant interaction, increases to a maximum and then decreases. This maximum seems to have the same characteristic for two surfactant series, one with 10 carbons and another with 13 carbons – with a HLB around 14.40 and a number of EO units close to the number of EO units in the E4210 ethoxylated chain. Regarding the number of carbons, it seems that the absorbance at the plateau, and thus potentially the dye-surfactant interaction, is also affected by the number of carbons. However, for these last two observations mentioned, this is only a hypothesis since data obtained are not enough to reliably conclude. From the results obtained, it looks like anionic surfactants give a higher absorbance at the plateau, and thus potentially greater dye-surfactant interactions, with E4210 than nonionic surfactants; but again, it would also have been necessary to study more anionic surfactants. In a surfactant mixture, a second surfactant does not seem to perturb the system suggesting a linear evolution of the absorbance at the plateau proportional to the ratio of each surfactant. However, all the interpretations of the dye-surfactant interaction results are tentative and require further studies to elucidate the correct value of the dye-surfactant binding constants. Moreover, in a surfactant mixture, synergy between them can occur so that a nonlinear behaviour should be observed.

Regarding the dye location, it has been observed that the UV-vis spectroscopy is only able to give an idea of the dye location by mimesis of the dye environment using the solvatochromic effect. SAXS is a better method to get the dye molecule's location within surfactant micelles. However, to know the exact position and where the interactions take place, the NMR remains the best method. Thus, from the results of these techniques, it can be affirmed that E4210 molecules are localised within the hydrophilic part of the micelles with both ethoxylated chains from the dye and the surfactant interacting together, but also close to the hydrophobic part of the micelles so that the aromatic part of the dye interacts with the surfactants' hydrophobic tail groups. In other words, the dye is located at, or close to, the hydrophobic/hydrophilic border.

References

[1] R. Christie, *Colour Chemistry*, 2001.

[2] M. J. Minch and S. S. Shah, 'Spectroscopic Studies of Hydrophobic Association. Merocyanine Dyes in Cationic and Anionic Micelles', *The Journal of Organic Chemistry* 44, no. 18 (1979): 3252–3255.

[3] S. S. Shah, G. M. Laghari, and K. Naeem, 'A Spectroscopic Study of Hemicyanine Dyes in Anionic Micellar Solutions', *Thin Solid Films* 346, no. 1–2 (1999): 145–149.

[4] M. Sarkar and S. Poddar, 'Studies on the Interaction of Surfactants with Cationic Dye by Absorption Spectroscopy', *Journal of Colloid and Interface Science* 221, no. 2 (2000): 181–85.

[5] S. Göktürk and M. Tunçay, 'Spectral Studies of Safranin-O in Different Surfactant Solutions', *Spectrochimica Acta Part A: Molecular and Biomolecular Spectroscopy* 59, no. 8 (2003): 1857–66.

[6] S. Göktürk and M. Tuncay, 'Dye-Surfactant Interaction in the Premicellar Region', *Journal of Surfactants and Detergents* 6, no. 4 (2003): 325–330.

[7] S. Fazeli, B. Sohrabi, and A. R. Tehrani-Bagha, 'The Study of Sunset Yellow Anionic Dye Interaction with Gemini and Conventional Cationic Surfactants in Aqueous Solution', *Dyes and Pigments* 95, no. 3 (2012): 768–75.

[8] A. R. Tehrani-Bagha and K. Holmberg, 'Solubilization of Hydrophobic Dyes in Surfactant Solutions', *Materials* 6, no. 2 (2013): 580–608.

[9] H. A. Benesi and J. H. Hildebrand, 'A Spectrophotometric Investigation of the Interaction of Iodine with Aromatic Hydrocarbons', *Journal of the American Chemical Society* 71, no. 8 (1949): 2703–2707.

[10] B. K. Seal, H. Sil, and D. C. Mukherjee, 'Independent Determination of Equilibrium Constant and Molar Extinction Coefficient of Molecular Complexes from Spectrophotometric Data by a Graphical Method', *Spectrochimica Acta Part A: Molecular Spectroscopy* 38, no. 2 (1982): 289–292.

[11] S. Göktürk and M. Tunçay, 'Spectral Studies of Safranin-O in Different Surfactant Solutions', *Spectrochimica Acta Part A: Molecular and Biomolecular Spectroscopy* 59, no. 8 (2003): 1857–66.

[12] M. Sarkar and S. Poddar, 'Spectral Studies of Methyl Violet in Aqueous Solutions of Different Surfactants in Supermicellar Concentration Region', *Spectrochimica Acta Part A: Molecular and Biomolecular Spectroscopy* 55, no. 9 (1999): 1737–1742.

[13] S. Yefimova, 'Spectroscopic Studies of Dye-Surfactant Interactions in Aqueous Solution in Pre- and Post- Micelle Formation Cencentration Ranges', *Functional Materials* 16, no. 1 (2009).

[14] P. F. Tavčer and J. Špan, 'Dye-Surfactant Interactions Studied Using Job's Method', *Textile Research Journal* 69, no. 4 (1999): 278–284.

[15] A. Agbabiaka, M. Wiltfong, and C. Park, 'Small Angle X-Ray Scattering Technique for the Particle Size Distribution of Nonporous Nanoparticles', *Journal of Nanoparticles* 2013 (2013): 1–11.

[16] H. Schnablegger and Y. Singh, *The SAXS Guide: Getting Acquainted with the Principles*, 2nd ed. (Austria: Anton Paar GmbH, 2011).

[17] J. Brunner-Popela and O. Glatter, 'Small-Angle Scattering of Interacting Particles. I. Basic Principles of a Global Evaluation Technique', *Journal of Applied Crystallography* 30, no. 4 (1997): 431–442.

[18] B. Weyerich, J. Brunner-Popela, and O. Glatter, 'Small-Angle Scattering of Interacting Particles. II. Generalized Indirect Fourier Transformation under Consideration of the Effective Structure Factor for Polydisperse Systems', *Journal of Applied Crystallography* 32, no. 2 (1999): 197–209.

[19] L. N. Guo et al., 'Solution Behavior of Dye-Surfactant Associations', *Journal of Colloid and Interface Science* 163 (1994): 334–46.

[20] C. Reichardt, 'Solvatochromic Dyes as Solvent Polarity Indicators', *Chemical Reviews* 94, no. 8 (1994): 2319–2358.

[21] M. Bergström and J. C. Eriksson, "A Theoretical Analysis of Synergistic Effects in Mixed Surfactant Systems," *Langmuir* 16, no. 18 (2000): 7173–81.

[22] Gong-du Zhou, *Fundamentals of Structural Chemistry* (World Scientific, 1993).

[23] R. J. Gillespie, 'The Valence-Shell Electron-Pair Repulsion (VSEPR) Theory of Directed Valency', *Journal of Chemical Education* 40, no. 6 (1963): 295.

6. Dye Deposition onto Fabric

As there are several kinds of fabrics, which differ according to their chemical composition, there are several classes of dye (discussed in Chapter 4, 4.1.5. Classification) capable of interacting with specific fabrics. In the dyeing process, surfactants are also used to act in different ways and represent about 37 % of the global surfactant market.[1] To understand properly dyeing mechanisms, it is therefore important to take into account dye-surfactant, dye-fibre and surfactant-fibre interactions. This section will talk about the dye-fibre interactions.

6.1. Introduction

6.1.1. Introduction on fabrics

Fabrics differ in their chemical composition/contamination and also in their property/morphology, texture and structure, which can affect the fibre wettability.[2] Surfactants are used to wet fabrics;[2] however, anionic surfactants have better wetting performance while nonionic have better deaeration properties (to have better wetting effects, surfactants must have an HLB in a range of 7-9).[1] Thus, according to the fibre structure and/or composition, the interactions between dyes and fibres will be affected by the surfactants as well as the dyeing.

The fibre classification is firstly done by their origin, i.e., either natural or made-made; then it is divided in terms of their chemical functionalities (see Figure 6.1).

Flax

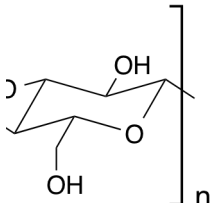

azotable dyes,
s, reactive dyes,

Protein

Wool | **Silk**

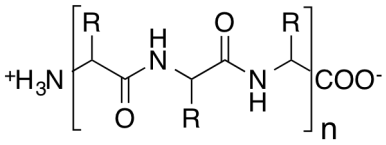

R = amino acids

Wool: cysteine, lysine, arginine, histidine, aspartic and glutamic acid

Silk: glycine, alanine, serine, tyrosine and aspartic acid

Dyed by: direct dyes, reactive dyes, acid dyes, metal-complex dyes

Regenerated
Transformation of natural polymer and particularly cellulose

Rayon | **Viscose** | **Lyocell** | **Acetate**

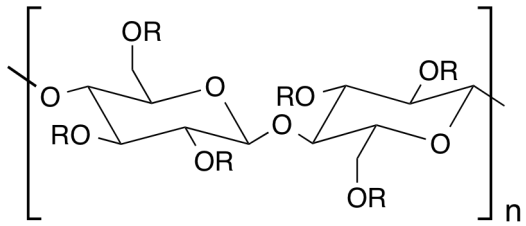

Cellulose Acetate (R = $COCH_3$ or H)

Viscose = Cellulose Xanthate (R = CS_2Na or H)

Dyed by: direct dyes, azo dyes, sulfur dyes, vat dyes, reactive dyes

Syntheti

Nylon

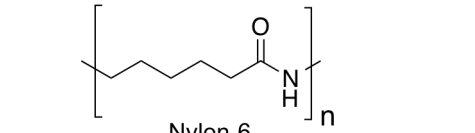

Nylon 6

Nylon 6,6

Dyed by:

Spandex

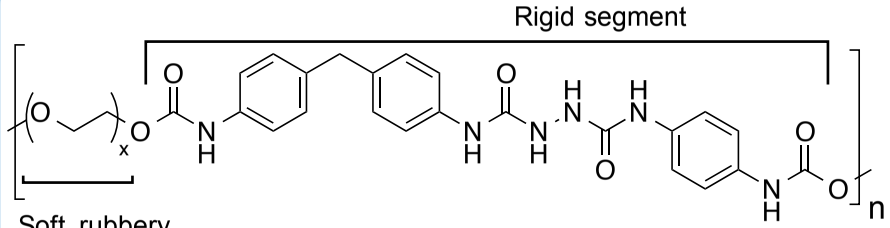

Rigid segment

Soft, rubbery segment

Dyed by: reactive dyes

Acrylic

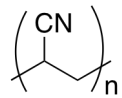

Dyed by:
cationic dyes,
anionic dyes,
dispersed dyes,
basic dyes

Polyole

Polypropy

Polyethyl

Dyed by:
dyes, disp
dyes, vat

6.1.2. Dye-fibre interactions

The main interaction between dye and fibre is the sorption of the dye onto the latter. The quantity of dye that sorbs onto the fibre is essentially governed by the different accessibilities of the fibre to the dye due to their differences in morphology, i.e. their surface areas, their accessible volumes and their electrical charges.[7] It has been shown that the fibre pore size distribution plays an important role in the fibre surface area because the pores have to be of a certain size to allow the sorption of the comparatively large dye molecules. The distribution of the fibre pore sizes, as well as the accessible volume for water, their internal surface area and their average pore diameter, can be accessed by column chromatography.[8] Additionally, if dye aggregation occurred, the accessible surface area for water would not change whereas the sorbed dye amount would be decreased, as many areas would become inaccessible to the bigger dye-aggregates. Overall, the relationship between pore sizes, molecule size and distribution coefficient appears to be very complex.[9,10] Thus the sorption is mostly governed by the morphology of the fibre but the electrical forces between fabric and dye also have to be considered as the electro-attraction or repulsion can affect the dye sorption.[11]

6.1.3. Dyeing process

Today, the dyeing process of materials is principally made industrially on a large scale. Prior to dyeing a textile, it generally has to be pre-treated[6] chemically or physically to remove all the textile impurities or the ones acquired during production that can affect the dyeing, and/or bleaching agents may be used to remove all traces of colours.

After this pre-treatment, the textile can be dyed following three common methods:[6] exhaustion dyeing (batch), continuous (padding) and printing.

In **exhaustion dyeing**, the dye is totally or partially soluble in the dyebath, where it is transported to the fibre surface by motion of the dye liquor or the textile. Then, the dye is adsorbed on the fibre surface to diffuse into the fibre and remain fixed to the fibre chemically or physically depending on the dye-fibre interactions. Usually exhaustion dyeing is conducted using dilute solutions of dye with a ratio by mass from 8:1 up to 30:1 of liquor to substrate. Auxiliaries, such as surfactants, are introduced into the dyebath before adding dyes in order to obtain a homogeneous

concentration of dye throughout the dyebath. As described above, the adsorption phase and the diffusion phase are the two main phases. During these phases, depending upon the dye used, the temperature and the pH can change to facilitate covalent fixation of the dye onto the textile. The dyeing is finished when the concentration in the fibre and the dyebath do not change significantly with time.

In **continuous dyeing**, the application and the fixation of the dye are carried out continuously in one simultaneous operation using working units assembled into a production line system including pre- and post-dyeing treatments. There are two types of dye application techniques: either by direct application of dye liquor by spraying, foam application, or printing; or by continuous immersion of the textile in a dyebath and removal of the excess of liquor by suction or squeeze rollers (padding) before being dried out. After drying, the dye is only deposited onto the surface of the textile and the next step is the fixation of the dye into the textile via a chemical reaction depending upon the dye and substrate involved (usually by heat).

In **printing**, direct printing is the most common method whereby the dyes are applied in a print paste form, containing thickeners and auxiliaries, via a roller or by screens. As for the padding, the textile is then dried out and steamed to allow the fixation of the dye into the textile.

Currently, some dyes, and particularly hueing or bluing dyes which exhibit good fabric deposition, are added in laundry detergents in order to give a “bluing” of white fabric to balance the yellowing of fabric which can occur after repeated laundering, thus giving a whiter fabric (and conversely, white fabrics also tend to become yellow over time due to oxidation, which causes the fabric to absorb more blue light and hence appear yellower). This is the case in Unilever’s[12] and Procter and Gamble’s[13,14,15] laundry detergents, which contain blue or violet dye at low concentration in the presence of surfactants. The dye has to have a good hueing efficiency value (defined by P&G) to get a good whitener effect and a good wash removal value to avoid the accumulation of dye into the fabric, which would give a bluish tint after repeated laundering. By this fact, in the context of this thesis, the use of hueing dyes is not to colour the fabric but essentially to give a whitening effect and thus the mechanism of dyeing could be assimilated to the exhaustion dyeing but with a much lower dye concentration which is transported to the fibre surface by motion of the textile and washing solution in the washing machine. Moreover, the dye is

chosen so that it is not fixed chemically to the fibre and can be removed in the next wash cycle in order to avoid long term overhue.

6.1.4. Dye sorption

During the dyeing process, there are three steps controlling the fabric dyeing, i.e. the dye sorption:[16]

- Transport of the dye through the dye bath to the fibre surface
- Adsorption of the dye at the fibre surface
- Diffusion of the dye from the surface to the interior of the fibre

The **transport of the dye** is essentially due to the flow of the dye liquor in the dyeing machine generated by a pump. In our case, for hueing dye in laundry products, the transport is done by water during the wash cycle after dissolution of the film containing the dye; assisted by the agitation of the washing machine. It is thus important to take into account the quantity of fabric incorporated into the machine: if there are too many fabrics, the agitation and thus the dye transport will be poor, increasing the staining risk.

The **adsorption of dye** at the fibre surface is either chemical or physical. The chemical adsorption refers to the chemical bonds between dye molecules and fibres. The physical adsorption is governed by the affinity of the dye for the fibre which is explained either by physical attractions forces (e.g. ion-dipole interaction, hydrogen-bonds, acid-base bonds or dispersion forces) or by mechanic effects due to the fibre pore size. The affinity may be calculated from the chemical potentials of dye molecules within the fibre, μ_f, and within the solution, μ_s, which are given by the Gibbs free energy relation where μ_f and μ_s are equal at equilibrium:[6]

$$\mu_f = \mu_s = \mu_f^\circ + RTlna_f = \mu_s^\circ + RTlna_s \qquad \text{Eq. 6.1}$$

where a is the activity, R the ideal gas constant and T is the temperature.

μ^o is the standard affinity which is the chemical potential of the molecule at standard conditions (at a temperature T = 25 °C (298 K) under a standard pressure p^o = 1 bar = 10^5 Pa).

It can then be defined as:

$$\Delta\mu^{\circ} = (\mu_f^{\circ} - \mu_s^{\circ}) = -RTln\frac{a_f}{a_s} \quad \text{Eq. 6.2}$$

or

$$-\Delta\mu^{\circ} = \left(\mu_s^{o} - \mu_f^{o}\right) = -RTlnK \quad \text{Eq. 6.3}$$

where K is the dimensionless equilibrium sorption constant.

The **diffusion** of the dye from the fibre surface to the interior of the fibre is the slowest step of the dyeing process and therefore determines the overall dyeing rate. Two models can describe the diffusion of a dye into a fibre: the Pore-Volume and the Free-Volume models.

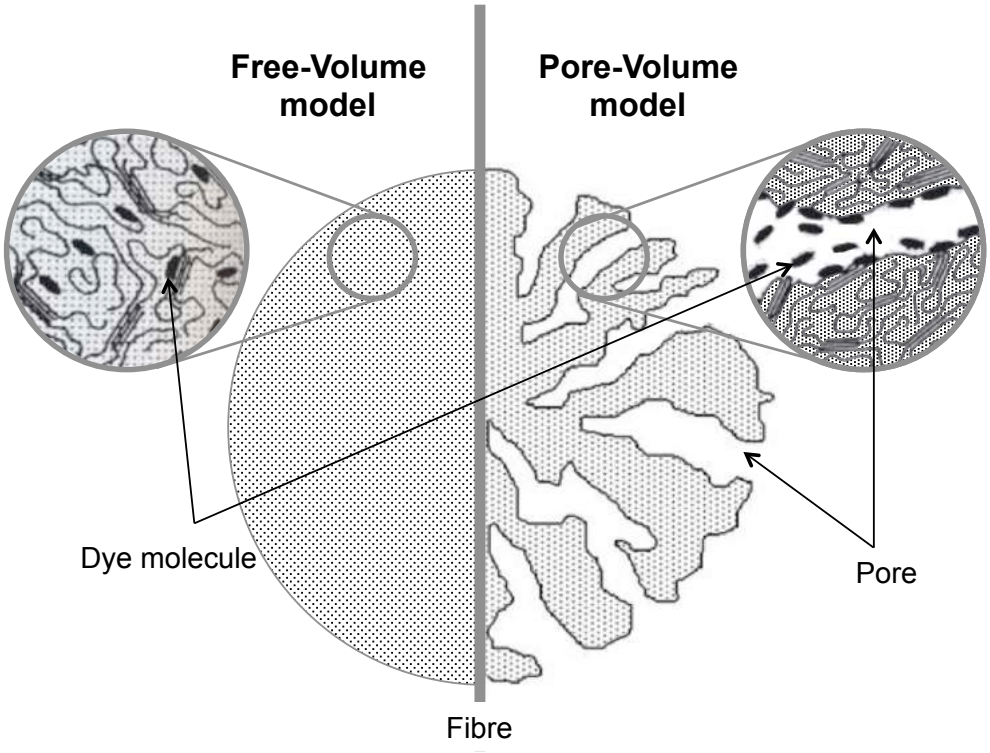

Figure 6.2: Difference between Pore-Volume model and Free-Volume model.

The Pore-Volume model was developed by Weisz and co-workers[9,10] and describes the fibre as possessing capillary channels where the dye in solution passes through. It is assumed that the measured diffusion coefficient is close to the coefficient in water if the diffusion takes place in the pore fibres; otherwise, due to mechanical obstruction of the fibre and physicochemical attractions between fibre and dye, the diffusion in the fibre is slower than in water. In other terms, the Pore-Volume model is used when it is assumed that pore fibres are interconnected with a width comparable to that of the dye to be adsorbed on the wall of these pores.

By contrast, in the Free-Volume model, the pore fibres are not taken into account; dye molecules enter the fibre through openings created by random movements of the amorphous polymer segments composing the fibre (crystalline regions of the fibre polymer being inaccessible to dye molecules). Thus, the diffusion rate is function of the mobility of the polymer chain segment. When the temperature increases, these movements and thus the free-volume increase, increasing the sorption of dye molecules.

Usually, the Pore-Volume model is preferred for organic fibre like cellulose, while the Free-Volume model is preferred for synthetic fibre like acrylic. But again, this also depends on the dye used.

6.2. Discussion

In this part will be presented and discussed all the results obtained using the method developed to get the potential dye staining onto fabric, the dye removal as well as the dye adsorption profile onto fabric. The validation method was used (as described in Chapter 2, 2.3.1. Validation method) to validate the method to determine the dye adsorption profile onto fabric. However, this validation method is typically used to validate analytical methods by comparing the results obtained by a new method with an older method (which P&G would like to change/improve for unknown reasons) or with a reference material. However, there was neither reference material nor standard method to get the small-scale dye adsorption onto fabric. Thus, the Excel file was modified in order to compare all the results with the average of all the measurements as a reference. Moreover, different levels of concentrations are usually used in the validation method. As the dye concentration has been fixed for all the experiments, the time was used for the dye adsorption test on a small scale in order to validate the method at any time (with a measurement every 15 or 30 minutes during 2 hours). The validation of the method to obtain the dye adsorption profile onto fabric in small-scale has given a good repeatability, in particular tolerance probability and acceptability limit values (90 % and 15 % respectively) were quite reasonable, which validated the method at any time.

6.2.1. Dye adsorption in small scale

6.2.1.1. Dye adsorption in small scale - Without surfactant

Initially the dye deposition onto the fabric was studied without surfactant to provide a control.

The five different fabrics described in Chapter 2, 2.1.3. Fabrics (terry cotton, flat cotton, knit cotton, polycotton and polyester) were used for the adsorption test in solutions without surfactant at concentrations of commercial E4210 of 1.24×10^{-4} mol L^{-1}. Also, to mimic the washing bath motion in the washing machine, a stirrer was added with a stirring kept constant for all the experiments. Thus, the procedure (described in Chapter 2, 2.3.3. Dye adsorption test in small scale) was done for three different masses of each fabric (with approximately $m_3 = 2 \times m_2 = 4 \times m_1$) in order to know if the deposition of dye was linear with the quantity of fabric. The amount of dye (in mole) adsorbed onto the fabric is then represented as a function of time, the type and mass of the fabric. Figure 6.4 shows the study of the deposition of commercial E4210. Similarly, the same procedure was used to study the deposition of commercial V200, at a concentration of 1.27×10^{-4} mol L^{-1}. Results for both absorption maximum at 492 nm and 575 nm are shown in Figure 6.9 and Figure 6.10, respectively.

Firstly, by comparing both pictures of the deposition of commercial E4210 and V200 onto these five fabrics (see Figure 2), it can be observed a better deposition for Terry cotton and Polycotton; and a lower deposition for Knit cotton and Polyester.

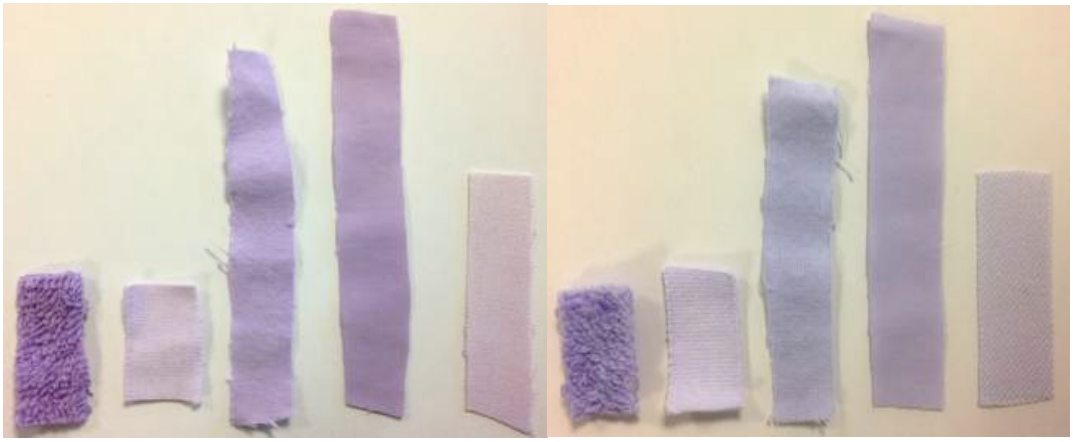

Figure 6.3: Adsorption of commercial E4210 and V200 respectively onto several fabrics: Terry cotton, Knit cotton, Flat cotton, Polycotton and Polyester from the left to the right.

This is confirmed by plotting the amount of dye adsorbed onto fabric vs. the amount of fabric as a function of the type of fabric for commercial E4210 and commercial V200 at λ_{max} = 492 nm and λ_{max} = 575 nm (see Figure 6.4, Figure 6.9 and Figure 6.10, respectively). These graphs also show that the dye deposition is quite linear with time and function of the quantity of fabric until the systems approach equilibria.

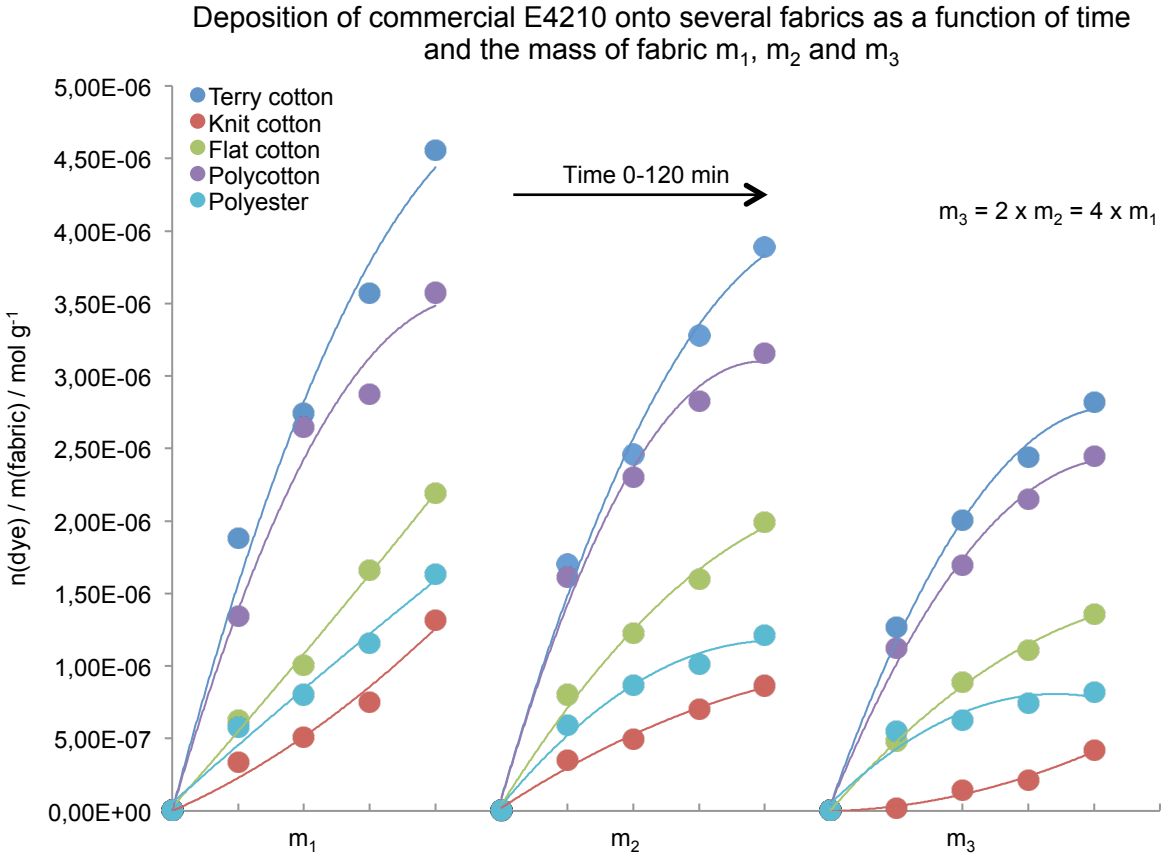

Figure 6.4: Deposition of commercial E4210 onto several fabrics as a function of time and the mass of fabric.

As most fabrics have the same composition (cotton), it can be suggested that the difference in dye sorption for the same dye is due to the difference in adsorption caused by the variation in weaving (see Figure 6.4) and the structural composition of each fabric, i.e. pore size between each fabric fibre (but also the nature of the fibre, cotton or polyester). As commercial E4210 is a bigger molecule than commercial V200, and assuming that the fabric pore size plays a key role in the dye sorption in the Pore-Volume model, dye sorption using V200 should be better than E4210. However, it was observed that the quantity of dye deposited onto fabric is similar for both dyes. It can thus be suggested that in this case, the Free-Volume model would be preferred for the sorption investigation and would be correlated with the

temperature as described previously. Note that all experiments of dye deposition test onto fabric in small scale were done at room temperature; it is thus not possible to confirm the preferred model and the change of dye deposition with the temperature. If the Free-Volume model is the best model, it can be suggested that interactions between each dye and fabric are different and that the long ethoxylate chain of E4210 plays a key role in its adsorption onto fabric (probably hydrophilic interactions between the dye's ethoxylate chain and cotton's alcohol functions) enabling it to adsorb despite its larger size to give almost the same adsorption onto fabric as V200, which is smaller.

As expected, the adsorption onto polyester fibre is lower than onto cotton fibre since it is more hydrophobic while both dyes are quite hydrophilic. Furthermore, note that the knit cotton is the fibre which possesses the poorest adsorption after polyester and that the polycotton is listed in second position. As the inverse exclusion chromatography was not available at the university, it was not possible to access the pore size distribution of each fabric to check if this would explain the difference in dye adsorption. SEM was thus performed on each fabric (see Figure 6.4) to look at the fibre, but nothing was obvious to validate the dye adsorption distribution.

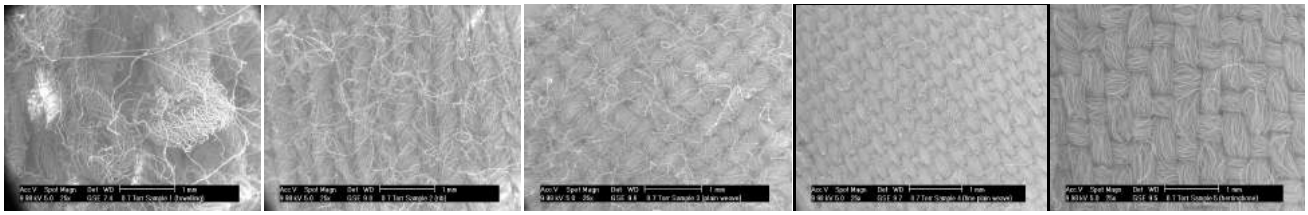

Figure 6.5: SEM pictures of fabrics: Terry cotton, Knit cotton, Flat cotton, Polycotton and Polyester from left to right.

Another method used to understand the difference in adsorption was to measure the time that a water droplet deposited at the surface of the fabric takes to be adsorbed onto the fabric but this was not following the same dye adsorption distribution. Moreover, note that even if a pre-treatment – which could explain the difference in adsorption – had been applied to the fabrics, several washes were performed by P&G in order to remove them. Moreover, a FTIR of each fabric was performed in order to see if a pre-treatment was present but nothing was evident (see Figure 6.6). Consequently, at this stage it was not possible to explain the difference in adsorption between each fabric to any great extent.

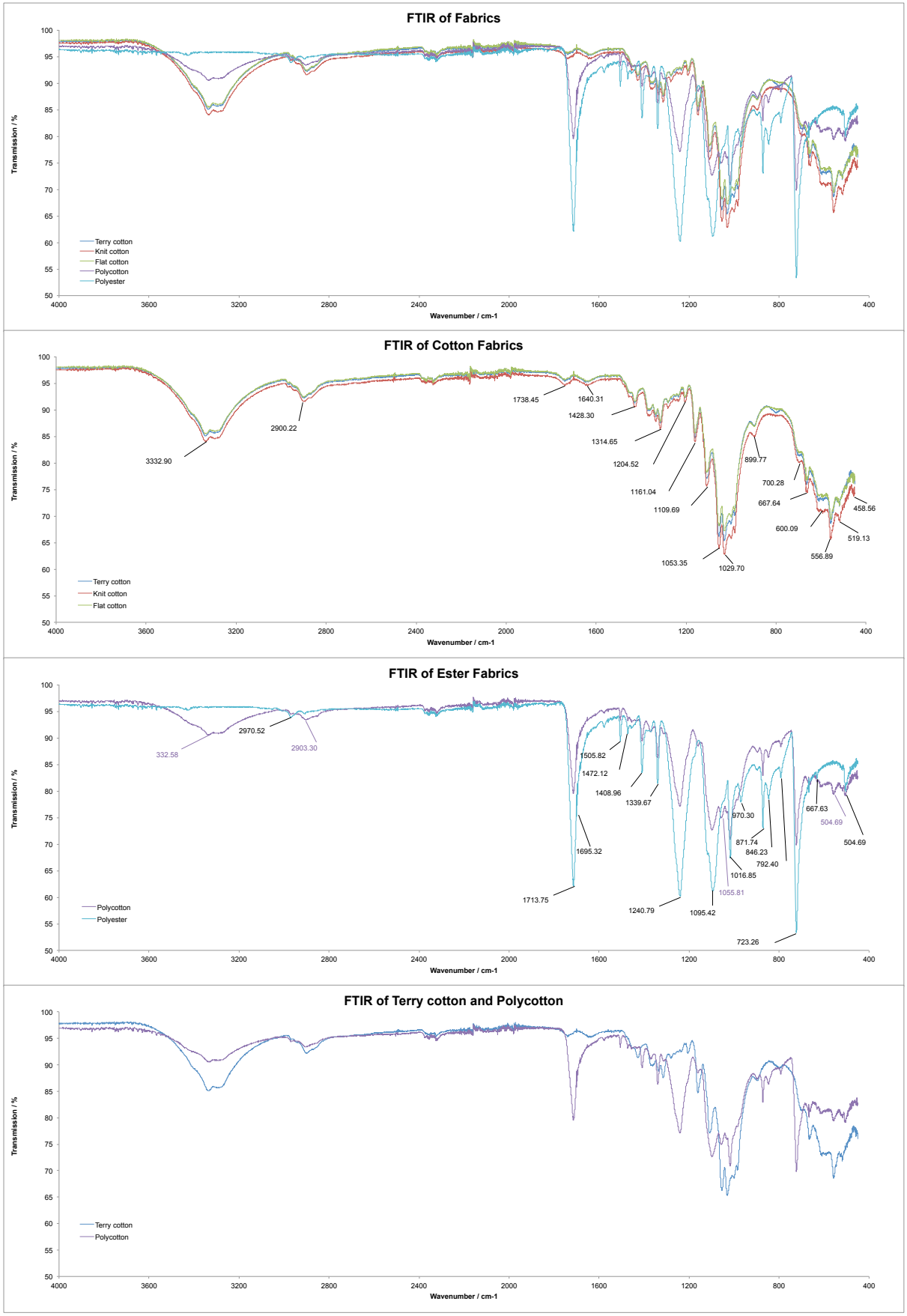

Figure 6.6: FTIR results of the five fabrics, cotton fabrics, ester fabrics and Terry cotton & Polycotton respectively from the top to the bottom.

The dye adsorption test was also performed with the purified form of E4210 at 10^{-4} mol L^{-1} in order to see the difference in dye adsorption in the dye solution as a function of time. The results are shown in Figure 6.7. The decreasing adsorption appears quite linear when the mass of fabric is low while the adsorption seems to decrease more rapidly with time when the mass of fabric increases. When comparing results of commercial and purified E4210 (Figure 6.4 and Figure 6.7, respectively), similar results are obtained in terms of dye adsorption profile (note that the data for polyester with a mass m_2 is missing due to an error in the experiment). However, the amount of dye adsorbed onto fabrics is lower for the purified E4210 than for the commercial E4210. This is either due to the solvent in the commercial dye, which helps in the dye adsorption by helping in the fabric wetting, or it could be due to errors from measurement (dye concentration between the commercial and the purified form, temperature, spectrophotometer (data on commercial form were obtained at Durham while those on the purified form were obtained at BIC)). This graph also shows us the importance of keeping the mass of fabric constant in order to compare all the results together, since the larger the mass of fabric, the more the absorbance of the dye solution decreases due to a higher amount of dye adsorbed onto fabric. For the same reason, the dye concentration must be constant for all the experiments.

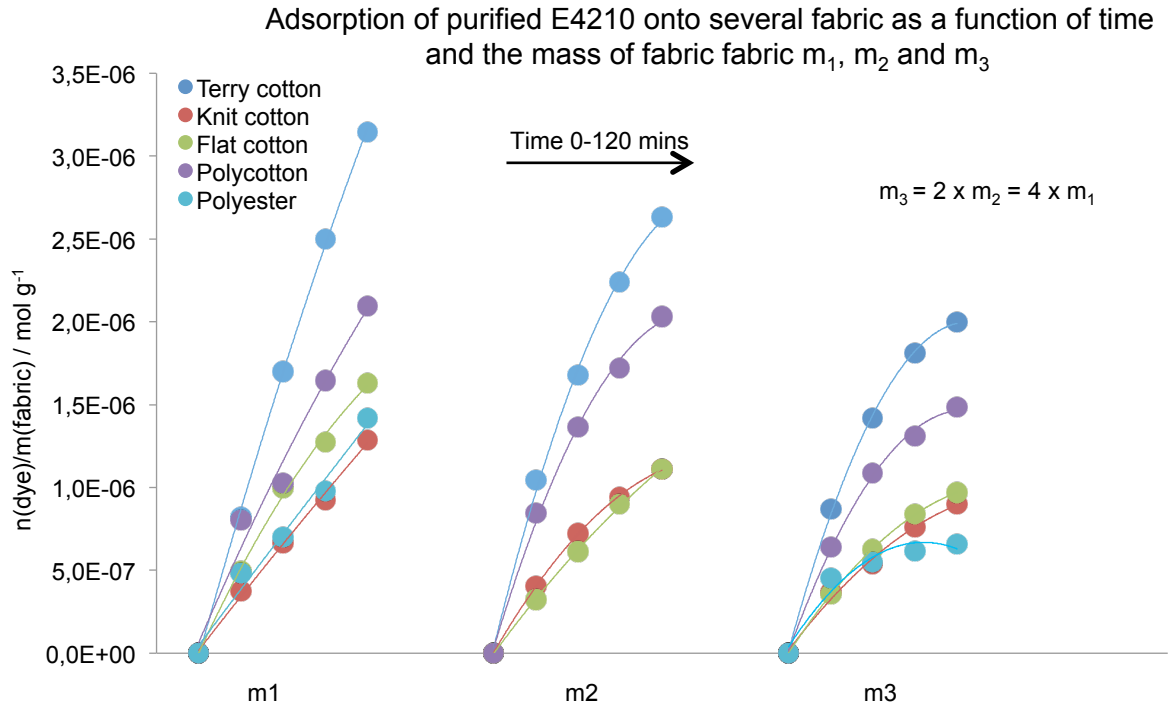

Figure 6.7: Deposition of purified E4210 onto several fabrics as a function of time and the mass of fabric.

Note that the fabric coloration for V200 is more blue than for E4210 (see pictures of dye deposition in Figure 6.3). This means that for commercial V200, the fabric coloration is essentially governed by the absorbance maxima of the dye monomer at λ_{max} = 575 nm (rather than the dye aggregate absorbance maxima at λ_{max} = 492 nm, which leads to more red observed). In comparison, E4210 has its absorbance maxima at λ_{max} = 542 nm, which leads to more violet observed (see Chapter 4 4.1.1. Origin of colour and interaction with light). Moreover, by comparing the absorbance of V200 in the presence of fabric (e.g. Terry cotton) as a function of the time for both adsorption peak maxima (see Figure 6.8), it can be observed that the absorbance at the first maxima at λ_{max} = 492 nm due to dye aggregates decreases linearly with time, while the absorbance for the second absorbance maxima at λ_{max} = 575 nm due to dye monomers remains almost constant with time.

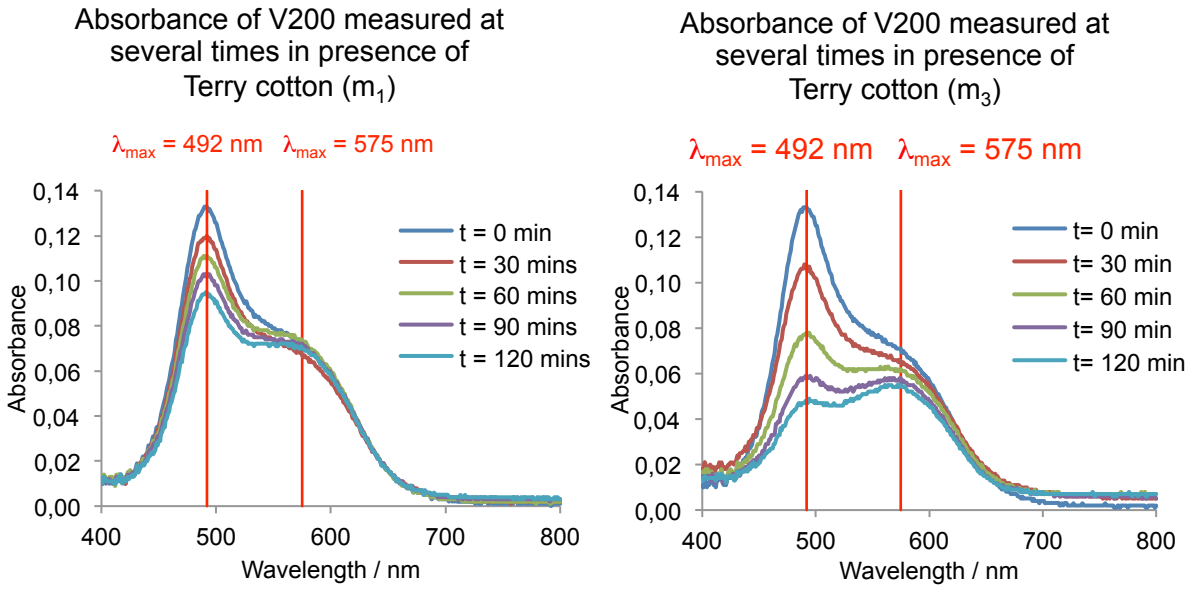

Figure 6.8: Absorbance of V200 as a function of time in presence of Terry cottons at mass m_1 on the left and higher mass, m_3, on the right.

Though at first it may seem that only the aggregate is adsorbing from the dye solution onto the fabric, it is much more likely that it is the monomer that is adsorbing but the equilibrium between monomers and aggregates in solution is then quickly re-established, with the aggregates in solution redispersing into monomers. This explains the negative values of mole of dye per mass of fabric when data are analysed only using the 575 nm peak, see Figure 6.10.

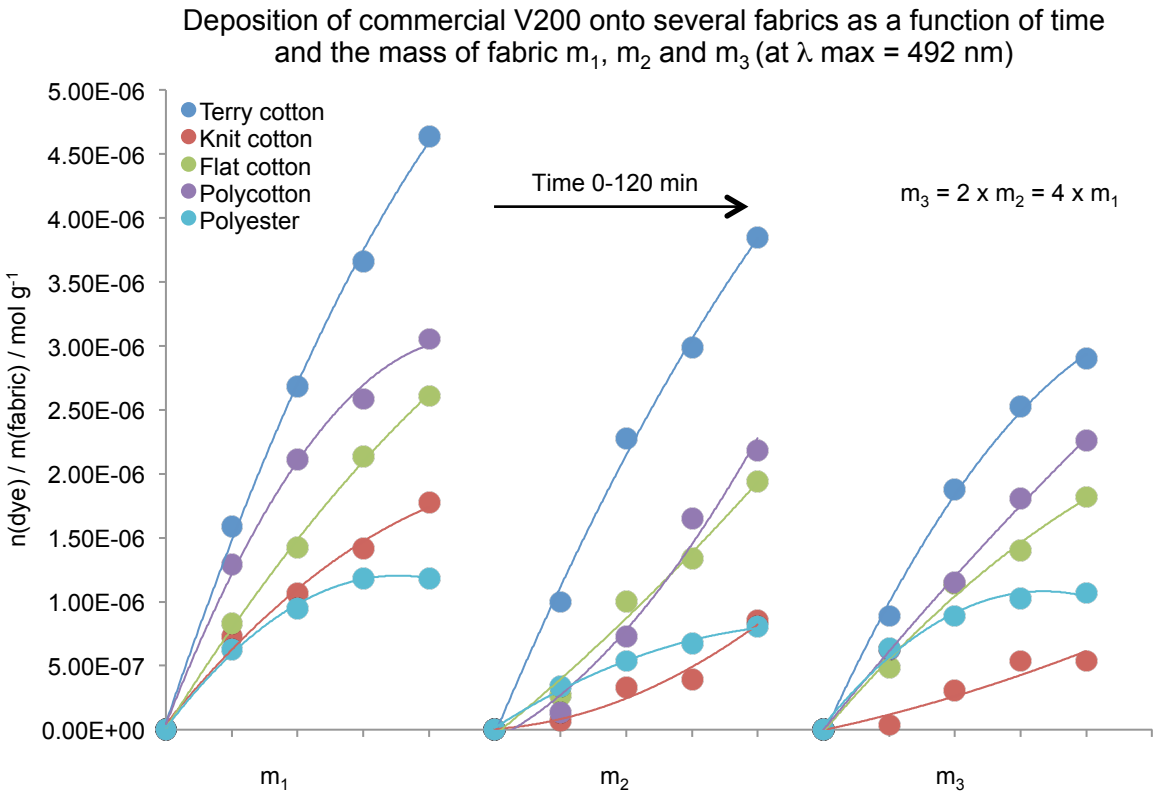

Figure 6.9: Deposition of commercial V200 (λ = 492 nm) onto several fabrics as a function of time and the mass of fabric.

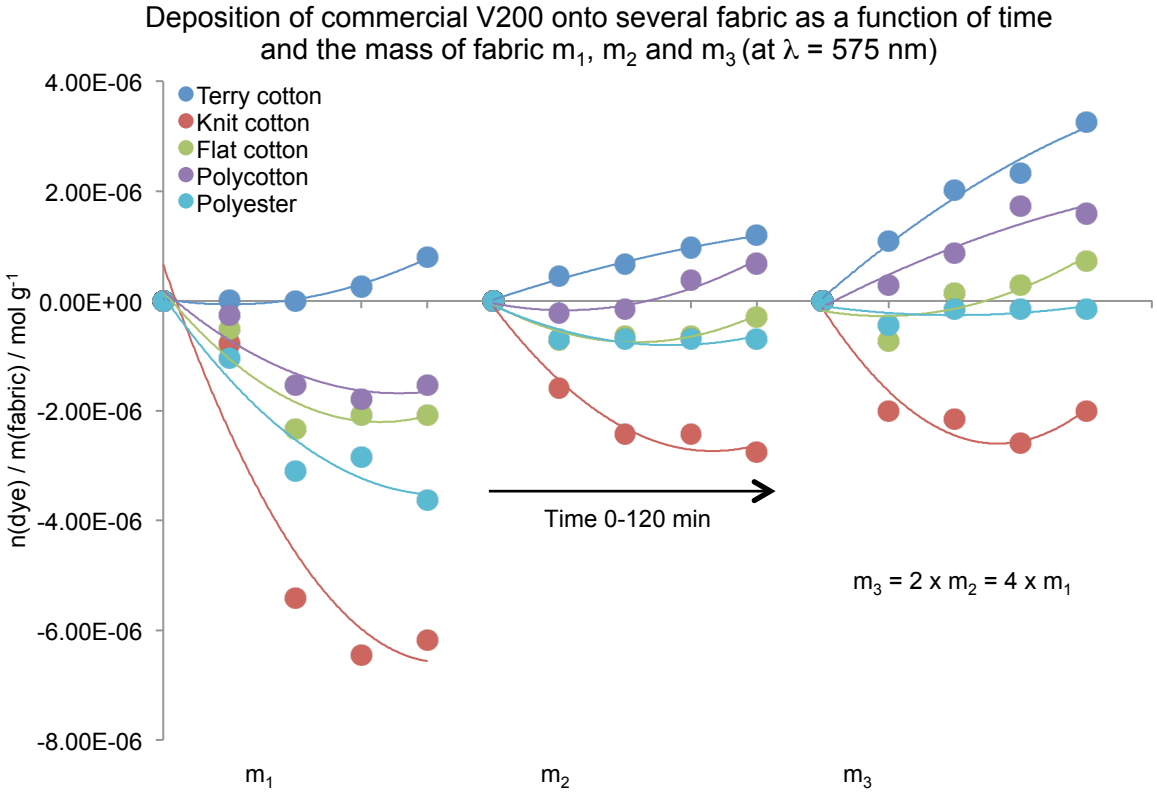

Figure 6.10: Deposition of commercial V200 (λ = 575 nm) onto several fabrics as a function of time and the mass of fabric.

Usually, like for E4210 (see Figure 6.4), the dye molecules are adsorbing onto fabric leading to a decrease in dye concentration in solution, visualised by the decrease of the absorbance as a function of time. As the adsorption is high onto terry cotton, the monomer of V200 is adsorbed onto fabric almost at the same rate as dispersion of aggregates onto monomers in solution; as explained earlier, this is what it can be seen in Figure 6.8 for m_1 and why the quantity of monomer adsorbed onto terry cotton looks almost zero as a function of time in Figure 6.10. When the quantity of terry cotton increases, the quantity of monomers adsorbed onto fabric increases and the rate of monomer adsorption onto fabric is initially higher than the dispersion rate of aggregate into monomers and so this leads to a decrease in both monomers and aggregates in solution and thus a decrease in absorbance for both peaks for fabric mass m_3. This is observed in Figure 6.8 and explains why it looks like the quantity of monomer adsorbed onto fabric increases as a function of time in .

Thus it seems that the monomer of V200 is preferentially adsorbed onto fabric. This could be tested by repeating the experiments at lower V200 dye concentration at which aggregation does not occur (i.e. below ~2 x 10^{-5} mol L^{-1}, see Chapter 4, Figure 4.14) and showing that dye adsorption still occurs efficiently. However, at this concentration the absorbance intensity is quite low (~ 0.25) and will then decrease again with the adsorption of dye molecules onto fabric, decreasing the reliability of the results. Because of this, a reflectance study on the coloured fabric was performed. As described in Figure 6.11, the incident light arrives to the surface of the object, which absorbs certain wavelengths of the light (this defines the absorbance profile) and the remaining wavelengths are reflected (this defines the reflectance profile), and a colour is then observed. Thus the reflectance $R(\lambda)$ is the opposite of the absorbance $A(\lambda)$ and using the reflectance profile it is possible to obtain the absorbance from the following equation:

$$A(\lambda) = \frac{1}{R(\lambda)} \qquad \text{Eq. 6.1}$$

By characterising the reflectance profile of the coloured fabric with V200, it is possible to know the wavelength of absorption of the dye onto the fabric; and thus to know if it corresponds to the monomer or the aggregate. For this, the diffuse reflectance spectroscopy (DRS) method was used. However, the types of reflection need to be considered and so specular reflections are differentiating from diffuse

reflections. Spectacular reflections result in incident light reflected off the top layer of the sample, the beam remains coherent and the angle between the reflected beam and the normal of the surface is the same as that of the incident beam. This can be observed in Figure 6.11, where the upper left section of the apple appears white. Diffuse reflections occur as the result of scattering, which may be caused by reflections from a non-uniform surface, or the incident light penetrating into the sample and after several reflections the light exits in a random direction leading to a spectral profile of the scattered light that is not the same as that of the incident light.

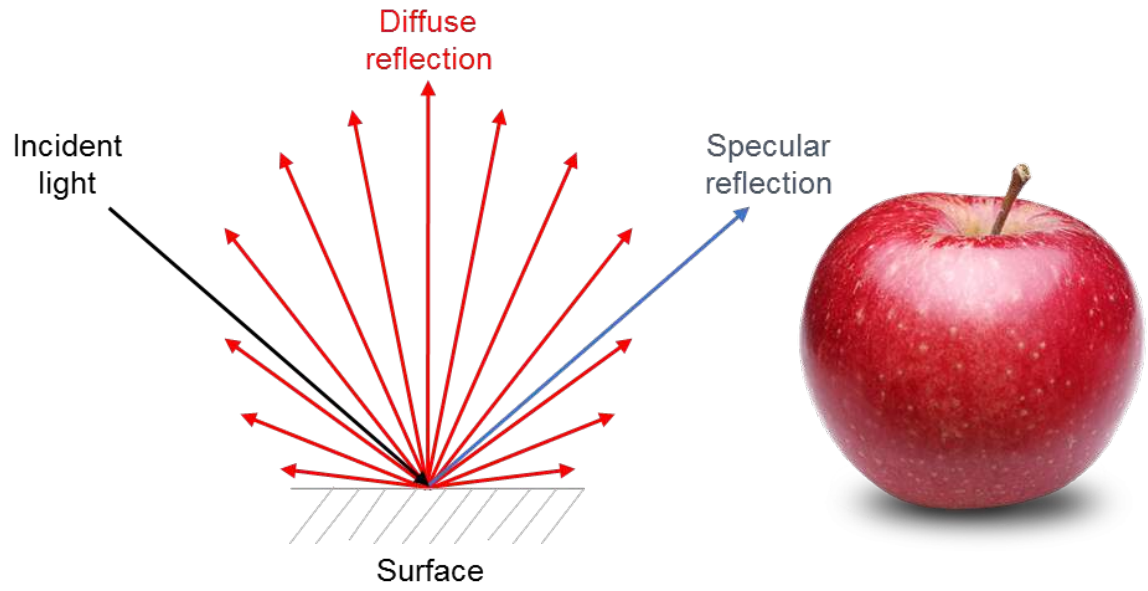

Figure 6.11: Beam paths in diffuse and specular reflections on the left, and a demonstration of each type observed on a partially reflective surface on the right.

DRS produces a reflectance spectrum that is independent of the light source and the detector used to measure it. For this, the sample is illuminated by a light source which is continuous in the entire spectral region of interest. The diffuse reflections are then collected, collimated and input into a spectrophotometer. To account for the non-uniform spectral power distribution of the light source, as well as any losses in the collection optics, diffuse reflectance is typically reported against a reference material.

In practise, this is carried out by recording the spectral density of reflected light from the sample (the fabric dyed by monomer and aggregate of V200 in this case) and a reference material (the fabric without dying) under uniform conditions. The relative reflectance $R(\lambda)$ of sample is then defined as the ratio of intensities I(λ) between the sample $I_s(\lambda)$ and the reference $I_r(\lambda)$ from the following equation:

$$R(\lambda) = \frac{I_s(\lambda)}{I_r(\lambda)} \qquad \text{Eq. 6.2}$$

A diffuse reflectance spectrum can be used to determine the colour of the object under any illumination. However, a reflectance spectrum can only account for the absorbance of a material. Luminescence can also contribute to the colour of an object but cannot be accounted for by DRS as it is dependent on the light source used to obtain it and cannot be readily decoupled. It has thus been produced the reflectance profile of a piece of fabric immersed in a concentrated solution of V200 containing aggregates and monomers of the dye (with an aggregate maximum in absorbance at 492 nm), as well as the reflectance profile of a piece of fabric immersed in a diluted solution of V200 containing only the monomer of the dye (with a maximum in absorbance at 575 nm). All the experiments were done in triplicate and the results of the reflectance profiles, as well as the absorbance profiles deducted from them, are presented in Figure 6.12. From this figure, as the absorbance of the aggregates is at 492 nm whilst for the monomers it is at 575 nm, it is observed that the monomer is preferentially adsorbed onto fabric.

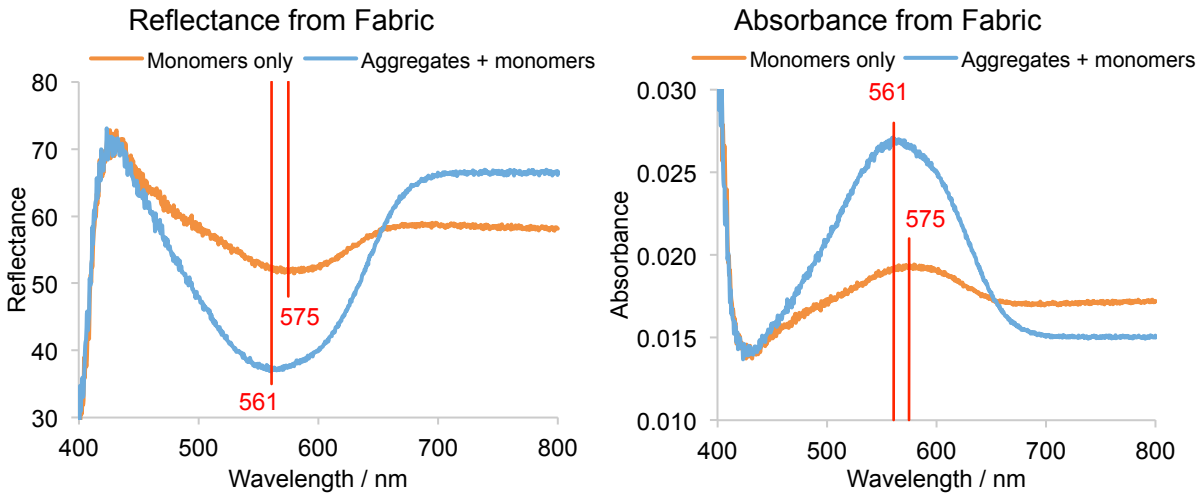

Figure 6.12: Reflectance profiles on the left and absorbance profile on the right of a piece of fabric immersed on a V200 solution containing aggregates and monomers of the dye, and a piece of fabric immersed in a V200 solution containing only monomers of the dye.

6.2.1.2. Influence of the agitation on the dye deposition

In order to study the influence of the agitation on the dye deposition onto fabric, the procedure was performed two times in triplicate. One time by adding a stirrer in the vial containing the solution with the piece of fabric, agitating the whole system (dye solution and piece of fabric). And another time without agitation, the dye solution and the piece of fabric being static. The results of absorbance loss (at λ_{max}) as a function of time are shown in Figure 6.13.

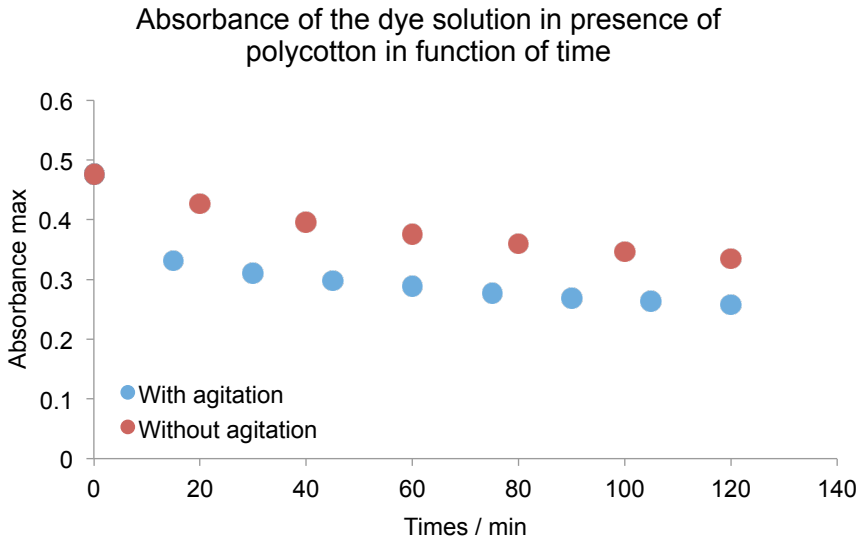

Figure 6.13: Influence of the agitation on the deposition of E4210 onto polycotton.

It is observed that the loss in absorbance due to the dye adsorption onto fabric is greater with agitation than without agitation, even though experiments with agitation had a lower mass of fabric (≈ 0.1004 g compared to ≈ 0.1021 g for no agitation). This shows the importance of agitation in achieving higher dye absorption onto fabric from solution. Moreover, this confirms the important role of dye diffusion in the boundary layer between the cloth and the bulk on dye deposition, since this will be increased with agitation. For this reason, a magnetic stirrer was used to achieve agitation and kept at the same level of agitation in all the experiments. However, this is quite subjective as it is difficult to measure the agitation and confirm that it is exactly the same in all experiments. This could also explain the difference in adsorption rate between each fabric that was not possible to explain.

6.2.1.3. Dye adsorption in small scale - With surfactant

The dye adsorption test developed previously was used to study the influence of surfactants on the dye deposition onto fabrics. For this, at the beginning a high concentration of surfactant was used in our experiments to mimic the surfactant concentration in the real product (e.g. the stock solution of $C_{10}E_{10}$ used for the determination of K_b, at high surfactant concentration, where f = 100 % of dye molecules incorporated in micelles). However, it has been shown (see Figure 6.14 at a surfactant concentration superior to 3×10^{-3} mol L^{-1}) that at this surfactant concentration, no absorbance loss occurs, meaning no dye adsorbs onto the fabric. This is confirmed by the fabric itself, which is still white with a light pink colouration (see Figure 6.15), either due to the remaining dye solution on the fabric during drying (since there is no rinsing step) or due to such a low amount of dye adsorbed onto the fabric that it is not detectable using our absorption loss method.

Thus, by decreasing the surfactant concentration under f = 100 %, the influence of the surfactant concentration on the dye deposition has been studied. For this, the method developed to study the adsorption in small scale by using polycotton, E4210 and several concentrations of $C_{10}E_{10}$ from below to above its CMC has been used (concentration above the CMC = 1.65×10^{-3} mol L^{-1} are shown in red on the graph). The experiment was done in triplicate and the results obtained are shown in Figure 6.14 and Figure 6.15. However, as the surfactant concentration has an influence on the dye adsorption band (see Chapter 5, 5.1.3. Dye-Surfactant interactions) and modifies the absorbance intensity, it was not possible to do a single calibration curve for all the surfactant concentrations. Moreover, as it is time consuming to do a calibration curve for each surfactant concentration, only the loss in absorbance as a function of time have been studied as it is correlated to the amount of dye adsorbed onto fabric. Thus, Figure 6.14 presents the difference between the absorbance at time t and 0 minutes (ΔA), to show the variation in the amount of dye adsorbed onto fabrics with time in order to have an idea on the influence of the surfactant on the amount of dye adsorbed onto fabric. Figure 6.15 shows polycotton swatches used for the dye deposition at different surfactant concentrations.

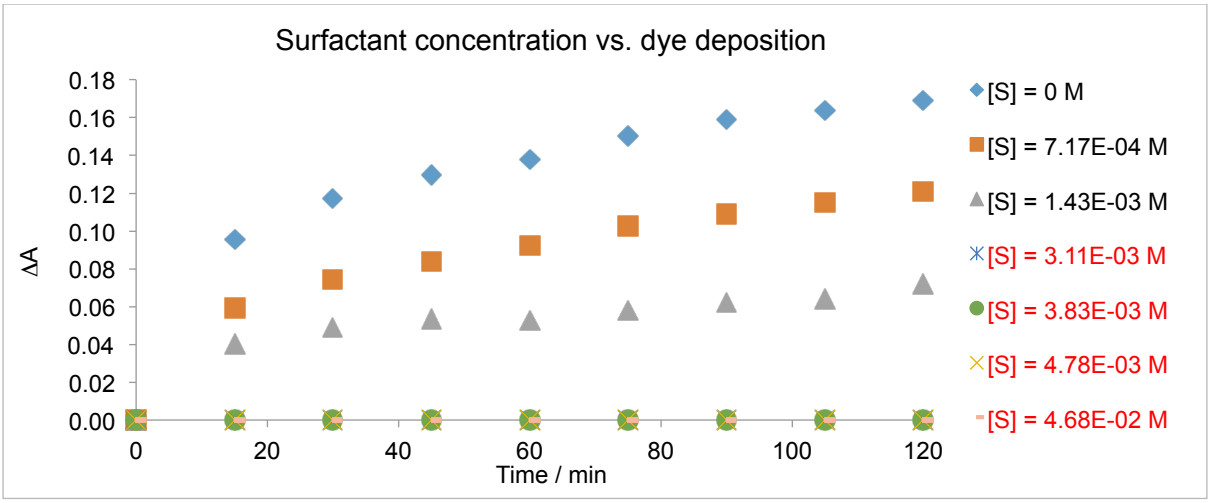

Figure 6.14: Influence of the surfactant concentration ($C_{10}E_{10}$) on the dye deposition (E4210) onto polycotton.

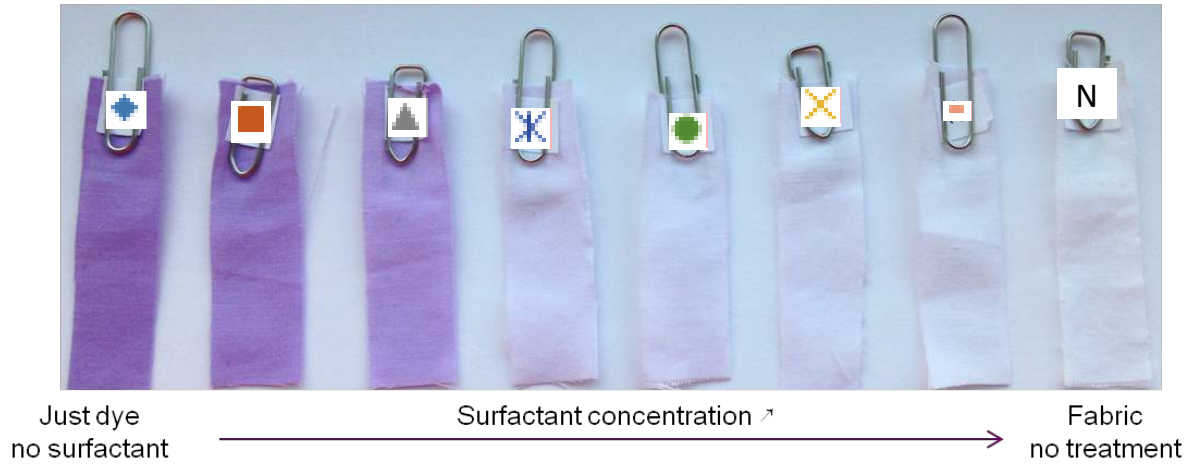

Figure 6.15: Polycotton after two hours dying with E4210 and different surfactant concentration ($C_{10}E_{10}$).

It can be observed that the dye deposition is greater in the absence of surfactant and then decreases when the surfactant concentration increases until there is almost no deposition above the CMC at f = 67.81 % (see Chapter 5, Figure 5.14), corresponding to a surfactant concentration of 3.11 x 10^{-3} mol L^{-1}, with only a light pink colouration occurring. This could be explained by two hypotheses. The first one would be explained by assuming that the dye-surfactant interactions are higher than those between dye molecules and fabric. Thus, the dye adsorption onto fabric decreases when the surfactant concentration increases since dye molecules are interacting with surfactant molecules and not the fabric; and when the CMC is reached, all or almost the dye molecules are incorporated in surfactant micelles and only interact with the fabric in a limited way, leading to almost no adsorption onto fabric. The second hypothesis would be to assume that the interactions between the

fabric and surfactant molecules are higher than the interactions between the fabric and dye molecules. Thus, surfactant molecules would be preferentially adsorbed onto the fabric leading to less free space for dye molecules to adsorb onto fabric. Moreover, this would imply that most of the surface of the fabric swatch is occupied by surfactant molecules above the CMC. This could be tested by increasing the fabric swatch size in order to see if dye adsorption increases, or by analysing the fabric swatches by spectroscopy (FTIR or DRS) to see if surfactants are present. Thus, it would be interesting to study and quantify the affinity of dye and surfactant molecules with fabric to compare with the dye-surfactant affinity (related to K_b).

Nine different people have compared all the fabric swatches in Figure 6.15 in terms of colour and colour intensity. All of them have found a difference in colour intensity between each fabric and seven of them have found the same order of colour intensity (form the lowest surfactant concentration to the highest). The other two have switched the samples [S] = 3.83 x 10^{-3} mol L^{-1} and [S] = 4.78 x 10^{-3} mol L^{-1}, which are quite difficult to differentiate. This means that a difference in dye deposition as a function of the surfactant concentration can be really seen. Regarding the hue of the colouration, some people considered this was due to 2 different dyes (between samples below and above the surfactant CMC) and some people have described the difference in hue by the colour intensity.

It is important to note that the value of f differs from surfactant to surfactant, depending on the affinity between the surfactant and the dye and thus K_b.

6.2.2. Staining test

In order to be in realistic conditions, a staining test was used to study the potential risk of staining of one formulation compared to one reference. For this, several formulations of the blue top compartment from the SUD were prepared, according to the nonionic formulation from P&G, using first only one surfactant per formulation in order to see the effect of that one, and then two surfactants per formulation – these are the same binary systems used for the determination of K_b with two surfactants – in order to see the influence of other surfactants on the risk of staining. For this, 1.5 g of each formulation was deposited on a pre-wet terry cotton fabric (as well as references for comparison) and left for 45 min. Then a rinsing step was needed, which was performed by dipping the fabrics twenty times in water to remove the

excess dye on the fabrics, before making a short machine wash at 30 °C with a little amount of basic detergent (P&G reference formulation: Jupiler nil brightener /perfume) to mimic realistic wash conditions (≈ 15 g). Note that before each wash cycle with fabrics, a short wash cycle at 95 °C with the emptied washing machine was performed in order to remove any detergent products in the washing machine. The fabrics were then dried at room temperature.

Afterwards, the *L, a* and *b* values of each stain (spots where the formulations were deposited) on the terry cotton fabrics as well as the *L, a* and *b* values of the terry cotton fabrics before making spots were determined using an Image Analysis System (IAS) – Digi Eye box (see Chapter 2, 2.2.6. Image Analysis Systems) – in order to determine the ΔE_s (see Chapter 4, 4.1.4. Characterisation of colours), which corresponds to the overall colour difference between the fabric before and after spots, which then characterises the staining. Thus, if ΔE_s is close to 0, this means that there is almost no staining and the greater the ΔE_s value, the greater the staining. All the experiments and measurements were done in triplicate. The composition of the blue tops used in this part is approximatively: 71 % of surfactant, 11 % of 1,2 propanediol, 8 % of water, 5 % of glycerine and 5 % of commercial E4210 (which correspond to 0.4 % of E410 active molecule) or 7 % of commercial V200 (which correspond to 0.4 % of V200 active molecule).

6.2.2.1. With one surfactant

6.2.2.1.1. E4210 vs V200

For this test, formulations used the Lutensol TO series (C_{13}) with either E4210 or V200, at 4.83 % or 1.20 % respectively, compared with a fresh (made less than 3 months ago) reference of Ambrosia 3 (ref A3: which is the current P&G formulation of the ionic blue top compartment) and a fresh reference of nonionic top (NI Top: formulation developed by P&G). The results of ΔE are presented on Figure 6.16. We have to note that for this study, the *L, a* and *b* values were determined using a KONICA MINOLTA Spectrophotometer CM-3610d and not the IAS. Figure 6.17 shows the fabrics used for the staining test with the different stains from formulations.

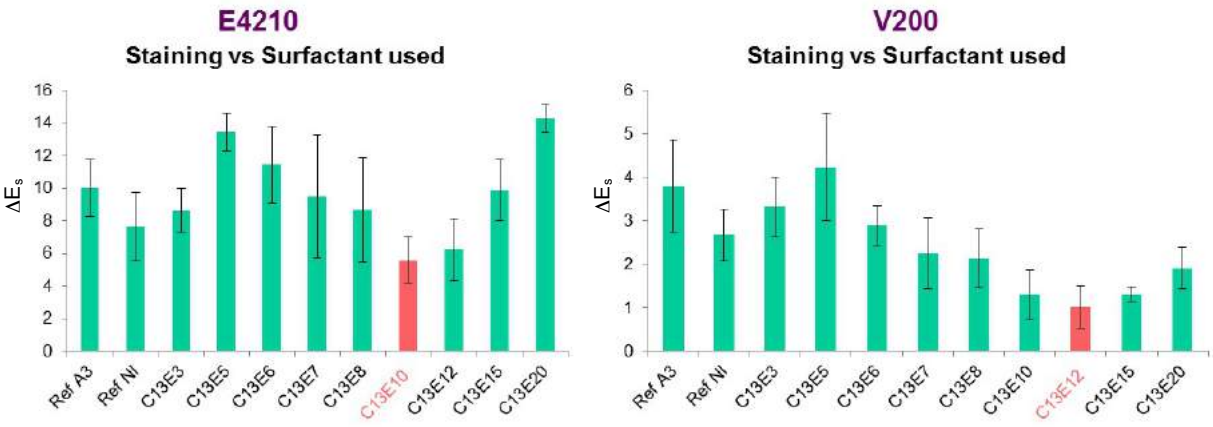

Figure 6.16: Staining vs. Dye and Surfactant used on Terry cotton.

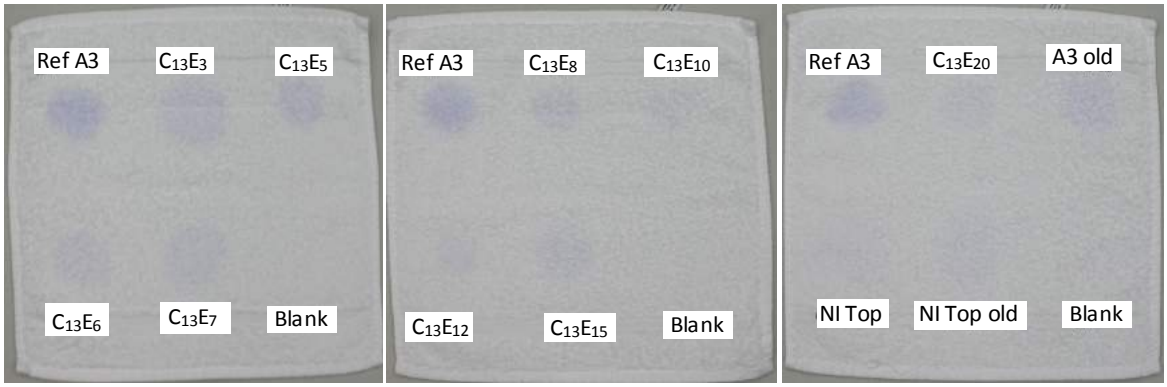

Figure 6.17: Influence of the surfactant on the staining using V200 and the Lutensol TO series (C_{13}).

From Figure 6.17 and Figure 6.16, it can be observed that the staining is in general decreased – up to 50 % depending on the surfactant used – using nonionic surfactants compared to the current ionic blue top used by P&G (Ref A3), agreeing with the findings of P&G from their previous work where they have noticed a decrease of the risk of staining using nonionic surfactants rather than using anionic surfactant. This could validate the initial hypothesis of assuming that interactions between dye molecules and nonionic surfactants are higher than with ionic surfactants due to potential electronic repulsions between dyes and ionic surfactants, with more dye-surfactant interactions decreasing the risk of staining. However, only one reference for the ionic formulation has been used and so comparison with several other ionic surfactants is required to fully validate this hypothesis.

Regarding the results between E4210 and V200, it can be observed that the staining is almost 50 % less important using V200 rather than E4210. Thus, even if E4210 is a more efficient technology than V200 (defined by P&G's dye supplier), it leads to a higher risk of staining, likely due to the long ethoxylated chain of E4210 which would bring more hydrogen interactions with fabric fibres compared to V200. It would be

interesting to compare the binding constant of a surfactant with both dyes, E4210 or V200, to see which is higher. Note that this effect may also be due to the greater colour intensity of E4210, which is higher than V200 since the molar extinction coefficient of E4210 is higher than V200's monomer (5066.5 L mol^{-1} cm^{-1} for E4210; 595.2 L mol^{-1} cm^{-1} and 1298.5 L mol^{-1} cm^{-1} respectively for the monomer and aggregate of V200). It can also be due to the fact that E4210 and V200 were not equimolar in the experiment in order to get almost the same hue intensity between both dyes due to difference in molar extinction coefficients. Thus, it would be interesting to look at results with equimolar dyes for efficiency comparison.
Now looking at the results within the same surfactant series, the staining seems to decrease until an optimum and then increase. The optimum number of EO is achieved at 10 or 12 EO groups for both dyes when using the $C_{13}E_j$ surfactant series.

6.2.2.1.2. Influence of the surfactant with E4210

In order to compare the results of staining tests with those obtained for the dye surfactant interactions, staining tests using the blue top composition as described earlier with the same surfactants used for the dye-surfactant interactions study and only E4210 were performed. However, it was not possible to study the anionic formulations using the same composition because of the high surfactant concentration in the blue top formulation (71 % in mass) and the poor solubility of LAS and SDBS leading to solid formulations. The results of ΔE_s are presented in Figure 6.18. For this study, note that the *L, a* and *b* values were determined using the IAS and this explains why the ΔE_s values using $C_{13}E_j$ surfactant are higher than those obtained previously. Nevertheless, the same trend was obtained, i.e. with a decrease in the risk of staining with the number of EO until an optimum at 12 EO groups followed by an increase in the risk of staining. Note though that the effect is small and within experimental error meaning a non-significant effect.

Regarding the results using the other surfactant series, $C_{10}E_j$, it seems that the opposite trend is observed with an increase in the risk of staining until a maximum at 9 EO groups and then a decrease. The risk of staining seems to be a bit lower using the surfactant series $C_{13}E_j$ rather than $C_{10}E_j$ but again, these relative changes are small and within experimental error and again non-significant.

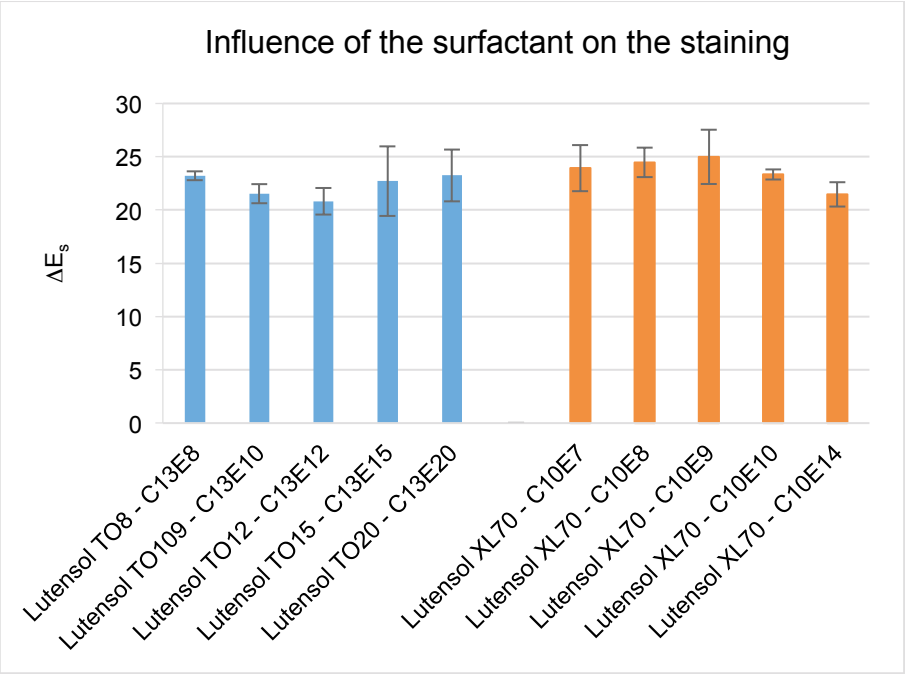

Figure 6.18: Influence of the surfactant on the staining using E4210.

The first hypothesis was that the risk of staining would be linked to the dye-surfactant interactions, i.e. the more the dye-surfactant interactions, the more the risk of staining is reduced. However, as explained in Chapter 5 – 5.2.1 Visualisation of the dye-surfactant interactions and binding constant – a problem occurred in getting the dye-surfactant binding constants and the tentative hypothesis where the absorbance at the plateau would be correlated to the intensity of the dye-surfactant interaction has thus been made, i.e. the greater the absorbance at the plateau, the greater the interactions between the dye and surfactant molecules. Thus, the results obtained using the staining tests (Figure 6.18) were compared with the absorbance at the plateau studying the dye-surfactant interactions using the spectrophotometric method (see Chapter 5, Figure 5.15) in order to see the relationship between dye-surfactant interactions and risk of staining.

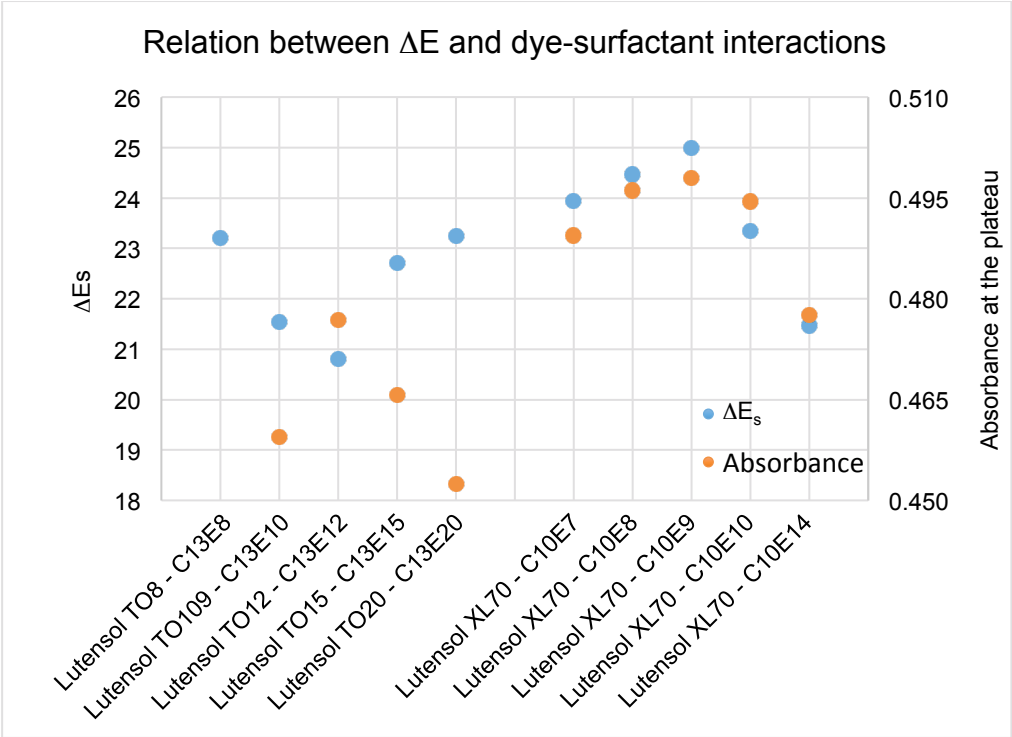

Figure 6.19: Relation between dye-surfactant interactions and risk of staining.

Looking at both results of staining tests and absorbance at the plateau for the $C_{13}E_j$ surfactant series (results on the left side on the graph), an opposite trend can be observed, corresponding to the same optimum value of 12 EO groups to reduce staining and increase dye-surfactant interactions. This would mean that when the dye-surfactant interactions increase, the risk of staining decreases and conversely. However, when looking at both results of staining tests and dye-surfactant interactions for the $C_{10}E_j$ surfactant series (results on the right side on the graph), the same trend can be observed with the same optimum value at 9 EO groups, with the risk of staining increasing when the dye surfactant interactions increase. As both surfactant series lead to the opposite trend in terms of risk of staining, while the dye-surfactant interactions follow the same trend, this means that either the trends observed in the ΔE_s values are not reliable or another mechanism takes place in the regulation of the dye adsorption onto fabrics in addition to the dye-surfactant interactions.

Indeed, it has to be taken into account the dye-fibre and surfactant-fibre interactions. There is likely an adsorption competition[9] between dye and surfactant molecules at the surface of the fabric. Note and remember that the risk of staining is essentially occurring – as well as measured in the staining test – when the

formulation is not well dissolved and directly in contact with the fabric; i.e. with a high surfactant concentration in a small contact area. Thus, if the surfactant-fibre interactions are higher than dye-fibre interactions, this would lead to a better adsorption of surfactant molecules at the fabric surface compared to dye molecules, leading to a decrease of the risk of staining. Conversely, if the dye-fibre interactions are higher than surfactant-fibre interactions, this would lead to a better adsorption of dye molecules to the fabric surface compared to surfactant molecules. However, in this case, the dye adsorption onto fabric would still be regulated by the dye-surfactant interactions.

In 1997, Biswas and Chattoraj[17] studied the polysaccharide-surfactant interactions and specifically, the adsorption of several cationic surfactants at the cellulose-water interface. From their work, they have found that the adsorption of cationic surfactant decreases with the decrease of hydrocarbon chain length of the surfactant. Applied to the nonionic surfactant used in this thesis, this would mean that the $C_{13}E_j$-fibre interactions are higher than $C_{10}E_j$-fibre and this would support the second tentative hypothesis: if the $C_{13}E_j$-fibre interactions are higher than E4210-fibre interactions while $C_{10}E_j$-fibre interactions are smaller than E4210-fibre ones, this would explain why the risk of staining is reduced using the $C_{13}E_j$ surfactant series rather than the $C_{10}E_j$ series. However, this would need more experiments and the measure of dye-fibre and surfactant-fibre interactions/affinity to confirm this tentative hypothesis.

6.2.2.2. With two surfactants – Binary system

In order to see the influence of another surfactant on the dye deposition of a blue top formulation already containing one surfactant, the risk of staining of several surfactant binary systems was studied. For this, the same blue top formulation as before was used varying the mass ratio of the two surfactants. The results of the risk of staining as a function of the mass fraction of each surfactant are presented in Figure 6.20.

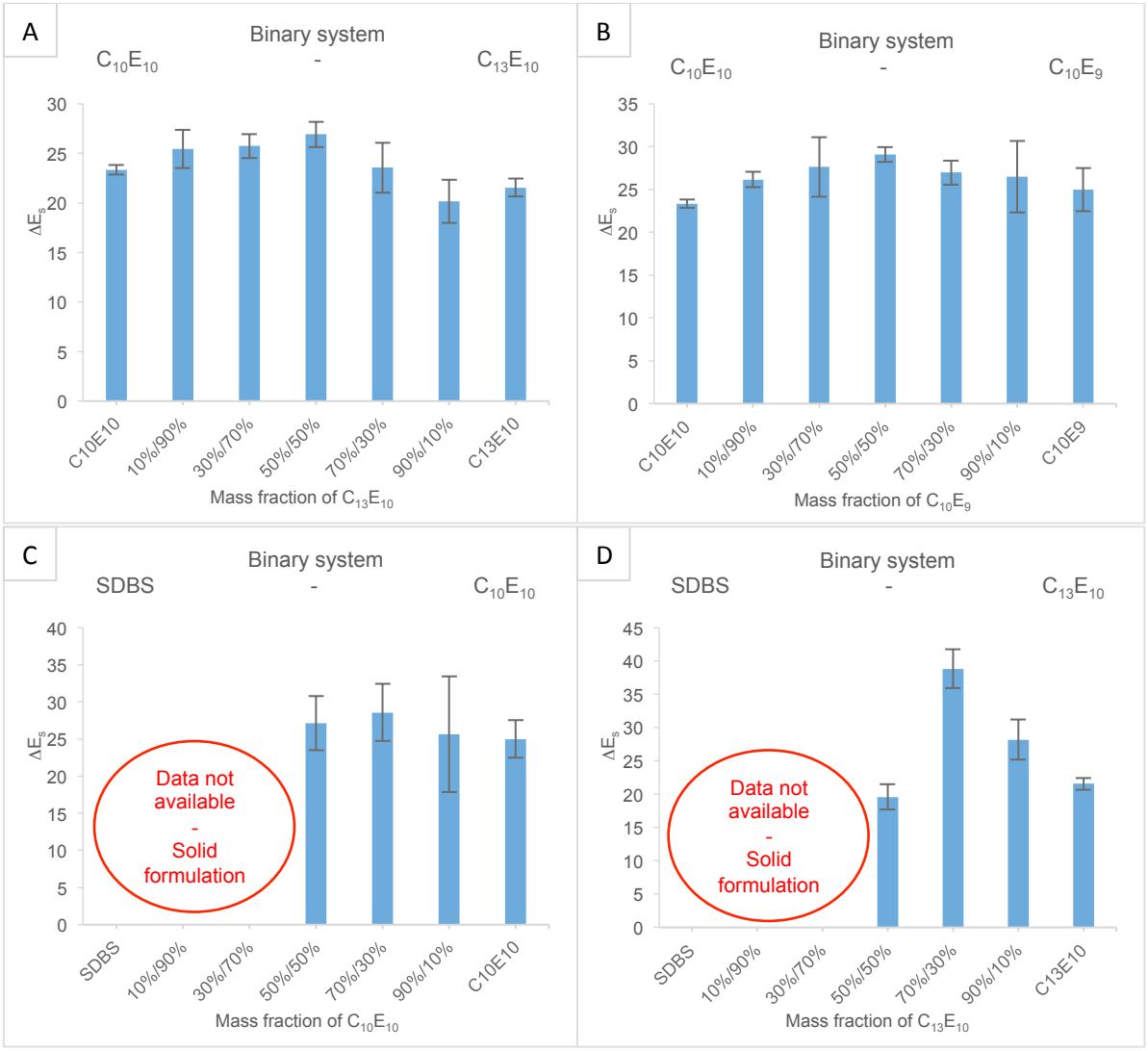

Figure 6.20: Evolution of the staining as a function of the surfactant ratio in mass in several surfactant binary system of A) $C_{10}E_{10}$ - $C_{13}E_{10}$, B) $C_{10}E_{10}$ - $C_{10}E_9$, C) SDBS - $C_{10}E_{10}$ and D) SDBS - $C_{13}E_{10}$.

Note that, due to the poor solubility of SDBS, a formulation containing a concentration of SDBS ≥ 35.5 % in mass (50% of SDBS from the 71% of surfactant in the blue top formulation) was leading to a solid formulation, which was not suitable for our tests. Thus, no data for these formulations was obtained. Looking at the results for the binary systems A and B, the risk of staining seems to increase to a 50/50 ratio in mass of both surfactants and then decreases, while regarding the absorbance at the plateau, and thus potentially the dye-surfactant interactions, it was evolving linearly suggesting that the total interaction depends on the ratio of each surfactant. This confirms again that there is another mechanism in addition to the dye-surfactant interactions affecting the dye deposition onto fabric. Moreover, it can be observed for the data available on the binary systems, C and D, that the staining is higher for the $C_{13}E_{10}$-SDBS formulations than with the $C_{10}E_{10}$-SDBS formulations

while it was smaller for the $C_{13}E_{10}$ formulation than the $C_{10}E_{10}$ formulation. Also, note that the viscosity for the $C_{13}E_{10}$-SDBS formulations seemed higher than the $C_{10}E_{10}$-SDBS formulations. This would mean that the viscosity of the formulation would also play a role in the dye deposition.

6.2.2.3. Influence of the viscosity on the dye deposition

In order to see the influence of the viscosity of the blue top formulation on the dye deposition, the viscosity of each formulation was measured at 25 °C using an Advanced Rheometer AR 2000 with a cone of 6 cm and 2 degrees at a shear rate from 0.1 s^{-1} to 10 s^{-1}. Note that the concentration of each surfactant in formulations was around 71 % in mass for each of them. The comparison between the risks of staining and the formulation viscosity are presented on Figure 6.21.

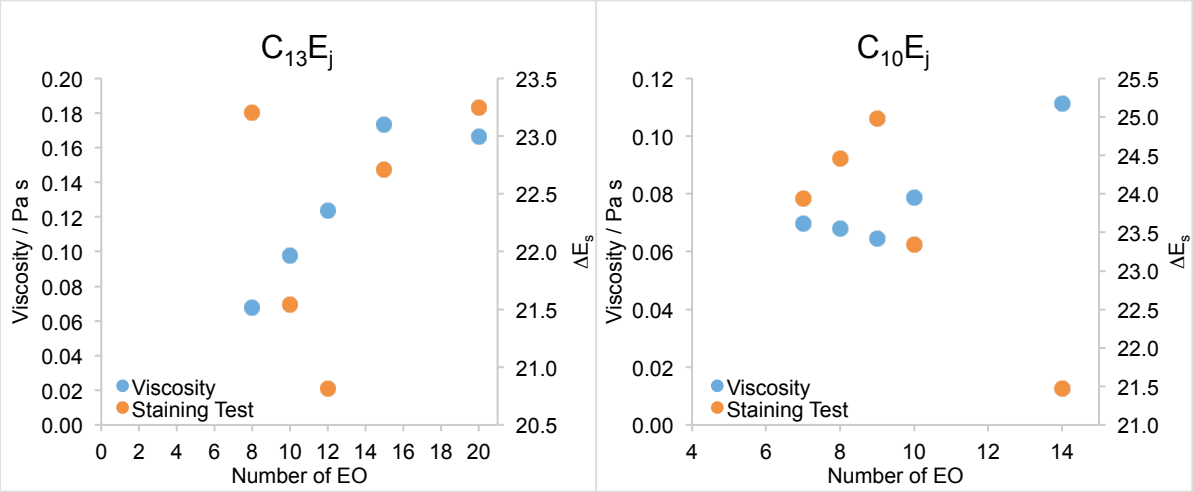

Figure 6.21: Comparison between the risk of staining and the viscosity of formulations using either the $C_{13}E_j$ series on the left, either the $C_{10}E_j$ series on the right.

Looking at the viscosity results with $C_{10}E_j$ shown in Figure 6.21, it seems that the risk of staining decreases when the viscosity of the formulation increases, however, the results are rather inconclusive. Moreover, in this case, the viscosity is essentially due to the choice of the surfactant which also has an incidence on the fabric surface and thus the dye adsorption. In order to confirm the role of the viscosity on the dye adsorption onto fabric, 6 formulations with the same amount of E4210 dye and without surfactant were produced. One with only water as reference with a viscosity of 0 Pa s, and 5 formulations containing a rheology modifier (Acusol from Dow Chemical at a pH around 3) at 1, 2, 3, 4 and 5 % in mass in water giving respectively a viscosity of 0, 800, 1900, 2900 and 5075 cP (1 cP = 0.001 Pa s). Then the same

formulations as before with a staining test have been used. All the measurements were done in triplicate and the results are presented on Figure 6.22.

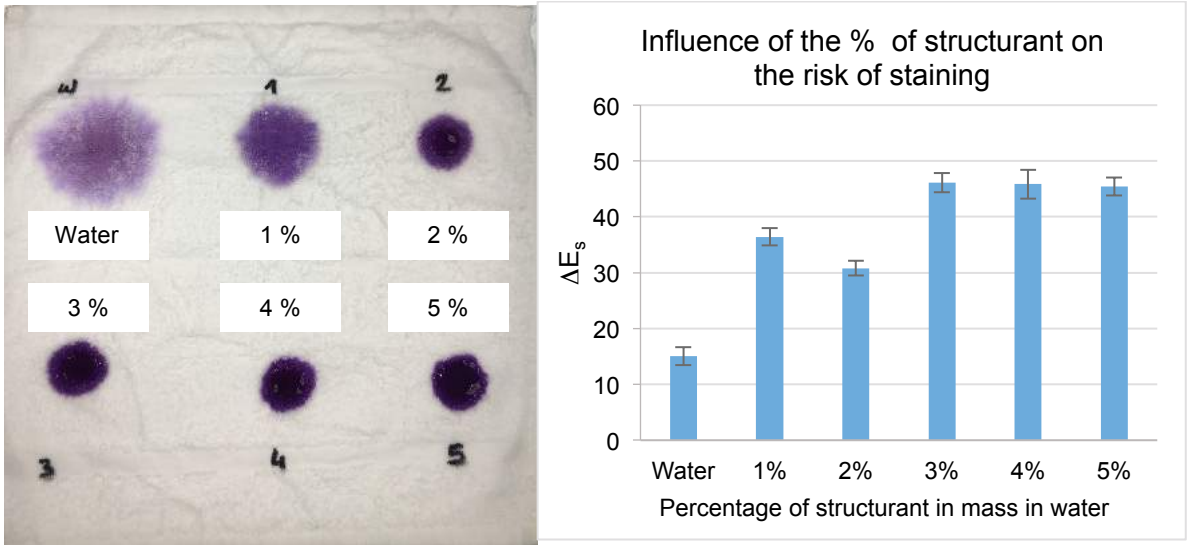

Figure 6.22: On the left: fabric after the deposition of 1.5 mL of each formations containing the same amount of E4210 dye in water only or with 1, 2, 3, 4 and 5 % of structurant. On the right: results of staining test as function of the % of structurant.

From Figure 6.22, the opposite effect as before with the risk of staining increasing as a function of the viscosity can be observed. This is probably due to the fact that when the formulation is more viscous, there are more adhesive forces between the formulation and fibre, while when the formulation is less viscous, the adhesive forces between the formulation and the fibre are weaker and result in greater expansion of the formulation through the fibre. However, as discussed in introduction of Chapter 5, surfactants can act as levelling agent to help the migration of the dye after initial uneven sorption onto fibre.[18] This would explain why the opposite effect is obtained in the presence of surfactant. This would also show that the effect of surfactant-fibre interactions in the dye deposition onto fabric would be more important than the viscosity of the formulation or event the dye-surfactant interactions.

6.2.2.4. Dye removal test

In the majority of literature concerning dye-surfactant interactions or the dye deposition onto the fibre, authors report on the industrial dyeing of fabrics. For this, they use dye baths with high concentration of dye molecules with the aim of getting the maximum of dye adsorption and a long-term dye fixation to the fibre. However, in the case of this thesis, the dying of the fabrics is not wanted but simply merely depositing the minimum number of dye molecules (involving a low dye

concentration) needed to counter the yellowish hue of white garments with time. Moreover, as hueing dyes are a technology intended to be used daily in washing machines, the ratio of dye molecules adsorbed and removed from the fabrics at each wash cycle has to be taken into account in order to avoid the long term overhue. Due to this, a dye removal test was developed (see Chapter 2, 2.3. Dye removal test) in order to gauge the ability of a formulation to remove dye from the fabric. The dye removal test was thus applied using the formulations containing the $C_{13}E_j$ surfactant series (see Figure 6.23) in order to see the effect of the number of EO groups on the dye removal and also to correlate the results obtained with the staining tests previously obtained. Then, the dye removal test was performed with only $C_{13}E_{10}$ at different level in mass in the formulation (keeping the other chemicals at the same level) in order to see the influence of the surfactant concentration on the dye removal (see Figure 6.24). Note that contrary to the staining test where ΔE_s defines the risk of staining with the more ΔE_s, the greater the risk of staining (ΔE_s being the difference in colouration between before the staining test – white fabric – and after the test – at the spot where the formulations were disposed); ΔE_r in the case of the dye removal test defines the ability of the formulation to remove the dye from the fabric, with the more ΔE_r, the more the dye is removed from the fabric (ΔE_r being the difference in coloration between before the dye removal test – coloured fabric with E4210 – and after the test – at the spot where the formulation were disposed).

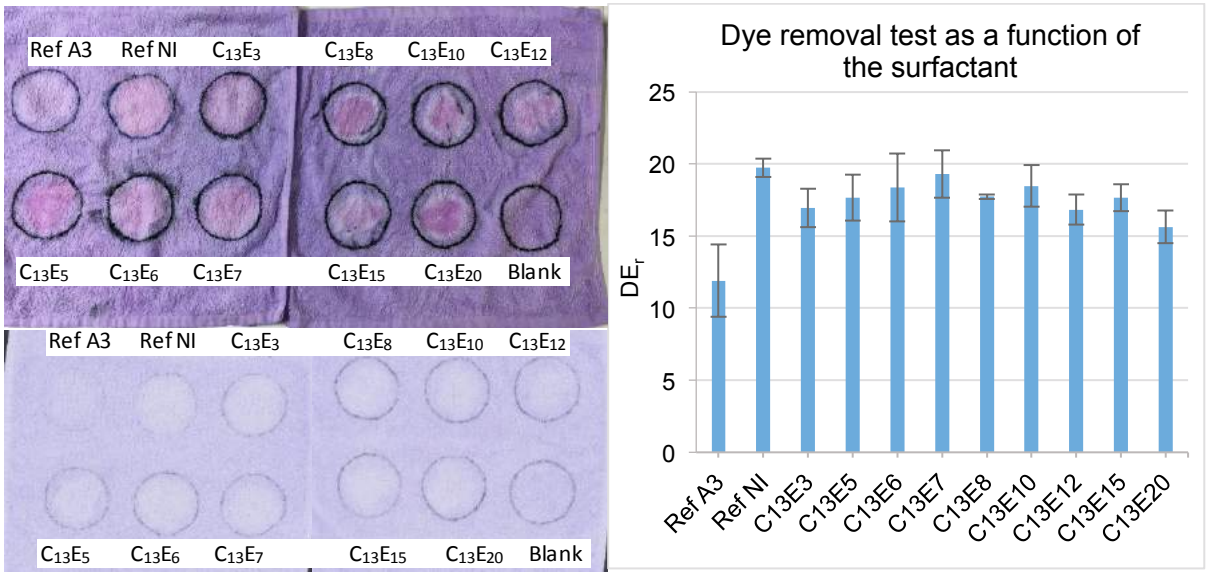

Figure 6.23: Dye removal test: On the top left, fabrics after 45 mins of the deposition step. On the bottom left, fabrics at the last step (after wash cycle and drying. On the right, results of dye removal test as a function of the surfactant within the $C_{13}E_j$ surfactant series.

First of all, looking at the fabric pictures in Figure 6.23, it can be observed on the top picture after 45 minutes of formulation deposition that the region where the Ref A3 formulation was deposited (1st spot from the top left) is whiter than the others, while the region where the Ref NI formulation was disposed (2nd spot from the top left) is also white but with some reddish/pinkish colouration while the fabric coloured with E4210 was purple (like outside spots). Note that in this context, the white "colouration" refers to the decolouration of the pre-coloured fabric, i.e. due to the dye removal. Now looking at the bottom picture after the complete dye removal test (i.e. after the wash cycle and drying step), it can be observed that the spot where Ref NI formulation was deposited (2nd spot from the top left) is whiter than the spot where the Ref A3 formulation was deposited (1st spot from the top left); meaning that the Ref NI formulation is more efficient than the Ref A3 formulation in terms of dye removal. This last observation is confirmed by the dye removal test results obtained in the graph in Figure 6.23, where ΔE_r is higher for the Ref NI formulation than the Ref A3 formulation. Regarding the $C_{13}E_j$ surfactant series' results, it seems that the ability of the formulation to remove dye from the fabric increases with the number of EO groups until an optimum of 7 EO groups and then decreases.Now comparing these results with the staining results obtained on Figure 6.16, it can be osberved that in general, a formulation which leads to a small risk of staining, leads to a high dye removal, except for the fact that the optimum point regarding the risk of staining was at 10 EO groups while it is at 7 EO groups for the dye removal.

From these observations and results, the following mechanism of dye removal in the presence of surfactant can be proposed. First, as suggested in 6.2.2.1.2. Influence of the surfactant with E4210, when a surfactant had higher interactions for fibres than with dye molecules, it leads to a better dye removal due to an adsorption competition between surfactant and dye molecules at the surface of the fabric. Secondly, when the dye-surfactant interactions are high, dye molecules are kept in surfactant micelles limiting the dye redeposition onto fabric and thus leading to a better dye removal action. This is supported by the fact that a white colouration (i.e. a decolouration of the pre-coloured fabric) using the Ref A3 formulation was observed, while using the Ref NI formulation, in addition to the white colouration, a reddish/pinkish colouration due to dye molecules incorporation into surfactant micelles was also observed (discussed in Chapter 5, 5.2.2. Dye location in surfactant

micelles). Thus, using the Ref NI, dye-surfactant interactions are higher than using the Ref A3 formulation, which leads to less dye redeposition onto fabric and thus a better dye removal action. However, note that there is still a dye deposition onto fabric since a result of 11.9 was obtained for the ΔE_s corresponding to the colour difference between the fabric without any treatment and the fabric after the dye removal test at a level of 20 % in mass of $C_{13}E_{10}$.

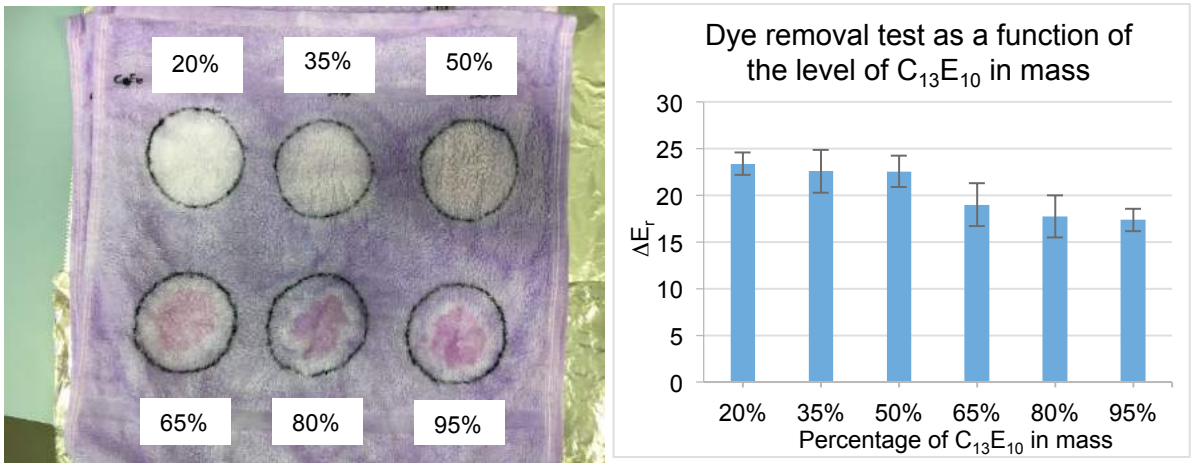

Figure 6.24: On the left, fabric after the dye removal test as a function of the level in mass of $C_{13}E_{10}$. On the right, Dye removal test as a function of the level of $C_{13}E_{10}$ in mass.

Looking at Figure 6.24, it can be observed that the dye removal decreases with the level of $C_{13}E_{10}$ with a high decolouration using 20 % in mass of $C_{13}E_{10}$. It also seems that there is a break point in the dye removal mechanism at a level of $C_{13}E_{10}$ superior to 50 % in mass with a significant decrease in dye removal and again the presence of reddish/pinkish colouration. However, it would need more experiments and especially surfactant-fibre interactions data in order to be able to go further in the interpretation of the results and to validate the mechanisms. A DRS and/or FTIR analyse could also be used on the fabric to see if surfactant molecules are present at the surface of the fabric which would explain a potential aggregation or dye molecules uptaken bu surfactant molecules (dye incorporated in surfactant micelles).

6.3. Conclusion

The method of dye adsorption in small scale developed in this thesis is a basic and good method to visualise but also quantify the dye deposition onto fabric. Moreover, even if it was not possible to determine the sensitivity and the limit of detection of dye molecules adsorbed onto fabric, this method seems a good and faster alternative to the common quantification method of dissolving the dye

molecules adsorbed onto fabric into solvents and then quantifying them by LC-MS. It allowed us to quickly see the difference in dye adsorption as a function of the nature and weaving of the fabric studied. However, several studies on the different fabrics used were performed in this thesis where no results were enabling to explain in any detail the difference in dye adsorption. Measurement of the fibre pore size distribution by inverse exclusion chromatography (not available at the university) would be invaluable for further studies here. In the presence of surfactant, it was observed a decrease of the dye deposition when the surfactant concentration increases with a break point when the surfactant CMC is reached, leading to almost no dye adsorption onto fabric (this is one of the limits of this method: limit of detection). At this point, a huge difference in colour intensity which decreases was also observed; and, to a lesser extent, a small change in the hue of the colouration, which looks pinker. This can be either due to the high decrease in colour intensity, or due to the fact that dye molecules are incorporated in surfactant molecules, leading to a solvatochromism effect.

From these observations, two hypothesis were made on the influence of surfactants on the dye deposition. The first one being that the dye-surfactant interactions would be higher than those between dye molecules and fabric, entrapping dye molecules in surfactant micelles and thus avoiding their interactions with fibres. The second one would be to assume that the interactions between surfactant molecules and fibres are higher than the interactions between dye molecules and fibres, leading to an adsorption competition and less free space at the fabric surface for dye molecules.

Using the methods developed in this thesis, some parameters have to be considered carefully. It is particularly important to keep the dye concentration and also the agitation constant within the same study for efficient comparison of results. Agitation favours the dye deposition by constantly renewing the presence of dye molecules at the boundary layer between the fabric and the bulk solution and improving the diffusion through fibres. In addition to this, the methods have some limits such as the limit of detection. First of all, a dye concentration acceptable for the absorbance measurements must be used, i.e. a dye concentration where absorbance should neither be too high or too small and where the Beer-Lambert law is validated. Moreover, when only a small change in dye concentration occurs (as

encountered during the experiments in the presence of surfactant), the sensitivity of the measurement is too weak. In addition to this, this method is not suitable for dye aggregation occurring in the concentration range of study. The DRS studies, have shown that the monomer of V200 is preferentially adsorbed onto fabric while the aggregate remains in solution and is redispersed into monomers to keep the equilibrium between monomers and aggregates in solution constant until all the aggregates are redispersed into monomer. This phenomena leads thus to a high perturbation in absorbance measurements when following only the adsorption of the monomer onto fabric with time.

In order to be in realistic conditions and study what happens daily in our washing machine when the SUD is badly dissolved and directly in contact with fabric, the staining test developed at P&G was used. This method was also modified to create the dye removal test. In addition to an IAS to determine the *L, a* and *b* values where the formulations were deposited, the staining test was thus used to determine the risk of staining by comparing the colour of the fabric before and after the deposition of a blue top formulation (left for 45 min, then rinsed and washed in a short wash cycle at 30 °C). A dye removal test was then used to determine the ability of a formulation (without dye) to remove dye from fabric by comparing the colour of a pre-coloured fabric before and after the deposition of the surfactant formulations. They are quite good methods to visualise and quantify the risk of staining and dye removal. However, they are not fast methods since there are several steps from the preparation of each fabric and formulations to the analysis of each spot by the IAS. Moreover, additional analysis must be carried out to quantify the amount of dye adsorbed/removed onto/from the fabric.

As observed by previous works from P&G, it has been shown that nonionic formulations can reduce the risk of staining compared to the current ionic formulation used by P&G. However, as this thesis has been focused on nonionic formulations, more comparisons with several ionic formulations would be needed to confirm this. It has also been shown that, even if E4210 is a more efficient technology, it comes with higher risk of staining likely due to the long ethoxylated chain of E4210, which brings higher interactions with cotton fibres than with V200. This can also be due to the difference in the molar extinction coefficient of E4210, which is higher than V200's.

Regarding the influence of the number of EO groups of the nonionic surfactant on the risk of staining, it seems that this depends on the number of carbons on the nonionic hydrophobic part. Indeed, using the $C_{13}E_j$ surfactant series, the risk of staining decreases to an optimum of 12 EO groups and then increases; while using the $C_{10}E_j$ surfactant series, the risk of staining increases slightly to a maximum of 9 EO groups and then decreases. Moreover, it seems that the risk of staining decreases by increasing the number of carbon on the nonionic hydrophobic part, but this would need more comparison with other carbon chain lengths to confirm this.

Looking at the effect of the formulation viscosity on the risk of staining, it has been shown that in the absence of surfactant (i.e. the viscosity only coming from a structurant), the risk of staining increases with the viscosity of the formulation. This is likely due to the fact that when the formulation is more viscous, there are more adhesive forces between the formulation and fibre leading to high interactions between dye molecules and fibres, while when the formulation is less viscous, the adhesive forces between the formulation and the fibres are weaker and lead to the expansion of the formulation through the fibre. However, when the viscosity is coming from the surfactant, we can observe the opposite trend, with the risk of staining decreasing with the increase of viscosity, showing the important role of surfactants in the dye adsorption.

By comparison with the results obtained in Chapter 5, 5.2.1. Visualisation of the dye interactions and binding constant, i.e. the absorbance at the plateau of dye solution in presence of increasing surfactant concentration with the tentative hypothesis that it would be correlated with the strength of the dye-surfactant interaction, it has been shown that stronger dye-surfactant interactions decrease the risk of staining using the $C_{10}E_j$ surfactant series. However, in the $C_{13}E_j$ surfactant series, it followed the opposite trend with the risk of staining increasing.

Regarding the dye removal, it has been observed that the risk of staining increases with the ability of the formulation to remove dye from fabric. However, while an optimum of the risk of staining was obtained at 12 EO groups, an optimum of dye removal was obtained at 7 EO groups. By comparing the dye removal between the ionic and the nonionic reference formulations, it has been observed that at the direct application of the formulation, the dye seemed more removed using the ionic

formulation; while after the washing cycle, the nonionic formulation had a better effect on dye removal.

All these observations and analysis results allow proposing the following tentative hypothesis on the dye adsorption mechanism in the presence of surfactant. It seems that two mechanisms take place. In the bulk, dye molecules are free in the formulation as well as incorporated in surfactant micelles. If the dye-fibre interactions are higher than the ones between surfactant and fibre, thus a simple dye adsorption onto fabric occurs, and so the dye micellisation controls and reduces the amount of dye-fibre interactions reducing the risk of staining. In this way, the greater the dye-surfactant interactions, the less there is a risk of staining. In addition to this, dye-surfactant interactions will also play a role of keeping dye molecules in suspension within surfactant micelles to avoid the redeposition onto fabric in the dye removal process.

However, if the surfactant-fibre interactions are higher than dye-fibre interactions, there is a competitive adsorption between them at the fabric surface. This would occur with a decrease in the hydrocarbon chain length of the surfactant increasing its affinity with cotton fibres. In this case, surfactant molecules are preferentially adsorbed at the surface of the fabric leaving less free space for the dye to adsorb at the fabric surface thereby decreasing the risk of staining. In the same way, when dye molecules are already adsorbed at the surface, surfactant molecules will displace dye molecules at the fabric surface. Thus, the more the surfactant-fibre interaction, the more the formulation is able to remove dye from fabric. Note that in reality, the risk of staining occurs when the formulation is not well dissolved and is directly in contact with the fabric; i.e. with a high surfactant concentration in a small contact area. It is more likely that when the SUD in normally dissolved, the surfactant and especially the dye concentration is much smaller on a small given area, leading to a normal and homogeneous dye adsorption onto fabric.

Thus, in any case, the dye-surfactant interactions have a role of controlling the adsorption kinetic by slowing down or limiting the dye-fibre interactions reducing the risk of staining. The surfactant also participates in the dye removal by avoiding the dye redeposition by keeping them in suspension within surfactant micelles. In addition to this, the choice of the surfactant is even more important since the risk of staining is reduced again if the surfactant-fibre interactions are stronger than dye-

fibre interactions. However, it would be necessary to study the surfactant-fibre and dye-fibre interactions directly to confidently interpret the results and fully validate these mechanisms.

References

[1] M. Showell, *Handbook of Detergents, Part D: Formulation* (CRC Press, 2006).
[2] E. Kissa, 'Wetting and Wicking', *Textile Research Journal* 66, no. 10 (1996): 660–668.
[3] W. Herbst, K. Hunger, and G. Wilker, *Industrial Organic Pigments: Production, Properties, Applications*, 3., compl. rev. ed (Weinheim: Wiley-VCH, 2004).
[4] K. Singha, 'Analysis of Spandex/Cotton Elastomeric Properties: Spinning and Applications', *International Journal of Composite Materials* 2, no. 2 (2012): 11–16.
[5] S. C. O. Ugbolue, *Polyolefin Fibres: Industrial and Medical Applications* (Elsevier, 2009).
[6] M. Clark, *Handbook of Textile and Industrial Dyeing: Principles, Processes and Types of Dyes*, (Woodhead Publishing, 2011).
[7] T. Vickerstaff, *The Physical Chemistry of Dyeing*, Second edition (Oliver and Boyd, London, 1954).
[8] A. Kongdee et al., 'Inverse Size Exclusion Chromatography - A Technique of Pore Characterisation of Textile Materials.', *Lenzinger Berichte* 82, no. 96–101 (2003): 193.
[9] P. B. Weisz and H. Zollinger, 'Sorption-Diffusion in Heterogeneous Systems. Part 3.—Experimental Models of Dye Sorption', *Transactions of the Faraday Society* 63 (1967): 1815–1823.
[10] P. B. Weisz and H. Zollinger, 'Sorption-Diffusion in Heterogeneous Systems. Part 4.—Dyeing Rates in Organic Fibres', *Transactions of the Faraday Society* 64 (1968): 1693–1700.
[11] F. M. Drumond Chequer et al., "Textile Dyes: Dyeing Process and Environmental Impact," in *Eco-Friendly Textile Dyeing and Finishing*, ed. M. Gunay (InTech, 2013).
[12] S. N. Batchelor and J. M. Bird, Bright detergent composition, WO2014012923 A1, issued 2014, Unilever Plc.
[13] E. S. Sadlowski and M. D. Cummings, Laundry detergent compositions with hueing dye, US7205269, issued 2007, The Procter & Gamble Company.
[14] E. S. Sadlowski and M. D. Cummings, Laundry detergent compositions with efficient hueing dye, US7208459, issued 2007, The Procter & Gamble Company.
[15] L. G. Brush et al., Fabric care compositions comprising hueing dye, US7235518, issued 2007, The Procter & Gamble Company.
[16] A. Johnson, *The Theory of Coloration of Textiles* (Society of Dyers and Colourists, 1989).
[17] S. C. Biswas and D. K. Chattoraj, 'Polysaccharide- Surfactant Interaction. 1. Adsorption of Cationic Surfactants at the Cellulose- Water Interface', *Langmuir* 13, no. 17 (1997): 4505–4511.
[18] R. Christie, *Colour Chemistry*, 2001.

7. Conclusion and Future Work

To summarise this thesis, the important results obtained for the investigation on the fundamental understanding of the underlying mechanisms and interactions in complex fluids governing the dye deposition in presence of surfactants will be presented. The different analytical techniques and methods developed during this thesis, their usefulness and limits will be also discussed. Also, when it is relevant, some guidance and/or future work to further study or fully validate some hypothesis will be proposed.

First, surfactants were described and characterised by tensiometry, which is a good and quite fast technique to determine the CMC, as well the decreasing surface tension of each surfactant. It has been shown that in addition to the cloud point for nonionic surfactants, there are key parameters for surfactant properties and their use. Indeed, a change in the surfactant structure, either in the hydrophilic part or in the hydrophobic part, will affect its properties. There are several ways to increase the surfactant HLB (i.e. an increase of the hydrophilicity or a decrease of the hydrophobicity) by either adding EO groups, either reducing the carbon chain. Note that a branched carbonic chain will be more hydrophilic than a linear surfactant. By increasing the hydrophilicity of surfactant, interactions with water molecules will increase. This leads to a better solubilisation of surfactant molecules increasing its CMC and cloud point. Conversely, a surfactant that is rather hydrophobic will tend to aggregate in water, decreasing its CMC and its cloud point.

Note that as P&G works have shown a better effect to minimise the risk of staining using nonionic surfactant. Thus, this thesis has been more focused on the nonionic surfactants studies (two nonionic surfactant series with either 13 carbons or 10

carbons, comprising a range of EO groups from 3 to 20). However, it would have been wise to also study different anionic surfactants to investigate the influence of several polar head groups and get more comparisons between nonionic and anionic surfactants. Moreover, even if a better range of EO groups was used, further studies would have been beneficial in understanding the effect of the alkyl chain length. However, surfactants with a number of carbons inferior to 10 and superior to 13 with a range of number of EO groups are either not available or too expensive. In addition, surfactants with a carbonic chain of less than 10 carbons will be less soluble in water or lose its surfactant properties.

Two hueing dyes of interest for P&G were then characterised. They are two azo polymeric dyes dissolved in a PEG solvent at an effective concentration of 8.00 % and 5.94 % by mass of E4210 and V200, respectively. E4210 exhibits a maximum in absorbance at 540 nm; while V200 exhibits a H-aggregation in water at a concentration above 2×10^{-5} mol L^{-1}, leading to a first maximum in absorbance at 575 nm for the monomer and a hypsochromic shift at 492 nm corresponding to the aggregate. A purification of E4210 was performed, but the spectrophotometric measurements have not pointed out a difference in the shape and maximum of the absorption band. Thus, due to the dye aggregation of V200 and the time-consuming and expensive purification of E4210, the commercial form of E4210 has been mainly used in the experiments.

The solvatochromic effect, which is responsible for bathochromic or hypsochromic shifts due to changes in the electronic state of chromophores was presented. It has thus been observed that a higher refractive index of a solvent leads to a bathochromic shift of the dye absorption band to a longer wavelength. Since the polarity and the refractive index of a solvent are correlated and as it is not always easy to determine the solvent polarity, this could be used to give an idea on solvatochromic effects. In the experiments, this solvatochromism effect was used to visualise the dye-surfactant interactions and found that the dye molecules were incorporated within the surfactant micelles. It has also been observed that from its structure, E4210 can exhibit a surfactant-like behaviour at high concentration (337 mg L^{-1}) by lowering the surface tension to 59.4 mN m^{-1}. However, the concentration of E4210 is very low in laundry products, and so the E4210 may just co-micellise with detergent surfactants.

After having characterised hueing dyes and surfactants, their interactions were characterised and investigated using the most common spectrophotometric method. As expected, it enables the visualisation of the incorporation of dye molecules in surfactant micelles. E4210 molecules start to interact with surfactant molecules leading to an increase of the absorbance intensity. Then, when the surfactant concentration increases to its CMC, it can be observed a shift of the absorption band caused by a change in the local environment surrounding the dye, showing its incorporation into micelles. Regarding V200, the solubilisation of the aggregates into monomers by the surfactant was first observed, followed by the incorporation of monomers into surfactant micelles.

The B-H equation was used to access the binding constant of the dye-surfactant complex by UV-vis spectrophotometry. However, even if this is a simple method, there are some parameters to be careful of, like the concentration of the dye regarding the surfactant concentration, which must be hundreds of times lower than the surfactant concentration in order to satisfy the B-H equation. In addition, the dye concentration and the temperature must be constant throughout the experiments since it can affect the final result. If the spectrophotometer can vary temperature (which was not the case for us), it is also possible to study the influence of the temperature on the dye-surfactant interactions or the dye deposition, for instance in the staining test, the blue top formulation temperature could be altered. The dye aggregates were not suitable for this study due to their absorbance shift; similarly any surfactants not solubilised sufficiently in water were also not suitable. One technique to help on this would be to use a solvent to solubilise better the dye aggregate or a more hydrophobic surfactant. However, this would lead to a solvatochromic effect and perturb the data analysis. Another alternative of the spectrophotometric method is the conductivity method proposed by D. Jocic[1], which can determine the degree of dye-surfactant interaction by determining the electrical conductivity of the dye solutions in the presence of surfactants. Also, it would have been interesting to use this technique in order to compare both methods and go further in the determination of the dye-surfactant complex binding constant, particularly with the study of V200 and more hydrophobic surfactants. Moreover, it

would have been easier to study the influence of the temperature on the dye-surfactant complex binding constant since we only need a hot plate.

Note that even if it was possible to visualise and characterise the dye-surfactant interaction using the B-H method, it was not possible to access the dye-surfactant complex binding constant from the experiments. Indeed, as the commercial E4210 effective concentration of 8.00 *wt%* was not taken into account, a huge difference in concentration between the dye and surfactant molecules was occurring. This was leading to all the dye being incorporated into the surfactant micelles for all the surfactant concentrations studied; creating a plateau of the maximum of absorbance that makes the B-H equation unusable. Alternatively to the B-H equation, the Job's method[2] could be used to study the dye-surfactant interactions.[3] This is a spectrophotometric method commonly used to determine the composition of complexes in solution as well as the association constant of the complex: very suitable for the method of continuous variations.

For this reason, a tentative hypothesis has been proposed where the greater the absorbance at the plateau, the greater the interactions between the dye and surfactant molecules. Making this hypothesis, it has been observed that an optimum of dye-surfactant interactions using both surfactant series (C13 and C10) occurs at a surfactant HLB around 14.40 and a number of EO units close to the number of EO units in the E4210 ethoxylated chain. Regarding the effect of the carbon chain length, this would need more comparison with other carbon chain lengths to reliably conclude. In the same way, it would also have been beneficial to study more anionic surfactants to compare with nonionic surfactants. Finally, it has been observed that the absorbance at the plateau, and thus potentially the dye-surfactant interactions, seems to evolve linearly suggesting that the dye-surfactant interactions are aditive. However, synergic effects should occur regarding the CMC of a surfactant mixture leading to a nonlinear behaviour. Thus, in the same way, the binding constant of a dye with a surfactant mixture should not be linear. All the interpretations of the dye-surfactant interaction results are tentative and require further studies to elucidate the correct value of the dye-surfactant binding constants.

Due to the spectrophotometric, SAXS and NMR studies, it has been possible to localise the E4210 molecules at the interface between the hydrophilic and

hydrophobic parts of the surfactant within the micelles, confirming its co-micellisation with surfactants.

To finish the investigation on the mechanisms of dye-surfactant interactions involved in the dye adsorption/removal onto fabric, dye deposition onto fabric in the absence and presence of surfactant using several methods was investigated. The method of dye adsorption on the small scale, which is a basic and good method to visualise and quantify the dye deposition onto fabric, allowed us to see the importance of keeping the agitation and dye concentration constant in the study. Accordingly, a difference in dye adsorption as a function of the fabric nature and fibre weaving has been observed. However, further studies are needed, especially the measurement of the fibre pore size distribution by inverse exclusion chromatography, to understand these results. Note that dye sorption seems to be similar between both dyes, E4210 and V200. However for V200, the DRS have shown that mainly monomers are adsorbing onto fabric with the aggregate in solution being redispersed into monomer to maintain the equilibrium between them both. In the presence of surfactant, the dye deposition decreases as a function of increasing surfactant concentration until the CMC is reached, where almost no dye adsorption onto fabric occurs. However, when a very small change in dye concentration occurs as in this case, the sensitivity of the measurement is too weak. Nevertheless, this method seems a good and faster alternative to the common quantification method of dissolving the dye molecules adsorbed onto fabric into suitable solvents and then quantifying them by analytical techniques such as LC-MS.

The staining test allowed being in realistic conditions in order to define the risk of staining from the blue top formulation. This method was also modified to create the dye removal test to define the ability of a surfactant formulation to remove dye from fabric. Using the staining test, it has been confirmed that a nonionic formulation can reduce the risk of staining compared to the current ionic formulation. But again, more experiments using different anionic surfactants would be needed to quantify this. Also, the hue intensity seems to be higher for E4210 than V200. This could be due to the difference in the molar extinction coefficient of E4210, which is higher than V200's, bringing a more intense hue. Thus, it has been shown that even if E4210 is a more efficient technology, it comes with a higher risk of staining, probably due to the long ethoxylated chain of E4210, which brings higher interactions with cotton fibres

than V200. To a first approximation, the risk of staining seems to be primarily a function of the carbon chain length and then a function of the number of EO groups with again, an optimum when it is close to the ethoxylated chain length of E4210.

A decrease in the risk of staining by increasing the number of carbons on the nonionic hydrophobic part has been observed, but this would need more comparison with other carbon chain lengths to confirm. By increasing the viscosity of the formulation, an increase of the the risk of staining due to adhesive forces between the formulation and fibre leading to higher interactions between dye molecules and fibres has also been shown. Thus, as it has been shown that the dye deposition can be influenced by the solvent (without surfactant), it would have been interesting to investigate the solvent's role on the dye deposition in a real context by varying the solvents and their ratio with surfactant in the blue top formulation. Due to the solvatrochromic effect, the spectrophotometer technique was not suitable for this investigation. However, insofar as the determination of dye-surfactant binding constants with both dye E4210 and V200 by future conductimetry experiments were successful, it would be suitable for this purpose. Moreover, coupled with data on V200 deposition onto fabric and affinity of V200 for fabric fibres, it would be possible to see the influence of both dye-surfactant interactions using E4210 or V200 on the dye deposition and so answer the following questions. Is the risk of staining increased using E4210 rather than V200 due to a better affinity of E4210 with fibre than V200, or due to stronger V200-surfactant interaction compared to E4210-surfactant interactions? In addition, to what extent do these two physicochemical actions occur and affect the dye deposition?

As it was not possible to obtain the binding constants of dye-surfactant complexes as explained earlier and in Chapter 5, 5.2.1., the dye deposition results has been compared with the absorbance at the plateau of the dye solution with increasing concentration of surfactant. In this, it was assumed the tentative hypothesis that this plateau is correlated with the intensity of the dye-surfactant interactions. Thus, it has been shown that dye-surfactant interactions followed the same trend in the risk of staining using the $C_{10}E_j$ surfactant series, while it followed the opposite trend using the $C_{13}E_j$ series. Regarding the dye removal, it has been observed the same trend as the staining test. This means that the risk of staining increases with the ability of the formulation to remove dye from fabric.

The experiments led thus to propose two tentative hypothesis on the two mechanisms governing the dye deposition in the presence of surfactant. The first one occurs when the interactions between surfactant molecules and fibres are higher than the interactions between dye molecules and fibres. In this case, there is an adsorption competition at the fibre surface between dye and surfactant molecules, leading to less free space at the fabric surface for dye molecules. The second mechanism occurs when dye-surfactant interactions are higher than those between dye molecules and fabric. By entrapping dye molecules in surfactant micelles, the number of dye interactions with the fibre are reduced and similarly, dye redeposition is reduced. This is why a good formulation that minimises the risk of staining will also maximise the dye removal and thus keep an equilibrium between dye molecules adsorbed and removed from fabric. Note that it is more likely that both hypotheses play more or less a role in the dye deposition. However, it would be necessary to quantify the surfactant-fibre and dye-fibre interactions to be able to go further in the interpretation of the results and fully validate these mechanisms.

An additional study would be to investigate the dye-surfactant interaction and the dye deposition in the presence of soil since the fabric washing process it is clearly important to consider the soil. By definition, the detergency is the ability to clean a surface through a bath containing surfactants involving physicochemical actions to remove soils from fabric. These physicochemical actions include the most effective removal mechanism, which is typically the solubilisation of soils by surfactants. Thus, it will be interesting to know to what extent the soil-surfactant interactions influence the dye-surfactant interactions and the dye deposition. It is likely possible that a solubilisation competition within surfactant micelles will occur. It will be important to address the following questions. Are the dye-surfactant interactions perturbed in presence of soil and if so, to what extent? What is the difference in affinity between 1. dye molecules and soils with surfactant and 2. dyes molecules and soils with fibre? What is the soil's influence on the dye deposition and on the risk of staining? If surfactant solubilises soils from fabric, how does this affect the dye molecules already adsorbed onto the fabric? What is the influence of the soil concentration? For these soil studies, we could use an oil to mimic a greasy soil that we could incorporate into our samples at varying concentration. In particular, this oil could be added into in our dye-surfactant solutions (used for the determination of the dye-

surfactant complex binding constant), in our blue top formulation, or by directly applying it onto our fabric swatches with a drying step before applying the blue top formulation.

References

[1] D. Jocić, 'Conductivity Measurement - A Simple Method for Determining Dye / Surfactant Interaction', *Textile Research Journal* 65, no. 7 (1 July 1995): 409–16.
[2] P. Job, 'Job's Method of Continuous Variation.', *Ann. Chem.* 9 (1928): 113–203.
[3] P. F. Tavčer and J. Špan, 'Dye-Surfactant Interactions Studied Using Job's Method', *Textile Research Journal* 69, no. 4 (1999): 278–284.

8. Appendix

NMR
E4210

- ^{1}H E4210
- NOESY E4210
- HSQCAD E4210

^{1}H E4210

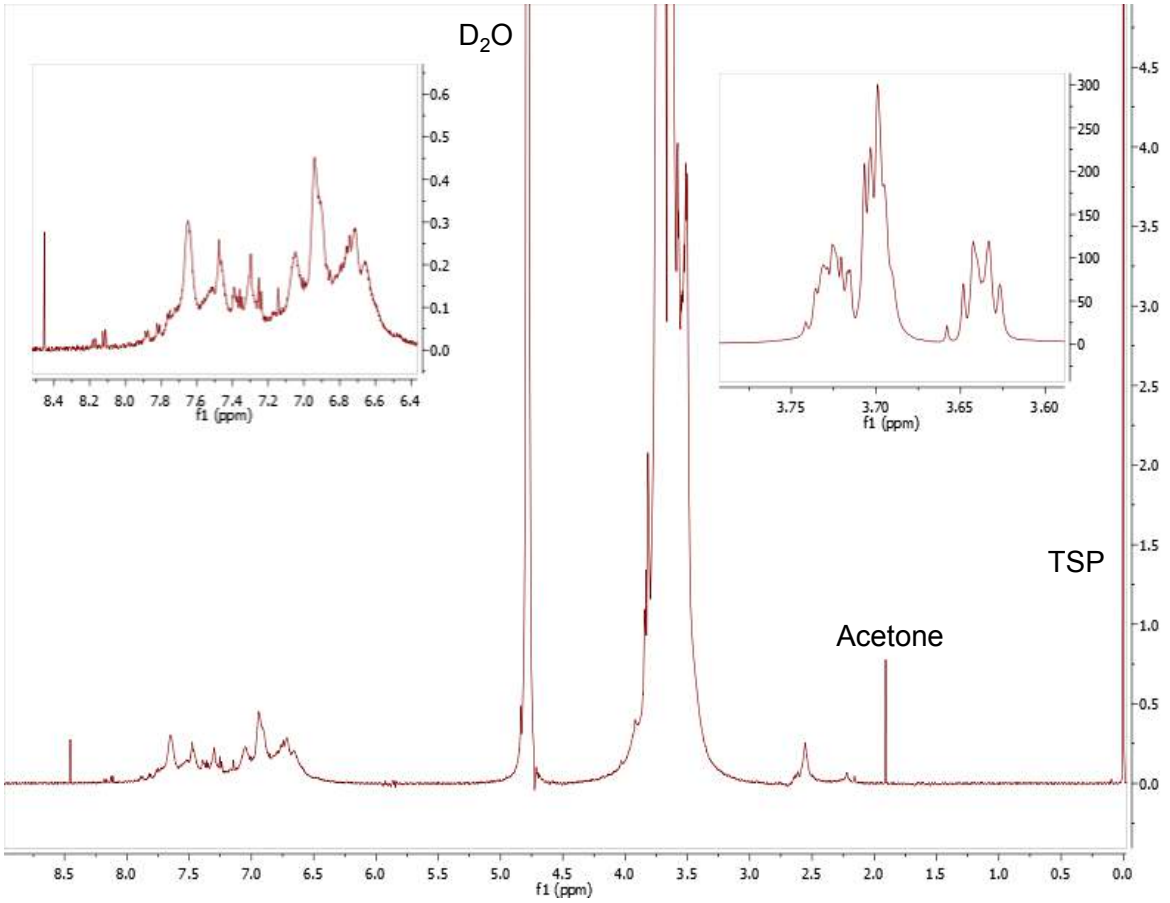

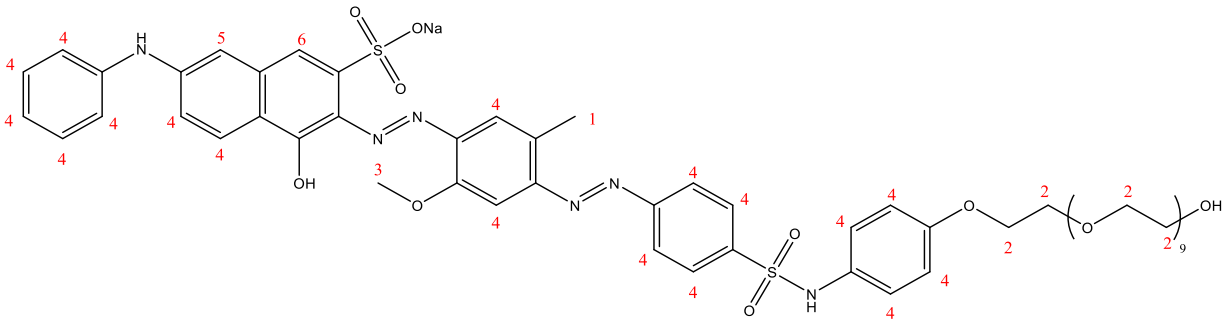

Assignment	Shift (ppm)	Shift (Hz)
TSP	0.00	0.00
Acetone	1.91	1144.20
1	2.56	1530.86
2	3.63 – 3.74	2174.29 – 2243.04
3	3.82	2287.74
D_2O	4.78	2866.25
4	6.66 – 7.65	3990.0 – 4584.97
5	7.79	4667.36
6	8.14	4883.22

NOESY E4210

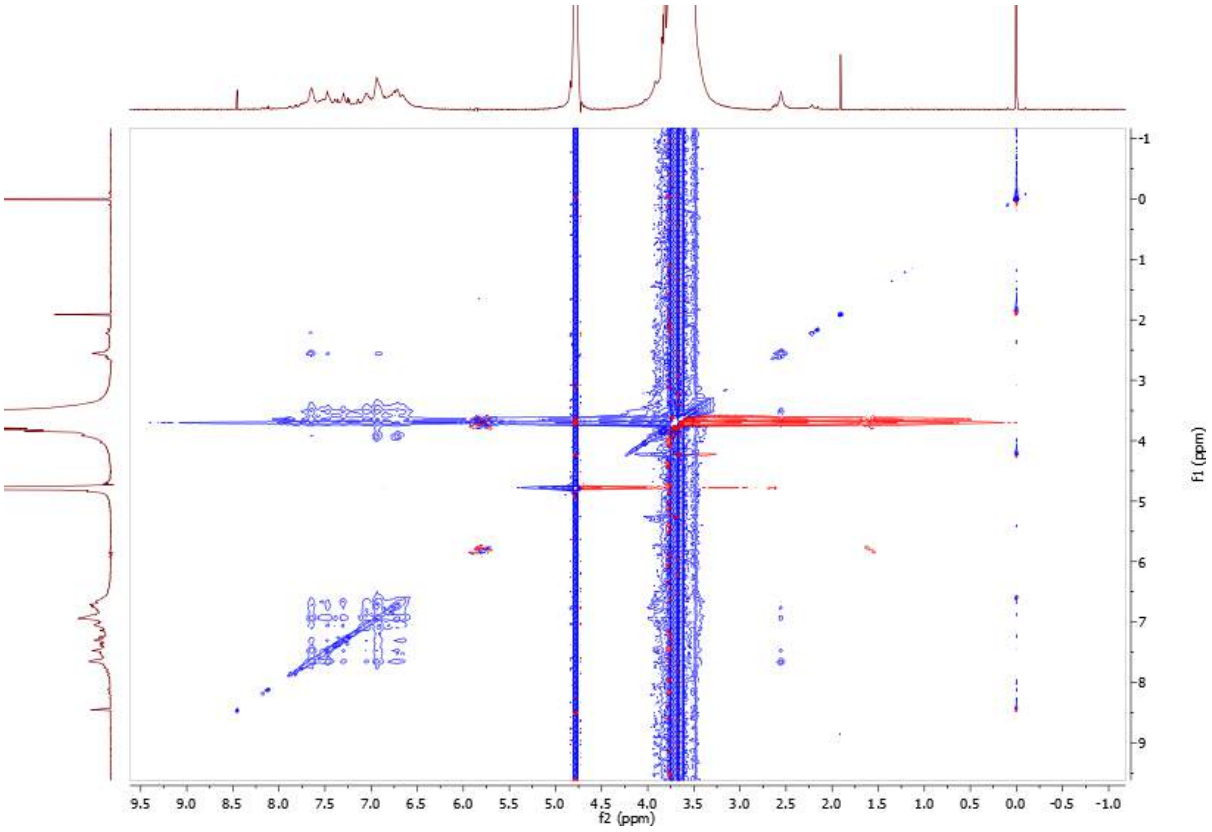

HSQCAD E4210

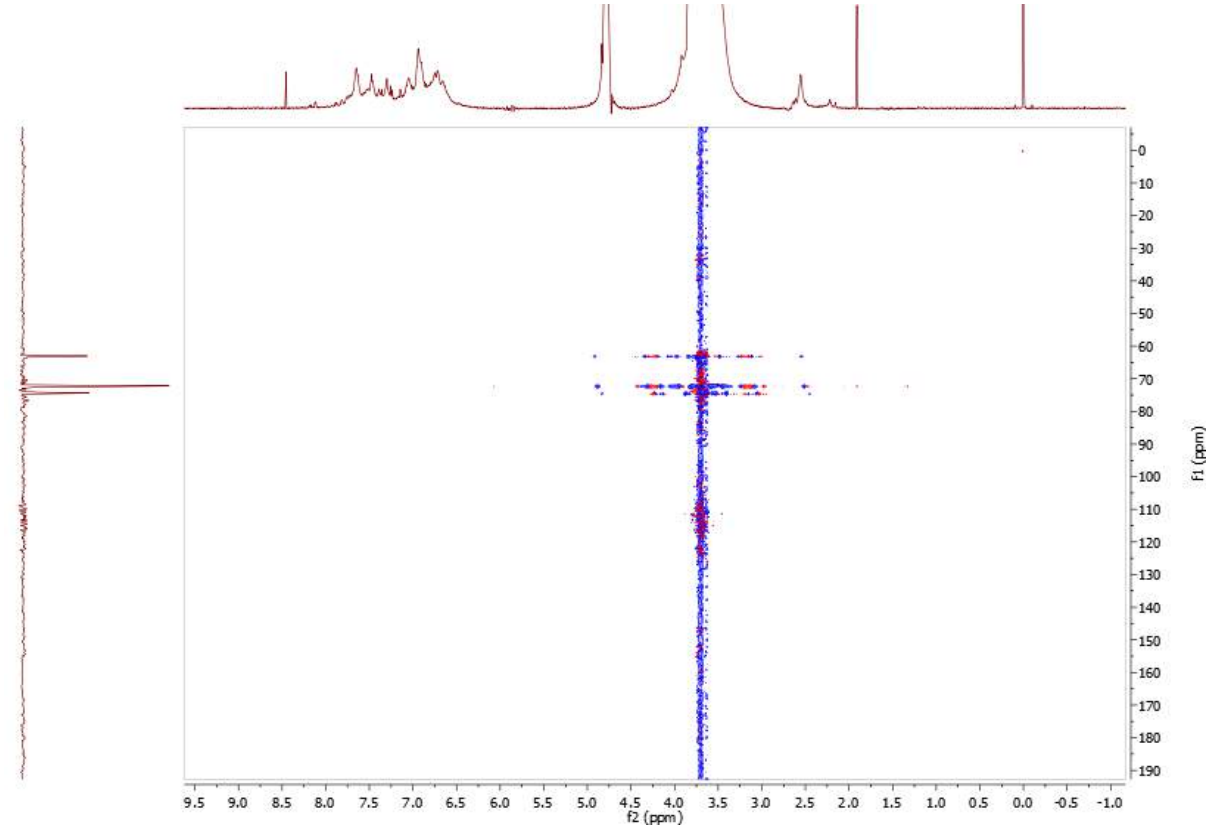

NMR
$C_{13}E_{10}$ – E4210

- ^{1}H $C_{13}E_{10}$
- NOESY $C_{13}E_{10}$
- HSQCAD $C_{13}E_{10}$
- ^{1}H $C_{13}E_{10}$ - E4210 complex
- NOESY $C_{13}E_{10}$ – E4210 complex
- ^{1}H $C_{13}E_{10}$ - E4210 complex comparison with pure samples
- NOESY $C_{13}E_{10}$ - E4210 complex comparison with pure samples

^1H $C_{13}E_{10}$

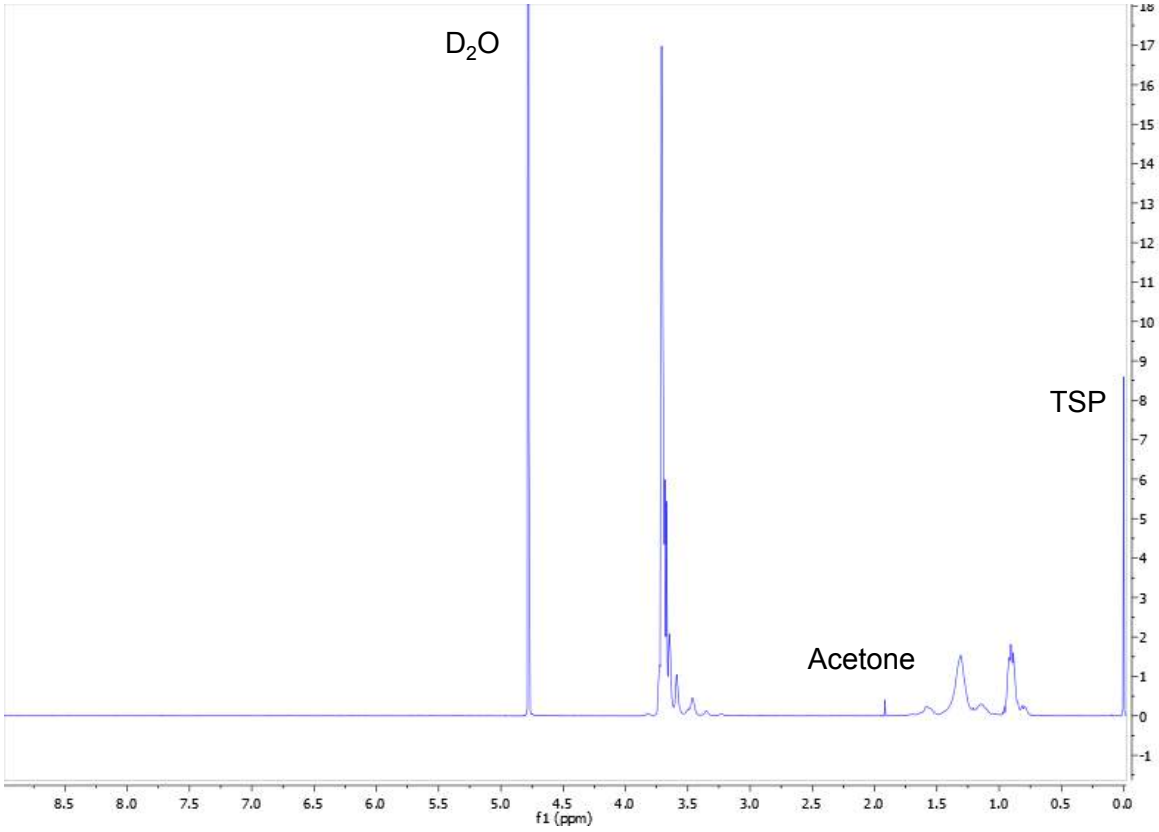

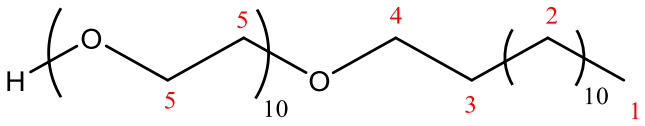

Assignment	Shift (ppm)	Shift (Hz)
TSP	0.00	0.00
1	0.91	543.34
2	1.31	784.29
3	1.59	951.57
Acetone	1.92	1149.09
4	3.59	2151.82
5	3.71	2224.07
D_2O	4.78	2864.47

NOESY $C_{13}E_{10}$

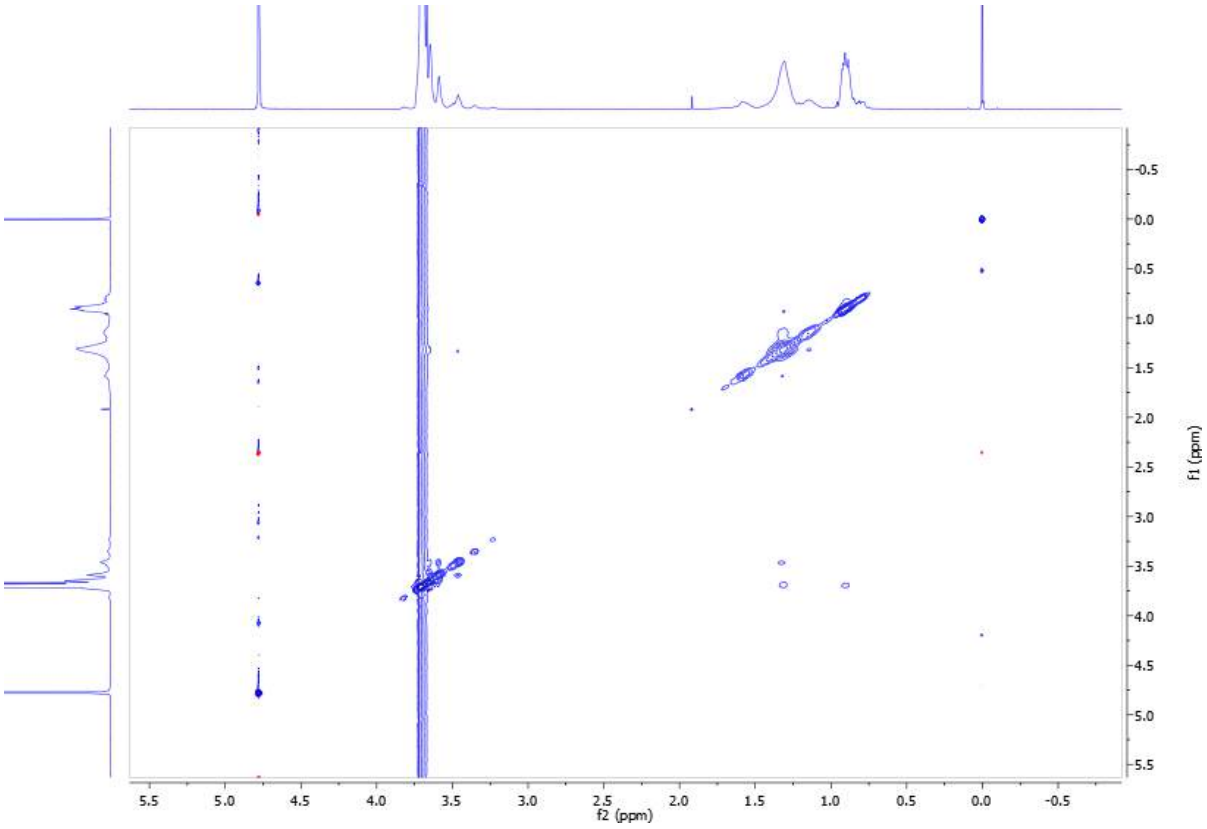

HSQCAD $C_{13}E_{10}$

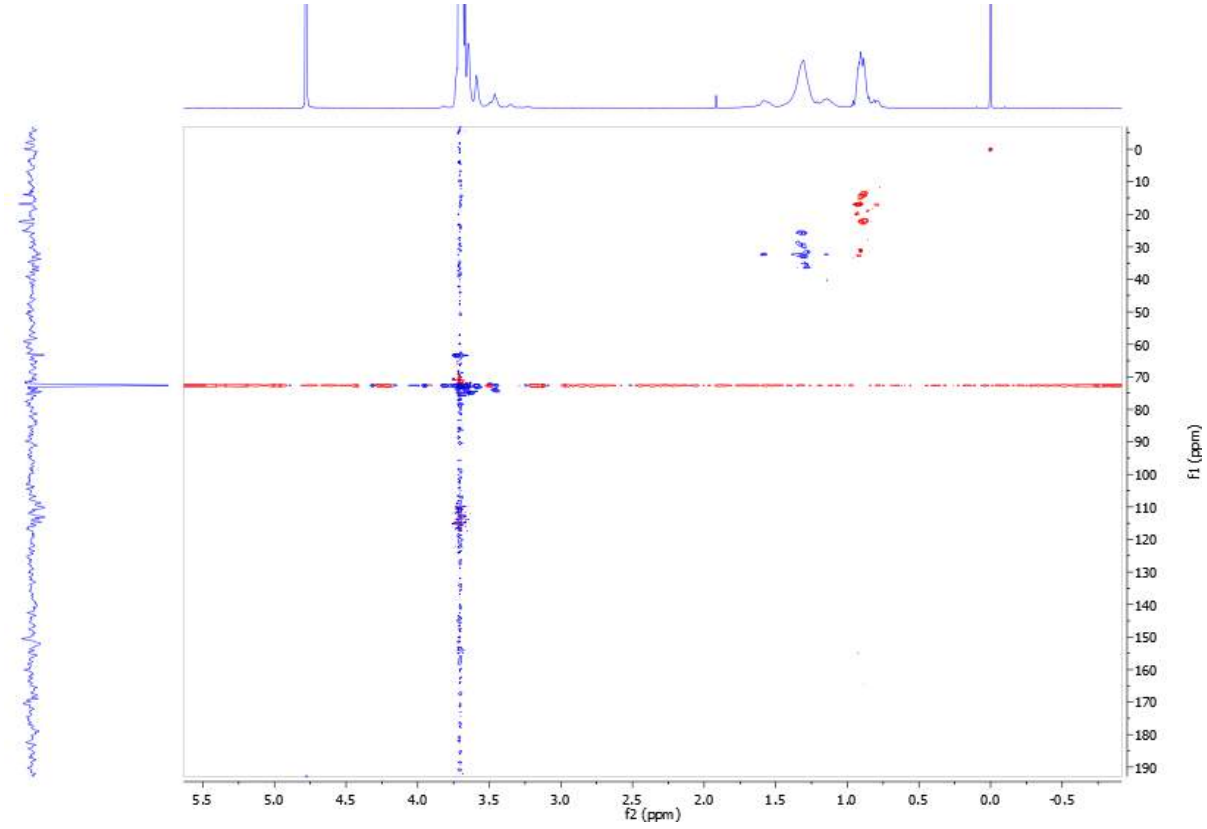

^1H $C_{13}E_{10}$ - E4210 complex

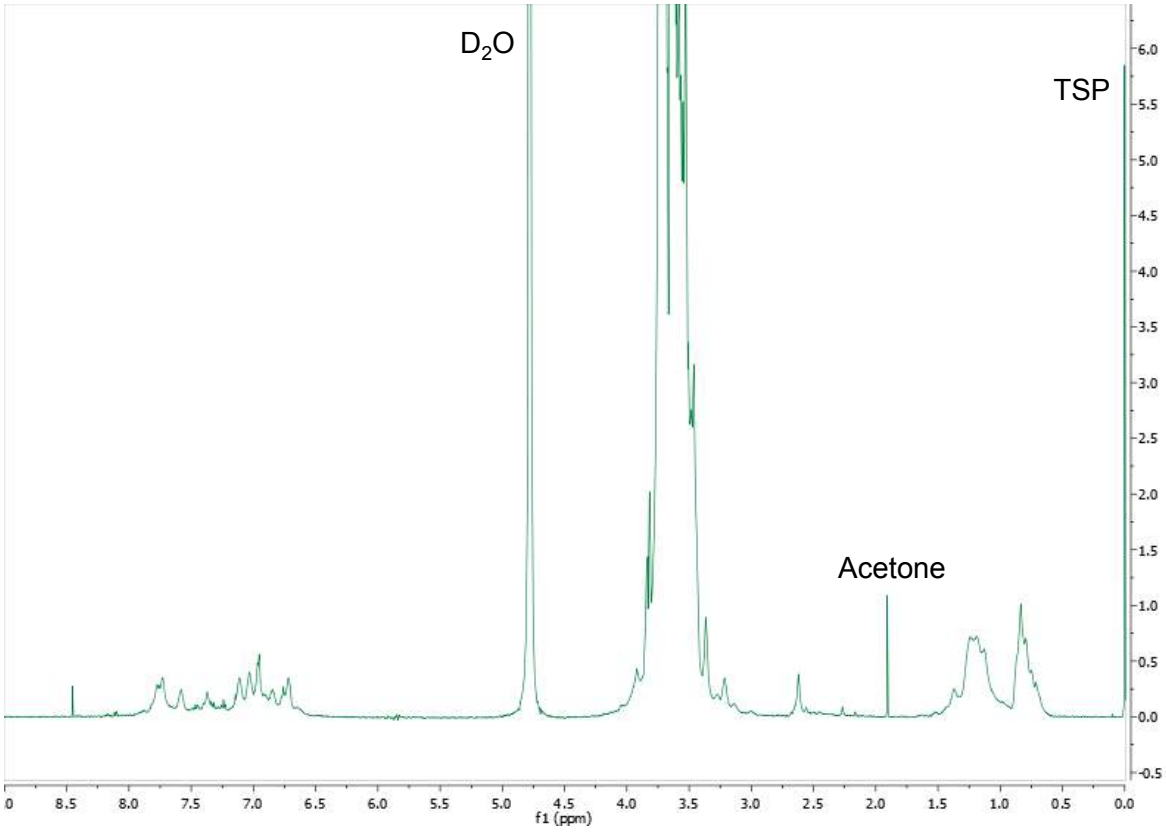

NOESY $C_{13}E_{10}$ - E4210 complex

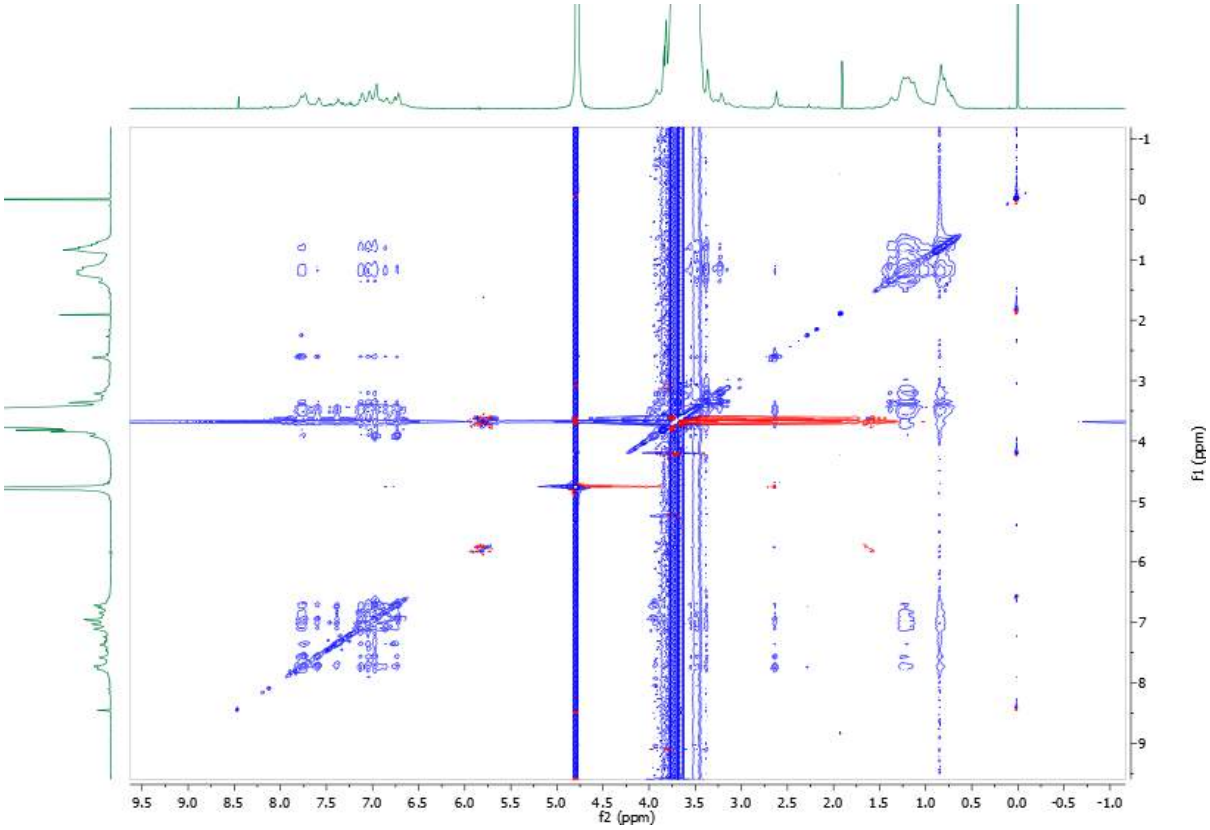

^{1}H $C_{13}E_{10}$ - E4210 complex comparison with pure samples

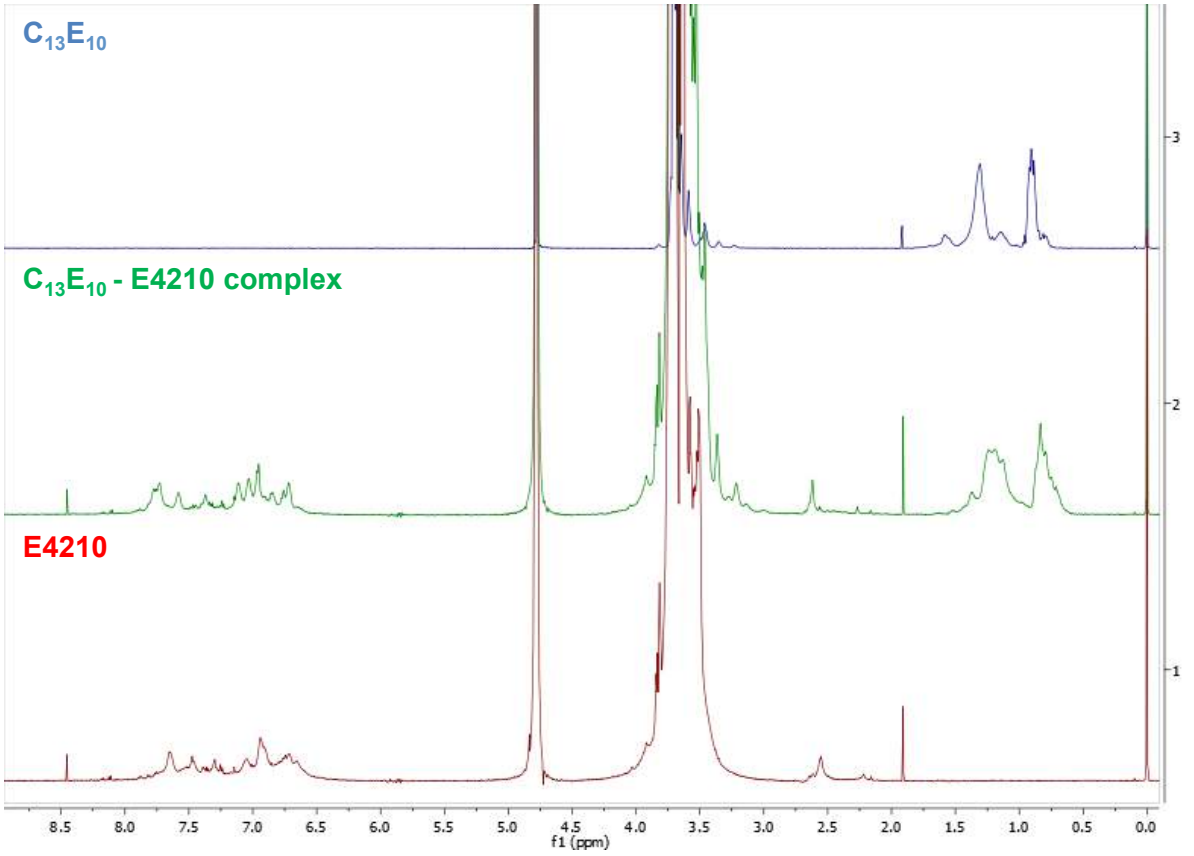

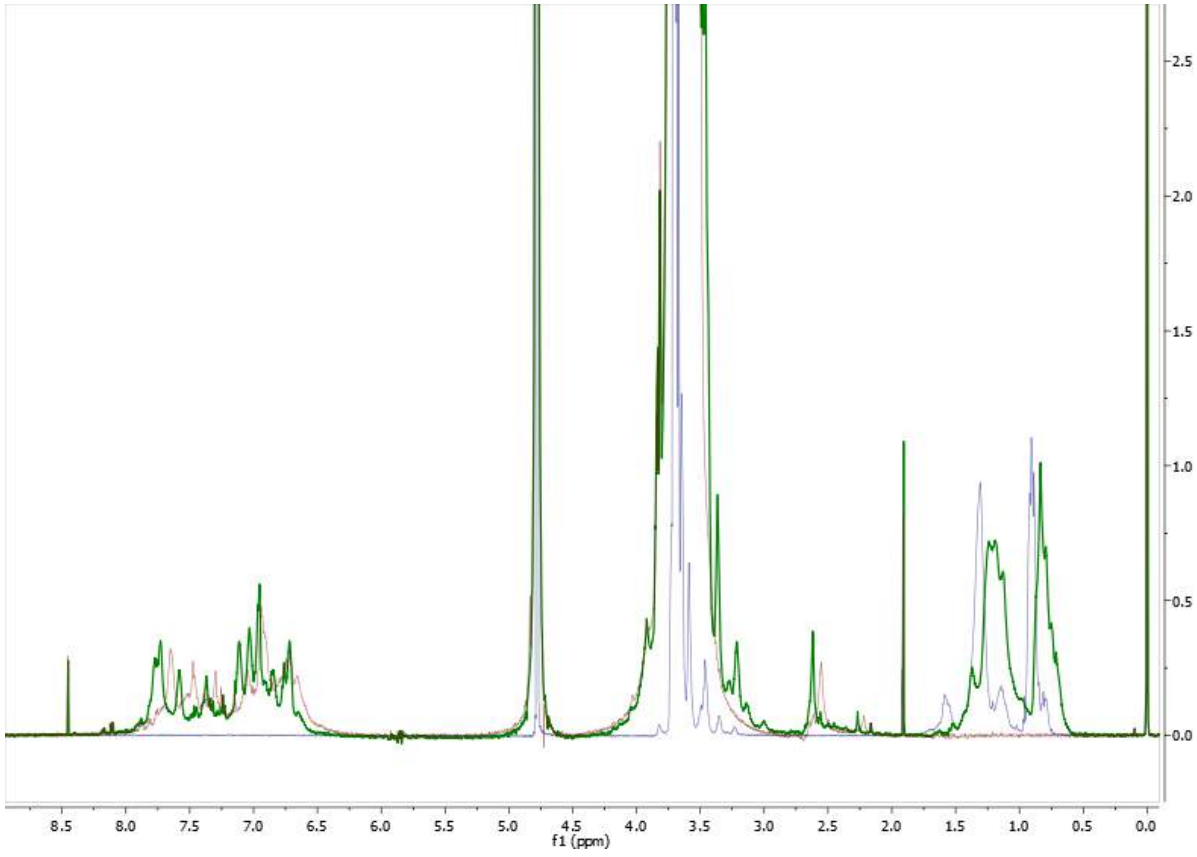

^{1}H $C_{13}E_{10}$ - E4210 complex comparison with pure samples

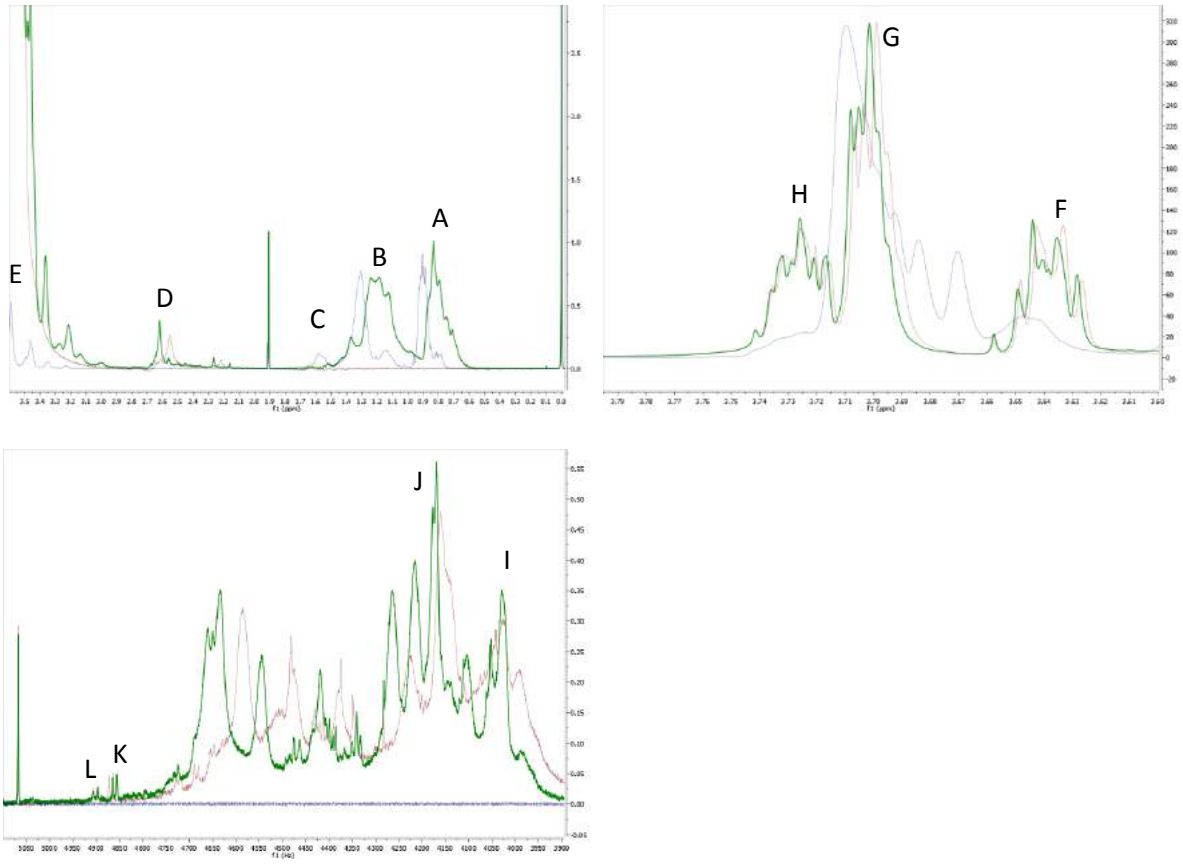

Assignment	$C_{13}E_{10}$ Shift (Hz)	E4210 Shift (Hz)	$C_{13}E_{10}$ - E4210 complex (Hz)	Delta Shift (Hz)
A	543.34		499.85	- 43.49
B	782.72		742.67	- 40.05
C	951.29		905.46	- 45.83
D		1530.86	1569.22	38.36
E	2151.07		2075.44	- 75.63
F		2178.23	2179.54	1.31
G	2224.07	2217.57	2219.07	- 5.00 / 1.50
H		2233.57	2233.69	0.12
I		4023.61	4026.22	2.61
J		4160.89	4168.42	7.53
L		4862.43	4856.03	- 6.40
M		4896.60	4897.12	0.52

NOESY $C_{13}E_{10}$ - E4210 complex comparison with pure samples

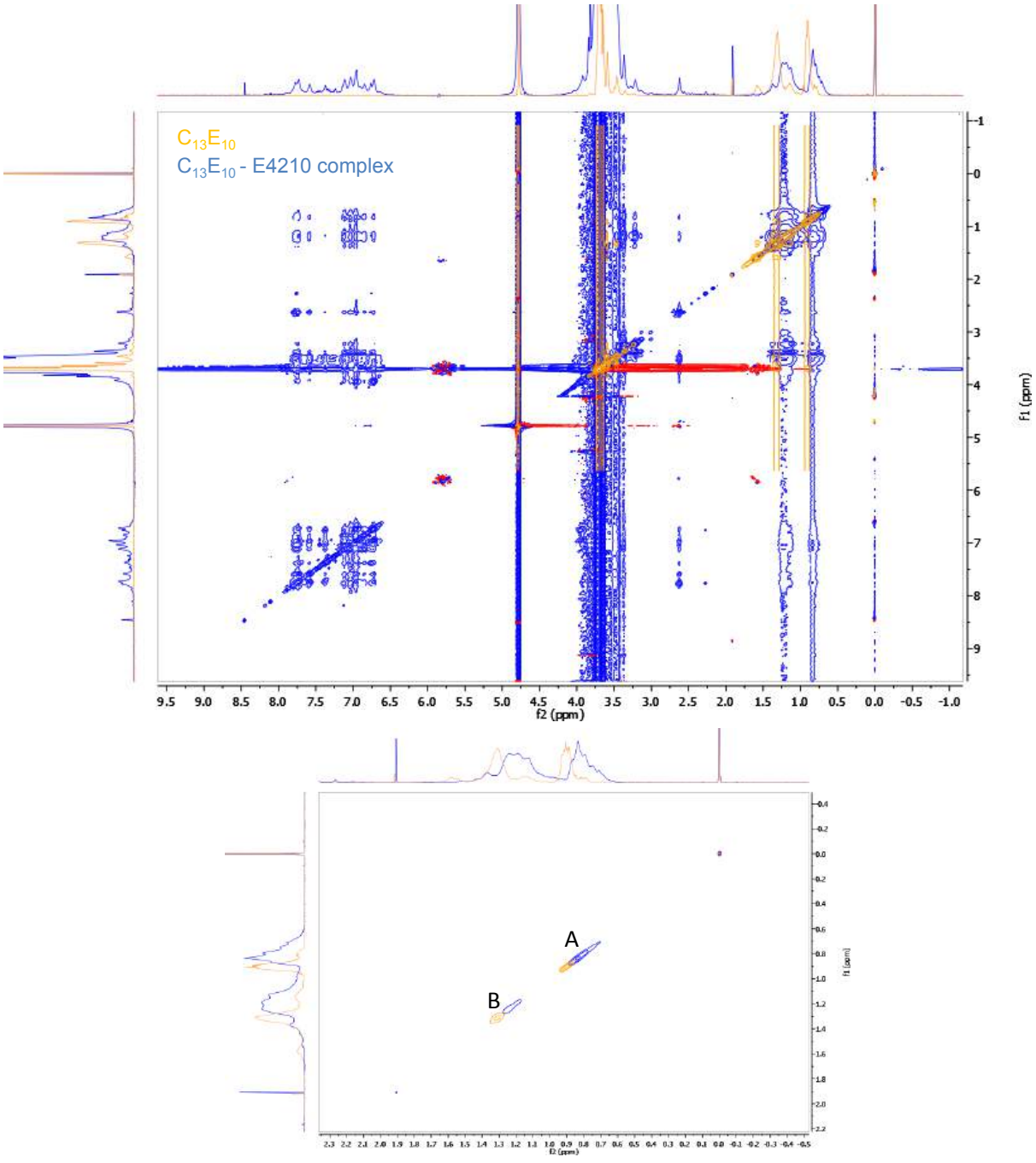

Assignment	$C_{13}E_{10}$ Shift (Hz)	E4210 Shift (Hz)	$C_{13}E_{10}$ - E4210 complex (Hz)	Delta Shift (Hz)
A	549.19		499.64	- 49.55
B	783.66		742.89	- 40.70

NOESY $C_{13}E_{10}$ - E4210 complex comparison with pure samples

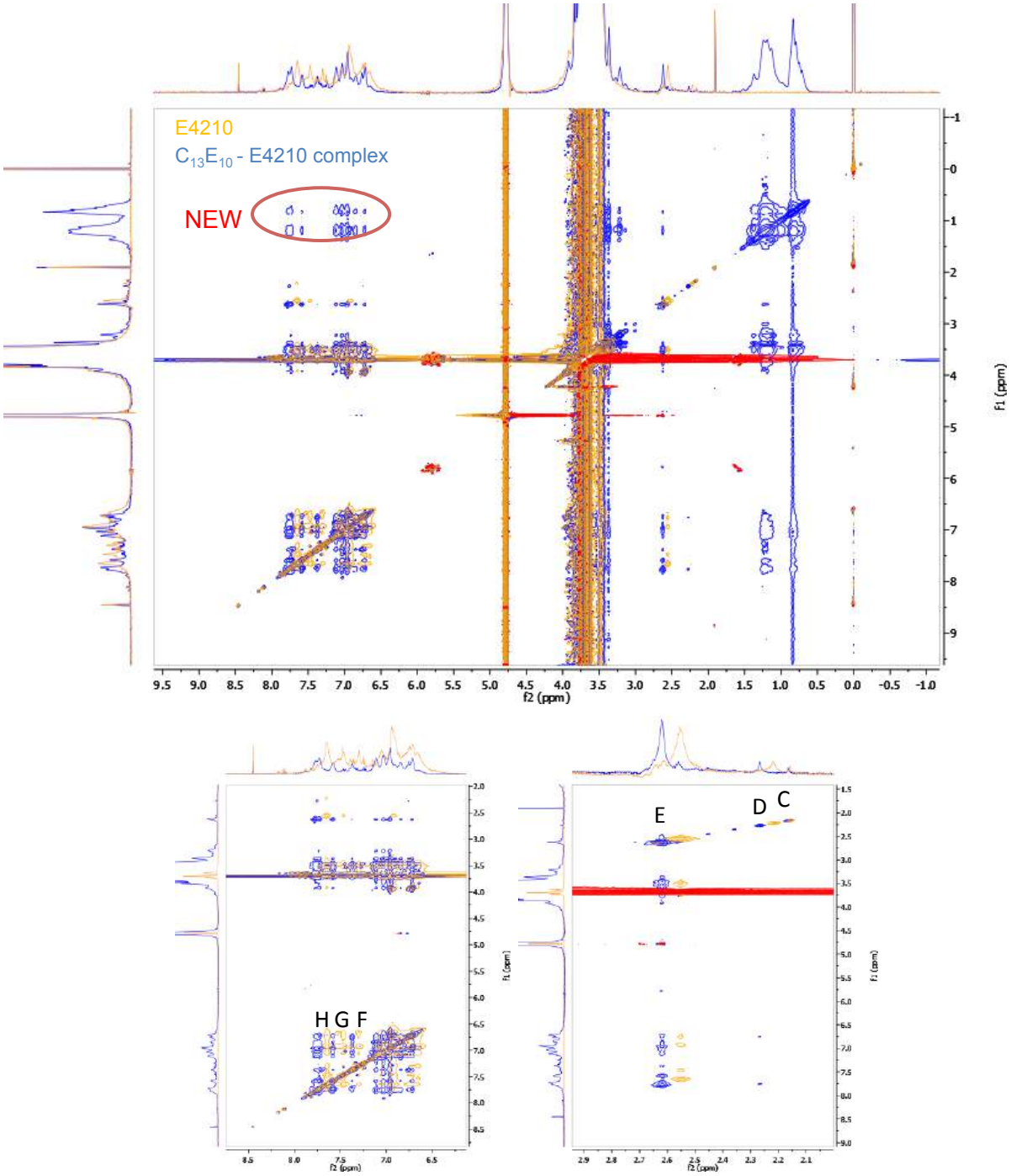

Assignment	$C_{13}E_{10}$ Shift (Hz)	E4210 Shift (Hz)	$C_{13}E_{10}$ - E4210 complex (Hz)	Delta Shift (Hz)
C		1292.91	1296.75	3.84
D		1329.03	1358.62	29.59
E		1529.21	1569.68	40.47
F		4375.90	4417.65	41.76
G		4478.05	4547.31	69.26
H		4584.94	4635.33	50.39

NMR
$C_{13}E_{20}$ – E4210

- ^{1}H $C_{13}E_{20}$
- NOESY $C_{13}E_{20}$
- HSQCAD $C_{13}E_{20}$
- ^{1}H $C_{13}E_{20}$ - E4210 complex
- NOESY $C_{13}E_{20}$ – E4210 complex
- ^{1}H $C_{13}E_{20}$ - E4210 complex comparison with pure samples
- NOESY $C_{13}E_{20}$ - E4210 complex comparison with pure samples

^1H $C_{13}E_{20}$

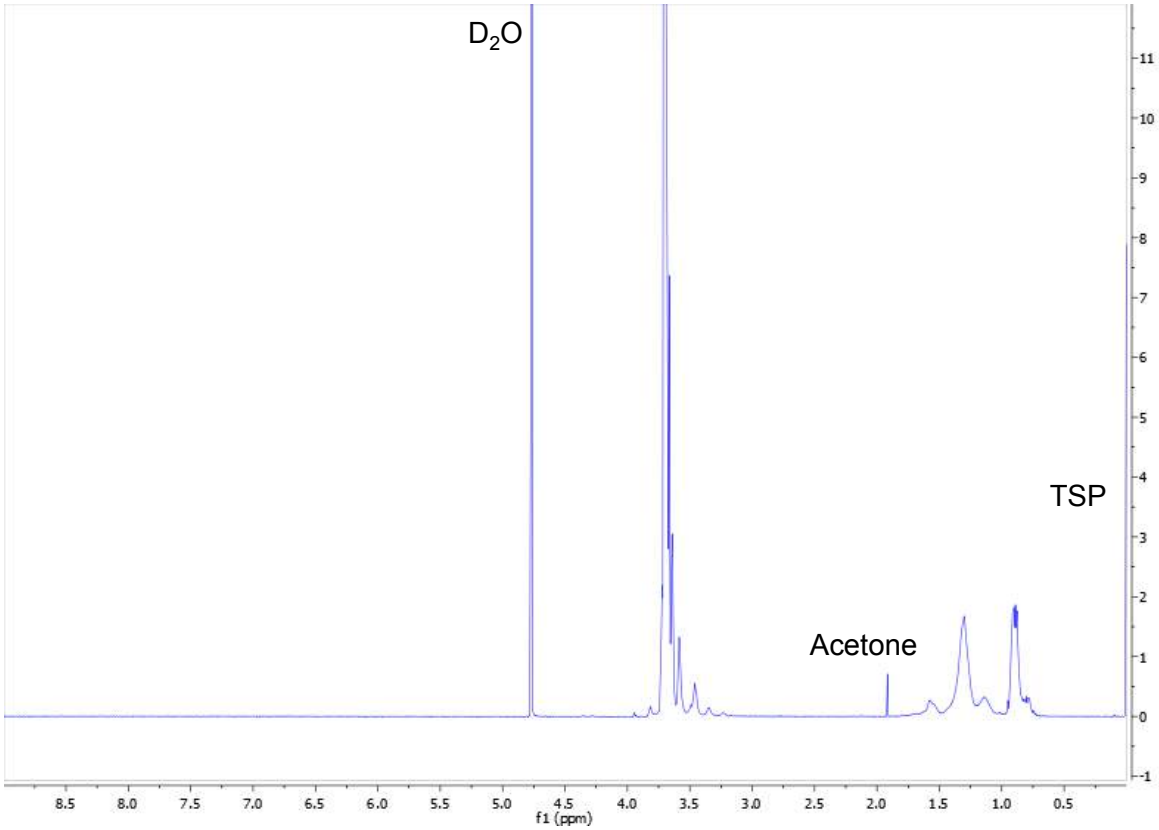

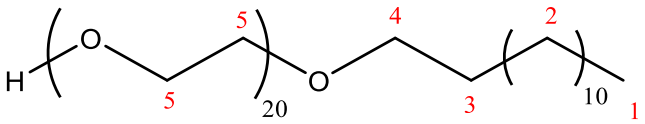

Assignment	Shift (ppm)	Shift (Hz)
TSP	0.00	0.00
1	0.90	533.37
2	1.30	779.67
3	1.57	942.85
Acetone	1.91	1147.78
4	3.58	2148.71
5	3.70	2220.82
D_2O	4.78	2865.75

NOESY $C_{13}E_{20}$

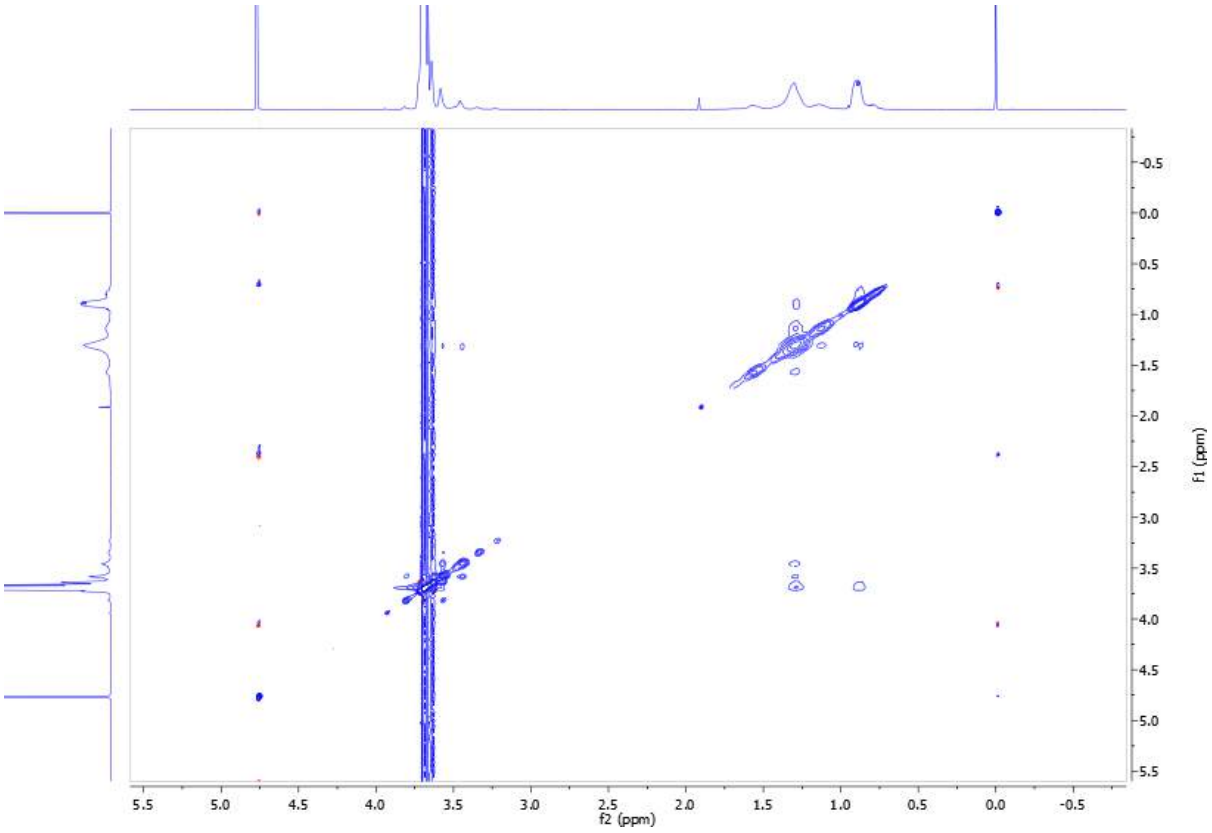

HSQCAD $C_{13}E_{20}$

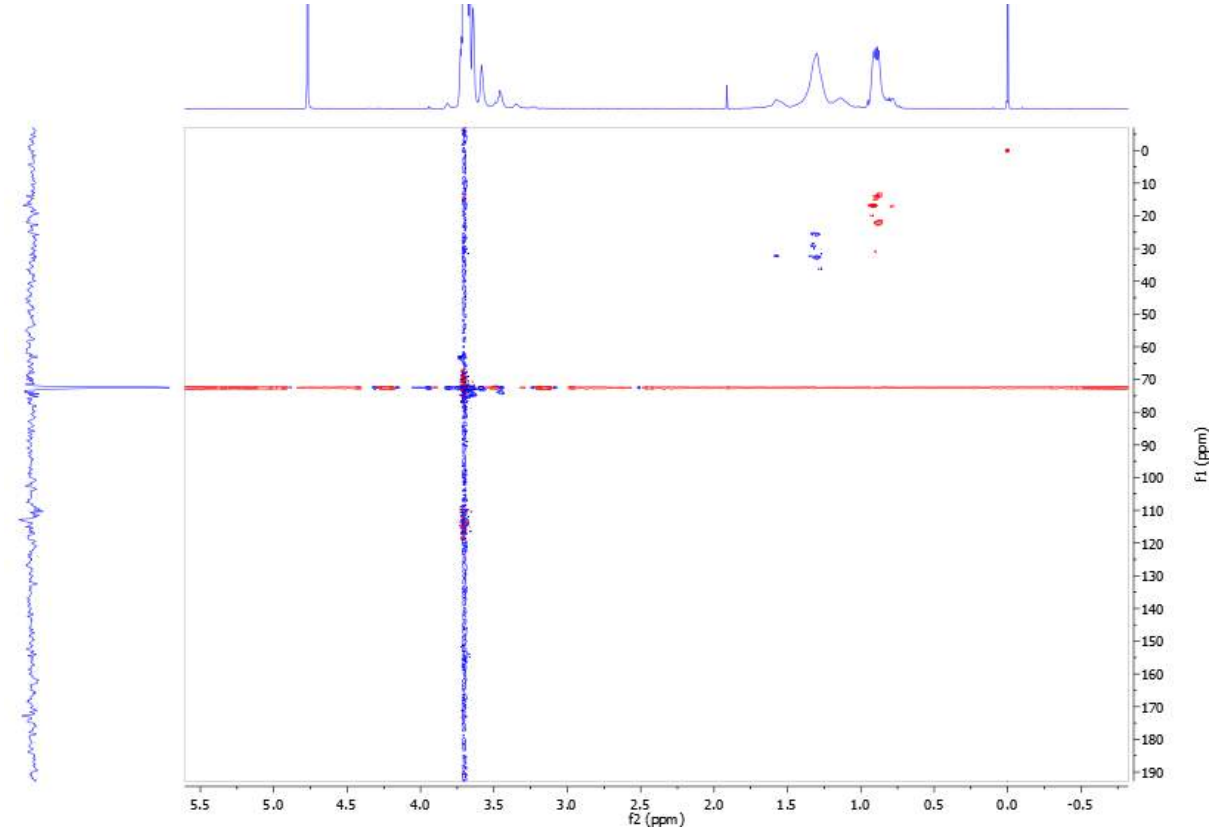

^1H $C_{13}E_{20}$ - E4210 complex

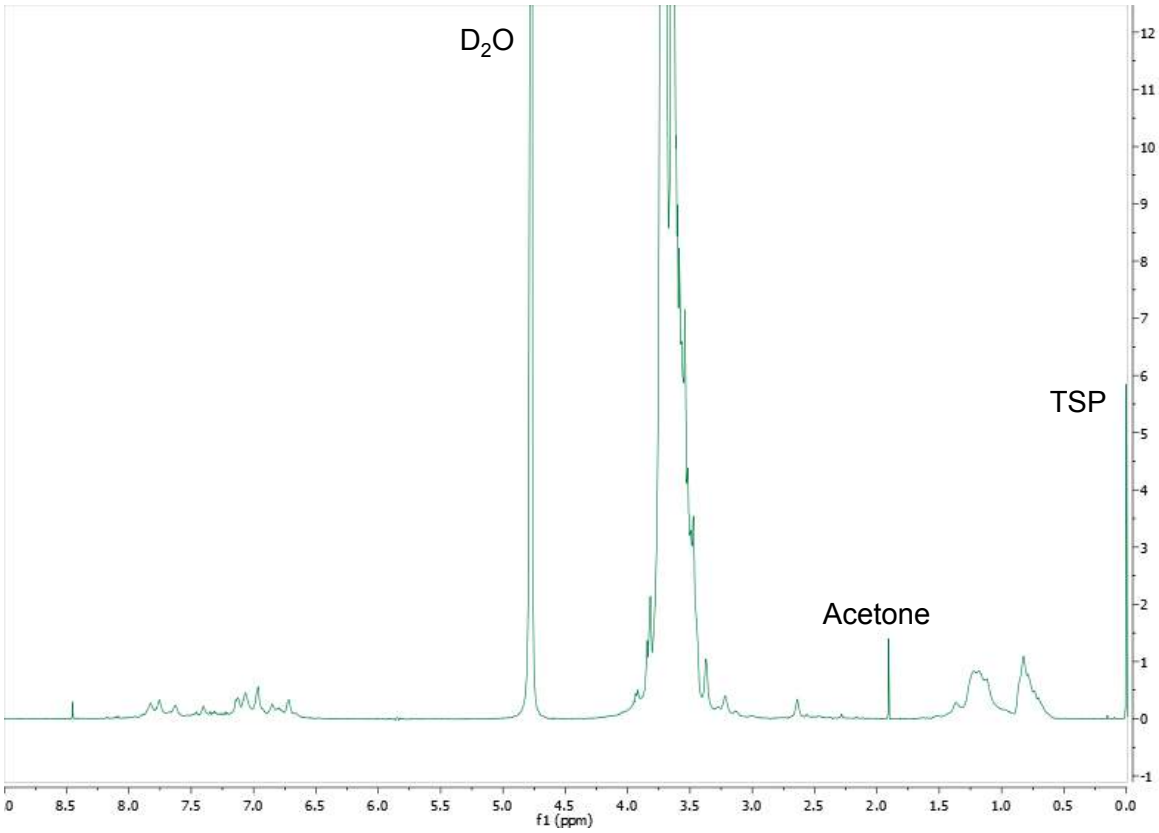

NOESY $C_{13}E_{20}$ - E4210 complex

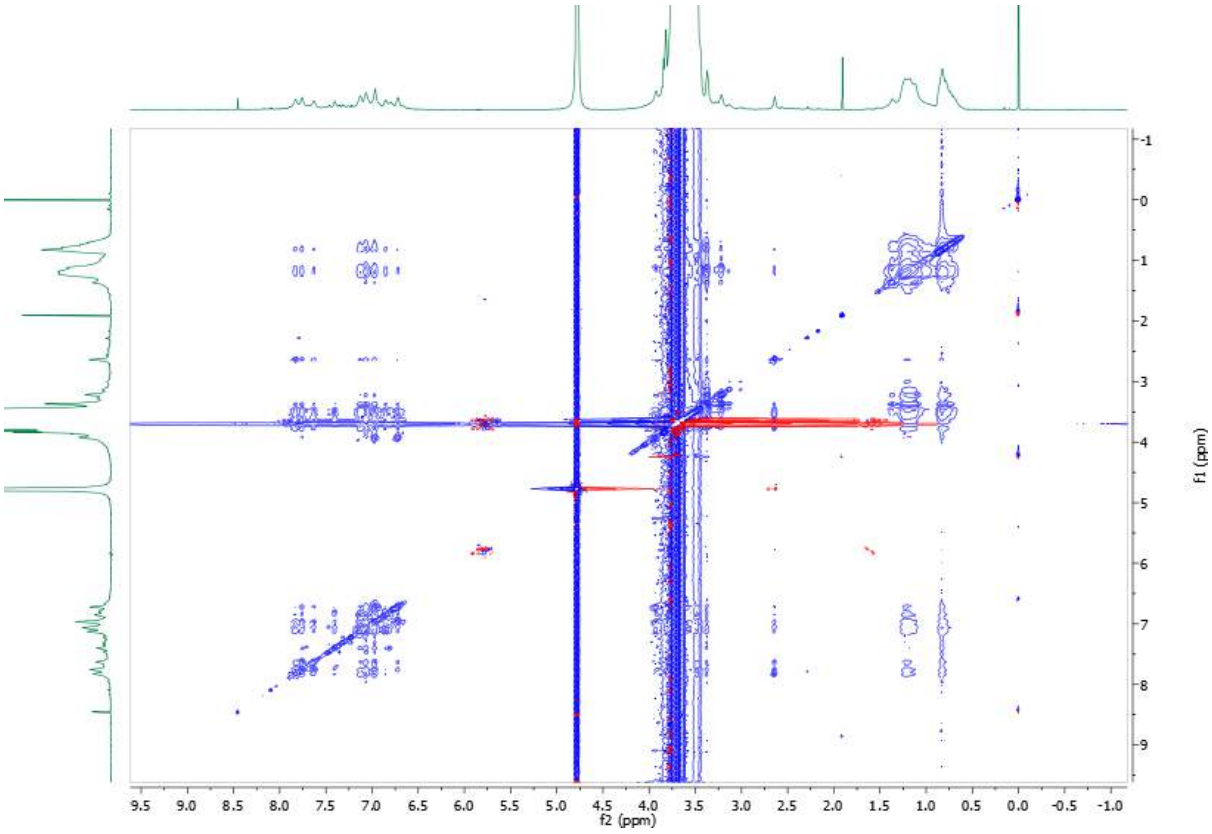

^1H $C_{13}E_{20}$ - E4210 complex comparison with pure samples

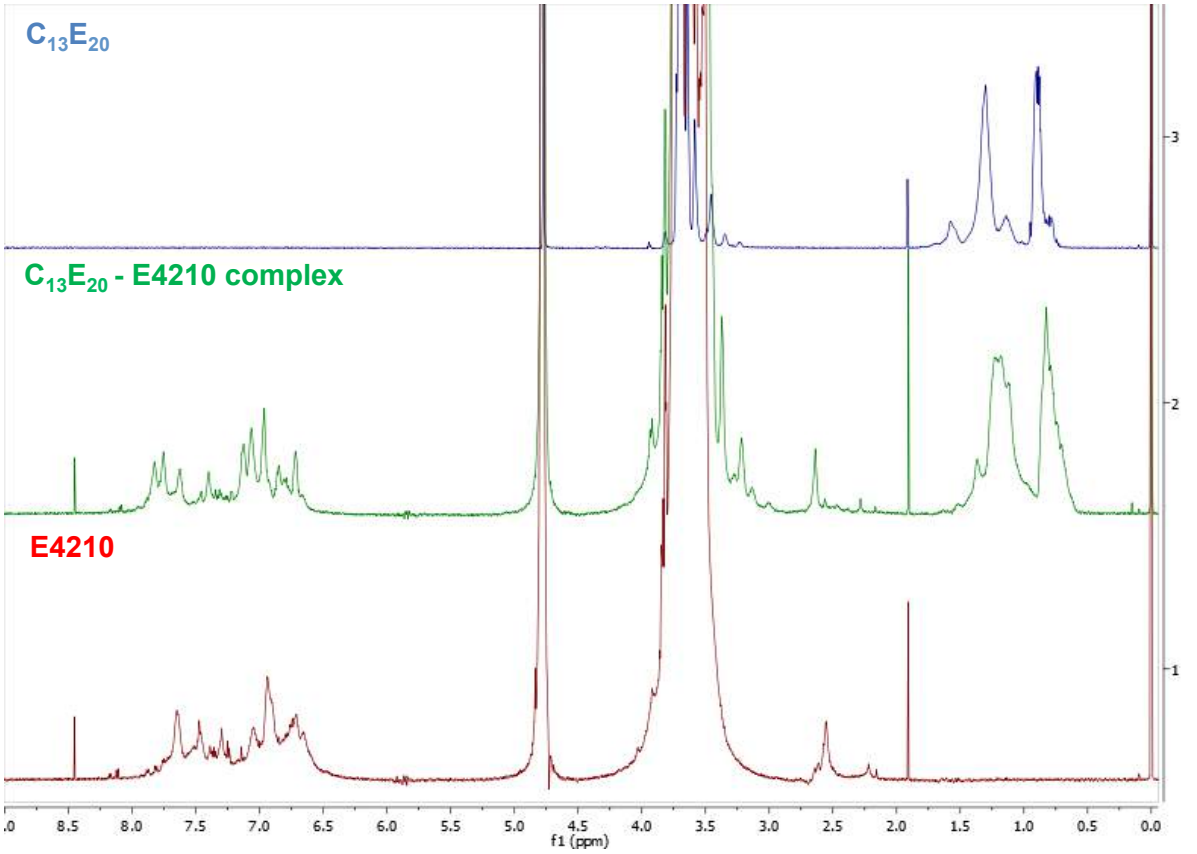

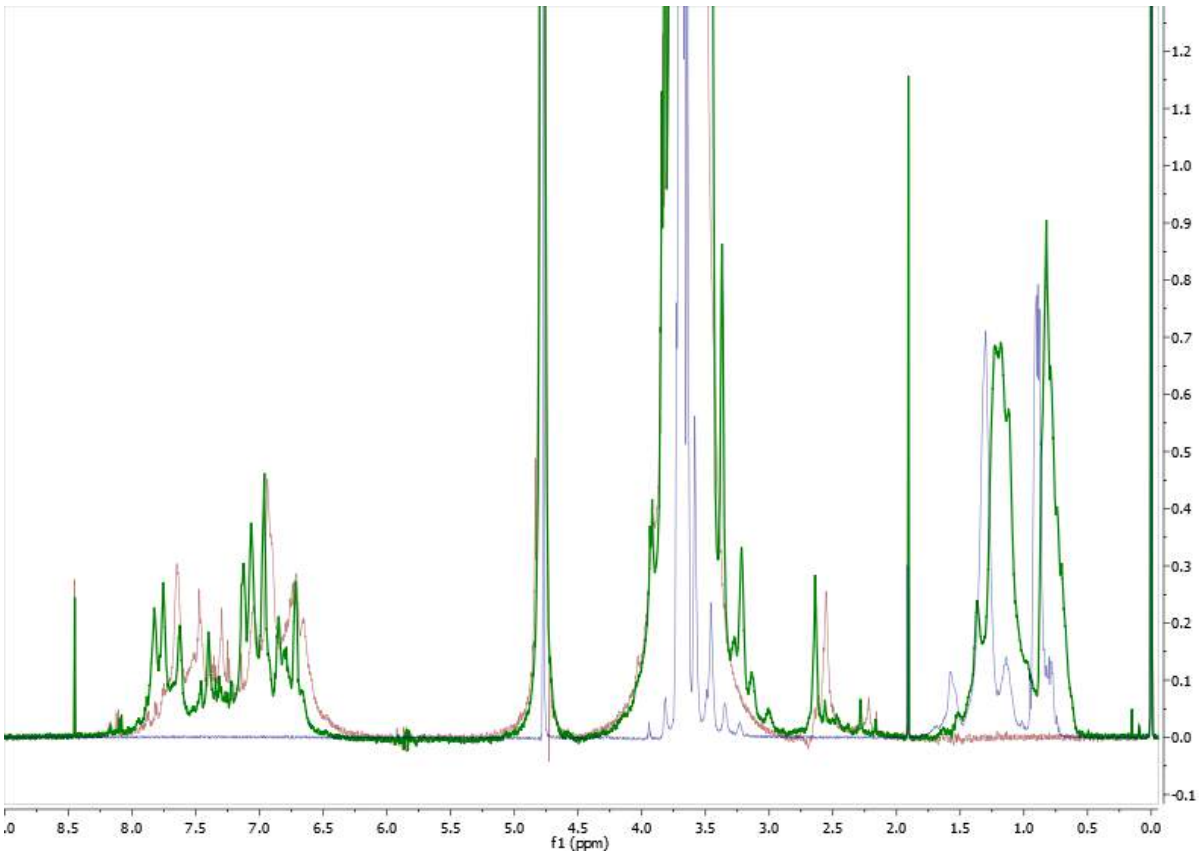

^{1}H $C_{13}E_{20}$ - E4210 complex comparison with pure samples

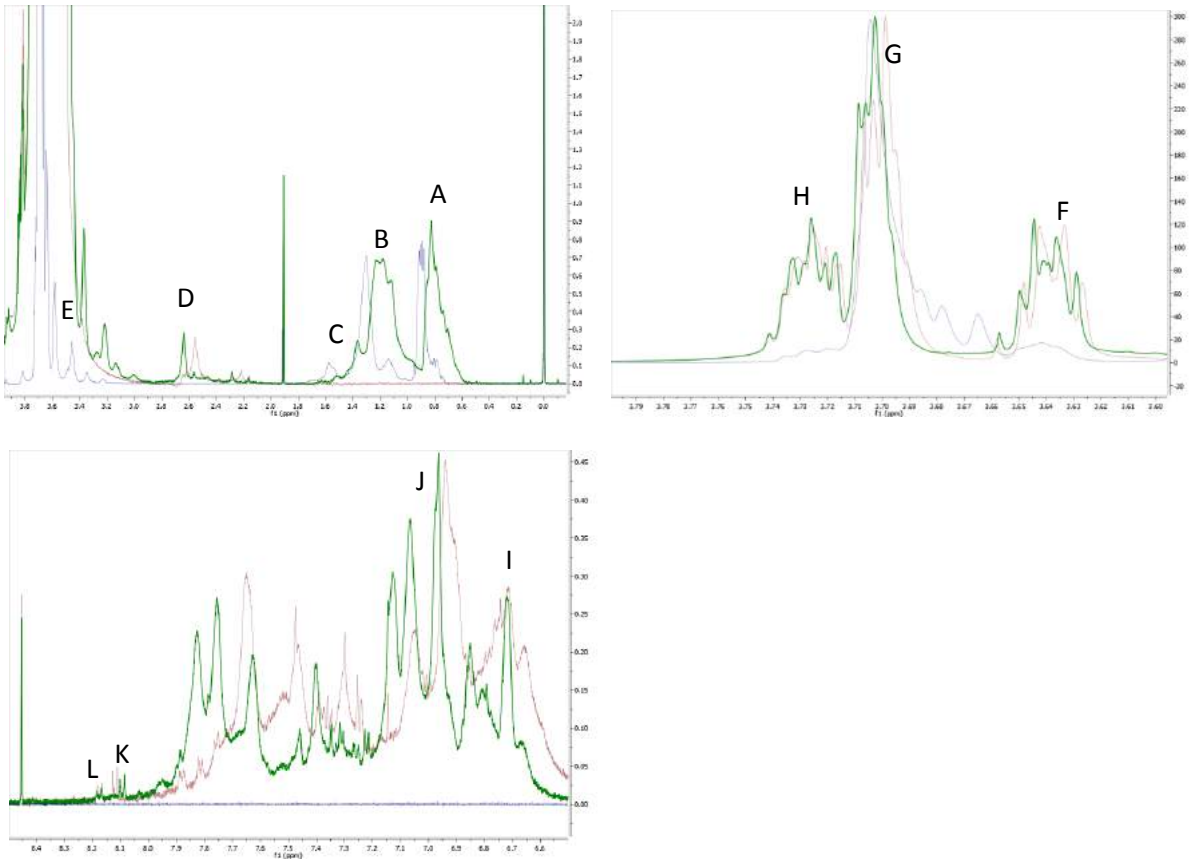

Assignment	$C_{13}E_{20}$ Shift (Hz)	E4210 Shift (Hz)	$C_{13}E_{20}$ - E4210 complex (Hz)	Delta Shift (Hz)
A	533.37		493.97	- 39.40
B	780.23		737.93	- 42.30
C	946.94		909.17	- 37.77
D		1532.15	1581.42	49.27
E	2073.73		2020.87	- 52.86
F		2178.23	2180.07	1.84
G	2220.82	2217.57	2219.76	- 1.06 / 2.19
H		2233.57	2233.78	0.21
I		4024.77	4027.67	2.90
J		4160.69	4174.82	14.13
K		4863.00	4847.41	- 15.59
L		4896.56	4897.57	1.01

NOESY $C_{13}E_{20}$ - E4210 complex comparison with pure samples

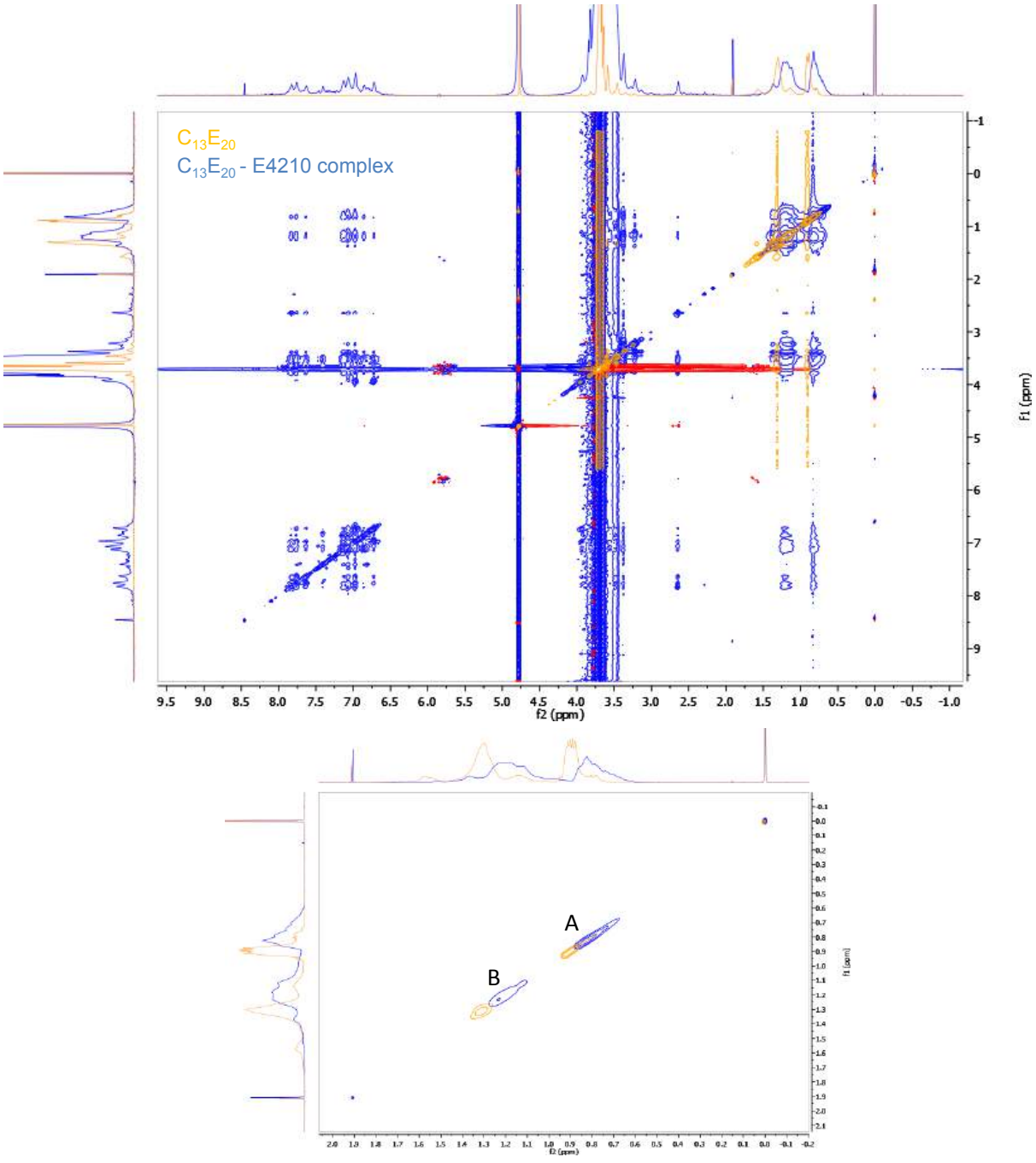

Assignment	$C_{13}E_{20}$ Shift (Hz)	E4210 Shift (Hz)	$C_{13}E_{20}$ - E4210 complex (Hz)	Delta Shift (Hz)
A	534.94		494.57	- 40.37
B	783.74		736.81	- 46.93

NOESY $C_{13}E_{20}$ - E4210 complex comparison with pure samples

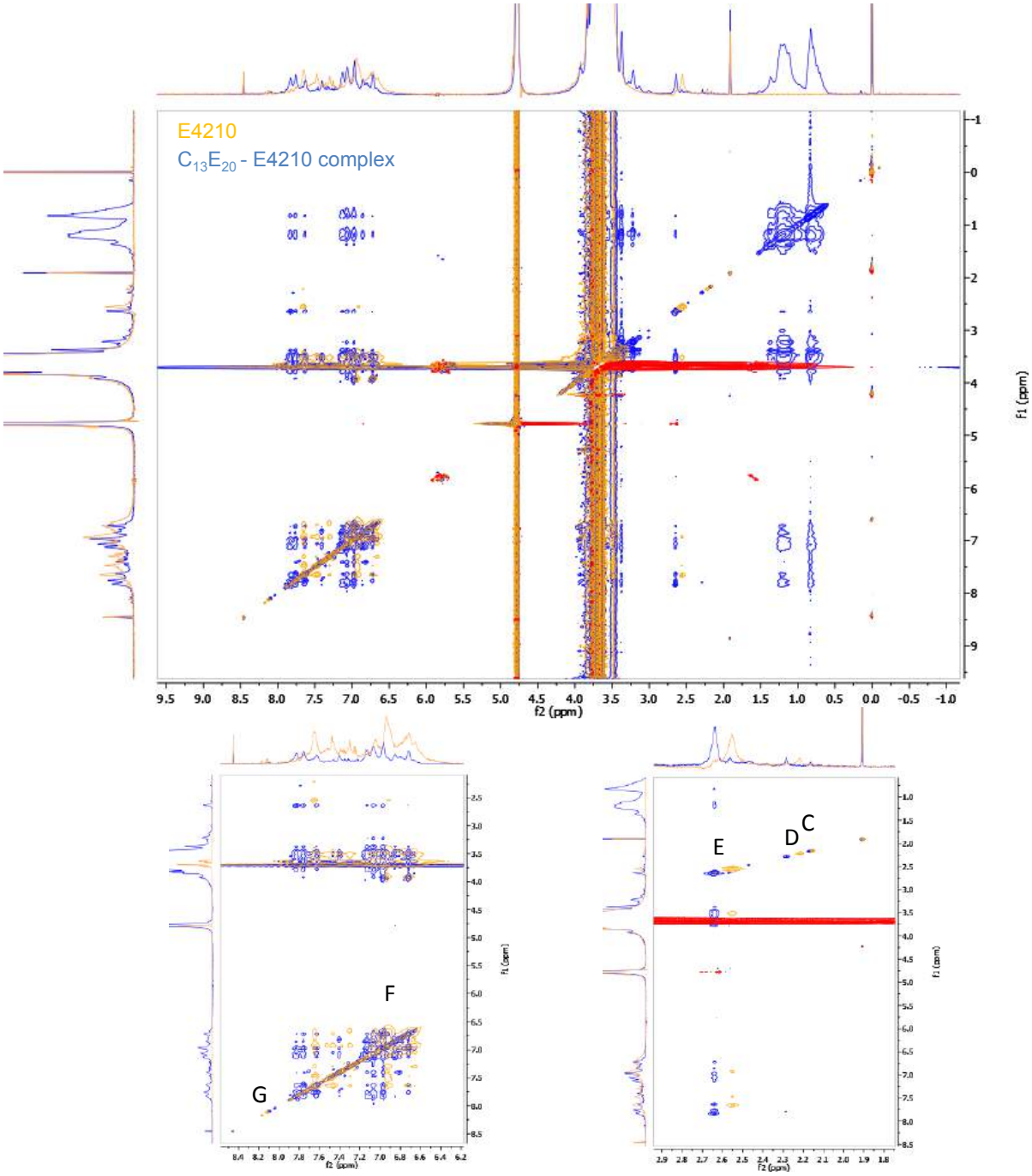

Assignment	$C_{13}E_{20}$ Shift (Hz)	E4210 Shift (Hz)	$C_{13}E_{20}$ - E4210 complex (Hz)	Delta Shift (Hz)
C		1291.78	1298.81	7.03
D		1328.11	1369.57	41.46
E		1529.90	1582.03	52.13
F		4157.73	4176.27	18.54
G		4861.12	4848.31	- 12.81

NMR
$C_{10}E_{10}$ – E4210

- ^1H $C_{10}E_{10}$
- NOESY $C_{10}E_{10}$
- HSQCAD $C_{10}E_{10}$
- ^1H $C_{10}E_{10}$ - E4210 complex
- NOESY $C_{10}E_{10}$ – E4210 complex
- ^1H $C_{10}E_{10}$ - E4210 complex comparison with pure samples
- NOESY $C_{10}E_{10}$ - E4210 complex comparison with pure samples

^1H $C_{10}E_{10}$

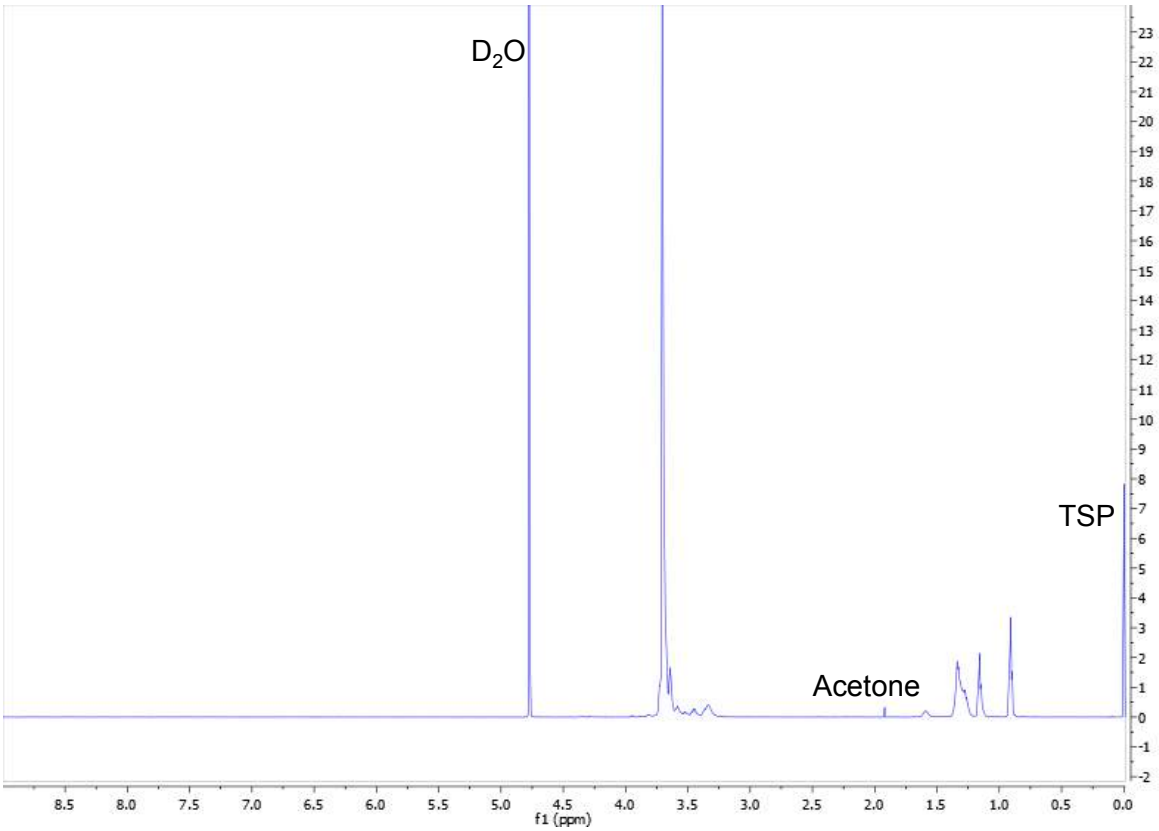

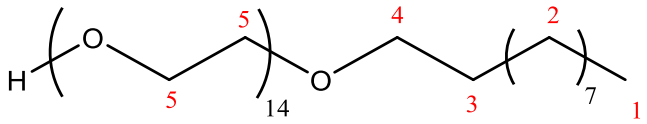

Assignment	Shift (ppm)	Shift (Hz)
TSP	0.00	0.00
1	0.91	545.38
1	1.16	695.23
2	1.33	796.96
3	1.60	957.95
Acetone	1.92	1149.89
4	3.34	1999.93
5	3.71	2221.53
D_2O	4.77	2861.02

NOESY $C_{10}E_{10}$

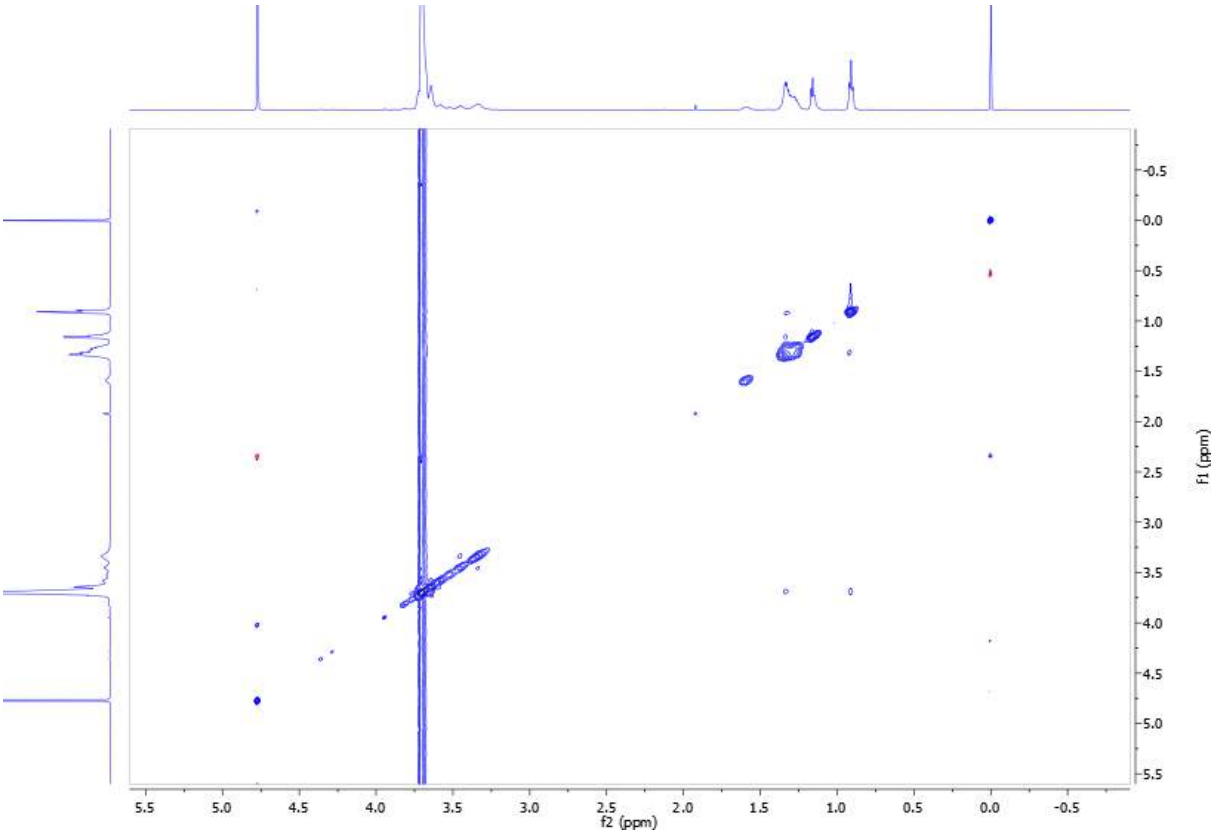

HSQCAD $C_{10}E_{10}$

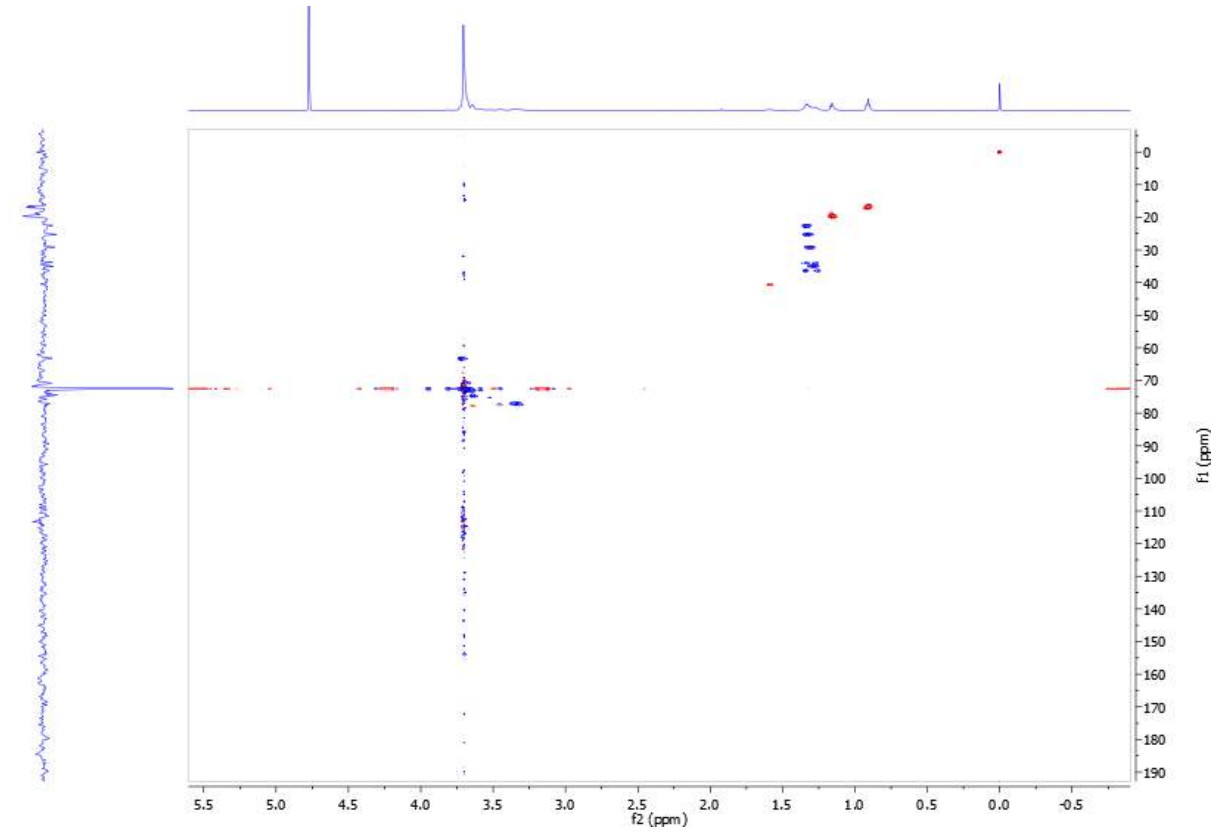

^1H $C_{10}E_{10}$ - E4210 complex

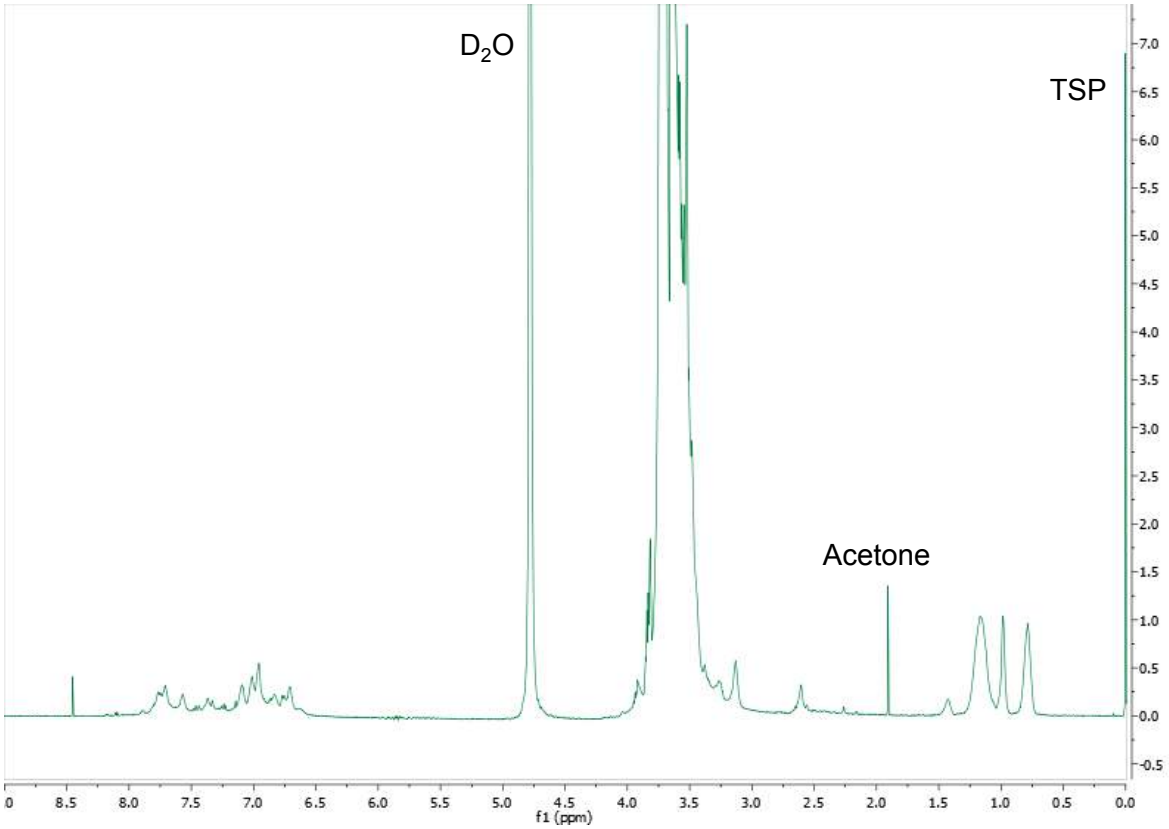

NOESY $C_{10}E_{10}$ - E4210 complex

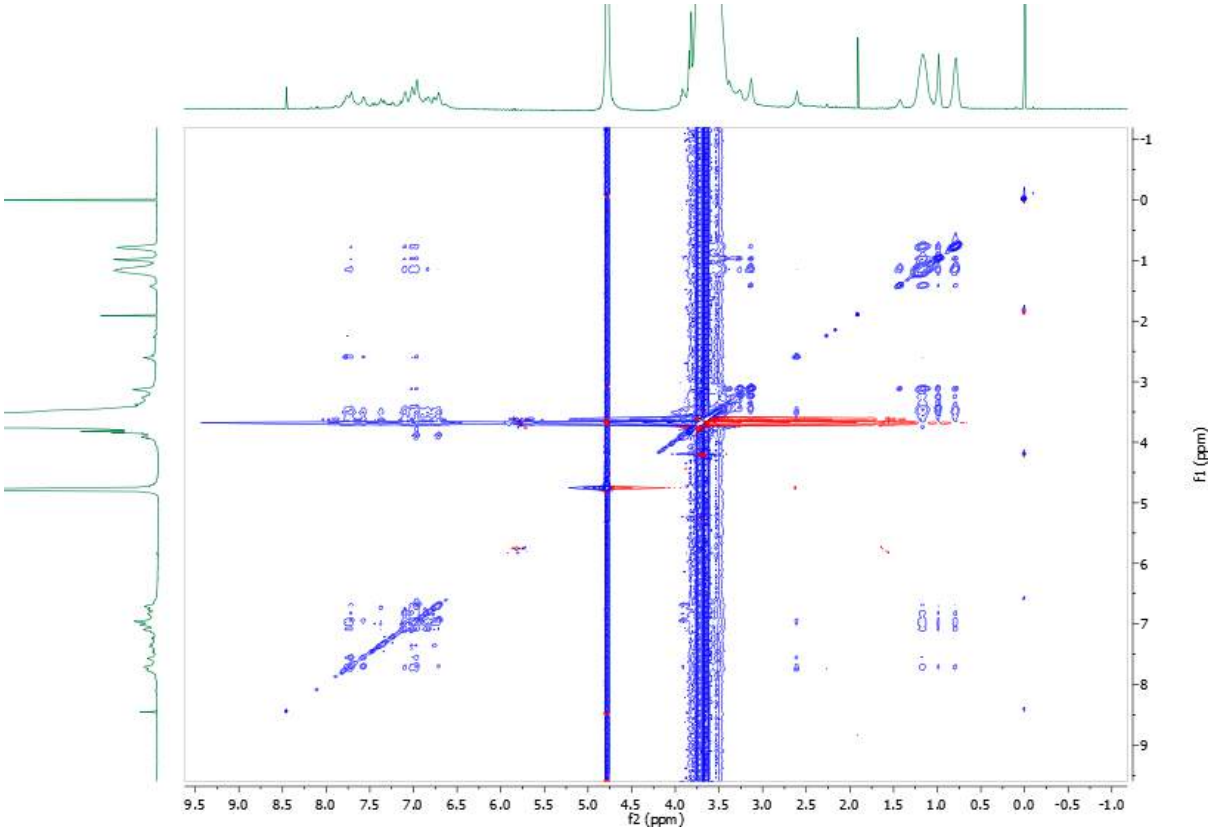

^{1}H $C_{10}E_{10}$ - E4210 complex comparison with pure samples

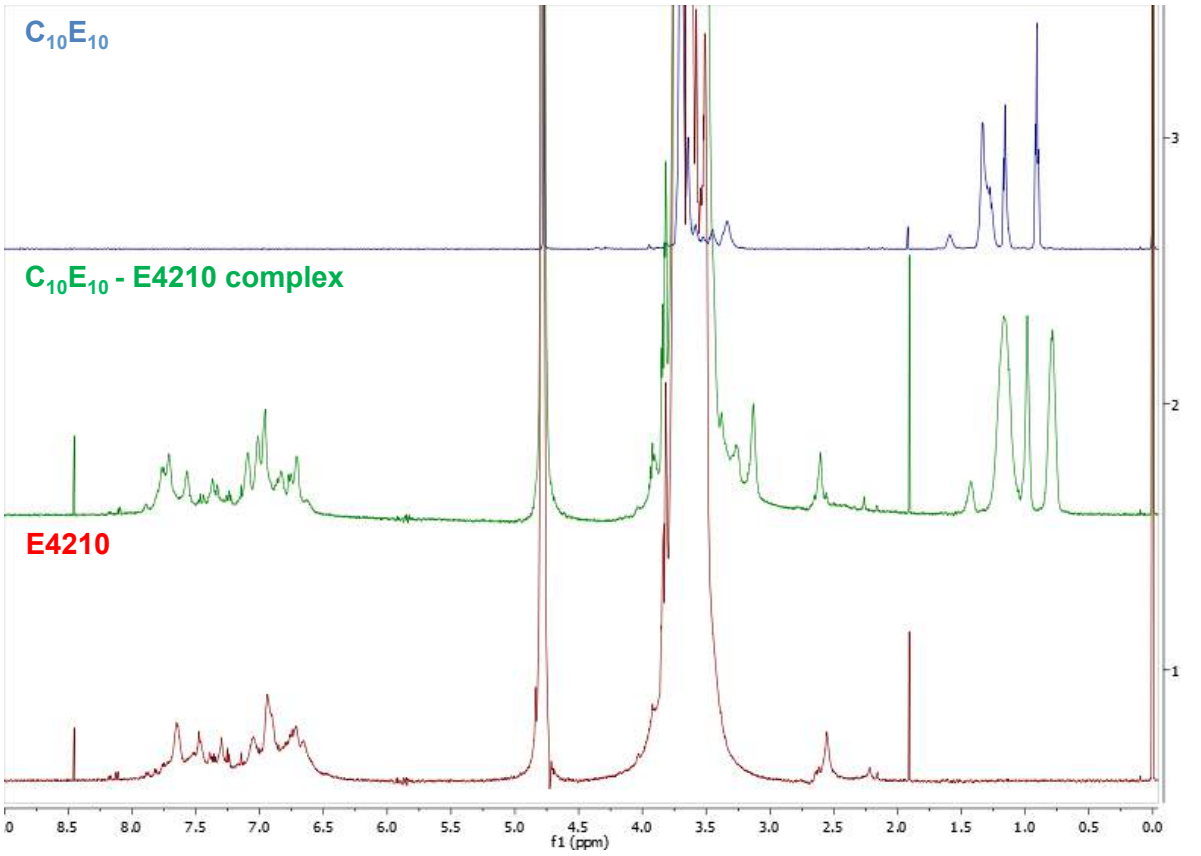

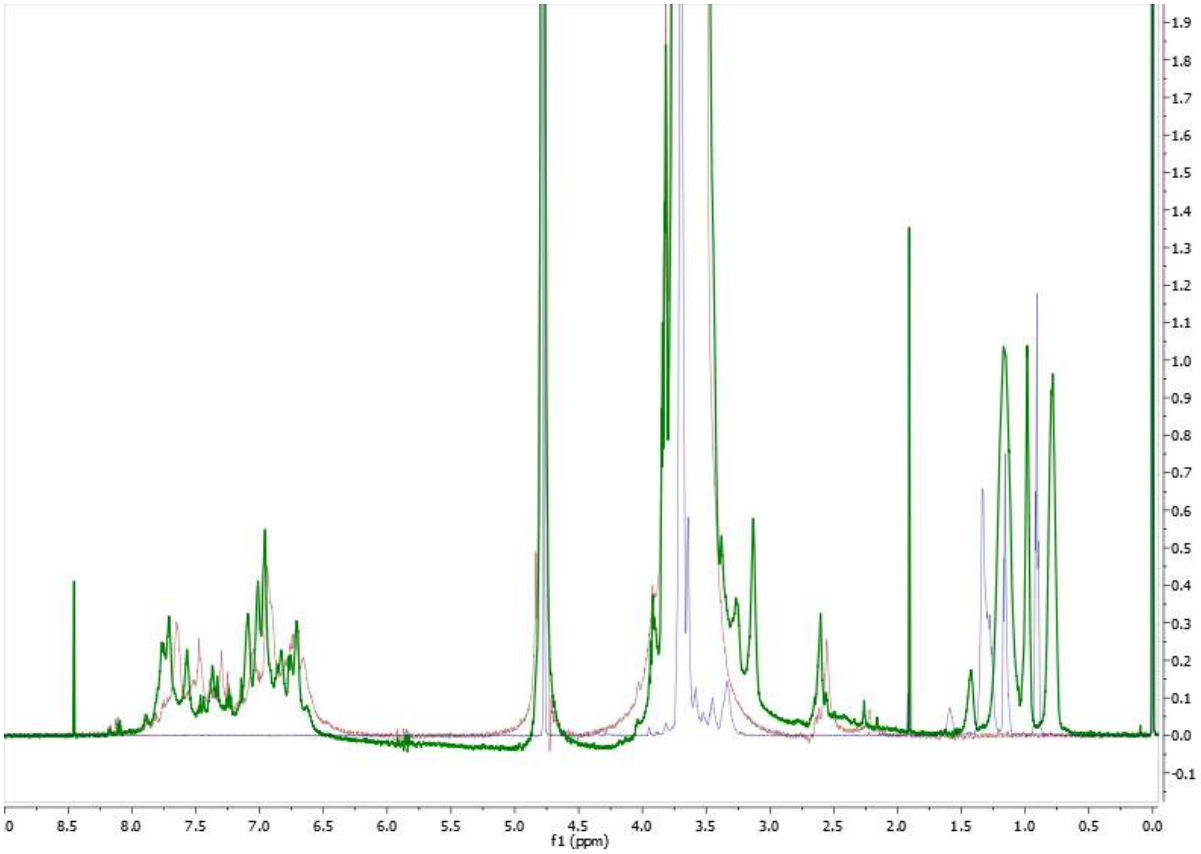

^1H $C_{10}E_{10}$ - E4210 complex comparison with pure samples

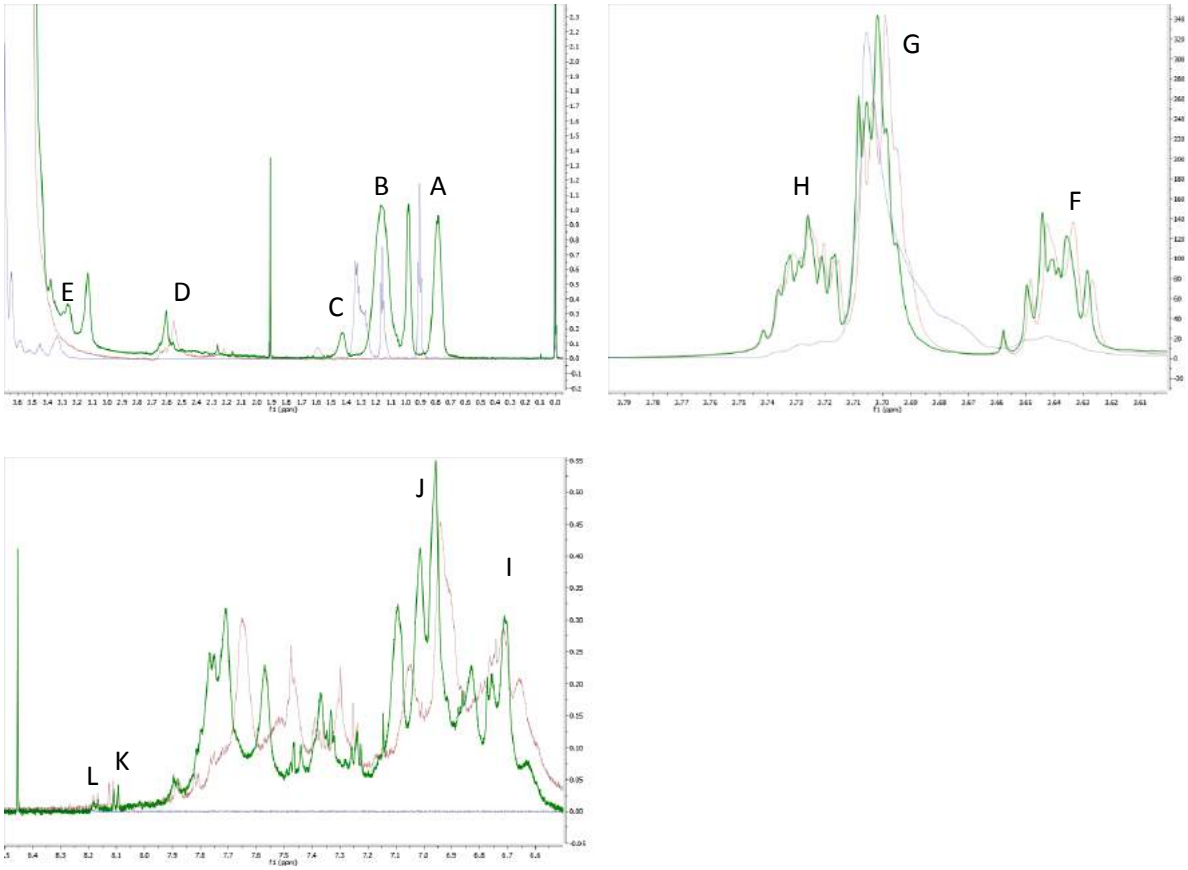

Assignment	$C_{10}E_{10}$ Shift (Hz)	E4210 Shift (Hz)	$C_{10}E_{10}$ - E4210 complex (Hz)	Delta Shift (Hz)
A	544.57		470.75	- 73.82
B	802.08		698.98	- 103.10
C	956.19		857.08	- 99.11
D		1531.39	1561.19	29.80
E	1998.23		1877.07	- 121.16
F		2178.23	2179.74	1.51
G	2251.53	2217.57	2219.25	- 32.28 / 1.68
H		2233.57	2233.80	0.23
I		4024.77	4022.73	- 2.04
J		4160.69	4170.71	10.02
K		4863.00	4853.01	- 9.99
L		4896.02	4896.83	0.81

NOESY $C_{10}E_{10}$ - E4210 complex comparison with pure samples

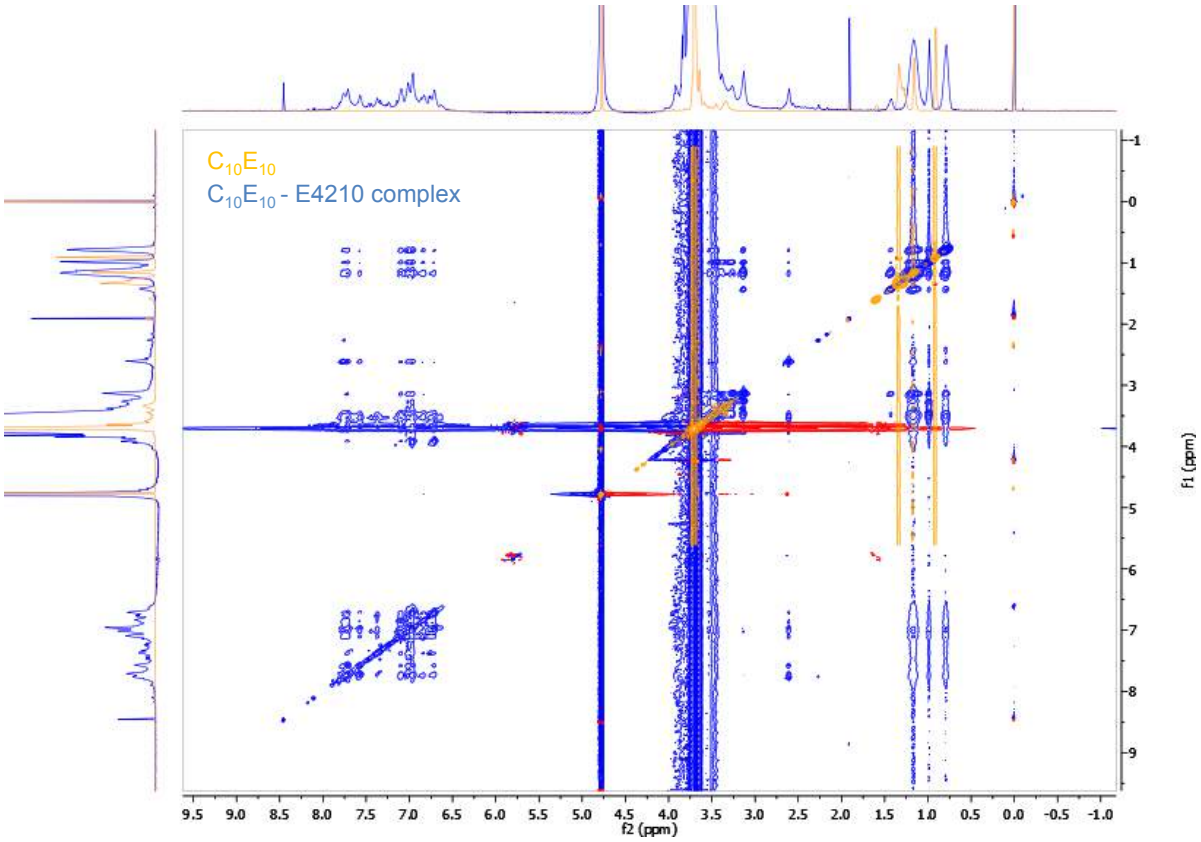

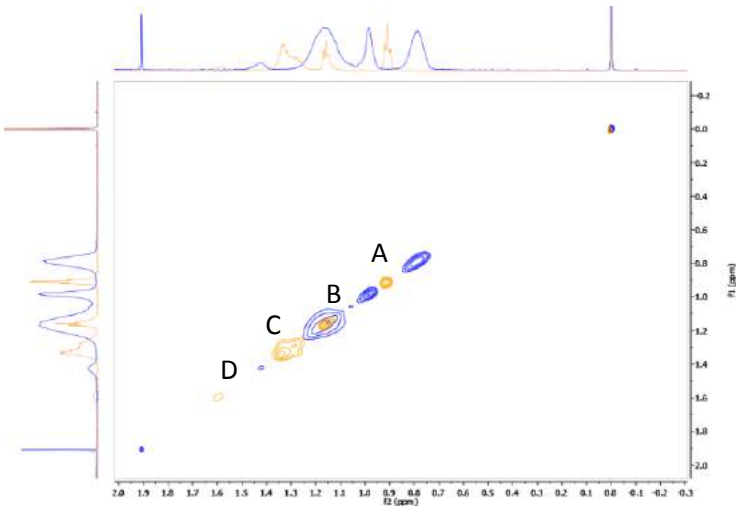

Assignment	$C_{10}E_{10}$ Shift (Hz)	E4210 Shift (Hz)	$C_{10}E_{10}$ - E4210 complex (Hz)	Delta Shift (Hz)
A	548.52		468.76	- 79.76
B	698.71		589.38	- 109.33
C	804.15		688.81	- 115.34
D	956.06		852.92	- 103.14

NOESY $C_{10}E_{10}$ - E4210 complex comparison with pure samples

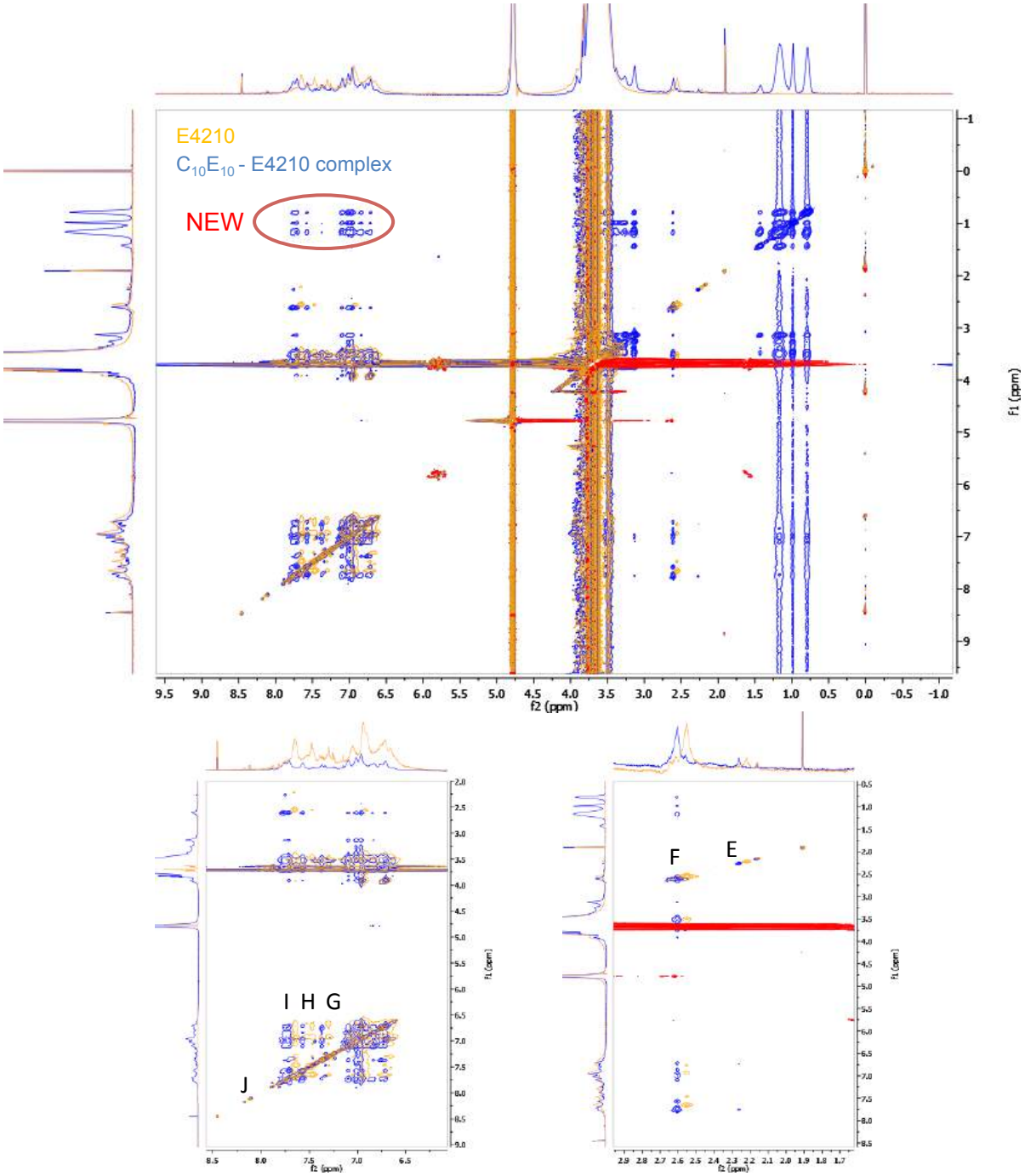

Assignment	$C_{10}E_{10}$ Shift (Hz)	E4210 Shift (Hz)	$C_{10}E_{10}$ - E4210 complex (Hz)	Delta Shift (Hz)
E		1327.94	1356.33	28.29
F		1530.50	1561.16	30.66
G		4378.12	4417.56	39.44
H		4475.36	4537.34	61.98
I		4583.15	4647.23	64.08
J		4861.78	4852.83	- 8.95

NMR
$C_{10}E_{14}$ – E4210

- ^1H $C_{10}E_{14}$
- NOESY $C_{10}E_{14}$
- HSQCAD $C_{10}E_{14}$
- ^1H $C_{10}E_{14}$ - E4210 complex
- NOESY $C_{10}E_{14}$ – E4210 complex
- ^1H $C_{10}E_{14}$ - E4210 complex comparison with pure samples
- NOESY $C_{10}E_{14}$ - E4210 complex comparison with pure samples

^1H $C_{10}E_{14}$

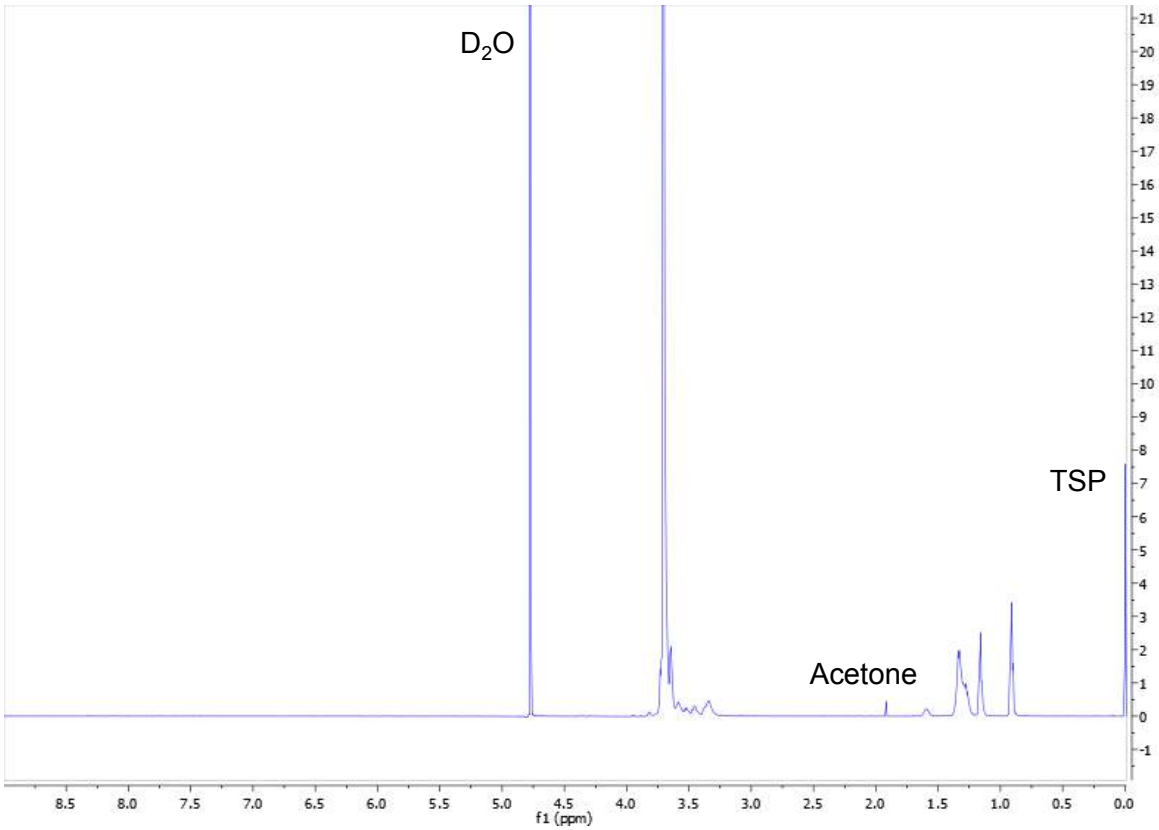

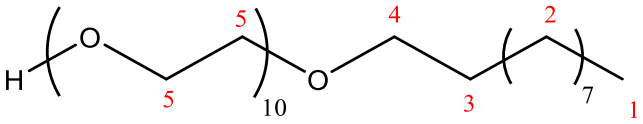

Assignment	Shift (ppm)	Shift (Hz)
TSP	0.00	0.00
1	0.91	544.57
1	1.16	694.41
2	1.33	796.15
3	1.59	954.73
Acetone	1.92	1150.89
4	3.35	2005.53
5	3.71	2222.53
D_2O	4.78	2865.75

NOESY $C_{10}E_{14}$

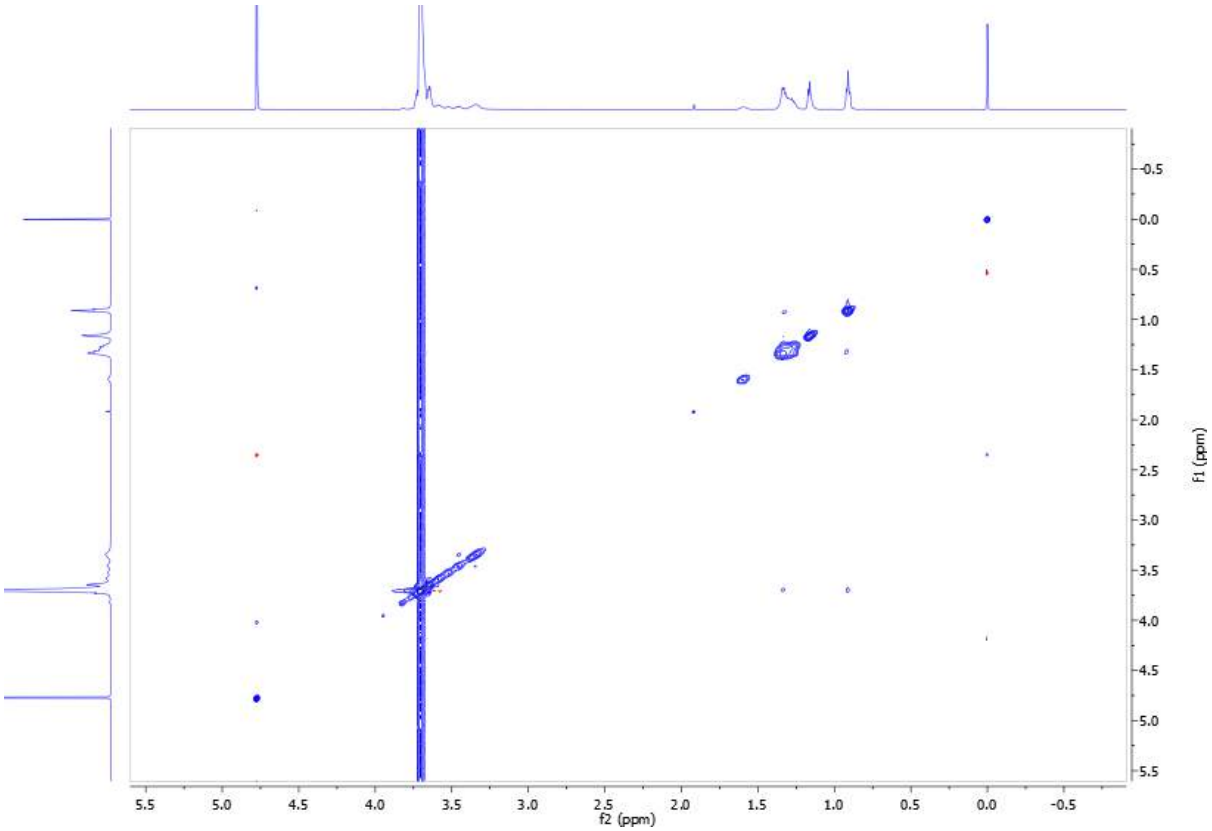

HSQCAD $C_{10}E_{14}$

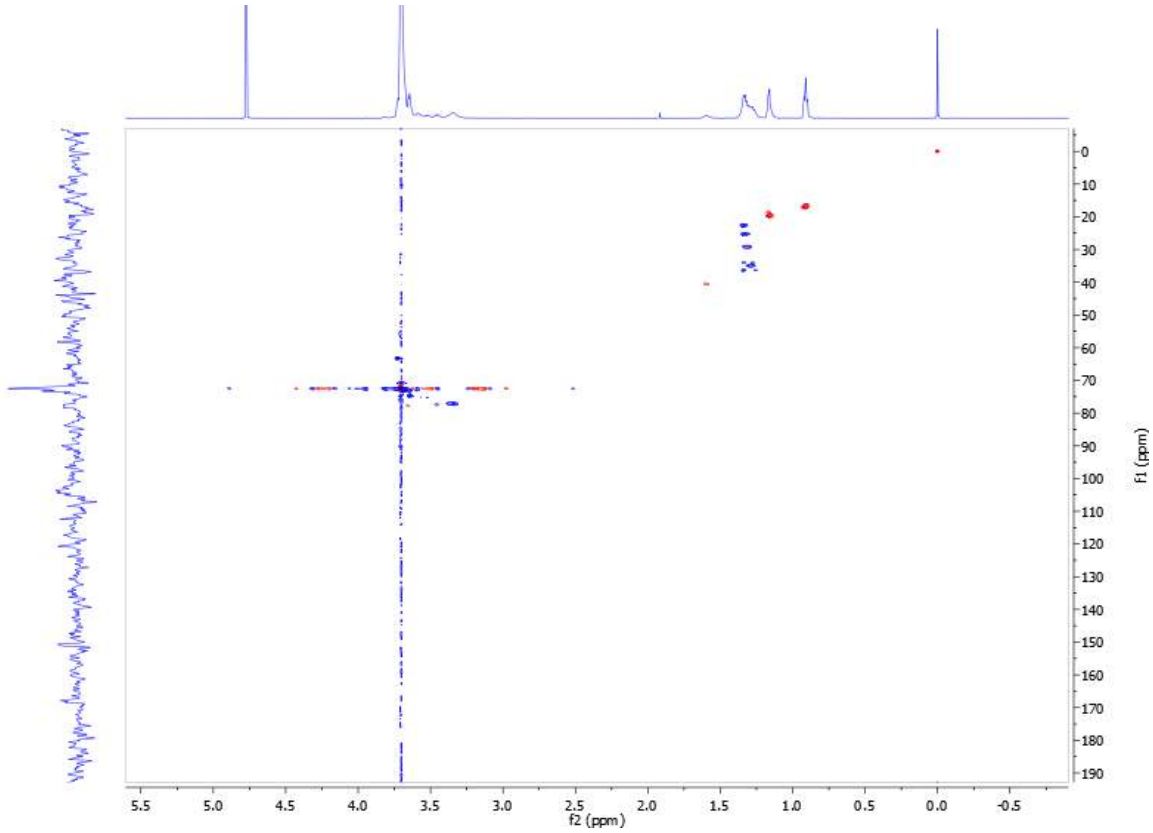

^1H $C_{10}E_{14}$ - E4210 complex

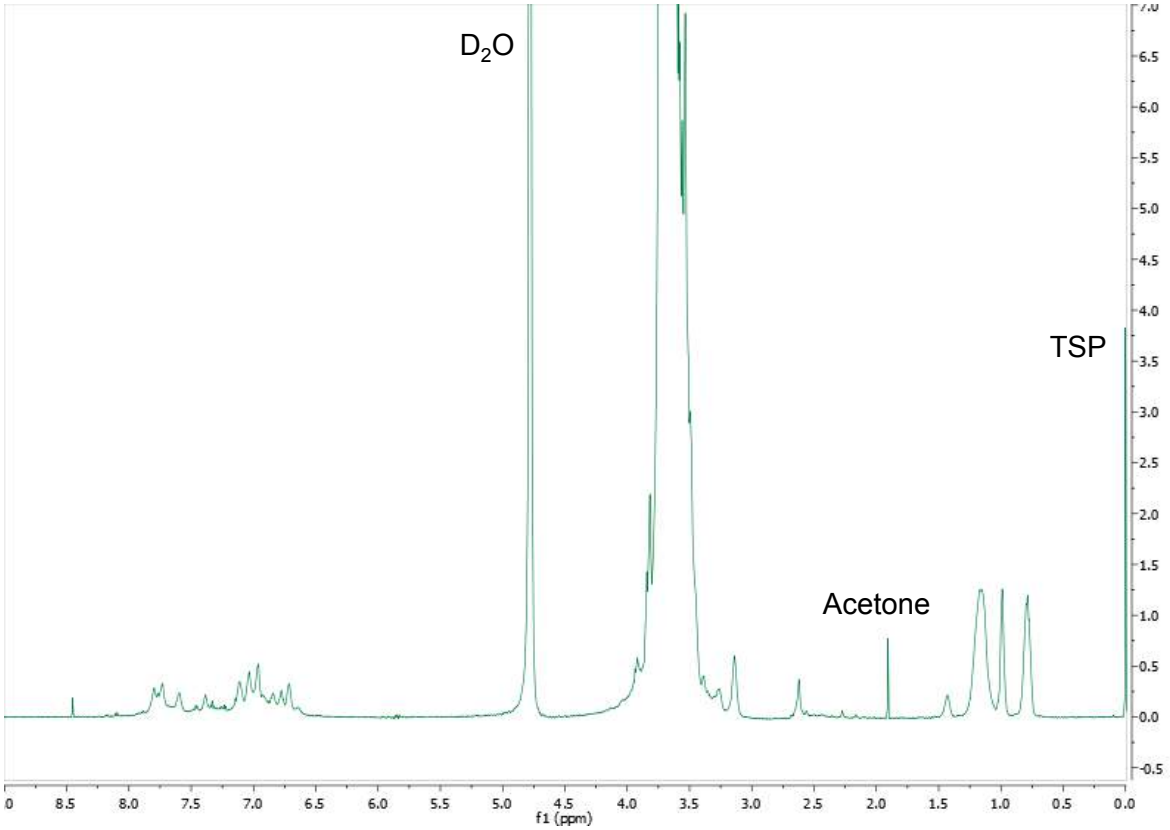

NOESY $C_{10}E_{14}$ - E4210 complex

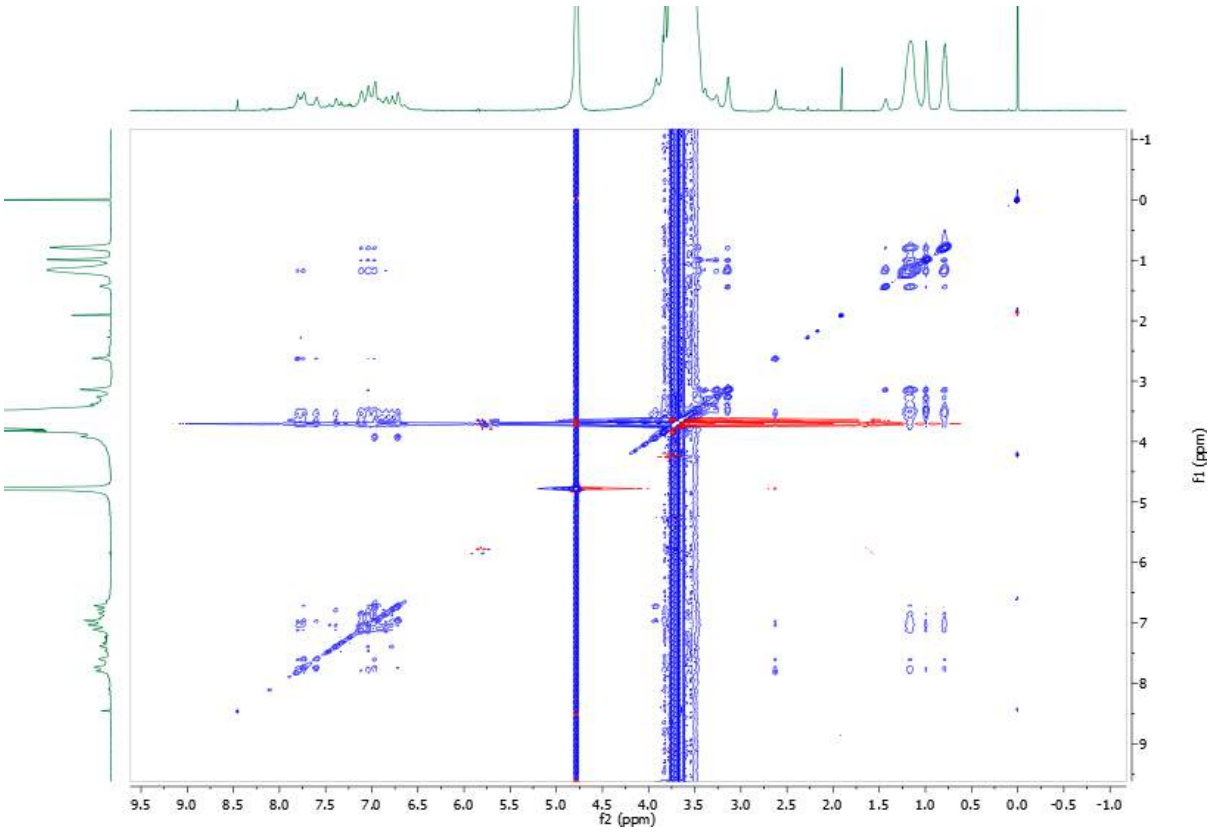

^{1}H $C_{10}E_{14}$ - E4210 complex comparison with pure samples

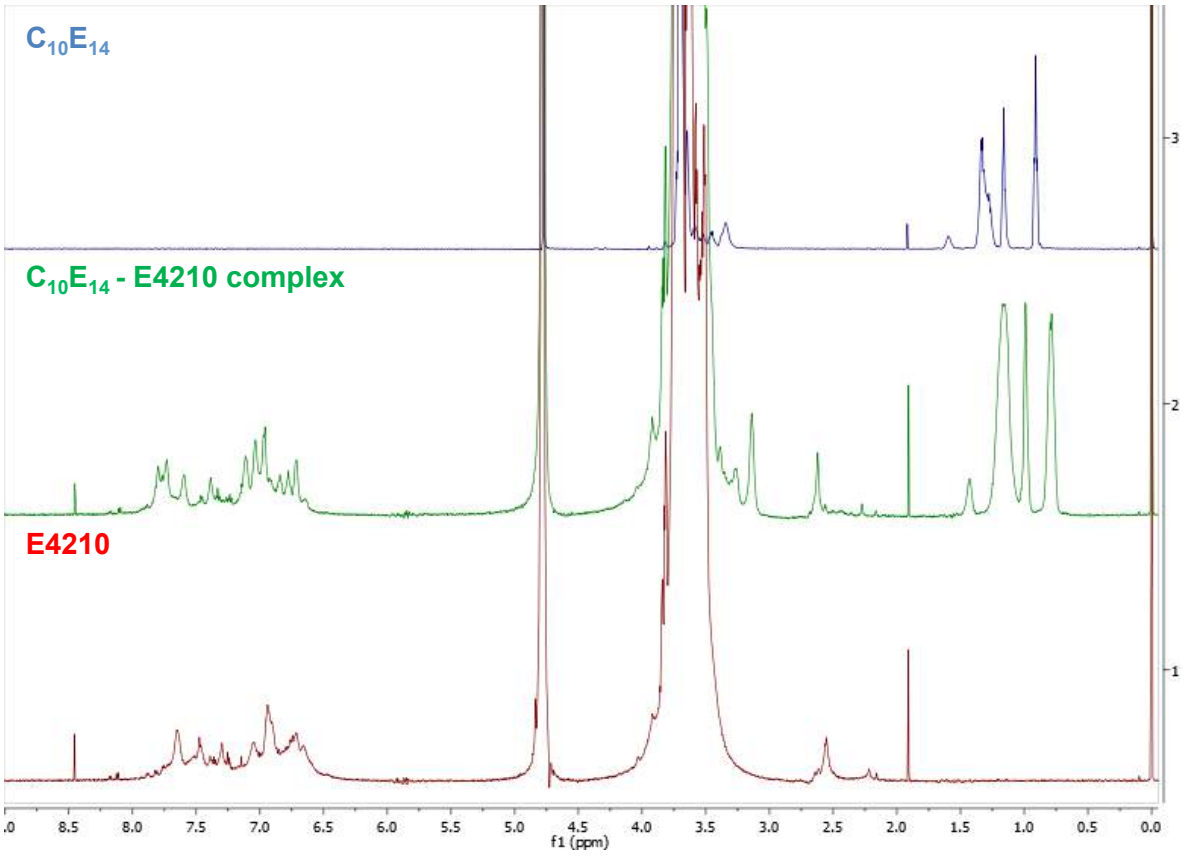

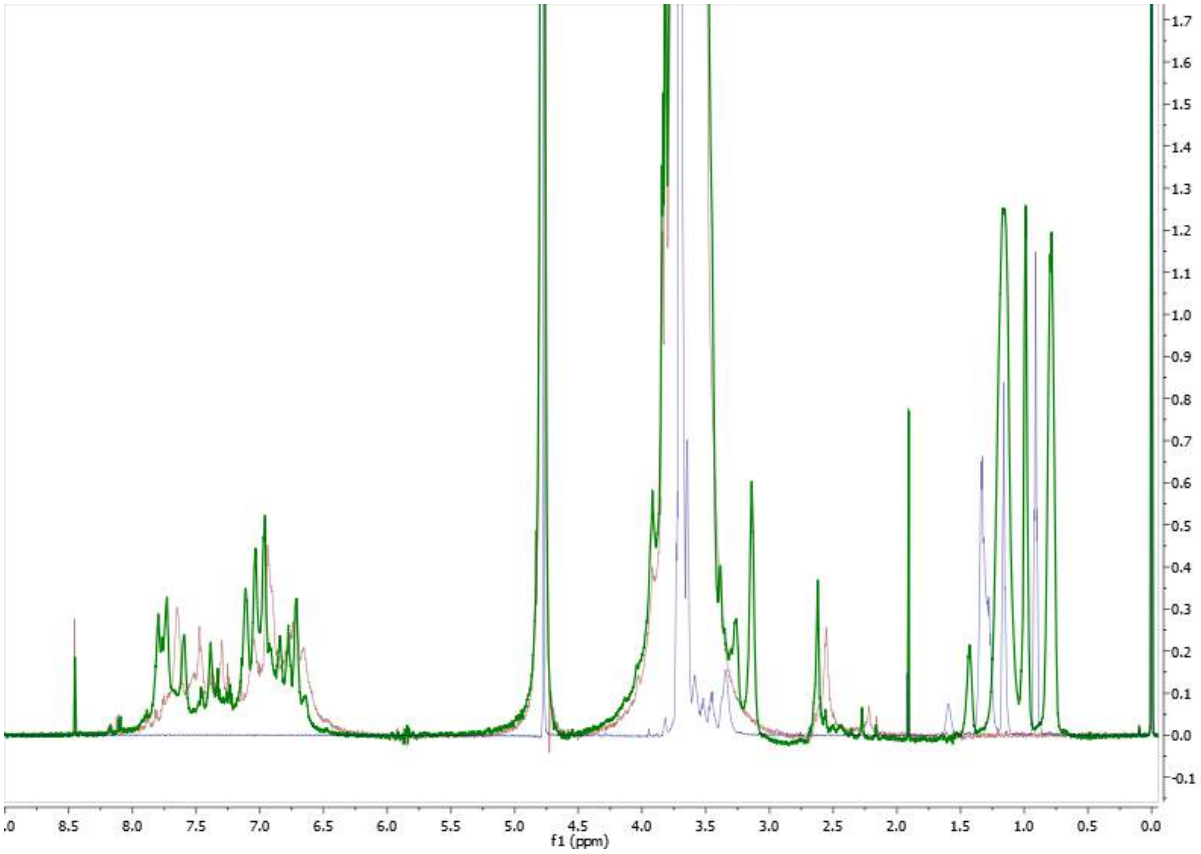

^{1}H $C_{10}E_{14}$ - E4210 complex comparison with pure samples

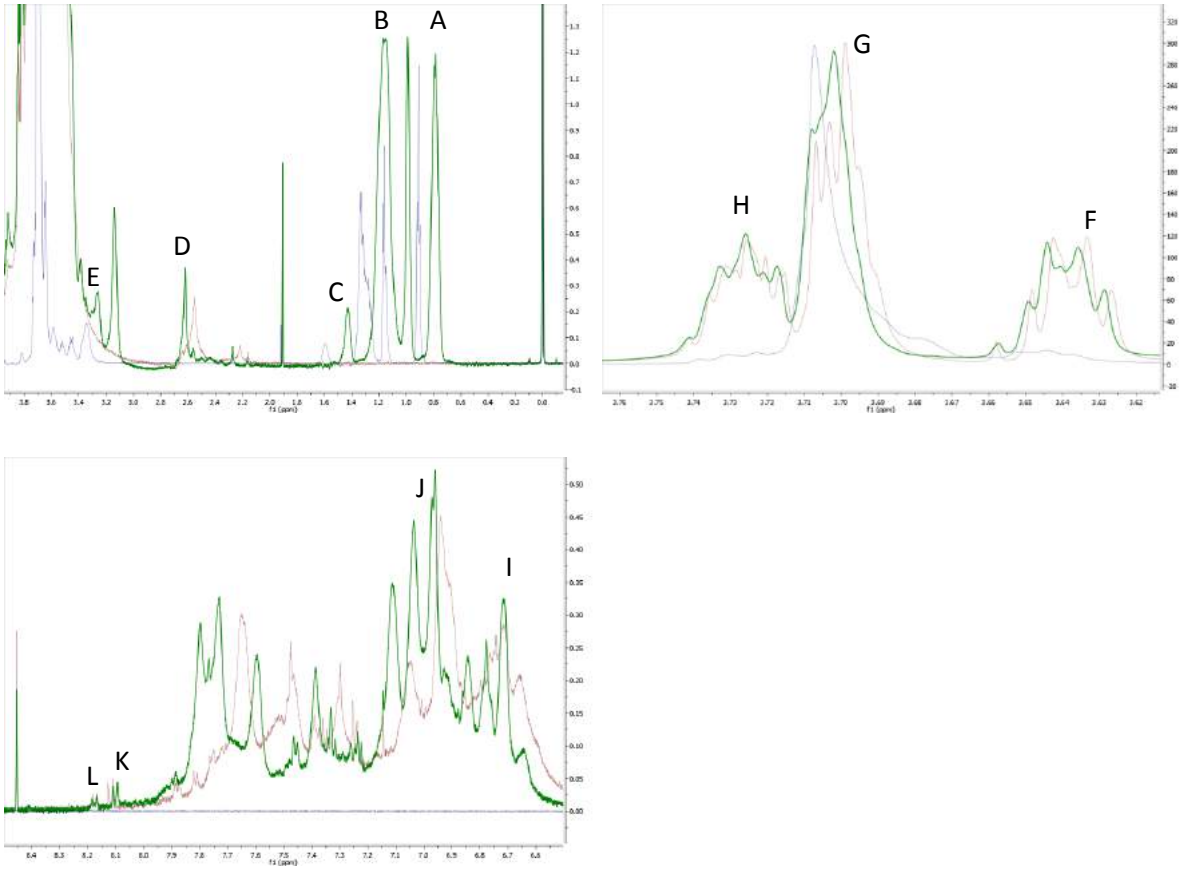

Assignment	$C_{10}E_{14}$ Shift (Hz)	E4210 Shift (Hz)	$C_{10}E_{14}$ - E4210 complex (Hz)	Delta Shift (Hz)
A	545.38		470.64	- 74.74
B	796.96		696.72	- 100.24
C	957.95		855.33	- 102.62
D		1530.59	1571.25	40.66
E	2005.53		1880.61	- 124.92
F		2178.23	2179.74	1.51
G	2222.53	2217.57	2219.37	- 3.16 / 1.80
H		2233.57	2233.69	0.12
I		4024.77	4025.16	0.39
J		4160.69	4172.04	11.35
K		4863.00	4852.52	- 10.48
L		4896.02	4897.14	1.12

NOESY $C_{10}E_{14}$ - E4210 complex comparison with pure samples

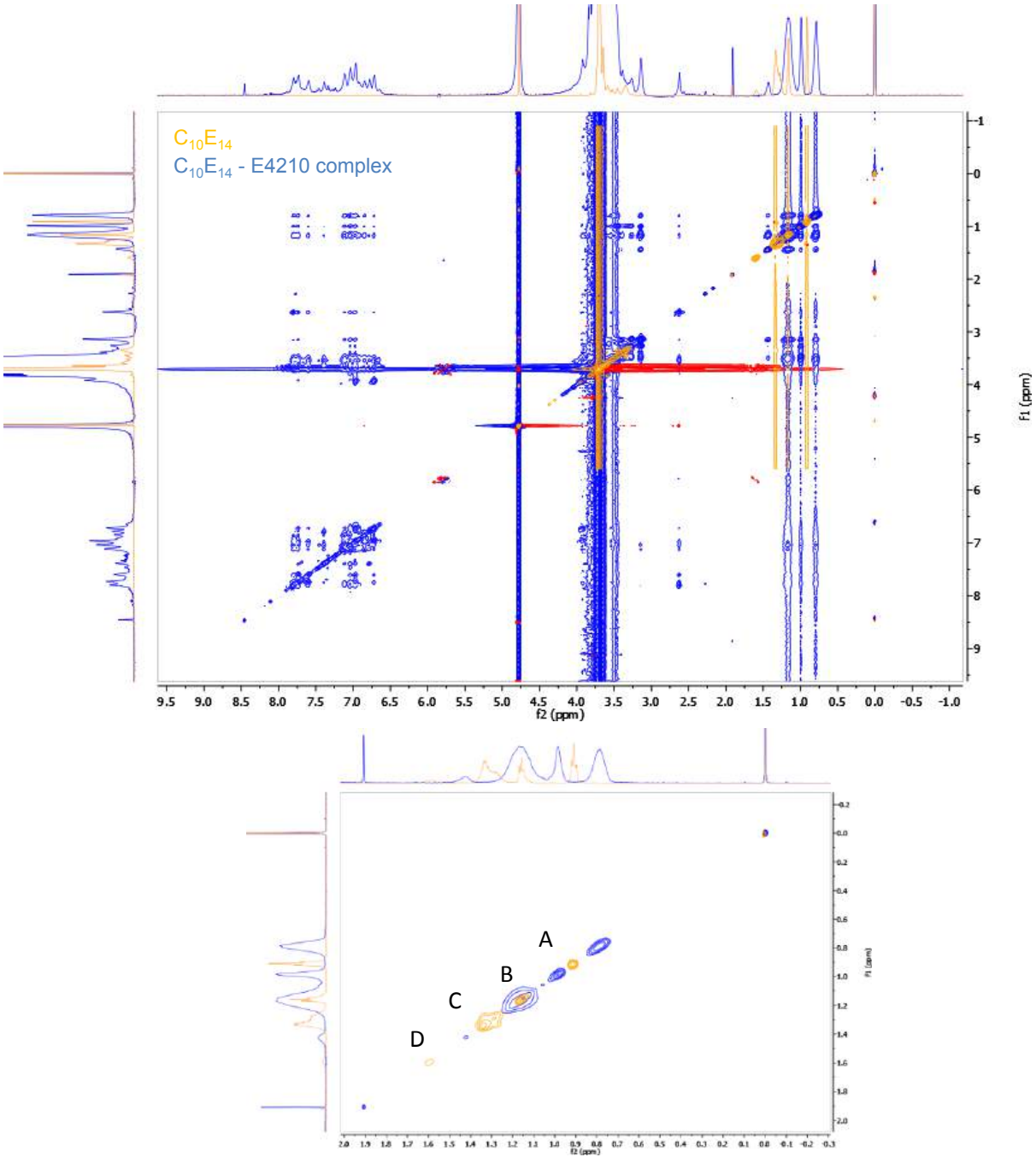

Assignment	$C_{10}E_{14}$ Shift (Hz)	E4210 Shift (Hz)	$C_{10}E_{14}$ - E4210 complex (Hz)	Delta Shift (Hz)
A	544.91		473.39	- 71.52
B	696.83		591.67	- 105.16
C	800.28		678.69	- 121.59
D	956.20		856.64	- 99.56

NOESY $C_{10}E_{14}$ - E4210 complex comparison with pure samples

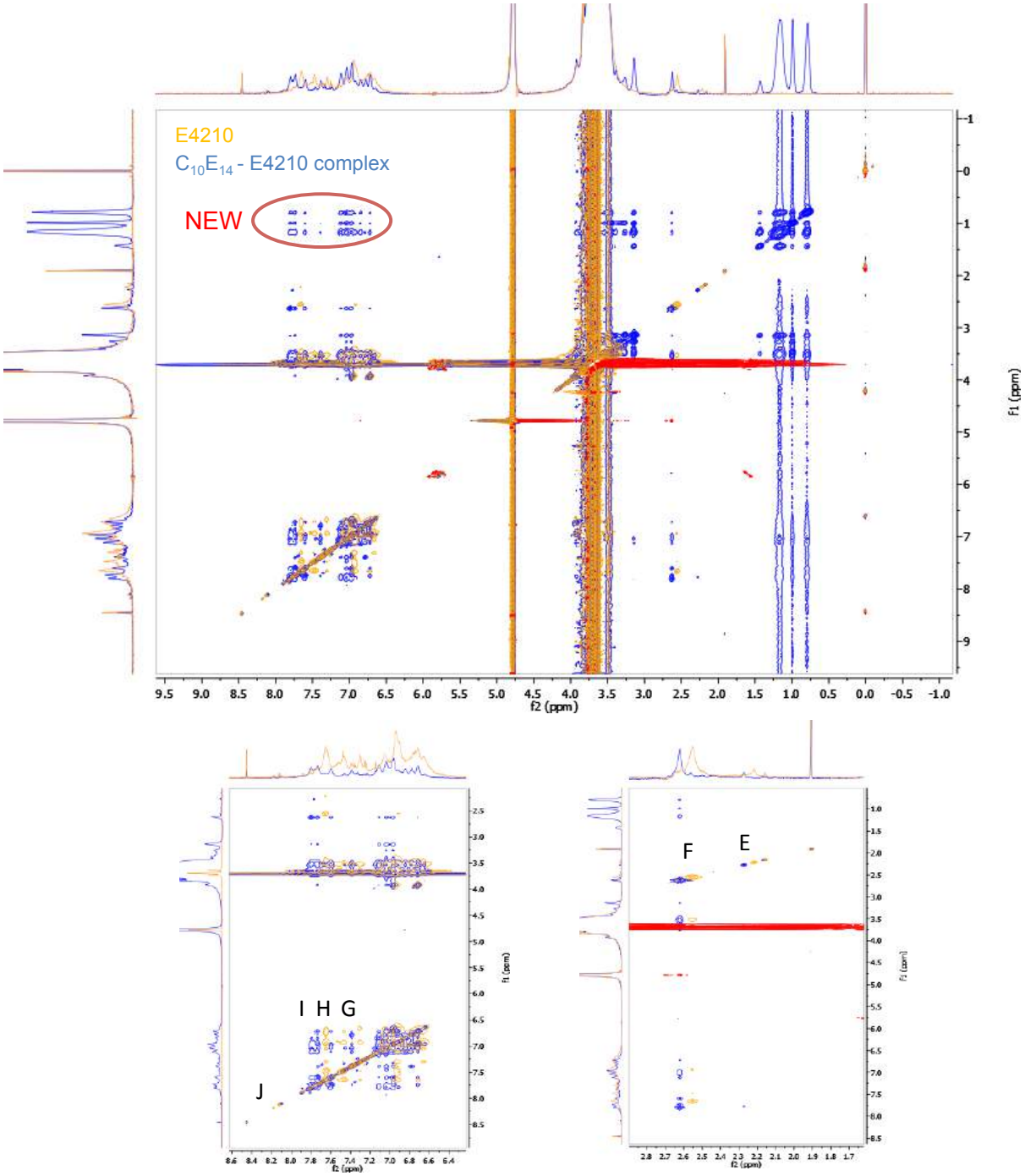

Assignment	$C_{10}E_{14}$Shift (Hz)	E4210 Shift (Hz)	$C_{10}E_{14}$ - E4210 complex (Hz)	Delta Shift (Hz)
E		1328.30	1361.67	33.37
F		1529.76	1570.33	40.57
G		4379.32	4423.20	43.88
H		4475.24	4556.41	81.17
I		4583.93	4639.03	55.10
J		4862.81	4853.11	-9.70

NMR
SDS – E4210

- ^{1}H SDS
- NOESY SDS
- HSQCAD SDS
- ^{1}H SDS - E4210 complex
- NOESY SDS – E4210 complex
- ^{1}H SDS - E4210 complex comparison with pure samples
- NOESY SDS - E4210 complex comparison with pure samples

^{1}H SDS

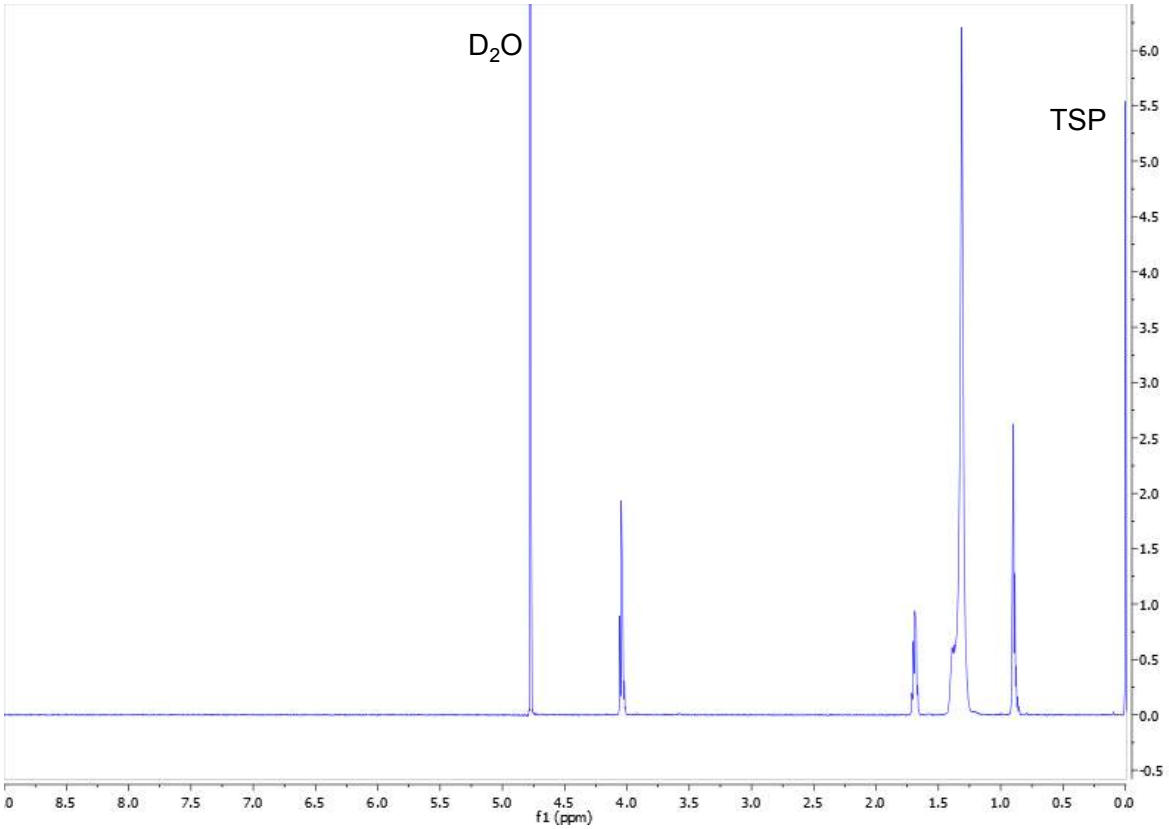

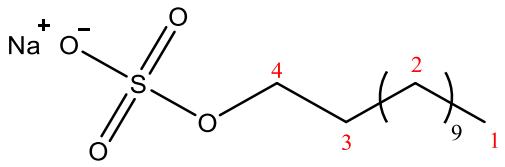

Assignment	Shift (ppm)	Shift (Hz)
TSP	0.00	0.00
1	0.90	538.13
2	1.31	786.57
3	1.69	1012.88
4	4.05	2425.71
D_2O	4.78	2862.75

NOESY SDS

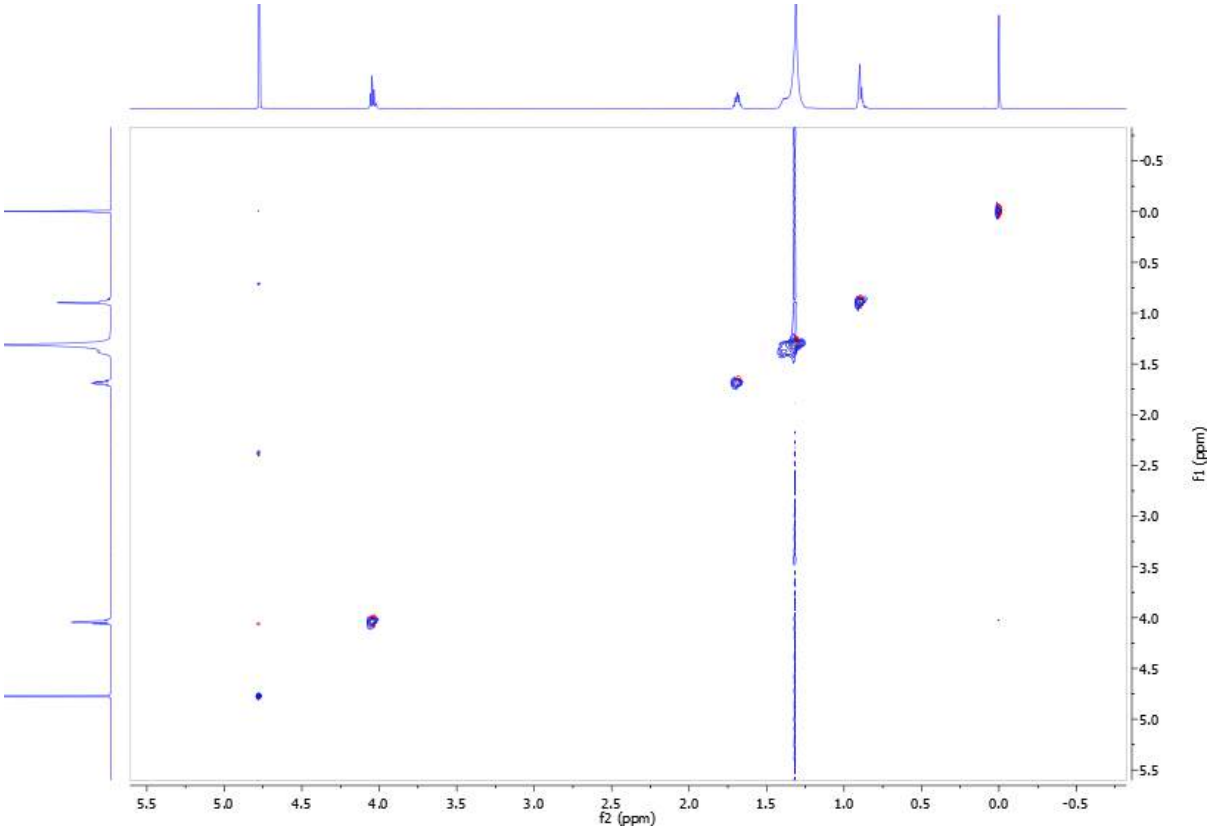

HSQCAD SDS

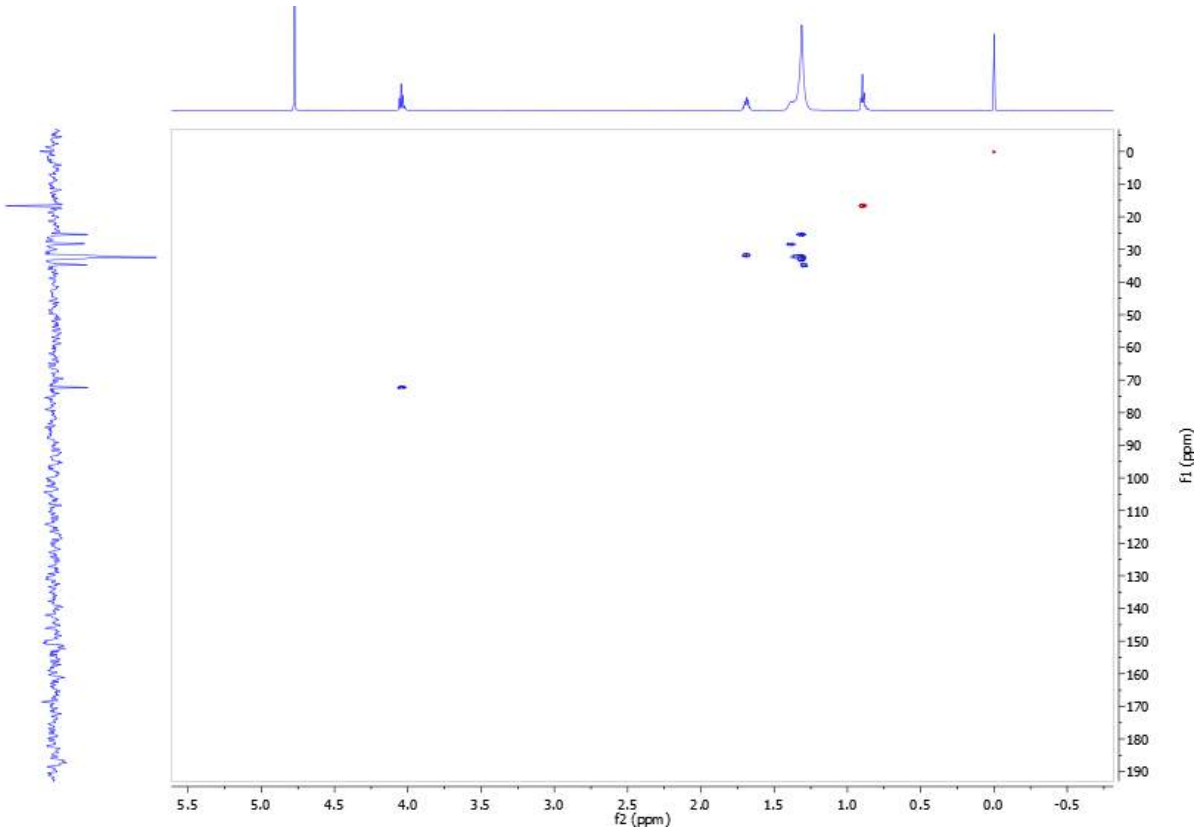

^{1}H SDS - E4210 complex

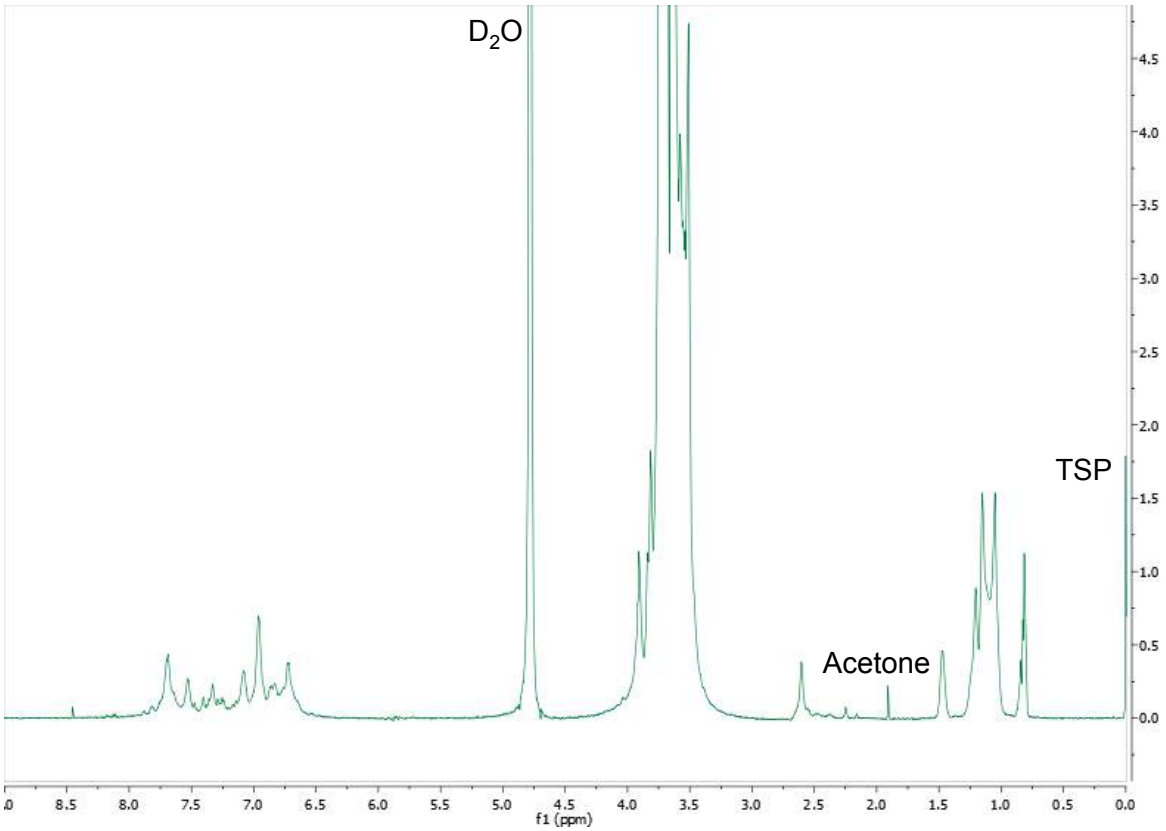

NOESY SDS - E4210 complex

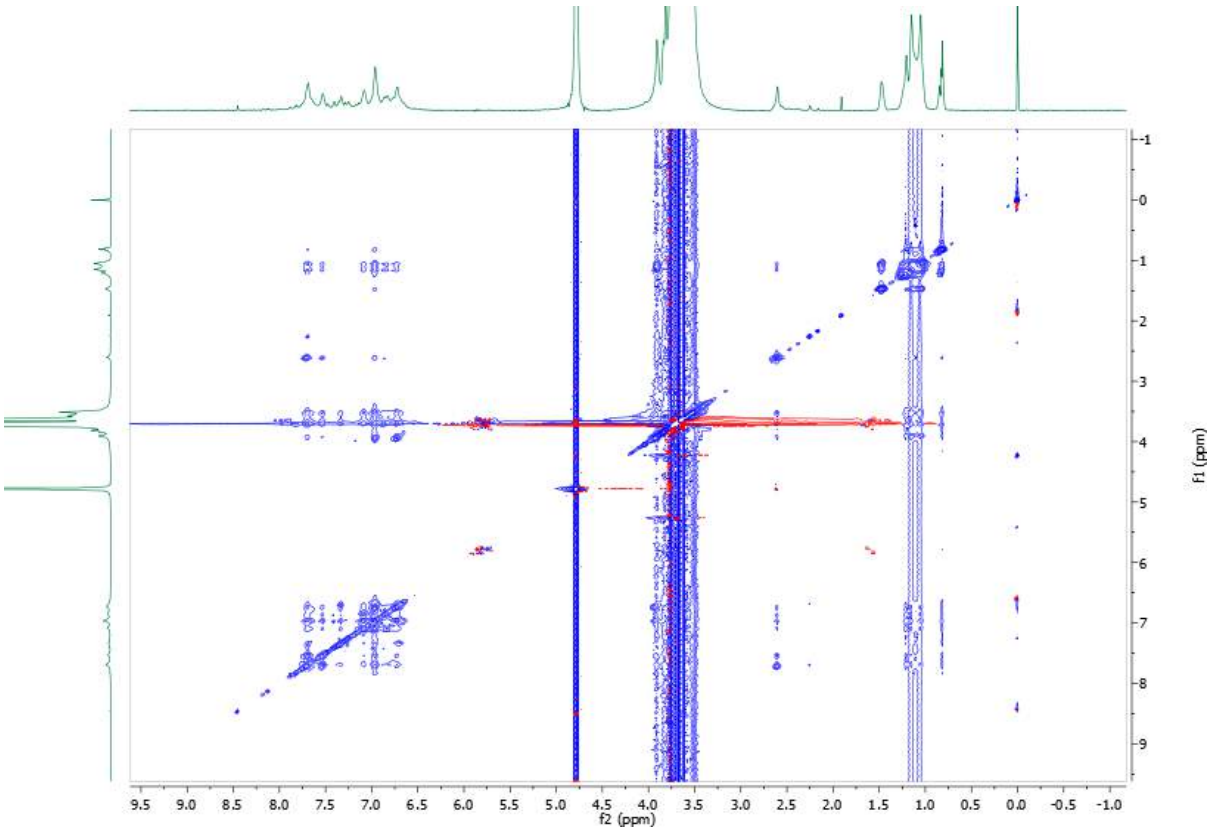

^{1}H SDS - E4210 complex comparison with pure samples

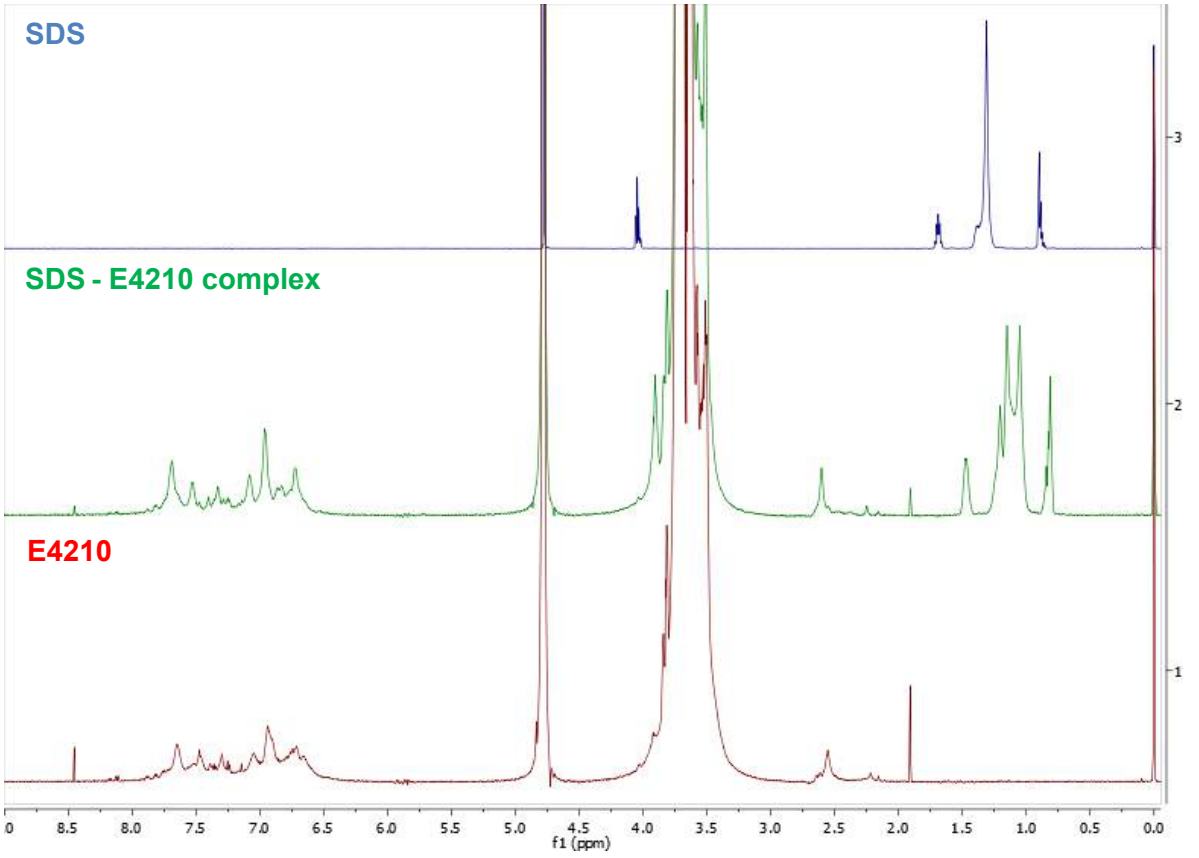

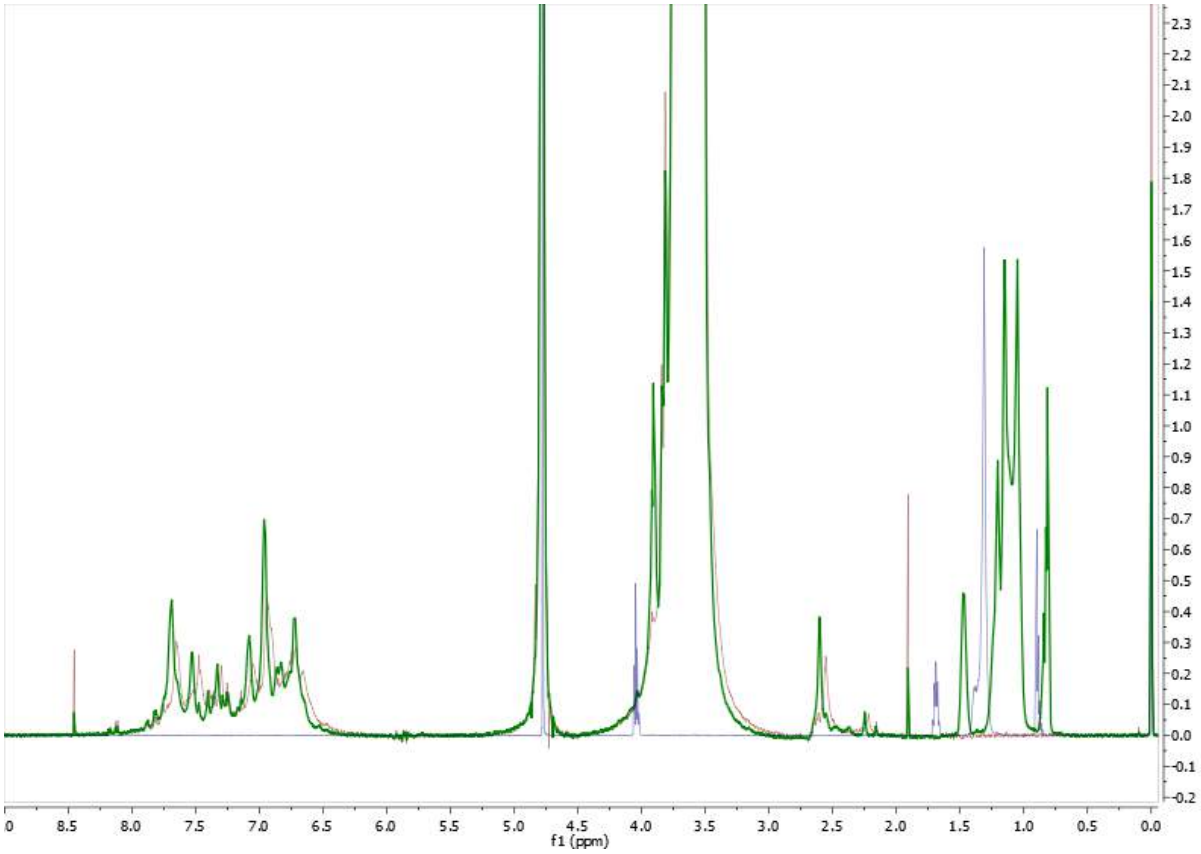

^{1}H SDS - E4210 complex comparison with pure samples

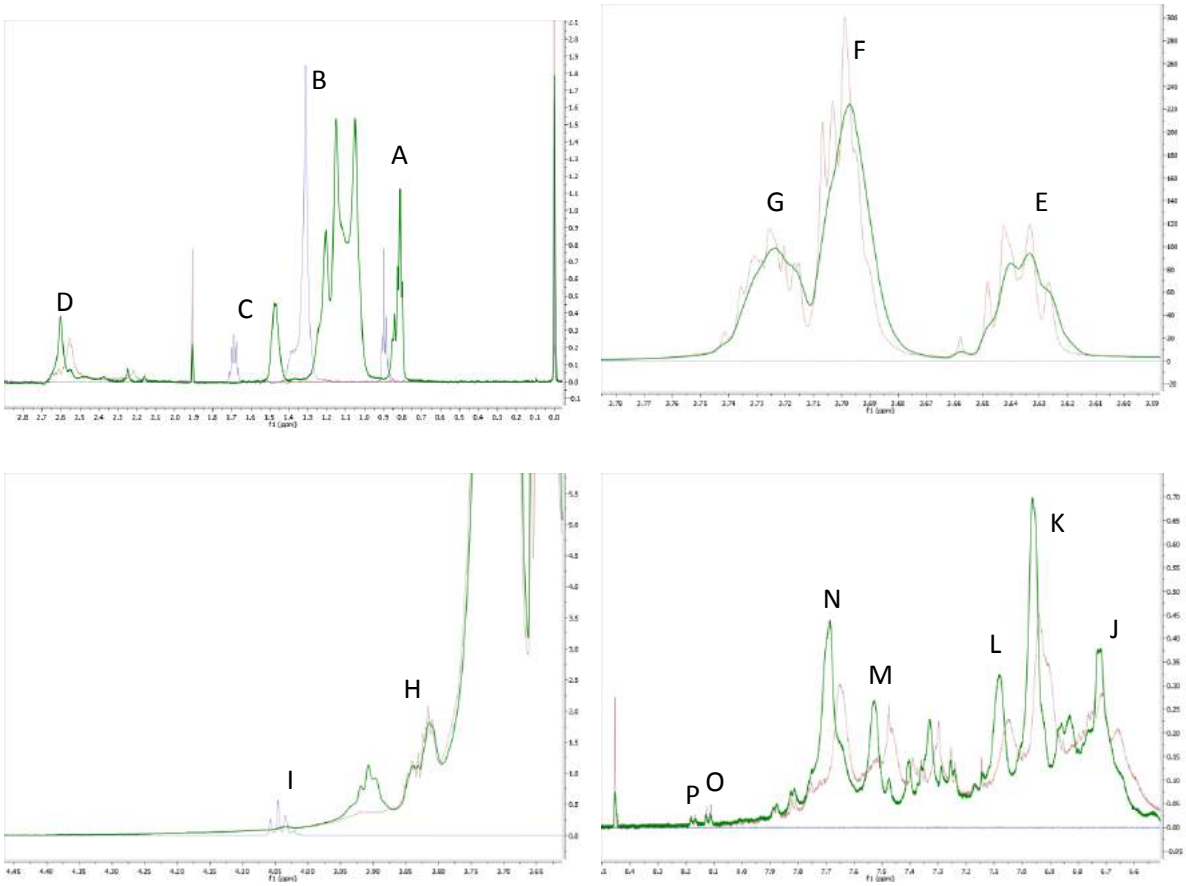

Assignment	SDS Shift (Hz)	E4210 Shift (Hz)	SDS - E4210 complex (Hz)	Delta Shift (Hz)
A	538.13		488.21	- 49.92
B	786.57		690.71	- 95.86
C	1012.88		883.51	- 129.37
D		1530.86	1560.49	29.63
E		2178.23	2178.32	0.09
F		2217.57	2216.56	- 1.01
G		2233.57	2232.24	- 1.33
H		2287.74	2286.80	- 0.94
I	2425.71		2342.74	- 82.97
J		4024.77	4031.09	6.32
K		4160.21	4175.31	15.10
L		4225.55	4244.41	18.86
M		4481.34	4513.76	22.42
N		4586.42	4608.97	22.55
O		4863.00	4865.35	2.35
P		4896.02	4897.12	1.10

NOESY SDS - E4210 complex comparison with pure samples

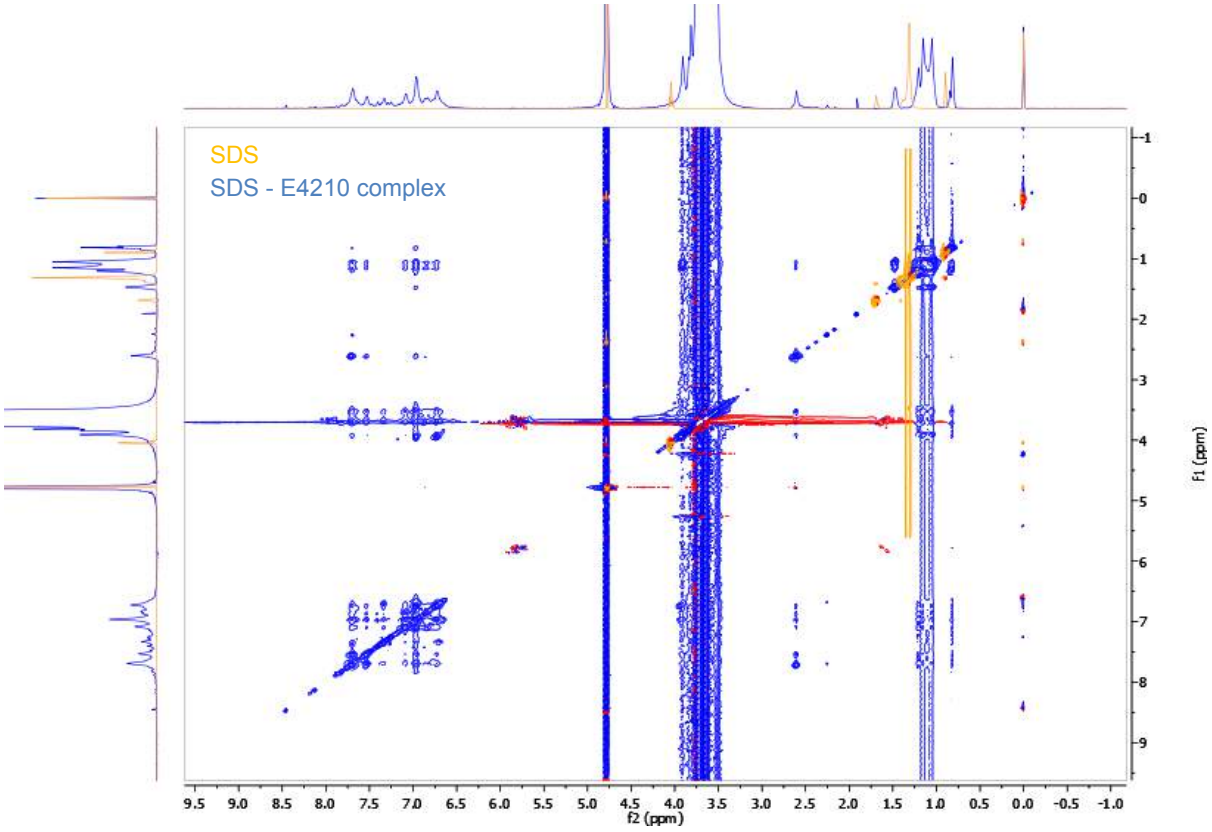

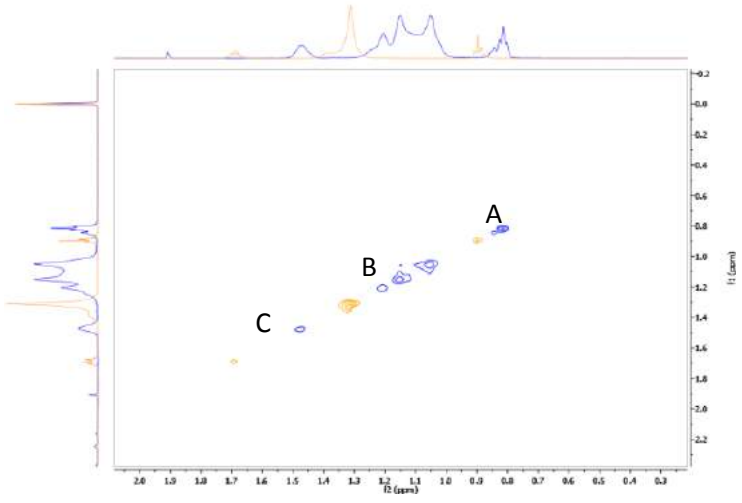

Assignment	SDS Shift (Hz)	E4210 Shift (Hz)	SDS - E4210 complex (Hz)	Delta Shift (Hz)
A	538.40		487.43	- 50.97
B	787.75		690.78	- 96.97
C	1014.83		886.10	- 128.73

NOESY SDS - E4210 complex comparison with pure samples

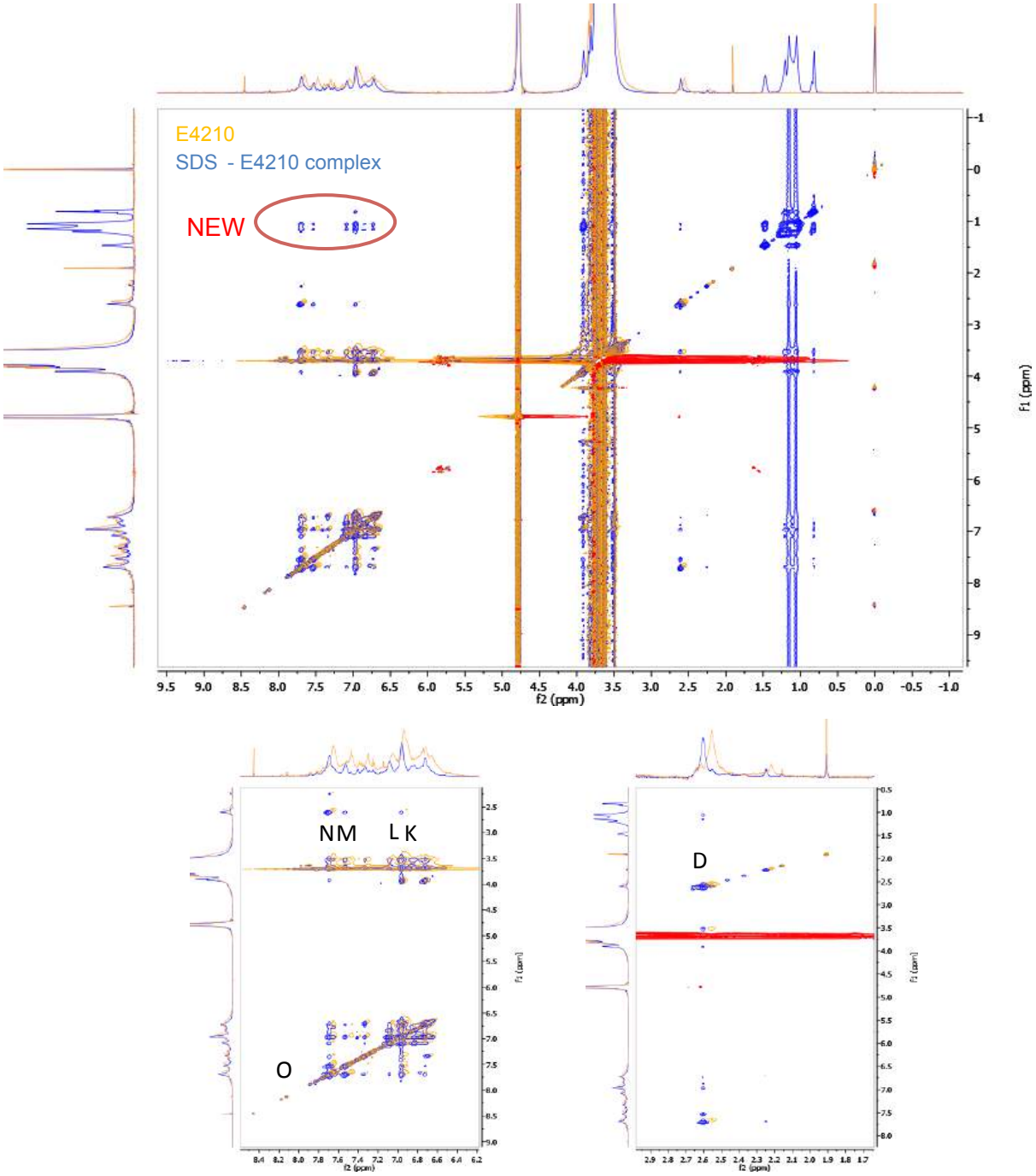

Assignment	SDS Shift (Hz)	E4210 Shift (Hz)	SDS - E4210 complex (Hz)	Delta Shift (Hz)
D		1531.23	1560.68	29.45
K		4160.05	4175.36	15.31
L		4225.94	4245.59	19.65
M		4479.57	4514.80	35.23
N		4587.72	4610.86	23.14
O		4862.98	4864.97	1.99

NMR
SDBS – E4210

- ^{1}H SDBS
- NOESY SDBS
- HSQCAD SDBS
- ^{1}H SDBS - E4210 complex
- NOESY SDBS – E4210 complex
- ^{1}H SDBS - E4210 complex comparison with pure samples
- NOESY SDBS - E4210 complex comparison with pure samples

^{1}H SDBS

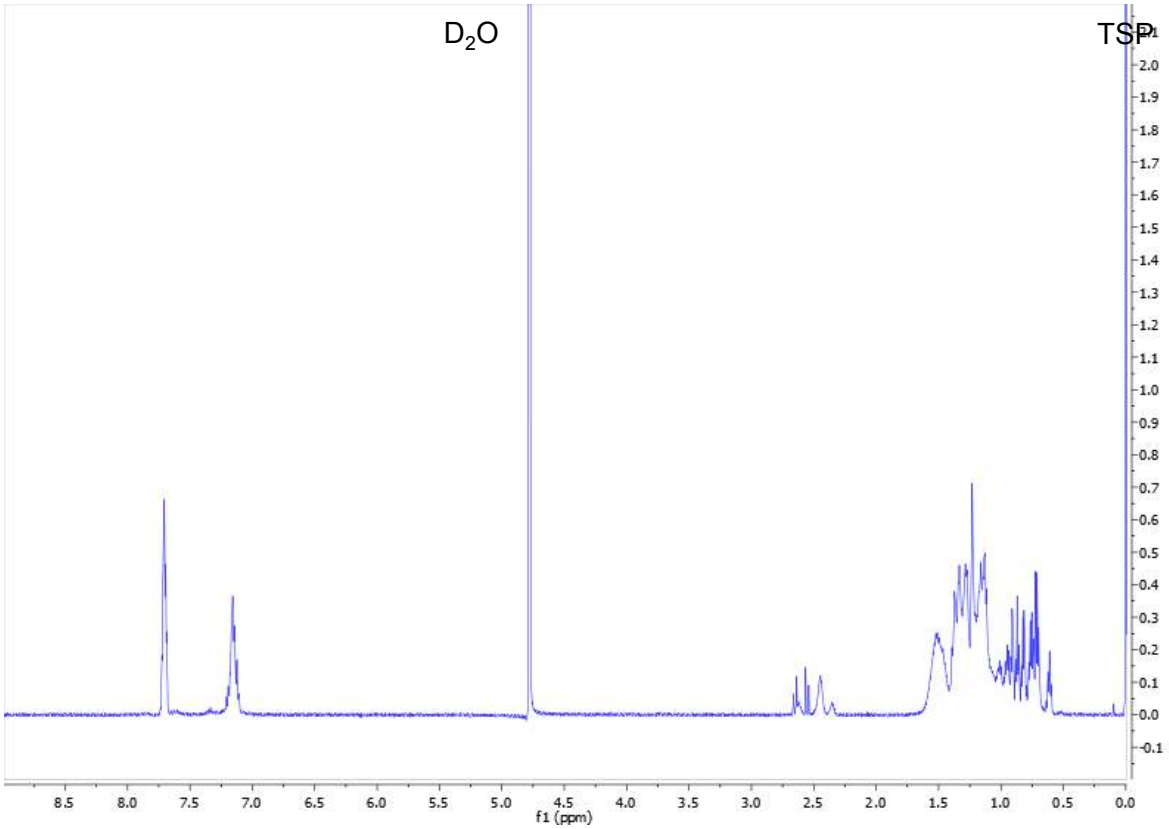

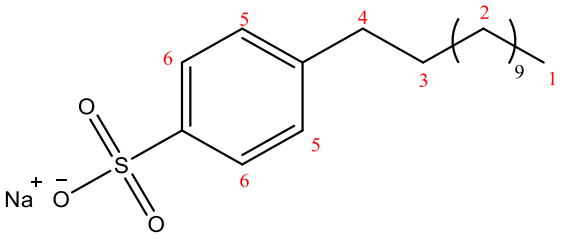

Assignment	Shift (ppm)	Shift (Hz)
TSP	0.00	0.00
1	0.61	366.03
2	0.70 – 1.37	419.00 – 823.08
3	1.51	905.82
4	2.35 – 2.66	1410.10 – 1597.13
D_2O	4.78	2865.75
5	7.16	4290.66
6	7.70	4619.23

NOESY SDBS

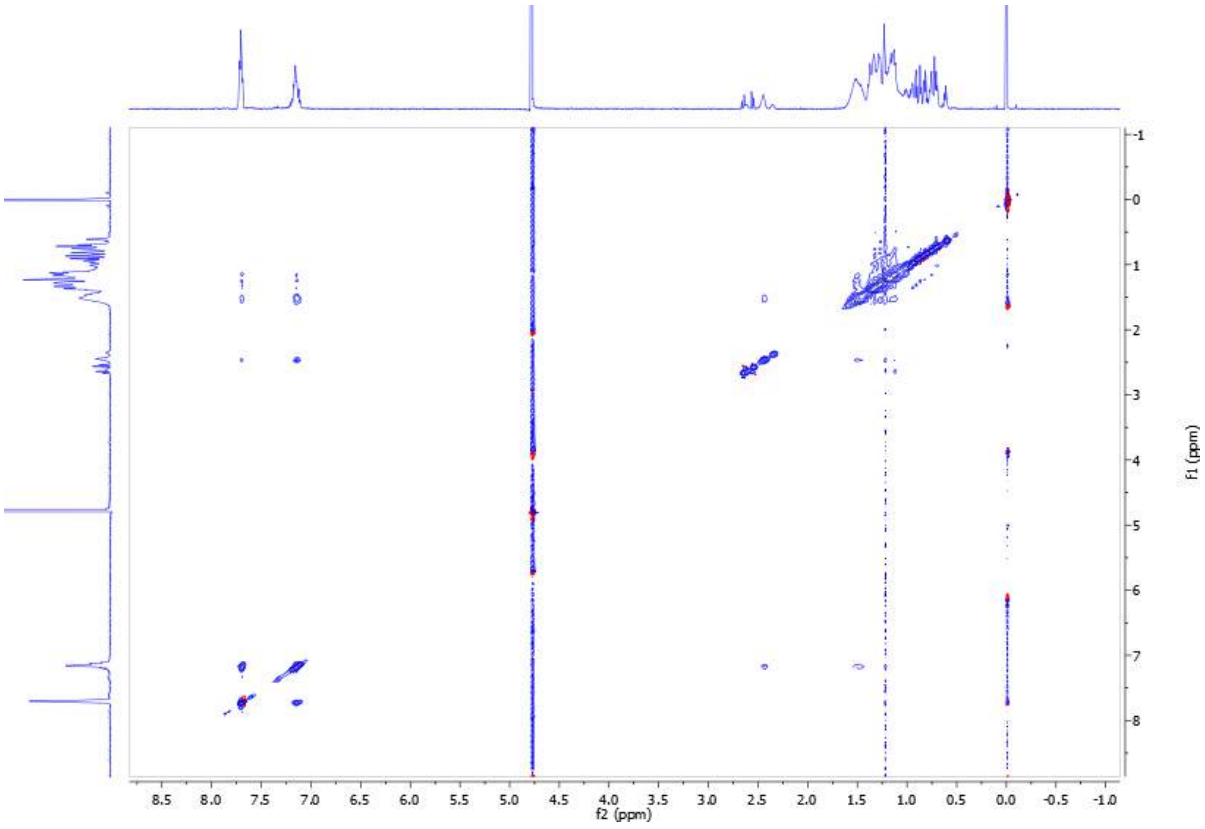

HSQCAD SDBS

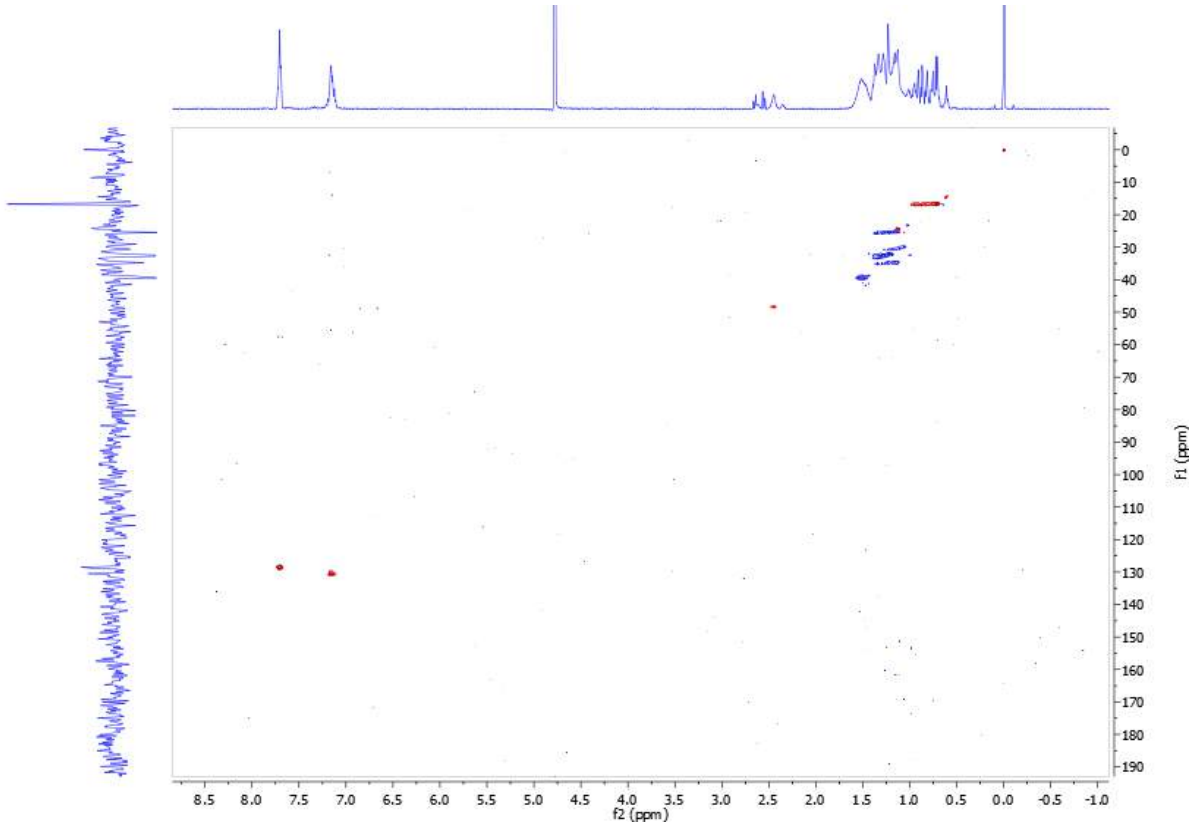

^{1}H SDBS - E4210 complex

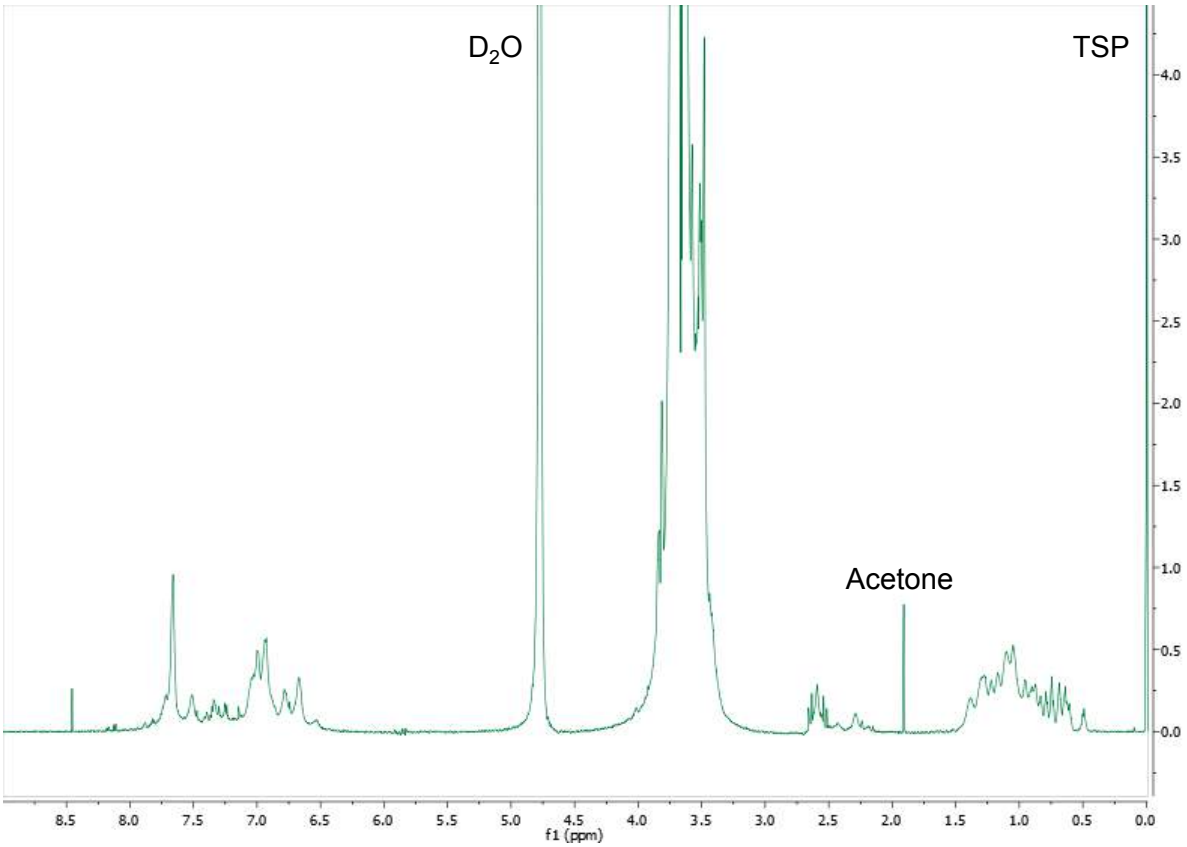

NOESY SDBS - E4210 complex

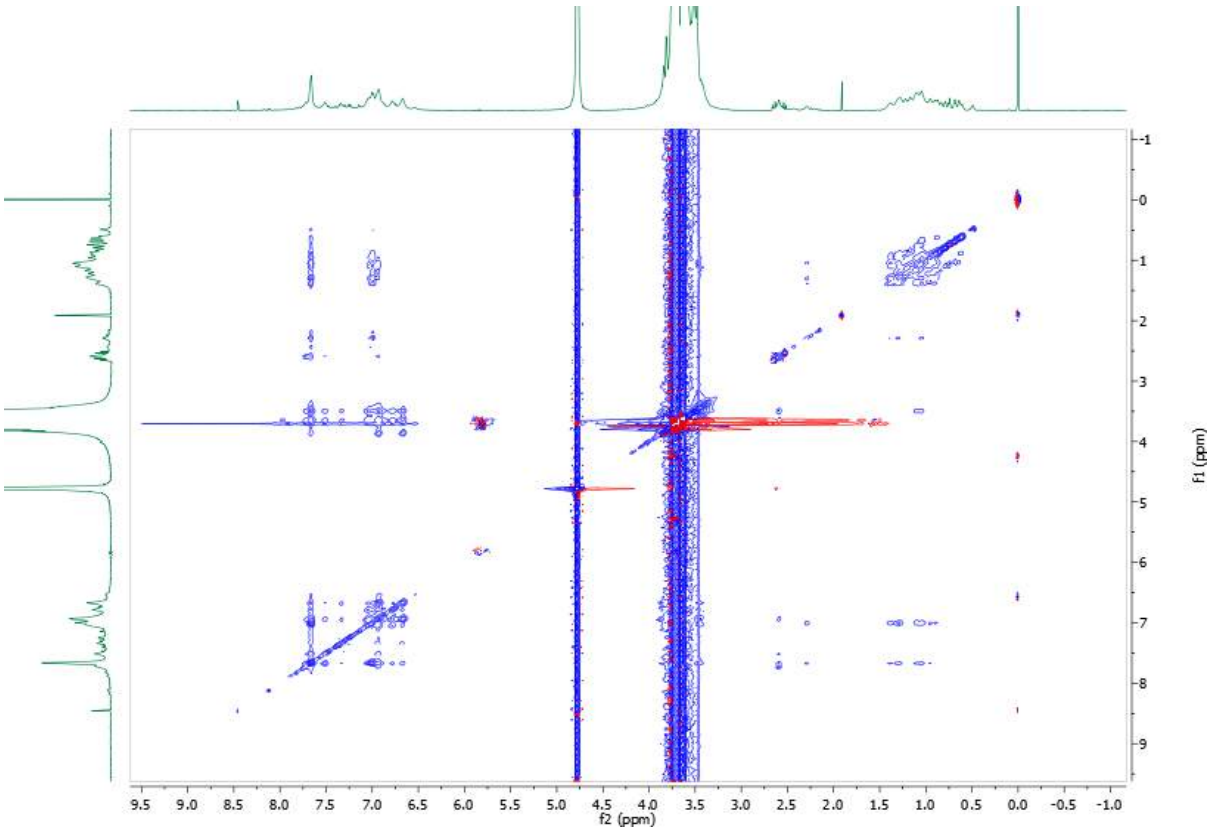

^{1}H SDBS - E4210 complex comparison with pure samples

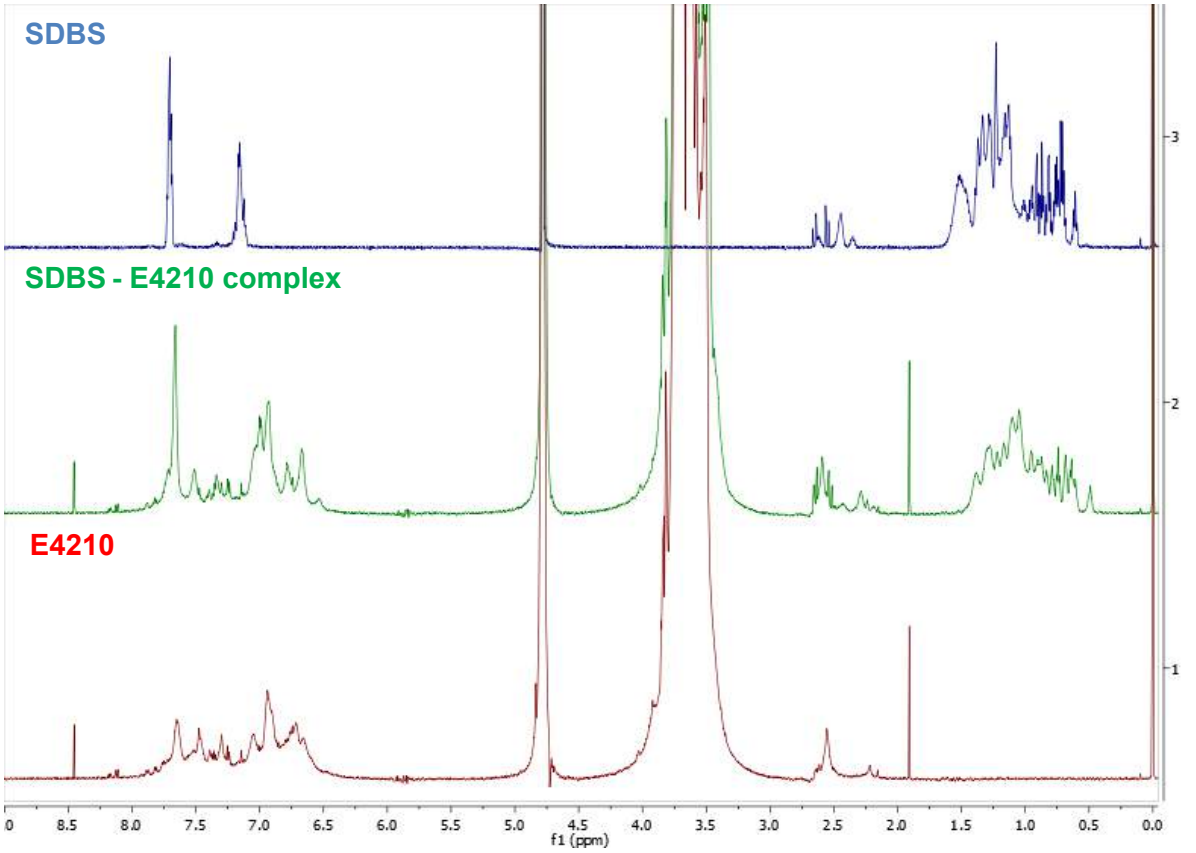

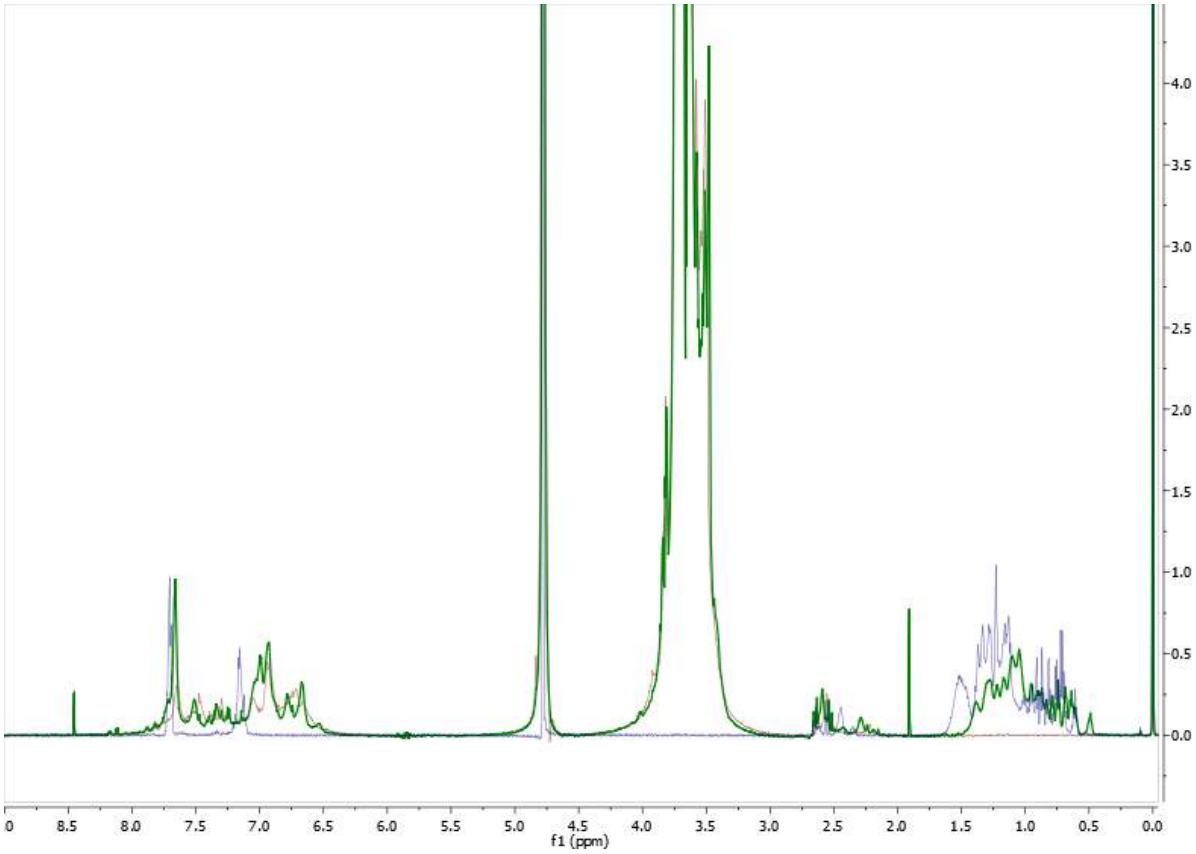

^{1}H SDBS - E4210 complex comparison with pure samples

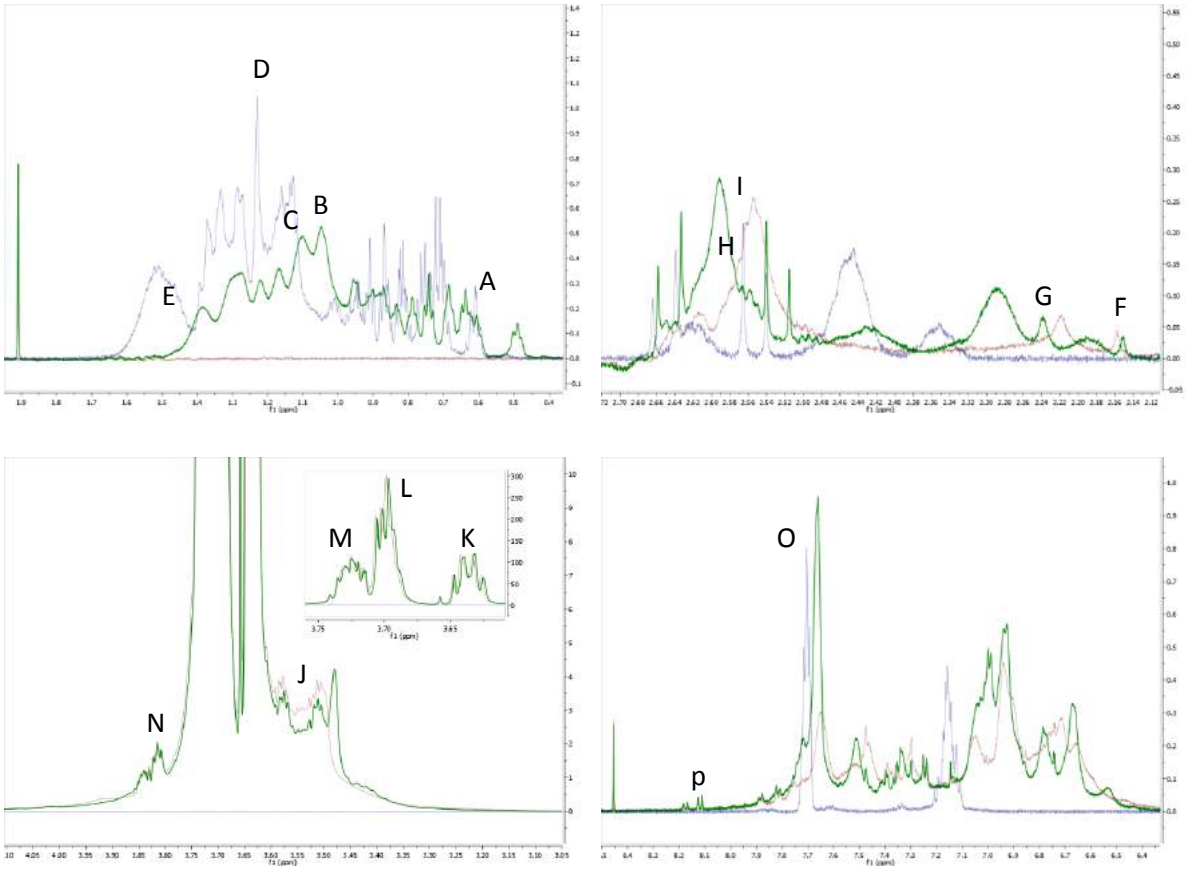

Assignment	SDBS Shift (Hz)	E4210 Shift (Hz)	SDBS - E4210 complex (Hz)	Delta Shift (Hz)
A	366.03		293.51	- 72.52
B	676.24		628.29	- 47.95
C	695.70		660.58	- 35.12
D	737.60		700.47	- 37.13
E	905.82		830.05	- 75.77
F		1293.52	1289.46	- 4.06
G		1329.98	1342.06	12.08
H	1560.03		1550.72	- 9.31
I		1530.86	1553.54	22.68
J		2105.67	2104.94	- 0.73
K		2178.23	2177.39	- 0.84
L		2217.57	2216.39	- 1.18
M		2233.57	2233.27	- 0.30
N		2287.74	2286.79	5.05
O	4619.23		4592.75	- 26.48
P		4862.48	4862.48	0.00

NOESY SDBS - E4210 complex comparison with pure samples

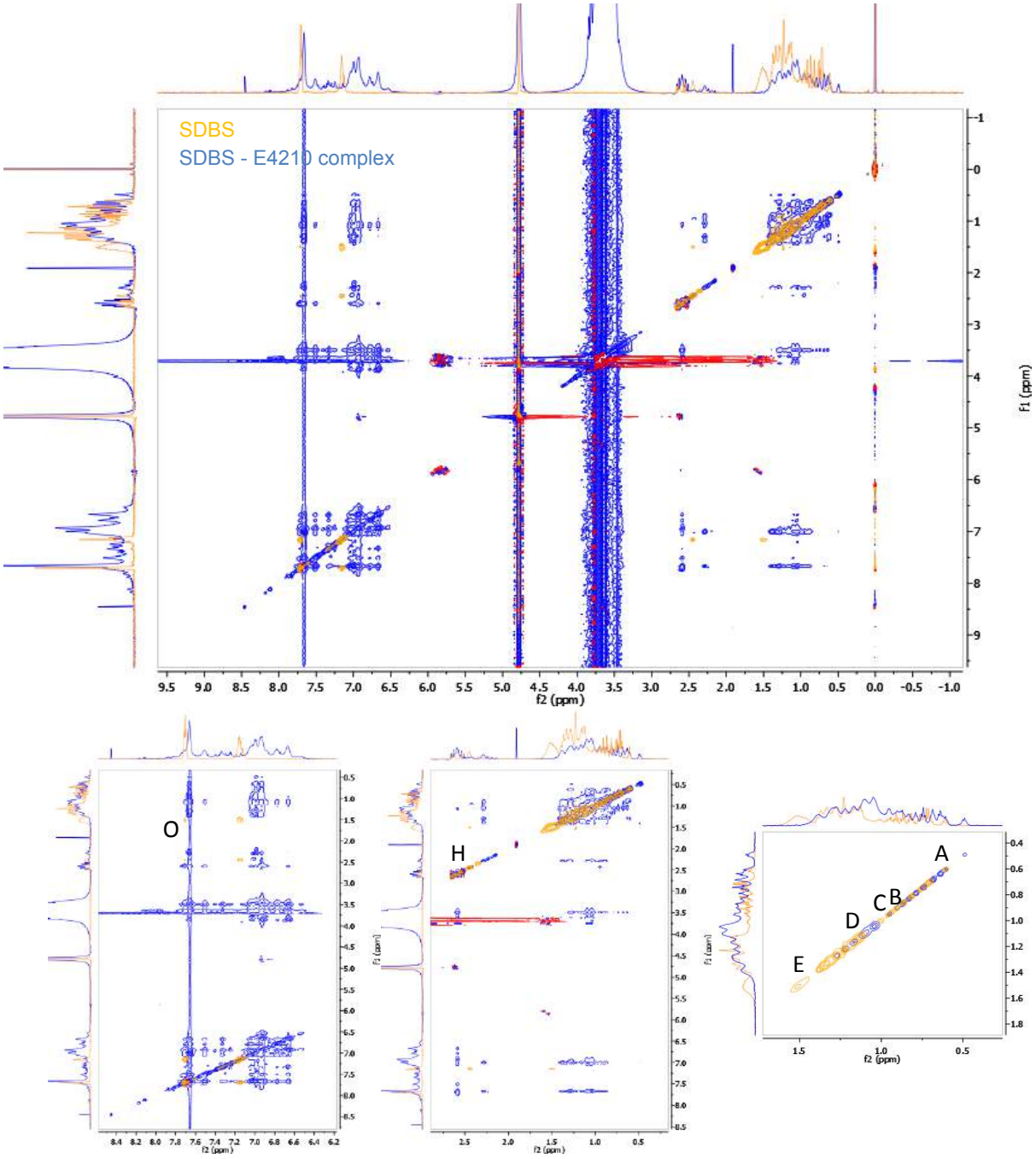

Assignment	SDBS Shift (Hz)	E4210 Shift (Hz)	SDBS - E4210 complex (Hz)	Delta Shift (Hz)
A	363.10		293.09	- 70.01
B	675.25		628.47	- 46.78
C	693.42		660.45	- 32.97
D	735.76		698.92	- 36.84
E	902.39		829.39	- 73.00
H	1557.50		1549.04	- 8.46
O	4618.65		4592.49	- 26.16

NOESY SDBS - E4210 complex comparison with pure samples

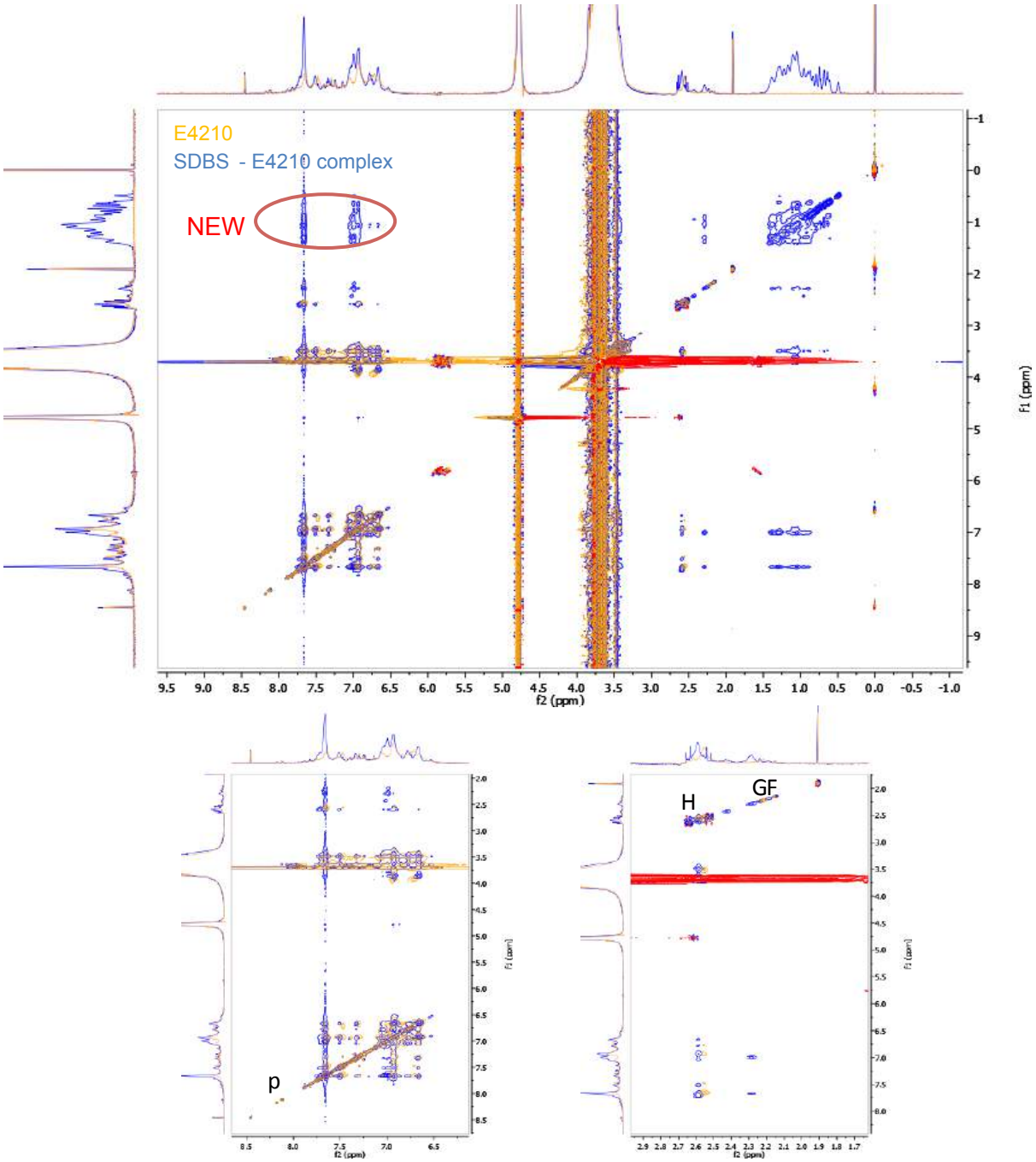

Assignment	SDBS Shift (Hz)	E4210 Shift (Hz)	SDBS - E4210 complex (Hz)	Delta Shift (Hz)
F		1293.57	1289.88	- 3.69
G		1329.53	1342.04	12.51
I		1530.35	1553.39	23.04
P		4862.70	4862.14	- 0.56